

UC San Diego

UC San Diego Electronic Theses and Dissertations

Title

Manipulating posttranslational modification in natural product biosynthesis

Permalink

<https://escholarship.org/uc/item/0sn8v44w>

Author

Foley, Timothy Leyden

Publication Date

2010

Peer reviewed|Thesis/dissertation

UNIVERSITY OF CALIFORNIA, SAN DIEGO

Manipulating Posttranslational Modification in Natural Product Biosynthesis

A dissertation submitted in partial satisfaction of the
requirements for the degree of Doctor of Philosophy

in

Chemistry

by

Timothy Leyden Foley

Committee in charge:

Professor Michael D. Burkart, Chair
Professor Stuart Brody
Professor Elizabeth A. Komives
Professor Emmanuel Theodorakis
Professor Jerry Yang

2010

Copyright

Timothy Leyden Foley, 2010

All rights reserved.

The dissertation of Timothy Leyden Foley is approved, and it is acceptable in quality
and form for publication on microfilm and electronically

Chair

University of California, San Diego

2010

DEDICATION

This dissertation is dedicated to my family and friends.

Most of all, to my mother, whose constant support and unwaivering acceptance of my decisions has been the cornerstone to my success, now and always. To my father, who bestowed upon me the desire for intellectual consummation and a curiosity about the physical world from an early age. To my brother, whose comradery and competition for attention at a young age allowed me to develop a drive for achievement. To my godparents, Ramona and Herb Gorecki, who have always been there as my surrogate extended family.

This dissertation is also dedicated to Erin Mesplou. Your love and support have provided me with the courage to complete my studies, without which this work would not have been possible.

EPIGRAPH

Very often, in the course of scientific experimentation,
a totally unexpected observation
is made that is either unrelated or only incidentally related to the problem under
immediate investigation. When it captures the attention of an alert,
inquisitive mind, this
observation may open the door for an entirely new study
that is often more fruitful than
that of the original design.

Earl Stadtman

TABLE OF CONTENTS

DEDICATION	iv
EPIGRAPH.....	v
TABLE OF CONTENTS	vi
LIST OF ABBREVIATIONS	x
LIST OF FIGURES.....	xii
LIST OF TABLES	xv
ACKNOWLEDGEMENTS	xvi
VITA.....	xviii
ABSTRACT OF THE DISSERTATION.....	xxii
Chapter 1 INTRODUCTION.....	1
NATURAL PRODUCTS.....	2
NONRIBOSOMAL PEPTIDES AND THEIR BIOSYNTHESIS	8
THIOTEMPLATE LOGIC.....	11
THIOESTER INTERMEDIATES	12
POSTTRANSLATIONAL MODIFICATION OF CP DOMAINS	13
PHOSPHOPANTETHEINYL TRANSFERASE ENZYMES	15
BIOMEDICAL RELEVANCE.....	17
PK AND NRP COMPOUNDS AS VIRULENCE FACTORS	18
DEVELOPMENT OF A CP-DOMAIN ISOLATION TECHNIQUE	19
TARGET ISOLATION PROCEDURE AND COMPLICATION.....	24

Chapter 2 SITE-SPECIFIC PROTEIN MODIFICATION: ADVANCES AND APPLICATIONS.....	27
ABSTRACT.....	28
INTRODUCTION	28
BIOCHEMICAL (<i>in vitro</i>) TOOLS.....	30
PROTEOMIC (<i>ex vivo</i>) TOOLS	34
CELLULAR IMAGING/RECOMBINANT TOOLS.....	38
CONCLUSION.....	42
ACKNOWLEDGEMENTS.....	45
Chapter 3 A HOMOGENOUS RESONANCE ENERGY TRANSFER ASSAY FOR PHOSPHOPANTETHIENYL TRANSFERASE.....	46
ABSTRACT.....	47
INTRODUCTION	47
MATERIALS & METHODS	50
RESULTS & DISCUSSION.....	54
CONCLUSIONS.....	73
ACKNOWLEDGEMENTS.....	73
Chapter 4 PHOSPHOPANTETHEINYL TRANSFERASE INHIBITORS AND SECONDARY METABOLISM	74
ABSTRACT.....	75
INTRODUCTION	75
RESULTS & DISCUSSION.....	79

CONCLUSIONS.....	93
MATERIALS AND METHODS.....	94
ACKNOWLEDGEMENTS.....	110
Chapter 5 A STRATEGY TO DISCOVER INHIBITORS OF BACILLUS SUBTILIS SURFACTIN-TYPE PHOSPHOPANTETHEINYL TRANSFERASE..	112
ABSTRACT.....	113
INTRODUCTION	114
MATERIALS AND METHODS.....	118
RESULTS	126
DISCUSSION	139
ACKNOWLEDGEMENTS.....	144
Chapter 6 PREPARATION OF FRET REPORTERS TO SUPPORT CHEMICAL PROBE DEVELOPMENT.....	146
ABSTRACT.....	147
INTRODUCTION	147
RESULTS AND DISCUSSION.....	150
MATERIALS AND METHODS.....	156
ACKNOWLEDGEMENTS.....	165
Chapter 7 INHIBITORS OF SURFACTIN-TYPE PHOSPHOPANTETHEINYL TRANSFERASE IDENTIFIED BY QUANTITATIVE HIGH THROUGHPUT SCREENING.....	167
ABSTRACT.....	168

INTRODUCTION	168
RESULTS	171
CONCLUSIONS.....	233
ACKNOWLEDGEMENTS	233
REFERENCES	234

LIST OF ABBREVIATIONS

4'-PP	4'-phosphopantetheine
ACP	acyl carrier protein
AT	acyl transferase
BSA	bovine serum albumen
CoA	coenzyme A
CP	carrier protein domain
DACM	7-dimethylamino-4-methyl-coumarin-3-maleimide
DMF	N,N-dimethylformamide
DMSO	dimethyl sulfoxide
DCM	dichloromethane
DH	dehydratase
ER	enoyl reductase
EtOAc	ethyl acetate
FITC	fluorescein-5-isothiocyanate
Fmoc	9-Fluorenylmethyloxycarbonyl
FRET	fluorescence resonance energy transfer
HATU	2-(1H-7-Azabenzotriazol-1-yl)-1,1,3,3-tetramethyl uronium hexafluorophosphate
HEPES	4-(2-hydroxyethyl)-1-piperazine ethanesulfonic acid
IC50	inhibitory concentration (50 percent)
KS	ketosynthase

MT	malonyl transferase
mCoA	modified-coenzyme A
PAP	3'-phosphoadenosine-5'-phosphate
PCP	peptidyl carrier protein
PPTase	phosphopantetheinyl transferase
RFU	relative fluorescence unit
R _f	relative mobility
TAMRA	tetramethylrhodamine-5-maleimide
TE	thioesterase
UV-VIS	ultraviolet-visible

LIST OF FIGURES

Figure 1.1 The central dogma of information flow in biological systems	3
Figure 1.2 Representative polyketide and nonribosomal peptide natural products.....	5
Figure 1.3 6-Deoxyerythronolide A biosynthetic pathway	7
Figure 1.4 Tyrocidine A Biosynthetic Pathway.	10
Figure 1.5 Thioester intermediates in PK/NRP biosynthesis	14
Figure 1.6 Posttranslational modification of carrier protein domains	16
Figure 1.7 Physiological transfer of acyl-phosphopantetheinyl arms by PPTase	20
Figure 1.8 Functional manipulation of CP domains with CoA analogues	22
Figure 1.9 Fluorescent labeling of CP domains	23
Figure 1.10 Scheme for the isolation of CP-containing enzymes	25
Figure 2.1 Biochemical methods for the Site specific labeling of proteins.....	32
Figure 2.2 <i>Ex vivo</i> techniques to identify posttranslationally modified proteins.	36
Figure 2.3 Enzymatic labeling techniques to image cells.	40
Figure 2.4 Image from cover of Curr. Ops. Chem Biol, vol 11, issue 1, 2007	44
Figure 3.1 Posttranslational modification of carrier proteins.	49
Figure 3.2 Fluorescence resonance energy transfer assay for phosphopantetheinyl transferase.....	55
Figure 3.3 Synthesis of assay components.	58
Figure 3.4 Probe selection and photophysical evaluation of the crypto-YbbR peptides.	62

Figure 3.5 Reaction progress and enzyme titration.	66
Figure 3.6 Determination of analysis timepoint and Z'.	69
Figure 3.7 Reproducibility of IC50 values for 3'-phosphoadenosine-5'-phosphate.	72
Figure 4.1 Isolation of carrier protein-dependent biosynthetic machinery.	77
Figure 4.2 Target validation in <i>Bacillus subtilis</i> Sfp ^{+/−}	81
Figure 4.3 Synthesis of anthranilate 4 <i>H</i> -oxazol-5-ones.	85
Figure 4.4 Design of a Förster resonance energy transfer assay for phosphopantetheinyl transferase.	87
Figure 4.5 Inhibition of PPTases from small 4 <i>H</i> -oxazol-5-one library.	88
Figure 4.6 Biological evaluation of 7ae in <i>Streptomyces coelicolor</i>	90
Figure 4.7 Working hypothesis of how PPTase inhibition increases natural product yield.	92
Figure 5.1 Assay Principle.	117
Figure 5.2 Assay Optimization.	127
Figure 5.3 Effect of different detergents on the reaction progress of the uncatalyzed enzyme in the Dark Quench system.	130
Figure 5.4 Sfp-PPTase Titration.	132
Figure 5.5 Reagent Stability.	134
Figure 5.6 Substrate and Product Mimetics.	135
Figure 5.7 LOPAC ¹²⁸⁰ qHTS.	137
Figure 6.1 Phosphopantetheinyl transferase assay format and commercially available chemical probes.	149
Figure 6.2 Synthetic route to Rhodamine WT-functionalized CoA.	151

Figure 6.3 Synthetic route to dark quencher p-nitrophenyl carbonate	153
Figure 6.4 Utilization of the new reagents in a triplicate robotic screen of the LOPAC1280 library.	154
Figure 7.1 Data cataloging for antibiotic analysis of LOPAC ¹²⁸⁰ hits.	172
Figure 7.2 qHTS Z' and control titration performance	176
Figure 7.3 waterfall plot of qHTS actives and inconclusives.....	180
Figure 7.4 Representative top actives.....	182
Figure 7.5 Compounds triaged for undesirable functionalities	183
Figure 7.6 Clusters of disparate active structures.....	185
Figure 7.7 Cyclohexa-/cyclohepta-/thiophene cluster	187
Figure 7.8 Thienopyrimidinone cluster.	188
Figure 7.9 3-amino-N-phenylbenzene sulfonamide cluster	189
Figure 7.10 Evaluation of thiourea active after resynthesis	231

LIST OF TABLES

Table 3.1 Summaried homogenous protocol for PPTase assay	68
Table 3.2 Statistical analysis of reaction progress curves.	70
Table 3.3 Day-to-day variability of assay statistics for the FRET-based PPTase assay	72
Table 5.1 Table 1. HTS Actives.	138
Table 7.1 Antibiotic activity of LOPAC ¹²⁸⁰ actives against <i>B. subtilis</i> M489	172
Table 7.2 Summary of qHTS data collection and performance.	174
Table 7.3 Curve class description for qHTS data analysis.	178
Table 7.4 Curve class distribution of qHTS data.	179
Table 7.5 Analysis of primary actives selected for follow up.	191

ACKNOWLEDGEMENTS

My work in the Burkart laboratory took a sharp right turn during my third year in graduate school, and blossomed into a fruitful collaboration with the NIH Chemical Genomics Center. As such, these fine results would not have been possible without the diligence of my collaborators at this center. The research described in my dissertation is published or in preparation for submission and my collaborators are cited in both the text and acknowledgements of each chapter. Permission has been extended to include this material. My thanks to all of these collaborators. I'd like to acknowledge my colleagues with whom I share authorship. Michael Burkart has provided insightful discussions, research direction, and contributed to the writing of each of these manuscripts.

Chapter 2 is based on a literature review published in Current Opinion in Chemical Biology on which I was the primary author.

Chapter 3 is adapted from work published in Analytical Biochemistry (2009) on which I was the primary author.

Chapter 4 is based upon work published in FEBS Journal (2009) for which I was primary author. Brian S. Young contributed synthetic expertise.

Chapter 5 is based upon work published in Molecular Biosystems (2010) on which I share co-primary authorship with Adam Yasgar. This work was completed in collaboration with the NIH Chemical Genomics Center, and contributors to this manuscript from this institution include Ajit Jadhav, Anton Simeonov and James

Inglese who extended their talents and experience in compound library screening and analysis.

Chapter 6 is based on work in that is being prepared for submission to Chemical Communications and I am the primary author. Adam Yasgar, Anton Simeonov and Ajit Jadhav provided experimental data and analysis.

Chapter 7 is based on work work that is ongoing in collaboration with the NIH Chemical Genomics Center for which I am a primary author. Adam Yasgar, Anton Simeonov executed the high throughput screen, James Inglese and Christopher Austin provided facility oversight without which the work would not have been possible. David Maloney synthesized the compounds that were characterized as potential leads, and Ajit Jadhav extended his expertise in data handling to make useful sense of the 5.2 million data points generated by the robot.

This dissertation is dedicated to my family and friends, and they deserve an acknowledgement as well. Thank you for years of love and unbridled support. I can't wait to start my adventure in our Nations Capitol and hope to be your knowledgable tour guide soon!

VITA

EDUCATION

- Ph. D. in Chemistry **2010**
University of California, San Diego
Department of Chemistry & Biochemistry
Title: “Manipulating posttranslational modification in natural product biosynthesis”
Advisor: Michael D. Burkart
- M.S. in Chemistry **2007**
University of California, San Diego
Department of Chemistry & Biochemistry
Focus in Organic Chemistry
- B.S. in Cell Biology and Biochemistry **2004**
University of California, San Diego
Division of Biology

AWARDS AND FELLOWSHIPS

- University of California, San Diego **2010**
Industry Professional Development Scholarship
- Merck & Co. **2004**
Summer Undergraduate Research Fellow
- Howard Hughes Medical Institute **2003**
Summer Undergraduate Research Fellow

PROFESSIONAL EXPERIENCE

- Graduate Student, University of California, San Diego* **2004-2010**
Department of Chemistry & Biochemistry
Advisor: Michael Burkart

Research Experience: Developed and implemented a FRET assay to identify

inhibitors of phosphopantetheinyl transferase enzymes. Designed and established a high throughput assay for the enzyme; played a leading role on a team of researchers aligned to execute a high throughput screen in conjunction with the NIH Chemical Genomics Center (NCGC). Responsibilities included assisting in grant writing to fund the project, personnel management and execution of the collaboration, interacting directly with the group leader at NCGC.

Initiated a team project to investigate the putative macrocycle forming thioesterase from the mycolactone biosynthetic pathway of *Mycobacterium ulcerans*. Included cloning, expression and purification of the enzyme, and implementation of an enzymatic assay.

Undergraduate Researcher, University of California, San Diego **2002-2004**
Department of Chemistry & Biochemistry
Advisor: Michael D. Burkart

Research Experience: Participated on a team that developed the first generation system for adapting Coenzyme A analogues to fluorescently or affinity label proteins that undergo posttranslational phosphopantetheinylation. This work was published in Chemistry & Biology.

Led a project to identify the source of *holo*-acyl carrier protein phosphodiesterase enzymatic activity in *Escherichia coli*. Activities included development of a fluorescence-based assay and execution of traditional protein fractionation techniques to purify the enzymatic activity.

TECHNICAL EXPERIENCE

Molecular biology: Genomic DNA isolation, polymerase chain reaction, expression construct design and assembly, DNA sequence analysis, restriction mapping, site directed mutagenesis, and bioinformatic analysis.

Biochemistry: enzyme assay development, protein expression, affinity purification, native protein purification via traditional chromatography, chromatography method development including ion exchange, size exclusion, hydrophobic interaction, and reverse phase techniques, polyacrylamide gel electrophoresis and western blot.

Synthetic chemistry: peptide synthesis, fluorescent probe design, synthesis and spectroscopic characterization (¹H-NMR, ¹³C-NMR, gCOSY and related 2D-NMR experiments, IR, UV-Vis, MS).

Tissue culture: adherent cell culture, hybridoma cell culture, cell line maintenance, antibody production and purification.

POSTERS & PRESENTATIONS

Foley, T.L.; Yasgar, A.; Jadhav, A., Maloney, D.; Inglese, J.; Austin, C.; Young, B.S.; Simeonov, A.; and Burkart, M.D. *Manipulating posttranslational modification in natural product biosynthesis: discovering inhibitors of phosphopantetheinyl transferase.* 6th Annual NIH Graduate Student Research Festival. Bethesda, MD. November, 2009.

Foley, T.L.; Young, B.S.; Burkart, M.D. *Synthesis and evaluation of anthranilate 4H-oxazol-5-one compounds to inhibit phosphopantetheinyl transferase involved in secondary metabolism.* 233rd National Meeting of the American Chemical Society. Chicago, IL. March, 2006.

PUBLICATIONS

Yasgar, A.*; **Foley, T.L.*;** Jadhav, A.; Inglese, J.; Simeonov, A.; Burkart, M.D. “A strategy to discover inhibitors of *Bacillus subtilis* surfactin-type phosphopantetheinyl transferase.” Molecular Biosystems *co-first author 2010 (*in press*).

Foley, T.L.; Young, B.S.; Burkart, M.D. “Phosphopantetheinyl transferase inhibitors and secondary metabolism.” FEBS Journal 2009 Volume 276 Issue 23, Pages 7134 – 7145.

Meier, J.L.; Niessen, S.; Hoover, H.; **Foley, T.L.;** Cravatt, B.F.; Burkart, M.D. *An orthogonal active site identification system (OASIS) for proteomic profiling of natural product biosynthesis.* ACS Chemical Biology 2009 Nov 20;4(11):948-57.

Lear, M.J.; Simon, O.; **Foley, T.L.;** Burkart, M.D.; Baiga, T.J.; Noel, J.P.; DiPasquale, A.J.; Rheingold, A.L.; La Clair, J.J. *Laetirobin from the parasitic growth of *Laetiporus sulphureus* on *Robinia pseudoacacia*.* Journal of Natural Products 2009 Nov;72(11):1980-7

Foley, T.L.; Burkart, M.D. “A homogenous fluorescence resonance energy transfer screen for phosphopantetheinyl transferase.” Analytical Biochemistry 2009 Nov; 394(1) 39-47.

Meier, J.L.; Barrows-Yano, T.; **Foley, T.L.;** Wilke C.L.; Burkart, M.D. *The unusual macrocycle forming thioesterase of mycolactone.* Molecular Biosystems 2008 Jun; 4(6) 663-71.

Foley, T.L.; Burkart, M.D. *Site-specific protein modification: advances and applications.* Current Opinion in Chemical Biology 2007 Feb; 11(1) 12-9.

La Clair J.J.; **Foley, T.L.;** Schegg, T.R.; Regan, C.M.; Burkart, M.D. *Manipulation of carrier proteins in antibiotic biosynthesis.* Chemistry & Biology 2004 Feb; 11(2) 195-201.

MANUSCRIPTS IN PREPARATION

Foley, T.L.; Yasgar, A.; Garcia, C.J.; Jadhav, A.; Simeonov, A; Burkart, M.D. *Economical preparation of reporters to support chemical probe development.* Chemical Communications (submitted).

Foley, T.L.; Wight, W.; Burkart, M.D. *A high sample density apparatus for protein electrophoresis* (manuscript in preparation).

Foley, T.L.; Kosa, N., Burkart, M.D. *On the mechanism of phosphopantetheinyl transferase* (manuscript in preparation).

Kosa, N.*; **Foley, T.L.*;** Burkart, M.D. *A broadly applicable fluorescence polarization screen for phosphopantetheinyl transferase* (manuscript in preparation).

(*) These authors contributed equally to this work

ABSTRACT OF THE DISSERTATION

Manipulating Posttranslational Modification in Natural Product Biosynthesis

by

Timothy Leyden Foley

Doctor of Philosophy in Chemistry

University of California, San Diego, 2010

Professor Michael D. Burkart, Chair

Fatty acids, polyketides and nonribosomal peptides are three classes of natural products that play critical roles in human health, disease and therapy. Investigations that lead to a broader understanding of their biosynthesis may one day allow scientists to engineer the biomanufacture of novel compounds with tailored chemistries and biological activities. A unifying characteristic between these classes of compounds is the posttranslational modification of their synthase enzymes with a 4'-phosphopantetheinyl (4'-PP) arm from a coenzyme A (CoA) donor, installed by phosphopantetheinyl transferase (PPTase).

We have previously described a method to chemoenzymatically install modified 4'-PP arms to heterologously expressed synthase enzymes through the use of CoA analogues that have been alkylated at the thiol terminus with fluorescent and affinity probes. We have since sought to extend this technique to the isolation of synthases from producer organisms, but this application was complicated by the efficiency of endogenous modification. This dissertation focuses on evaluating the use of PPTase inhibitors to enable the extension of our technique to these organisms.

Chapter 1 provides an introduction to this work, and Chapter 2 reviews the current literature regarding the site-specific labeling of proteins. Chapter 3 details the development of a homogenous resonance energy transfer assay for PPTase. Chapter 4 confirms endogenous phosphopantetheinylation as the source of complication, and evaluates known PPTase inhibitor architectures for this application; revealing the limited spectrum of activity of these compounds.

As such, this dissertation also reports efforts to identify a new inhibitor scaffolds by the screening of large chemical libraries. Studies toward this include Chapter 5, describing optimization of the assay process described in Chapter 3 for this purpose. Chapter 6 details the preparation of reporters to support this large scale robotic screen. Chapter 7 applies the results of Chapters 5 and 6 through an automated high throughput screen of over 311,000 compounds, and details efforts to nominate a lead structure for further optimization to develop a PPTase chemical probe.

Chapter 1
INTRODUCTION

NATURAL PRODUCTS

For thousands of years, Man has looked to Nature for remedies to cure disease and alleviate human suffering. Many of the drugs we take today to treat ailments ranging from the headache and common cold, to life threatening cancer, bacterial and parasitic infection, to compounds enabling feats of modern medicine including coronary bypass and tissue transplant, are based on chemical structures produced by Nature. (Kingston and Newman, 2005, Newman and Cragg, 2004b, Newman and Cragg, 2004a, Newman et al., 2003, Newman et al., 2002, Cragg and Newman, 2001, Cragg et al., 1997) It is fascination with the ability of Nature to provide compounds of intriguing structure and exquisite biological activity that natural product chemists strive to further the work of ancient shaman, refining known treatments for human disease and discovering new leads for therapeutic development. (James, 1999, Anhauser, 2003, Newman and Cragg, 2007)

As natural product chemists, we seek not only to identify new compounds with desired biological activity, but also to understand the mechanisms of their biosynthesis, with the goal that obtaining a broad knowledge base that may eventually lead to the future engineering of advanced non-natural intermediates for further chemical elaboration, as well as the methods to engineer the biomanufacture of designed structures (Cane et al., 1998, Strohl, 2001, Du et al., 2001). We can apply the central dogma of biology, Figure 1.1, to resolve the molecular details involved with the assembly of these molecules. It is not a far reach of reason to consider this principle when asking where do these modern marvels come from?



Figure 1.1 The central dogma of information flow in biological systems

DNA is encoded in an organism's genome, and is transcribed into functional (ribosomal and translational) and coding (messenger) RNAs by the transcriptional machinery. The coding sequences (mRNA) are then translated by the ribosome into proteins. These proteins are the primary source of catalytic and functional activities in living systems. Extension of this information flow allows one to reason that if a function or activity can be detected (a phenotype), then the genome encodes a locus responsible for the observation.

If the compounds are yielded from a biological system, then there must be enzymes that catalyze the chemical transformations necessary for their assembly. These enzymes are proteins, and must be assembled by the ribosome through decoding of messenger RNA (mRNA). This mRNA is the product of the transcriptional machinery responsible for preparing transient copies of genetic information for application. And thus, the information that encodes for the enzymes responsible for manufacturing a natural product is genetically based and archived within the DNA of the producer organism.

With the advent of modern molecular biology, this rationale has been applied to the molecular cloning the enzymes that constitute an entire biosynthetic pathway at the DNA level, and pathway reconstitution in heterologous hosts (Nielsen, 1998, Hutchinson, 1998). This capacity, converting a nonproducer to producer organism by transformation with isolated foreign DNA, has academic and industrial importance; serving to enhance our understanding of these pathways at the genetic and biochemical levels, as well to provide access to desired compounds from engineered organisms when the natural host proves recalcitrant to traditional strain improvement methods.(Kao et al., 1994)

Natural products can be grouped into five classes of compounds: terpenes, alkaloids, glycosides, polyketides and nonribosomal peptides. This thesis will focus on the latter two classes, detailing efforts to isolate and manipulate representative enzyme complexes that produce such molecules. Some exemplary chemical structures that are produced from these pathways are shown in Figure 1.2. Their central role as the topic of this work warrants, a further discussion of the general routes to their biosynthesis

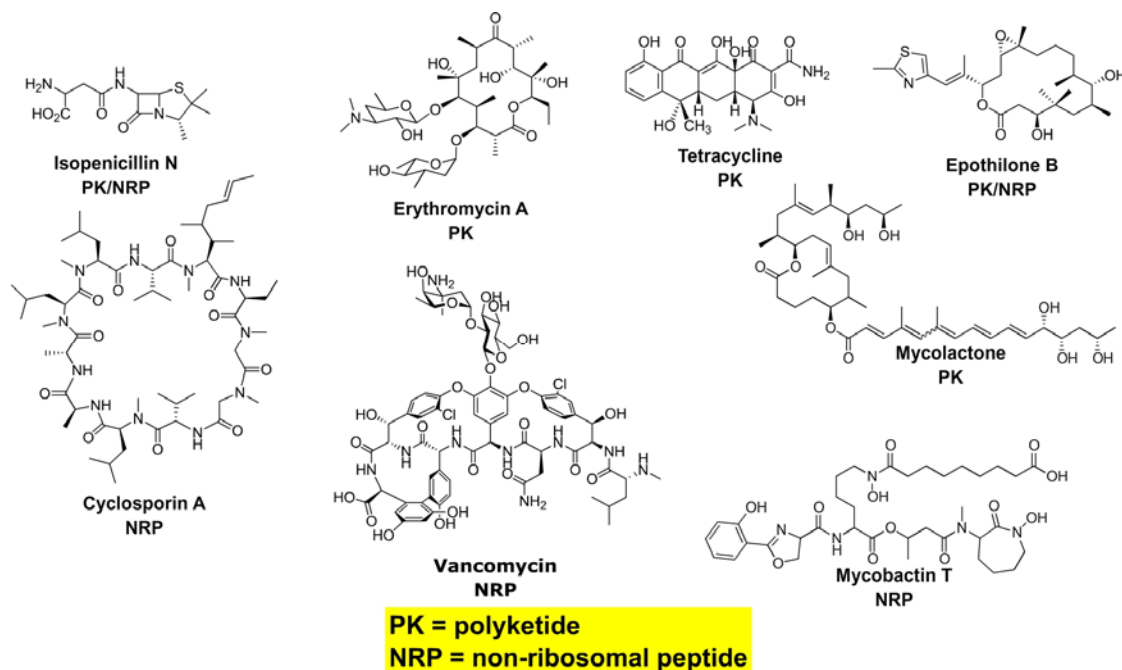


Figure 1.2 Representative polyketide and nonribosomal peptide natural products.

Polyketides (PK) and nonribosomal peptides (NRP) are two classes of natural products that are used to combat all facets of human disease. Shown are compounds from these classes that are currently used in the clinic including the antibiotics isopenicillin N, erythromycin A, tetracycline and vancomycin; potential new anticancer agent epothilone B; and the immunosuppressant cyclosporin A (to prevent allograft rejection). A number of virulence factors produced by bacterial pathogens belong to these compound classes. Three such representatives of these virulence factors include the mycolic acids and Mycobactins, produced by *Mycobacterium tuberculosis* and are essential for pathogenicity, as well as mycolactone, the causative agent responsible for the necrotic nature of Buruli's ulcer.

POLYKETIDES AND THEIR BIOSYNTHESIS

Polyketides are a class of natural products that exhibit a broad spectrum of biological activities, and are a rich source of many treatments and therapies in use today. (Newman et al., 2003, Cragg et al., 1997) The compounds are produced by the polymerization of acetate and propionate units in a manner very much paralleled in primary metabolism by fatty acid production. (Walsh, 2003) Differing between these, however, are the complexities of the enzyme systems. Fatty Acid Synthase (FAS) is an iterative enzyme complex where the catalytic core contains one set of each enzymatic domain that function multiple times to assemble the product (palmitic acid) from an acetate starting material and eight rounds of polymerization and reduction. While polyketides can be assembled by a similar iterative fashion of a minimal enzyme complex (i.e. iterative type I, type-II and type-III PKSs), a much greater level of diversity may be present. Rather than utilizing single catalytic domains that function multiple times to assemble a single product, the modular PKS (type-I PKS) is best described as a “molecular assembly line” and house a unique enzymatic domain for every step that is required for product formation.

To further discuss these assembly lines, a schematic of the biosynthetic machinery responsible for the assembly of 6-deoxyerythronolide, the aglycone core of erythromycin, is given in Figure 1.3. This pathway is composed of three gene products, DEBS1, DEBS2 and DEBS3; each being discrete polypeptides that house multiple enzymatic domains. Each of these polypeptides can be divided into discrete repeating units, referred to as

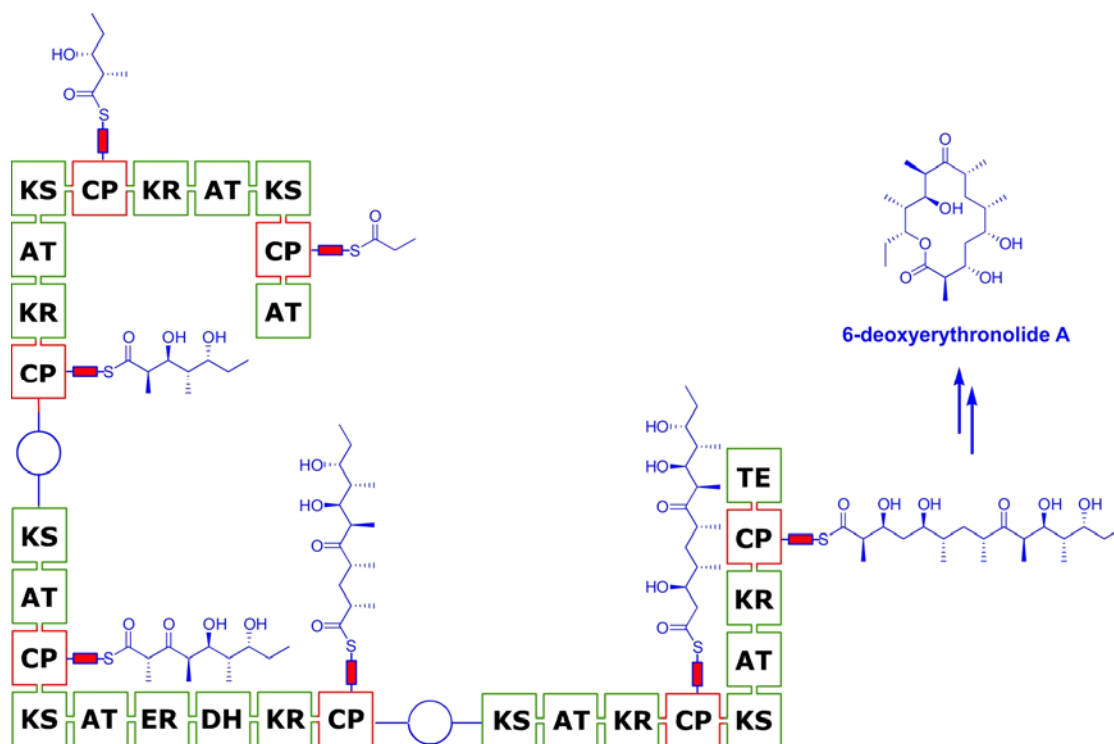


Figure 1.3 6-Deoxyerythronolide A biosynthetic pathway

Fatty acid, polyketide and nonribosomal peptides are assembled by multienzyme complexes that polymerize and elaborate small carboxylic and amino acid monomers to form the final product. Unifying to the biosynthetic pathways is the tethering of the nascent chain to the synthases through a thioester linkage, within a carrier protein domain (CP). This bond is not appending the B-sulfhydryl group of a cysteine residue, but a 4'-phosphopantetheinyl arm. Depicted above is a lego diagram of the 6-deoxyerythronolide A megasynthase with fully elaborated intermediates. This complex is comprised of three proteins of approximately 300 kDa each that form a "molecular assembly line" to produce the aglycone core of erythromycin.

modules, that are responsible for incorporating a single 2-carbon unit of the final product. The general arrangement of enzymatic domains within a module is ketosynthase (KS) , acyl transferase (AT), dehydratase (DH), enoyl reductase (ER), ketoreductase (KR) and acyl carrier protein (CP); and are tethered in this orientation by the peptide backbone. The KS, AT and CP domains of module are essential, and the presence or absence of the accessory domains (KR, DH and ER) determine the reduction level of the module's product, as well as stereochemistry of resultant (hydroxyl) chiral centers that arrive from incomplete hydrogenation of the growing ketide chain. It is noteworthy that, of the required domains, the CP region does not catalyse a chemical reaction, but serves as an anchoring point to tether the nascent polymer to the enzyme as it is extended and elaborated. Therefore, these domains likely serve a purpose to enhance production rates by substrate channeling through preventing diffusion of elaborate intermediates away from the complex. (Walsh, 2003)

NONRIBOSOMAL PEPTIDES AND THEIR BIOSYNTHESIS

Nonribosomal Peptides (NRP) are a class of secondary metabolites yielded in the laboratory by the fermentation of bacteria and fungi, and similar to the polyketides, possess a broad array of activities.(Newman et al., 2003, Cragg et al., 1997) These compounds are assembled by the polymerization of amino acids. As their name suggests, NRPs are produced through mechanisms independent of the ribosomal system, and are neither encoded directly in the genome nor dependent on messenger RNA for their assembly. Thus, the chemical structures of these molecules are not limited to L-enantiomers or the 20 proteogenic amino acids which are hallmarks of

this class; and they can contain alternative connectivities about sidechain functional groups, a functional subclass that are denoted as depsipeptides. (Walsh, 2003)

The biochemical machineries that manufacture these compounds, the nonribosomal peptide synthases (NRPS) is similar in logic to the type-I PKS systems, but bear different mechanisms of activation and polymerization that warrant further discussion. Analogous to the Type-I PKS systems is the repeating linear arrangements of active sites in the primary structure of the polyenzyme, which can be divided again into modules that contain all of the enzymatic domains responsible for the incorporation of one monomer unit into the polymer. A minimalized module from an NRPS contains three regions, the adenylation domain (AT), condensation domain (C) and peptidyl carrier protein (PCP) or thiolation domain (T). The former domains (AT and C) are catalytic, while the latter (PCP) domain serves an analogous purpose to the ACP domain of PKS enzymes, acting as a tether to hold and sequester the nascent polymer as it is assembled. (Walsh, 2003) As shown in Figure 1.4, these modules are arranged in the primary sequence in the order AT-PCP-C, and may contain accessory catalytic domains that include the epimerization domain (E) responsible for the interconversion of L- and D- arrangements about the α -carbon of the bound amino acid, and the cyclization domain (Cy) that catalyzes intramolecular formation of oxazolidine and thiazolidine rings from serine, threonine and cysteine residues, respectively, after their incorporation into the growing product. Release of the final product is accomplished canonically by a thioesterase domain (TE) fused to the C-terminus of the final PCP-domain.

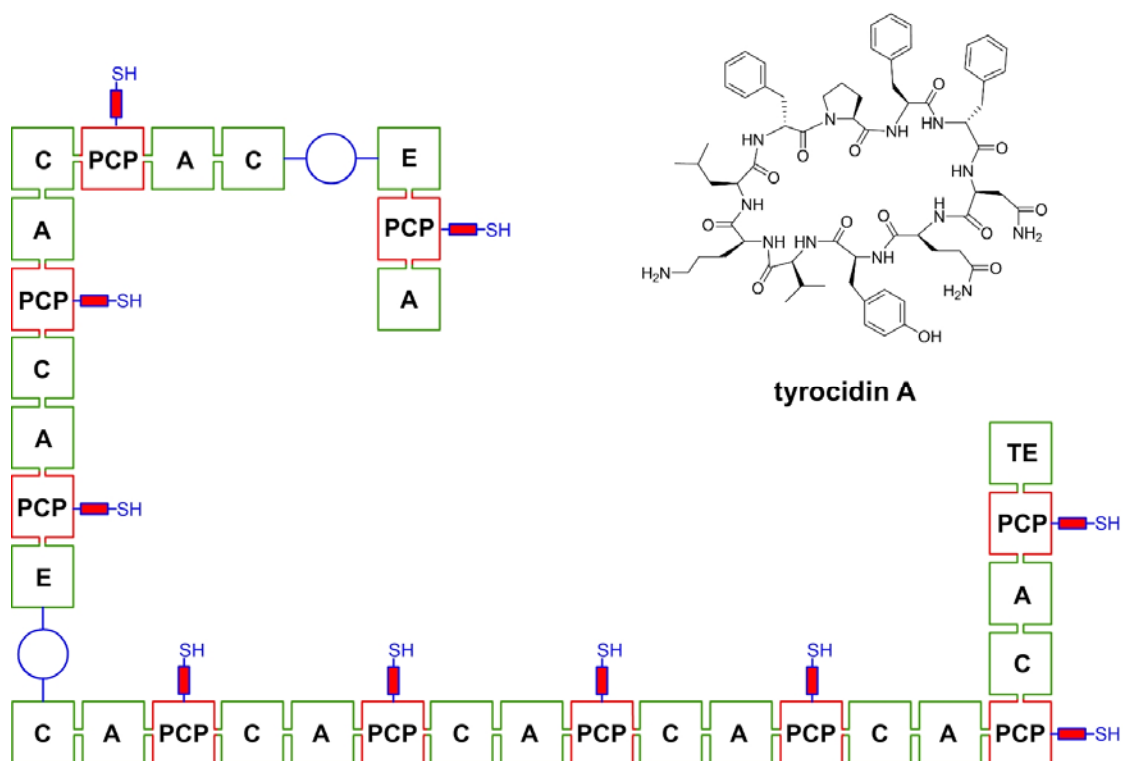


Figure 1.4 Tyrocidine A Biosynthetic Pathway.

Tyrocidine is biosynthesized by three proteins TycA, TycB and TycC. These proteins are represented here in lego diagram, with each cube representing an individual catalytic domain. The nascent chain of tyrocidine is bound to the enzyme through a thioester bond to the thiol attached to each PCP domain.

THIOTEMPLATE LOGIC

Since PK and NRP compounds are not produced from a genetic code, the identity of monomeric units incorporated into the product is tied to the genes of a producer organism indirectly, through the isomeric and functional specificity of the synthase enzymatic domains. The primary selectivity for monomers is accomplished by the AT and A domains, respectively, who are responsible for loading the monomers onto the carrier protein (CP) domains of their respective modules. These monomers are held on the CP domains through a thioester bond, and this, coupled to the modular nature of PK and NRP systems has led to the description of the rationale for the biosynthesis of these compounds as the thiotemplate logic of biosynthesis (Cane et al., 1998, Walsh, 2003). The lego-like arrangement of modules in these systems has not gone overlooked, as the field of metabolic engineering has strived to harness this similarity to an assembly line to design and produce unique polyenzymes containing a linear arrangement of modules with specificity for the monomers that in theory would produce a novel metabolite of known chemical structure.(Hutchinson and McDaniel, 2001, Hutchinson, 1994, Hoffmann, 2000) Unfortunately, these efforts have been stricken with low yields and the undesired production of shunt metabolites, and revealed that the design and assembly of a functional metabolic pathway requires multiple levels of refinement. (Hutchinson, 1998, Kao et al., 1994, Bedford et al., 1995, Kim et al., 1995, Kealey et al., 1998, Pfeifer and Khosla, 2001) Protein-protein interaction at the inter- and intramodular level has been hypothesized as the complicating road block, resulting in a lack of cooperativity in the pathway and

vanishingly small yield of the desired product. (Meier and Burkart, 2009a, Meier and Burkart, 2009b, Mercer and Burkart, 2007, Worthington et al., 2008)

These efforts would be aided by a further understanding of the natural enzyme systems at the biochemical level, but high yield of PKS and NRPS proteins by recombinant production is obscured by an incompatibility of the genes, both their sheer size and codon bias, with *Escherichia coli* host systems.(Pfeifer and Khosla, 2001) Further complicating is the relative low expression levels in the endogenous producer, a problem that has still not been resolved in the *Streptomyces lividans* host system.(Anne and Van Mellaert, 1993, Binnie et al., 1989, Payne et al., 1990, Sathyamoorthy et al., 1996, Zirkle et al., 2004) Given this low abundance of starting material, these studies would be further aided by the development of a purification technique that would leverage the chemistries inherent to PKS/NRPS enzymes; along with the multiplicity which each enzymatic domain exists within a modular enzyme complex.

THIOESTER INTERMEDIATES

In examining the chemistries inherent to PKS and NRPS pathways, the CP domain stands alone as the sole unifying domain that appears with multiplicity in both classes. This small domain serves as a tethering point for the nascent polymer as it is extended and elaborated, but serves no explicit catalysis. Its role is analogous to Coenzyme A (CoA), acting as a carrier for activated ester intermediates, providing a handle for molecular recognition events and enhanced portability between different enzyme active sites. Additionally similar to CoA, the CP domain holds the activated

monomers and intermediates in a thioester bond that provides for polymerization reactions by acting as a leaving group upon nucleophilic attack, as well as acidifying the protons α - to the acyl-group carbonyl, allowing for a number of chemical reactions to occur, including enhanced rates of decarboxylation of loaded malonic acids in PKSs and epimerization of loaded amino acids in NRPS pathways. (Walsh, 2003)

POSTTRANSLATIONAL MODIFICATION OF CP DOMAINS

Interestingly, the thioester bond that binds the monomers and intermediates to CP domains is not about the β -sulfhydryl group of a cysteine residue. This thiol functional group is installed to the proteins posttranslationally, and is embedded in a 4'-phosphopantetheinyl (4'-PP) group. The 4'-PP group is the functional "arm" of CoA that allows for translocation of acyl groups within active site of CoA utilizing enzymes, and it is an interesting and yet not completely understood event of evolutionary convergence. (Mercer and Burkart, 2007)

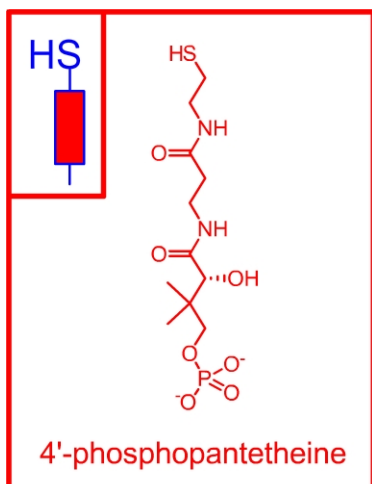


Figure 1.5 Thioester intermediates in PK/NRP biosynthesis

As fatty acids, polyketides and nonribosomal peptides are produced, they are tethered to CP domains of the synthases through a thioester linkage. This linkage is not about a β -sulfhydryl group of a cysteine residue, but a 4'-phosphopantetheine arm.

PHOSPHOPANTETHEINYL TRANSFERASE ENZYMES

This posttranslational modification to CP domains is performed by a class of structurally distinct and evolutionarily conserved enzymes: the phosphopantetheinyl transferases (PPTases). PPTase enzymes (Enzyme Code 2.8.7.x) bind magnesium, and use the translated *apo*-CP domain and CoA as cosubstrates to produce the posttranslationally modified *holo*-CP domain and 5'-monophosphoadenosine-3'phosphate (PAP) as reaction products (Figure 1.6). (Lambalot et al., 1996b)

Crystallographic studies have revealed a novel protein fold, and thus PPTases constitute a new enzyme superfamily.(Parris et al., 2000, Reuter et al., 1999) Early biochemical data suggested an ordered bi-bi mechanism for this enzyme, with the CP domain binding first.(McAllister et al., 2000) Crystallographic analysis of a nonproductive ternary complex containing Ca^{++} in place of the catalytic Mg^{++} , however, revealed a structure with the CoA sandwiched between the enzyme and CP substrate, strongly suggesting a reversed order of binding. (Parris et al., 2000, Bunkoczi et al., 2007)

The PPTase enzymes can be grouped into three classes based upon primary sequence.(Lambalot et al., 1996b) The first two classes, the AcpS-Type and Sfp-Type PPTases, are free standing soluble enzymes, while the third denotation, the Fungal FAS PPTases, are integrated into the megasynthase polypeptide. This third classification of PPTase bears strong homology to the Sfp-Type PPTases, and is N-terminally fused to the fungal FAS at it's C-terminus.(Crawford et al., 2008) Congeners of this third class are exceedingly rare, with the only known natural product pathway containing such a fusion having recently been described in an

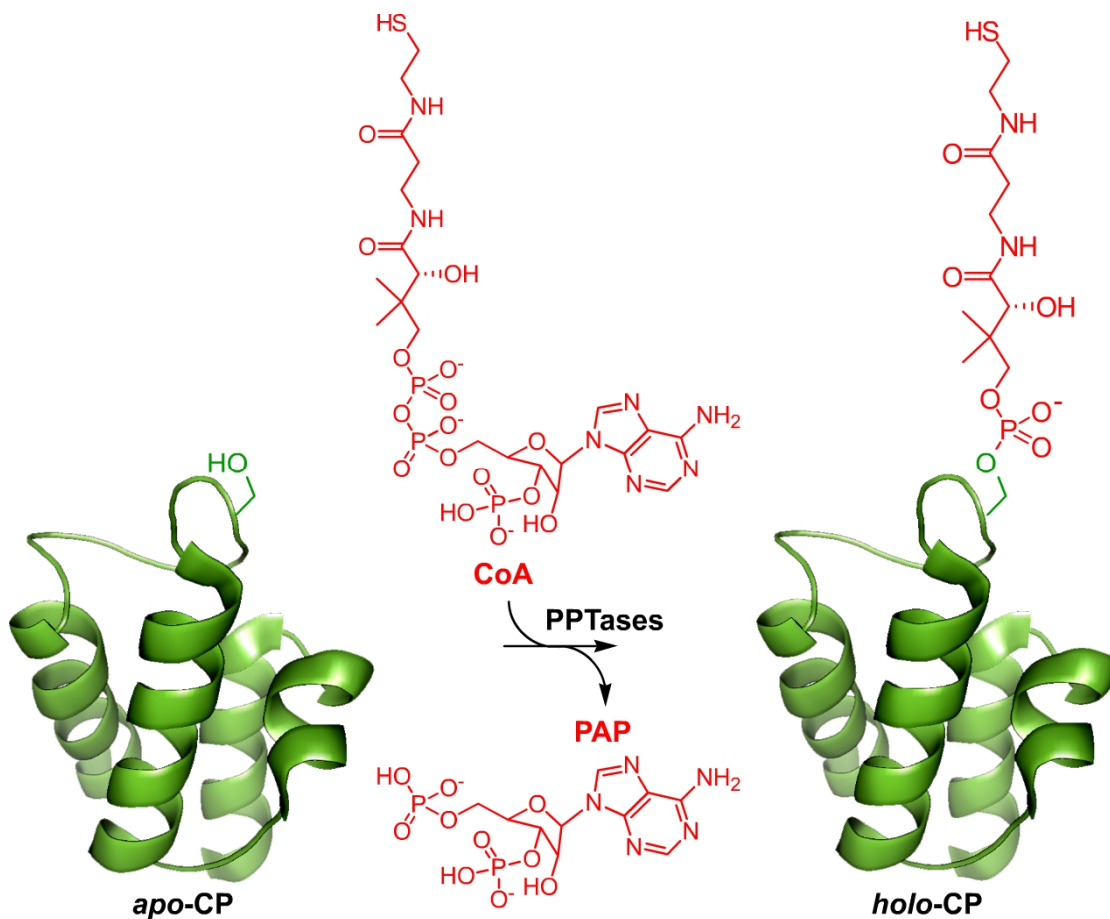


Figure 1.6 Posttranslational modification of carrier protein domains

A unifying characteristic of the biosynthesis of PK and NRP compounds is the tethering of the nascent polymer to carrier protein domains (CPs) of the synthase via thioester linkage through a 4'-phosphopantetheinyl arm that is posttranslationally installed from coenzyme A (CoA) to the apo-CP by a phosphopantetheinyl transferase (PPTase). This modification creates the holo-CP and 3'-phosphoadenosyl-5'-phosphate (PAP), rendering the synthase catalytically active.

enediyne biosynthetic pathway. (Horsman et al., 2009) For all purposes, discussions of PPTase enzymes in this dissertation will discreetly pertain to the AcpS- and Sfp-type classes.

BIOMEDICAL RELEVANCE

The biochemistry of PPTase enzymes was first unveiled by Vagelos *et al.* during rigorous investigations seeking to characterize the FAS-specific cofactor to which nascent fatty acids were tethered during production in *E. coli* (ACP). (Elovson and Vagelos, 1968, Powell et al., 1969, Prescott et al., 1969) Some 30 years transgressed before the subject of phosphopantetheinyl transfer reentered the literature, after revolutions in molecular biology and DNA sequencing enabled studies of heterologous metabolic pathway reconstitution, and it was the diligent work of Lambalot and Walsh that identified the *acpS* locus of *E. coli* using a reverse genetics approach. (Lambalot and Walsh, 1995) The Locus they arrived at was formerly annotated as *dpj* (downstream of *pdxJ* involved in pyridoxal phosphate anabolism). (Lam et al., 1992a, Takiff et al., 1992) Subsequently, the same function was mapped, based on sequence homology to *acpS*, to the *sfp* locus of *Bacillus subtilis*. (Quadri et al., 1998a, Lambalot et al., 1996b) a gene whose product had been previously linked to the regulation of secondary metabolite production, (Nakano et al., 1992, Nakano et al., 1988, Nakano and Zuber, 1989, Nakano and Zuber, 1990) but had been presumed to serve at the transcriptional level.

Given that the *dpj* locus had previously been characterized as an essential gene to *E. coli*, (Takiff et al., 1992, Lam et al., 1992b) observed by polar effects elicited on

the locus by interruption of the *pdxJ* reading frame, the annotation of a biochemical activity to the gene product along with the absence of a homologue in human, validated the enzyme as a target for inhibitor development with the goal of identifying antibacterial compounds with a new mode of action.(Chu et al., 2003a, Gilbert et al., 2004, Joseph-McCarthy et al., 2005b) At the initiation of these dissertation studies, two groups had reported compounds with antagonistic activity against AcpS, (Chu et al., 2003a, Gilbert et al., 2004, Joseph-McCarthy et al., 2005b) and these are discussed in detail in Chapter 4.

PK AND NRP COMPOUNDS AS VIRULENCE FACTORS

We have harnessed PK and NRP compounds for centuries for the purpose of treating human conditions, but this is not the original purpose in Nature. Bacteria and fungi manufacture these compounds as chemical warfare agents,(Walsh, 2003) weapons in the battle for survival and competition to colonize food sources. A number of these compounds have also been linked as chemical agents that impart infectivity to these groups of organisms, rendering them pathogenic to animals and humans. (Chalut et al., 2006b) (Quadri et al., 1998b) (Reed et al., 2004) (Portevin et al., 2004, Bhatt et al., 2007) As we gain further understanding of host-pathogen interaction, and identify virulence factors (VFs) whose ablation renders the organism unviable in disease setting, we find new avenues to target for therapeutic development. This has not gone unnoticed, and numerous investigations have begun to specifically target PK and NRP VF production to evaluate the viability of this route for medicinal application. The regulatory role of PPTase in these pathways has received a particular amount of

attention, and groups are interested in identifying and evaluating PPTase inhibitors to treat tuberculosis, aspergillosis, fungal infection, cancer and obesity. (Chalut et al., 2006b, Strickland et al., 2009, Horbach et al., 2009, Guo and Bhattacharjee, 2004, Oberegger et al., 2003, Bunkoczi et al., 2007)

DEVELOPMENT OF A CP-DOMAIN ISOLATION TECHNIQUE

The work in this dissertation is an extension of the research I performed under direction of Michael D. Burkart while an undergraduate in the Division of Biology at the University of California, San Diego. This work sought to develop a technique to selectively isolate PKS and NRPS proteins based on the specificity of phosphopantetheinylation. (La Clair et al., 2004b) This work was based on two observations: First, Sfp, the canonical representative of the Sfp-Type PPTases, had been demonstrated to possess a broad specificity with regard to the CP substrate, and will install 4'-PP groups to both PKS and NRPS enzymes. Second, it had been shown that Sfp, and AcpS for that matter, possess a high tolerance for appendages to the thiol of CoA, and will transfer an entire acyl-4'-PP group onto *apo*-CP domains (Figure 1.7). This latter observation is physiologically relevant in most organisms, as the intracellular CoA pool is present primarily as various acyl-CoAs, and very low relative concentrations of free thiol CoA (CoA-SH). While it seems that this would be problematic for PKS/NRPS enzymes, since reactive monomers need to be loaded successively to achieve flux through the pathway, an accessory stand alone

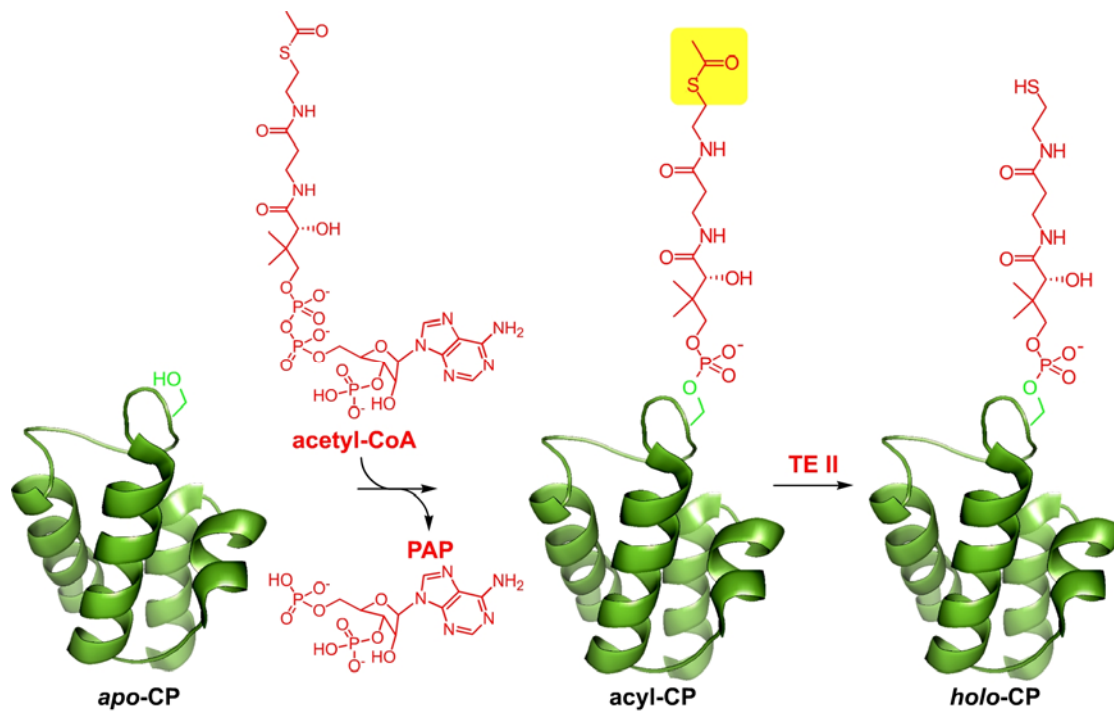


Figure 1.7 Physiological transfer of acyl-phosphopantetheinyl arms by PPTase

In most organisms, CoA does not exist in the free thiol form. Rather, activated forms (acetyl-CoA, malonyl-CoA) are more prevalent. Many PPTases demonstrate promiscuity for CoA analogs, and an external thioesterase (TE II) enzyme hydrolyzes these thioesters subsequently.

thioesterase (Type-II TE) (Steller et al., 2004) is associated with most secondary metabolite gene clusters that serve the purpose of hydrolyzing misprimed and decarboxylated acyl groups from megasynthase CP domains (Figure 1.7), generating the catalytically relevant *holo*-CP containing the free acceptor thiol.(Steller et al., 2004)

We sought to leverage these two characteristics, and ask if the appendage to the thiol of CoA was not an acyl- group, but a reporter molecule, would the enzyme catalyse transfer to apo-CP domains? If viable, this would allow for the chemoenzymatic installation of diverse functionality to CP-containing proteins.

We chose to conjugate the reporters to CoA using malimide chemistry (Figure 1.8), since the soft Michael acceptor provides facile access to the thioether derivatives after reaction, and this bond would provide a stable linkage that would not be susceptible to hydrolysis or scattering (nonspecific amidation of amino-groups) one might expect by using the native thioester configuration. We have termed this state of posttranslational modification, where the prosthetic group thiol is irreversibly alkylated with a reporter, to be the *crypto*-form of the proteins, since the protein is neither *apo*- nor biochemically active. We chose to investigate a collection of fluorescent and affinity reporters that would allow us to visualize labeled proteins after separation by SDS-PAGE (with a fluorescent reporter) or detect them indirectly via far-western blot using the biotin derivative in conjunction with an streptavidin-alkaline phosphatase (streptavidin-AP) conjugate. Some exemplary data of this work is shown in Figure 1.9 where three type-II ACP domains were selectively labeled and visualized by transillumination with ultraviolet light after separation by SDS-PAGE.

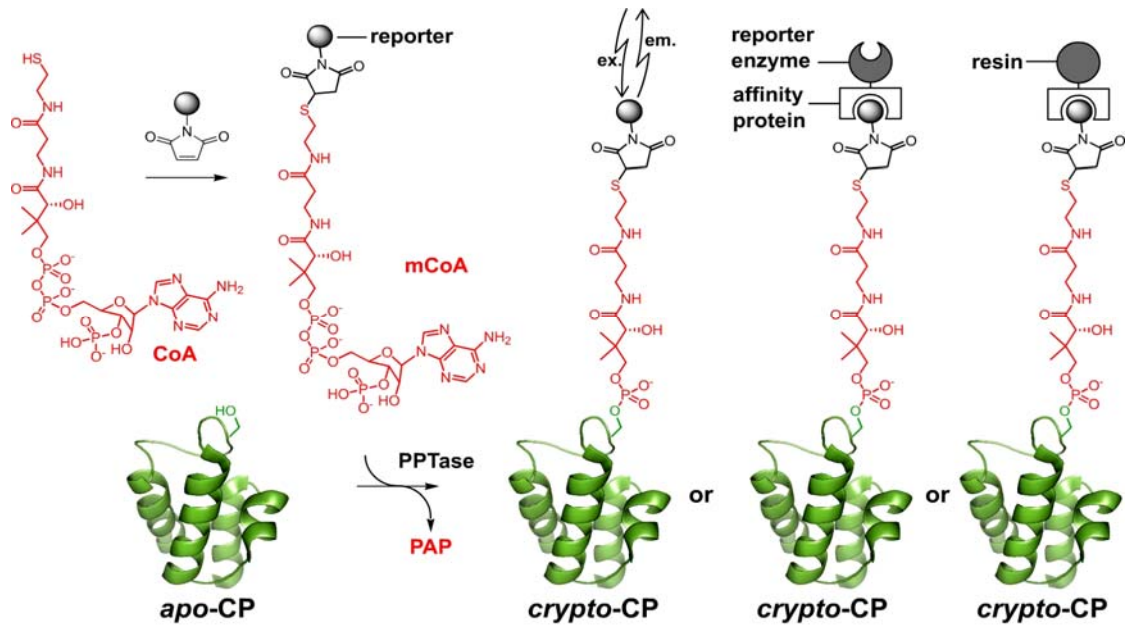


Figure 1.8 Functional manipulation of CP domains with CoA analogues

A PPTase is used to catalyze the labeling of apo-CP with mCoA to yield 4'-phosphopantetheine derivatives crypto-CP and PAP. Fluorescent reporters can be used to visualize CPs at specific excitation and emission wavelengths. Alternatively, conventional affinity labels (i.e., biotin) can be used to mark carrier proteins for Western blot or for purification by affinity chromatography with resin-bound affinity proteins.

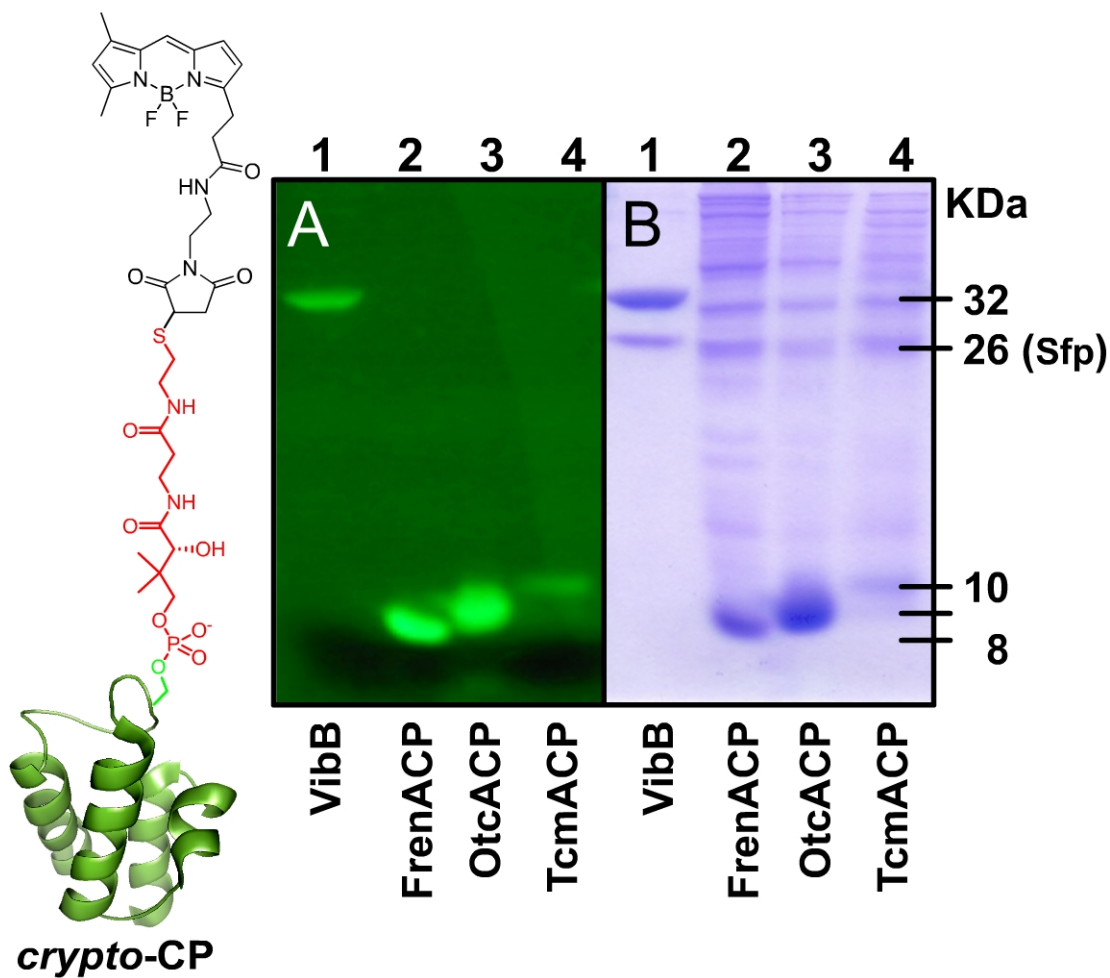


Figure 1.9 Fluorescent labeling of CP domains

Fluorescent visualization of CPs from *E. coli* crude cell lysate after incubation with BODIPY-tagged CoA and Sfp. A.) VibB (lane 1) is a small NRP CP domain. FrenACP (lane 2), OtcACP (lane 3), and TcmACP (lane 4) are three type II PK CP domains. The fluorescent band corresponding to VibB was excised from the membrane and subjected to N-terminal amino acid sequencing by Edman degradation. The first 10 amino acids of the returned sequence, "maipkiasyp", mapped to VibB when searched with BLAST against 1.4 million sequences in GenBank B. B.) Coomassie stain of the same gel.

It is also noteworthy that we also utilized the biotin reporter as a handle for selective purification, with the aid of streptavidin immobilized on agarose beads, and this is further detailed in Chapter 4.

TARGET ISOLATION PROCEDURE AND COMPLICATION

With the technique validated, we turned our attention to the labeling and isolation of Type-I PKS and NRPS enzymes from the crude cellular extracts of producer organisms, as outlined in Figure 1.10. Briefly, we sought to prepare protein extracts from these organisms at timepoints in culture when metabolite production could be verified to be occurring, and modify the proteins to their *crypto*-form to enable their detection and isolation. As described in the initial disclosure, we were intermittently able to detect what is hypothesized to be the DEBS enzymes from *Saccharopolyspora erythraea*, but in these contexts we at no time observed the robust labeling that had become routine when heterologously expressed proteins were used as substrates.

Given that we could observe the presence of these proteins by total protein staining (data not shown), and the robust nature of phosphopantetheinylating reaction with mCoA derivatives, we presumed the source of our complication to be the efficiency of modification performed by PPTases expressed endogenously by the producer organisms. Work detailing the confirmation of this is presented in Chapter 4.

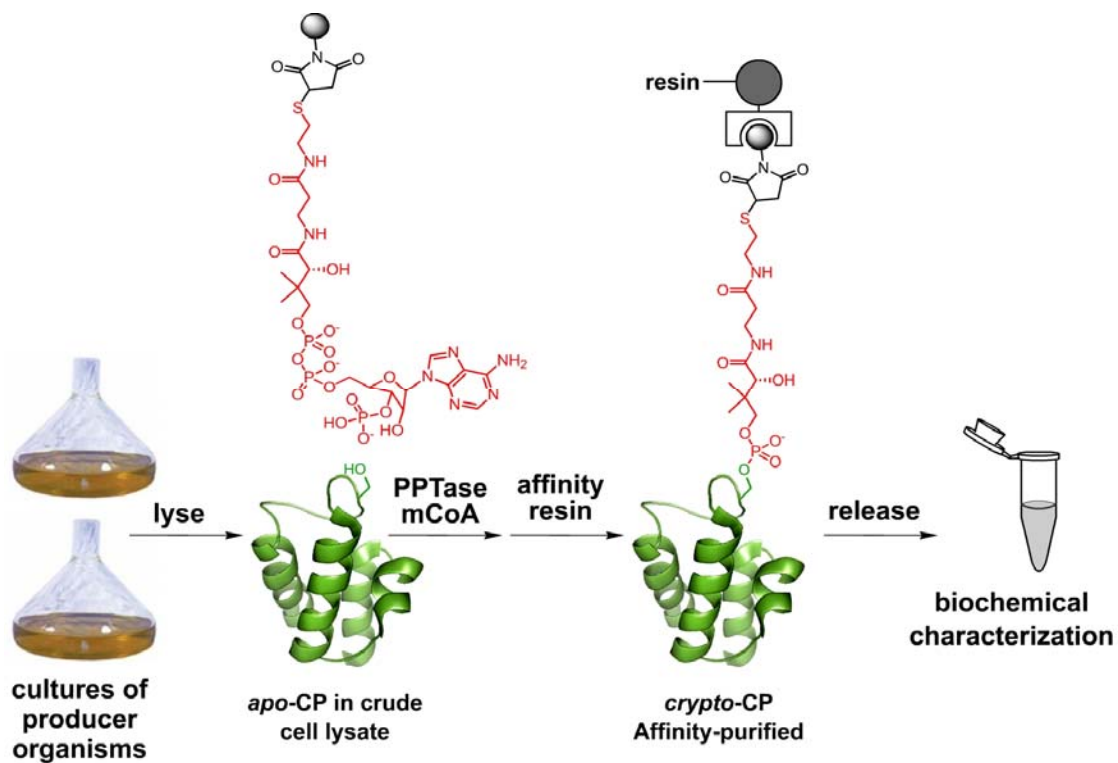


Figure 1.10 Scheme for the isolation of CP-containing enzymes

Cultures of producer organisms are grown to a point where the desired compounds are produced. These cultures are lysed and *apo*-synthases are converted to their *crypto*- form bearing an affinity label. This tag is leveraged by affinity chromatography. Isolated synthases are then released from the resin and are capable of being characterized biochemically.

With our developed technique being requisite on obtaining PKS/NRPS proteins in the apo-state, my work embodied in this dissertation has focused on a single goal: to identify a means of increasing *apo*-CP concentrations in crude cell extracts. Herein described are efforts to evaluate the use of small molecule inhibitors of PPTases as chemical probes to further the utility of our phosphopantetheinylation technique, and encompass studies including enzyme assay design, inhibitor synthesis, biochemical and biological inhibitor evaluation, assay component synthesis and automated high throughput screening of large compound collections to pan for new compound architectures with antagonistic activity against PPTase enzymes.

Chapter 2

SITE-SPECIFIC PROTEIN MODIFICATION: ADVANCES AND APPLICATIONS

ABSTRACT

Currently, chemical methods to modify proteins in a sequence-specific manner have not been realized. Posttranslational modification with functionalized substrate analogues provides an avenue to install unique reactivity to proteins in a sequence-specific manner; and these can be leveraged for isolation, detection and identification. Further application of these systems to covalently attach reporter probes to proteins by exploitation of this machinery provides a new avenue for the imaging of cellular processes that avoids nonspecific labeling and probe scattering, complications observed in other nonenzymatic methods of protein targeting.

INTRODUCTION

Although methods to acquire whole genome sequences have become routine, analysis of these data have made it apparent that the bulk of genomic content encodes putative genes whose products serve unknown function. Realization that the complexity of this body of information cannot be digested by current computational and genomic methods has fueled development of new techniques for functional characterization. Posttranslational modifications complicate these investigations, and their vital role in modulating activity *in vivo* suggests that traditional profiling techniques will not arrive at a comprehensive understanding of this material.

Elucidation of modification pathways, as a means to better understand these mechanisms of activation and regulation, has bred a field of scientists conducting interdisciplinary studies performing chemical transformations in biological contexts to solve elusive problems. These studies have found biochemical systems with exquisite sequence specificity and, through delicate probing of their chemical selectivity, have identified permissive substrate analogues with functionality immune to cellular chemistries. These analogues can be leveraged for fluorescent visualization or isolation, allowing insight into cellular localization of the individual populations of proteins being modified for their identification. The robust nature of these techniques has prompted thought into their application to additional biological problems, and their orthogonality to other cellular processes has further extended their use from proteomic analysis and genomic annotation to the imaging of biochemical processes at the cellular level.

In this review, we focus on recent advances in the biochemical and proteomic fields toward the ability to label proteins site-specifically, as well as new applications of posttranslational modification toward cellular imaging. Being an abridged summary, this is by no means a substitute for other recent discussions of work toward activity based protein-profiling (Saghatelian and Cravatt, 2005) or tools for cellular imaging (Giepmans et al., 2006), does not span the scope of engineered systems that utilize overt knowledge of the protein system (exemplified in (Takaoka et al., 2006)), and will not cover material that was adequately described previously (Chen and Ting, 2005, Miller and Cornish, 2005). Herein, as a continuation of this annual series, we

discuss recent advances in the labeling proteins site-specifically that are of interest to the chemical biology community.

BIOCHEMICAL (*in vitro*) TOOLS

General techniques for *in vitro* chemical labeling of native (non-fusion) proteins have been utilized for many years, but increasingly find themselves less applicable, in part due to the reactivity limitations of the 20 proteinogenic amino acids. These methods utilize selective chemistries that exploit solvent-accessible thiols and amines (from cysteine and lysine residues respectively, as well as the N-terminus) and more recently carboxylates (of aspartate, glutamate and the C-terminus) (Hermanson, 1996). While these species can be differentiated from each other, current methods do not provide an avenue for specific, single-site modification due to the multiplicity at which these moieties exist on the protein surface. As such, resultant labeling reaction product pools are composed of congeners with vary degrees of modification about a number of sites. Members of these pools may not behave identically, and it cannot be overlooked that modification of certain surface residues results in perturbation of protein-protein interactions by disruption of recognition elements. In attempts to circumvent this, protein chemists have sought to develop methods that impart reactivity to residues found less frequently on the protein surface not traditionally considered handles for such manipulation. Many research groups have adapted organic cross-coupling reactions to aqueous conditions seeking to exploit the reactivity of aromatic sidechains with transition metal catalysts or electrophilic species (for an excellent review of recent advances see (Antos and Francis, 2006)). While these

methods utilize new chemistries, they still do not guarantee utility of single-site derivitization, especially when structural information that demonstrates a single solvent-accessible residue is unavailable; a luxury not afforded to those studying new or complex protein systems.

An approach to this end has recently been demonstrated by Francis et al. utilizing an oxidative deamination reaction to strip the N-terminal amino group from various proteins (Gilmore et al., 2006). This technique, which entails treatment of isolated proteins with pyridoxal phosphate, is specific to the N-terminus due to the increased acidity of the α -proton, and installs α -keto functionality (Figure 1A). Gentle reaction conditions insure that aliphatic amines of lysine residues do not react, thus a single handle on each protein is installed that can be subsequently derivatized through a number of various enamine chemistries, including reaction with hydrazine or alkoxyamine probes.

While this technique avoids potential perturbation of activity that recombinant methods impart, it is limited in scope to proteins that meet requirements of N-terminal solvent accessibility, methionine processing, and terminal residue identity (β -functionalized amino acids are unreactive). More complicating, though, is the general fact that very few chemical processes of proteins proceed quantitatively, and this is no exception. Researchers are left with a product pool containing both singly labeled and unlabeled proteins. Separation of this mixture through traditional methods can prove to be quite arduous. In work towards this end, another publication from the same group describes a technique to address this complication with cyclodextrin resin (Nguyen et al., 2006), an affinity matrix that differentiates mixtures of substances with

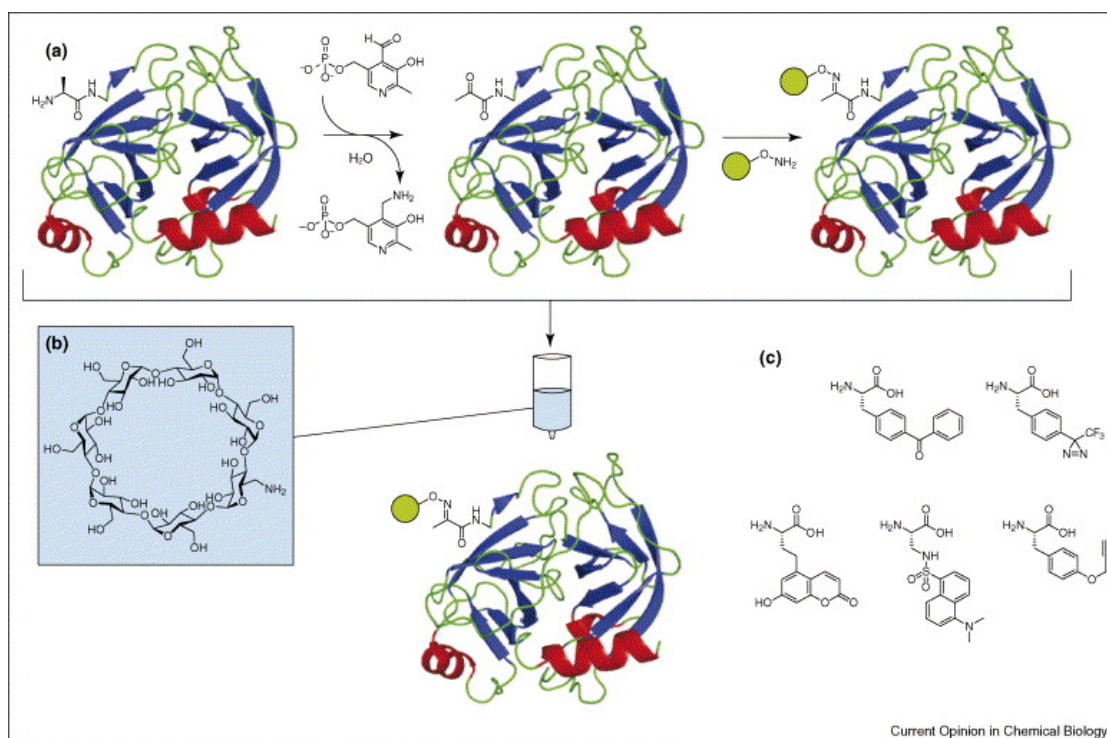


Figure 2.1 Biochemical methods for the Site specific labeling of proteins.

(A) Proteins containing permissive N-terminal residues (here represented as alanine) can be selectively deaminated oxidatively by treatment with pyridoxal phosphate to generate a α -keto residue and pyridoxylamine (Gilmore et al., 2006). Subsequent conjugation to an alkoxyamine-appended fluorophore yields a product pool of unlabeled and monolabeled proteins. Affinity chromatography of this mixture affords selective isolation of the protein conjugate (Nguyen et al., 2006). (B) Alternatively, methods to incorporate non-natural amino acids allow the installment of a number of bioorthogonal chemical functionalities, including photoreactive moieties for crosslinking experiments, intrinsically fluorescent residues and for biophysical and imaging applications, or an alkyl-terminating residue for click and staudinger-based investigations (Xie and Schultz, 2006). Protein structures were rendered using PyMOL [39]. All proteins shown are followed by the Protein Data Bank accession number for the structural data from which the representation was rendered. Trypsinogen (PDB: 1G36) used as a default representative protein.

varying degrees of aromatic and hydrophobic constituents on their surface. Use of this resin affords efficient separation of organically labeled proteins (Figure 1A) and should aid protein chemists by facilitating the preparation of homogeneously labeled protein preparations for use in analytical FRET-based studies, native-protein binding interactions, and *in vitro* experiments. This technique also promises important application toward enrichment of proteins and peptides containing unique aromatic substituents, such as those that have been enzymatically labeled with reporter analogues.

An alternative method to direct chemical modification is to impart distinguishable functionality during translation, described in the work of Shultz's group (reviewed in depth (Xie and Schultz, 2006)). This technique, utilizing a number of genetic manipulations to paired-sets of tRNA and tRNA-synthetases, has been amply discussed in review literature [1,2,4,5] and has expanded the genetic code to include over 30 additional unnatural amino acids, including those with alkynyl- and azido- appended functionalities for 'click' and Staudinger-based investigations, photoreactive sidechains for crosslinking, and intrinsically fluorescent coumaryl- and dansyl- moieties allowing insight to localization and trafficking at the cellular level (Figure 1B). This system meets criteria of minimal tag size (1 amino acid mutagenesis) and homogeneous populations (where the amber codon is placed at the N-terminus, truncation due to early-stop produces an oligopeptide that does not manifest itself in purified protein pools), but finds itself dependant upon cellular uptake of non-biogenic amino acid substrates from culture medium that is supplemented with these in large quantities to ensure incorporation. The recent

adaptation of this technique to yeast (Chin et al., 2003) and mammalian cell culture (Zhang et al., 2004) stands to expand its scope of applicability from an *in vitro* biochemical protein preparation tool to a staple of *in vivo* functional interrogation studies on multiple levels.

PROTEOMIC (ex vivo) TOOLS

In the proteomic arena, exhaustive effort has been put forth to develop new techniques to allow for the identification of posttranslationally modified proteins. More than 200 nontemplated alterations of protein surfaces are known to occur (Yan et al., 1989), and these play important roles in enzyme regulation, signal transduction, protein half-life and subcellular localization. Of these, phosphorylation is of particular interest to researchers due to its ubiquitous nature, playing a pivotal role in development, cell division, and oncogenesis. While current strategies can allow researchers to computationally identify potential phosphorylation motifs and enrich pools of phospho-proteins, they do not afford for the direct analysis of proteins owing their phosphorylated status to a single given kinase. In efforts to achieve this, Shokat has honed a technique utilizing an engineered ‘analogue specific’-kinase (*as*-kinase) and dually derivatized ATP to uniquely label the enzyme’s substrates (Allen et al., 2005). Specifically, the adenosine-binding site of a kinase is mutated to accommodate an N⁶-benzylation of the purine ring, a chemical modification that renders the nucleotide unrecognizable by cellular kinases due to its increased bulk. In addition, the N⁶-benzyl-adenine is functionalized with a γ -thiophosphate that, upon transfer to proteinacious targets, installs a nucleophile with unique pKa that can be leveraged for

site-specific labeling. This moiety can be modified with various electrophile-conjugated haptens and tags that readily allow for immunoprecipitation of the protein and detection by in gel visualization and western blot (Figure 2A). The principal drawback of this strategy is that, like other *ex vivo* techniques, it requires that enzyme substrates are in the *apo*-state at the time of extract preparation, necessitating the use of transgenic *as*-kinase cell lines cultured with *as*-targeted inhibitors or global dephosphorylation to prime the lysates before analysis.

Additionally, notable advances have been made aiming to selectively isolate and detect glycoproteins based on monomer constitution of the glycan (Saxon and Bertozzi, 2000, Dube et al., 2006, Sprung et al., 2005, Vocadlo et al., 2003, Sawa et al., 2006, Rabuka et al., 2006). These reports share a common methodology pioneered by Bertozzi (Saxon and Bertozzi, 2000), but are distinctly unique due to the complex nature of carbohydrate chemistry. Of these, a particularly interesting pair detail efforts to analyse fucosylation events, a modification demonstrated to gate certain secretory pathways, immune system recognition, and cancer biology. These studies come separately from the Bertozzi (Rabuka et al., 2006) and Wong (Sawa et al., 2006) groups and describe the synthetic preparation, validation, and application of azido- and alkynyl-modified fucosugars toward detection and isolation of their containing

glycans. In addition, the latter report describes the optimization of a new alkynyl-probe for click-based investigations that becomes fluorogenic only after reaction with azido- species. With this in hand, imaging was performed using fixed preparations from cells cultured with azidofucose; allowing assessment of fucosylglycan accumulation in the golgi and on the cell surface (Figure 2B). Many

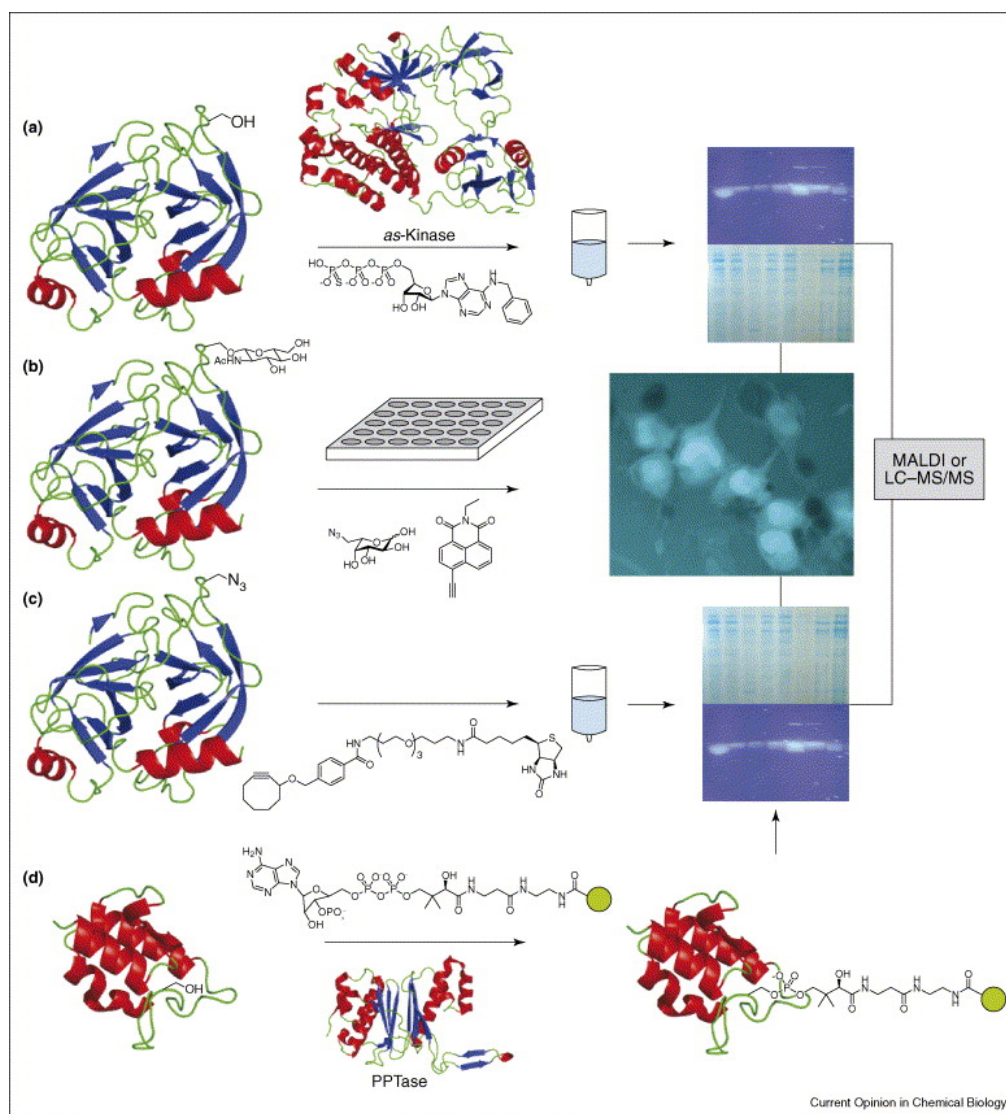


Figure 2.2 *Ex vivo* techniques to identify posttranslationally modified proteins.

(A) *apo*-substrates of an engineered *analogue specific*-kinase (*as*-kinase) (PDB: 1KSW) can be selectively labeled with N⁶-benzyl-ATP- γ -thiophosphate (AT*P γ S), subsequently derivitised by reactivity of their thiophosphate modification, and visualized in gel (Allen et al., 2005). (B) Glycosylated proteins encoded to be fucosylated within the cell (here represented by an O-linked N-acetylglucosamine residue) can be modified by metabolic delivery of 6-deoxy-6-azidofucose. Subsequent ‘click’ modification of fixed cell preparations with alkyne naphthamide probes can be microscopically imaged, visualized in gel, or identified by MALDI or LC/MS/MS (Sawa et al., 2006). (C) Proteins engineered to contain alkyne-azide species can be modified in the absence of catalyst with reporter- appended cyclooctynes for isolation, visualization, and identification (Agard et al., 2004). (D) *Apo*-carrier proteins (PDB: 1ACP) can be enzymatically phosphopantetheinylated with CoA derivatives by a phosphopantetheinyl transferase (PPTase) (PDB: 1QRO) to be visualized, isolated and identified (La Clair et al., 2004b). All proteins shown are followed by the Protein Data Bank accession number for the structural data from which the representation was rendered. Trypsinogen (PDB: 1G36) used as a default representative protein. Protein structures were rendered using PyMOL [39]. All proteins shown are followed by the Protein Data Bank accession number for the structural data from which the representation was rendered. Trypsinogen (PDB: 1G36) used as a default representative protein.

groups seek to apply the selectivity of the Huisgen [3+2] cycloaddition to live systems, however these efforts are often retarded by the toxicity of Cu^+ -based catalysts and slow rates of the uncatalysed reaction. This new probe provides a complimentary technique that may facilitate the development biocompatible catalysts.

Alternatively, Bertozzi and colleagues have recently evaluated strained alkynes as a means to obviate catalyst requirements (Agard et al., 2004) and found a cyclooctyne that reacts facilely under physiological conditions in the absence of Cu^+ (Figure 2C). It was demonstrated to efficiently label surface-exposed glycoconjugates and recently utilized in a bacterial cell-surface display method to screen tRNA synthetase mutagenic libraries for non-natural amino acid permissibility (Link et al., 2006). We await analysis of their cellular permeability and literary precedent toward their *in vivo* application.

Phosphopantetheinylation, a posttranslational modification of interest to metabolomics and natural products communities, entails the enzymatic transfer of the 4'-phosphopantetheinyl arm of coenzyme A (CoA) to conserved serine residues found in stand alone carrier proteins (CP) and synonymous domains of small-molecule biosynthetic enzymes. These polypeptide regions support the nascent chains of fatty acids, polyketides and nonribosomal peptides during elongation steps of biosynthesis. Selective analysis of these events would facilitate identification and manipulation of biosynthetic proteins and their genes from producer organisms. Discovery of Sfp, a phosphopantetheinyl transferase (PPTase) with broad substrate specificity regarding both carrier domain selectivity and appendages about the thiol of CoA (Lambalot et

al., 1996b) paved the way for our work demonstrating the preparation of CoA derivatives and their application to the fluorescent and affinity probe labeling of these proteins for detection and isolation (La Clair et al., 2004b) (Figure 2D). Additionally, we have detailed a modular synthesis of CoA (Mandel et al., 2004) that is readily amenable to derivative preparation, allowing investigations into the preparation of activity-based probes (Worthington, 2006) for isolation of enzymes recognizing CoA or CP-tethered substrates.

CELLULAR IMAGING/RECOMBINANT TOOLS

Posttranslational modifications have also been investigated as potential new avenues for the imaging of cellular processes. The enzymes that govern some of these processes demonstrate stringent sequence requirements regarding their proteinaceous substrates but are tolerant of derivatizations made to the small-molecule undergoing ligation: such characteristics make them ideal for *in vivo* applications. Studies to minimize recognition motifs have led to the shortening of these polypeptide substrates from large (>70 residues) proteins to short (5-15) peptides less likely to interrupt fusion partner function. The current status of these applications has been summarized (Giepmans et al., 2006, Chen and Ting, 2005, Miller and Cornish, 2005), but given the high level of interest in this field, some recent advancements have been made that warrant discussion.

The versatility of the aforementioned phosphopantetheinylation technique was recognized by a number of other groups who have utilized CP-fusion systems to prepare protein arrays (Yin et al., 2004) and microscopically image proteins at the cell

surface (Yin et al., 2005a, Meyer et al., 2006b, Meyer et al., 2006a). While the specificity and kinetics of this system are satisfactory for this latter application, its major criticisms (Chen and Ting, 2005, Miller and Cornish, 2005) focus upon the CP-fusion partner size (70 – 90 amino acid) and cell impermeability of CoA analogues (due their anionic nature at physiological conditions). Prior efforts to shorten the protein recognition element proved to be unsuccessful until recently when Walsh utilized phage-display screening of *Bacillus subtilis* genome fragments to arrive at an 11 amino acid ‘minimalized’ phosphopantetheinylation motif (Yin et al., 2005b). This motif was shown to be versatile as a modification handle when fused to either of the protein termini or inserted into loops between secondary structural elements.

Toward accessing membrane permeable tags, we sought to investigate the metabolic delivery of functionalized pantothenic acids (vitamin B5) as a means to furnish CoA analogues to proteins inside the cell (Figure 3A). Propitiously, the CoA biosynthetic

pathway enzymes accept fluorescent pantothenate analogues *in vitro* (Worthington and Burkart, 2006) and are cell permeable (Clarke et al., 2005b). We also sought to minimize the chemical preparation of these analogues, ideally making them accessible to laboratories lacking synthetic capabilities and have found simple analogs containing the pantoic acid moiety for facile uptake and *in vivo* conversion into CoA analogs (Meier et al., 2006a). This system stands to be evaluated in

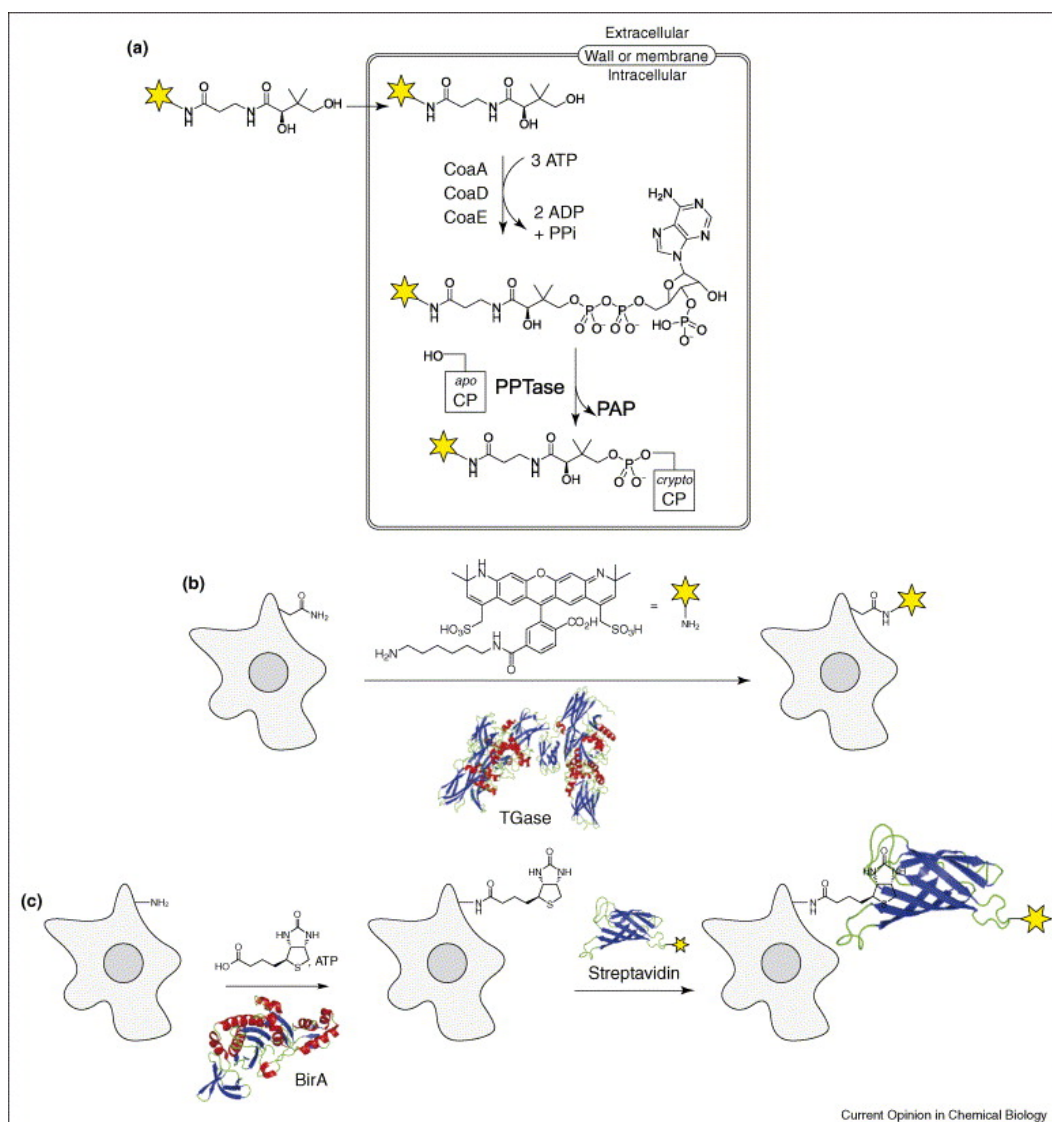


Figure 2.3 Enzymatic labeling techniques to image cells.

(A). Fluorescent pantoic acid derivatives can be metabolically converted into coenzyme A and attached to carrier proteins by coexpressed phosphopantetheinyl transferase in *E. coli* (Clarke et al., 2005b). (B) Cell surface proteins fused to glutamine-containing Q-tags can be fluorescently labeled by incubation with amine-terminating fluorophores and transglutaminase (TGase) (PDB: 1L9M) (Lin and Ting, 2006). (C) Live cells expressing membrane proteins containing AP-fusions can biotinylated by treatment with biotin, ATP and biotin ligase (BirA) (PDB: 1HXD) (Chen et al., 2005, Howarth et al., 2005). Further labeling with monovalent streptavidin (PDB: 1STP) conjugated to fluorophores allows for imaging without aberrant modulation of receptor function (Howarth et al., 2006). Protein structures were rendered using PyMOL [39]. All proteins shown are followed by the Protein Data Bank accession number for the structural data from which the representation was rendered. Trypsinogen (PDB: 1G36) used as a default representative protein.

eukaryotic and mammalian systems, where little information is known regarding potential localization of CoA pools and CoA-dependant enzymes.

Another method recently described by Ting utilizes transglutaminase (TGase) to catalyse the interconversion of the γ -amido nitrogen of glutamine residues with those of small alkylamine-appended probes (Lin and Ting, 2006) (Figure 3B). In this work, surface-targeted proteins fused to Q-tags (7 amino acid glutamine-containing peptide sequences recognized by TGase) were expressed in HeLa cells and efficiently labeled by guinea pig liver TGase with cadaverine-appended reporter and affinity probes. The resultant derivatizations could be visualized by fluorescent microscopy or immunodetected by western blot. The authors suggest a limited applicability of this technique to extracellular labeling, stating caviats which include competition with endogenous TG substrates (both small amines and nonspecific reaction with cellular proteins) and the low concentration of cytosolic Ca^{++} (an essential cofactor for the TGase). Future work in this arena stands to screen other TGases for increased Q-tag specificity as well as differential metal dependence, but it may find a most useful application in analysis of ER resident proteins (where Ca^{++} is abundant) and intracellular trafficking, a field where such methods have not been realized.

Finally, Ting and colleagues have also advanced their previously discussed technique (Chen and Ting, 2005) using *E. coli* biotin ligase (BirA) to covalently attach biotin to a lysine residue found within a 15 amino acid acceptor peptide (AP) sequence (Figure 3C). The initial studies (Chen et al., 2005, Howarth et al., 2005) found that cells expressing receptors containing AP at the N-terminus were readily biotinylated for imaging after incubation with fluorophore-appended streptavidin. The

technique was extended to dissociated hippocampal neurons in culture. Here, limitations are presented by inherent characteristics of the avidin family of proteins. Structurally, these polypeptides exist as multivalent tetramers. Treatment of live cells with such proteins leads to aggregation of the targeted receptors on the surface, potentially resulting in aberrant receptor activation and/or inhibition of endocytosis. Attempts to monomerize avidins have been made, but given that the biotin binding site is constituted at the multimerization-interface, such constructs have proven inaccessible. The Ting group remedied this through the preparation of a monovalent tetramer by refolding denatured 3:1 stoichiometric mixtures of mutant and wildtype streptavidins, respectively (Howarth et al., 2006). These experiments generate a distribution of products about the five possible associations, but efficient separation is imparted by encoding a hexa-histidine tag on the mutant subunits and separating the mixture via immobilized metal-chelate chromatography.

CONCLUSION

Site-specific labeling of proteins with small molecules stands to advance the understanding of biological systems through several pathways. Newly developed techniques will provide protein chemists the ability to prepare homogeneous substrate pools for biophysical studies. Permissive substrate analogues to analyze modification events will further our understanding of these key modes of activity modulation. Advanced computational assignment of putative gene product function will further the continuing quest to decipher the genetic code. Finally, the extended application of enzyme-mediated labeling to cellular imaging presents new methods to analyze

protein function *in vivo*. Given the versatility of these techniques, the future awaits further application and publicity to promote their adoption by the biological community for whom they have been developed.

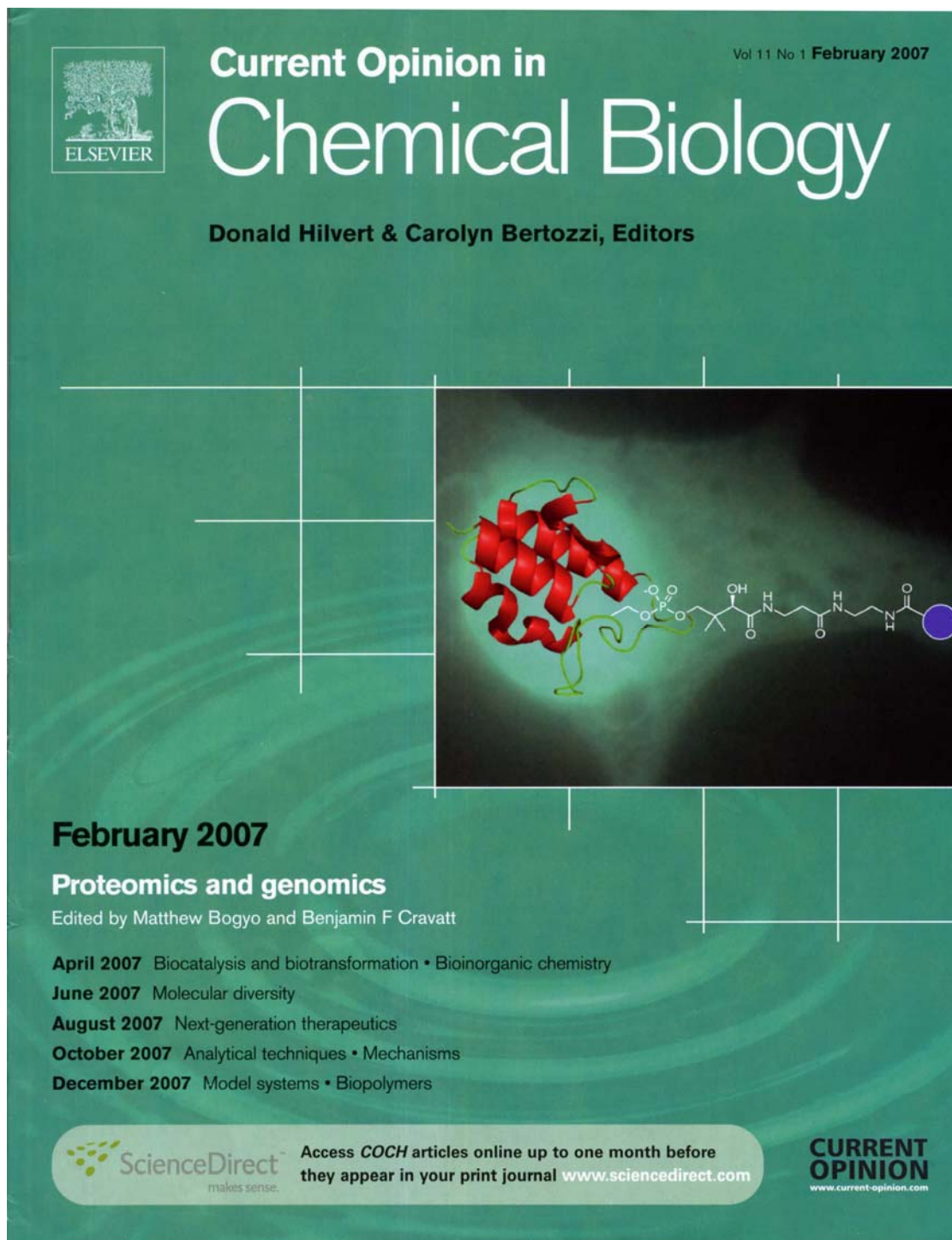


Figure 2.4 Image from cover of Curr. Ops. Chem Biol, vol 11, issue 1, 2007

ACKNOWLEDGEMENTS

Chapter 2, in whole, is a reprint of material published in *Current Opinion in Chemical Biology* (2007) Vol. 11, pp 12-9. I was the primary author of this work.

Chapter 3

A HOMOGENOUS RESONANCE ENERGY TRANSFER ASSAY FOR PHOSPHOPANTHETIENYL TRANSFERASE

ABSTRACT

Phosphopantetheinyl transferase plays an essential role in activating fatty acid, polyketide and nonribosomal peptide biosynthetic pathways, catalyzing covalent attachment of a 4'-phosphopantetheinyl group to a conserved residue within carrier protein domains. This enzyme has been validated an essential gene to primary metabolism and presents a target for the identification of antibiotics with a new mode of action. Here we report the development of a homogenous resonance energy transfer assay utilizing fluorescent coenzyme A derivatives and a surrogate peptide substrate that can serve to identify inhibitors of this enzyme class. This assay lays a blueprint for translation of these techniques to other transferase enzymes that accept fluorescent substrate analogues.

INTRODUCTION

A unifying characteristic in the biosynthesis of fatty acid, non-ribosomal peptide, and polyketide compounds is the tethering of the nascent polymer to small carrier protein domains of the synthases through thioester linkage about a phosphopantetheinyl (4'-PP) arm. This 4'-PP is installed on the proteins post-translationally from coenzyme A (CoA) **2** on a conserved serine residue by action of phosphopantetheinyl transferase (PPTase) enzymes, converting them from their *apo- 1* to *holo- 4* form (Fig. 1). This modification is essential for synthase activity, and ablation of the PPTase gene precludes natural product production (Lambalot et al., 1996a, Quadri et al., 1998a, Barezzi et al., 2004, Finking et al., 2002), or in the case of fatty acid biosynthesis, renders the organism unviable (Lambalot and Walsh, 1995,

Barekzi et al., 2004, Finking et al., 2002). Within bacteria, there exist two major classes of enzymes within the PPTase superfamily: the AcpS-type and the Sfp-type (Lambalot et al., 1996a). Grouping in these designations are made based on primary sequence, and their canonical representatives, AcpS of *Escherichia coli* and Sfp of *Bacillus subtilis*, are structurally distinct (Parris et al., 2000, Reuter et al., 1999).

It has been demonstrated that *acpS* is an essential *E. coli* gene (Lam et al., 1992a, Takiff et al., 1992), thus validating it as a target for inhibitor development with the potential to treat multi-drug resistance. Indeed, a number of groups have begun focused programs to develop AcpS inhibitors (Chu et al., 2003c, Gilbert et al., 2004, Joseph-McCarthy et al., 2005b, McAllister et al., 2000, Payne et al., 2007) and several candidates have recently been discussed (Chu et al., 2003c, Gilbert et al., 2004, Joseph-McCarthy et al., 2005b). In addition to fatty acids, a number of compounds are produced from 4'-PP dependent pathways that have been identified as virulence factors, and disruption of their biosynthesis has received much attention as a new angle for therapeutic development (Neres et al., 2008, Stirrett et al., 2008, Ferreras et al., 2008, Cisar et al., 2007, Meier et al., 2008). We have been intrigued by the central role of phosphopantetheinylation in these metabolic pathways, and are interested in studying the potential effects that PPTase inhibitors may have on the coordinate attenuation of numerous aspects of pathogenicity.

While AcpS-directed inhibitor development has been reported (Chu et al., 2003c, Gilbert et al., 2004, Joseph-McCarthy et al., 2005b, McAllister et al., 2000, Payne et al., 2007), this work has generally omitted screening protocols. The only described method utilizes homogenous time-resolved fluorescence resonance energy

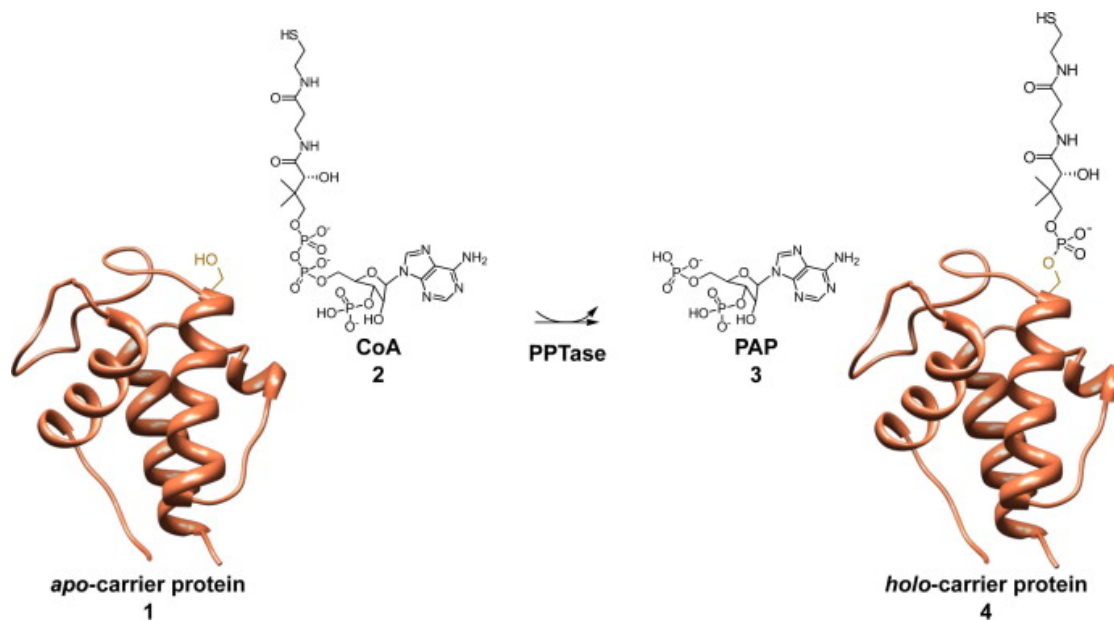


Figure 3.1 Posttranslational modification of carrier proteins.

The translated apo-carrier proteins **1** and coenzyme A **2** react with PPTase to generate 3'-phosphoadenosine-5'-phosphate (PAP) **3** and holo-carrier proteins **4**.

transfer (HT-RF) as a means for activity determination (Gilbert et al., 2004). We found replication of this technique beyond our capabilities due to limitations imposed by instrumentation, and we desired the use of readily available and affordable biochemical reagents. Herein we report the development of a homogenous fluorescence resonance energy transfer (FRET) screen for the two canonical PPTase representatives, AcpS and Sfp. This method is simple, requiring only addition of reagents to reaction wells of a microtiter plate, and is herein validated as a process to identify inhibitors of these enzymes. Furthermore, we describe the details that led to successful development of this screen, so it may serve to blueprint assay design for other transferase enzymes that accept reporter-modified substrate analogues.

MATERIALS & METHODS

General

7-dimethylamino-4-methyl-coumarin-3-maleimide (DACM) and *N,N,N',N'*-tetramethylrhodamine-5-maleimide (TAMRA) were purchased from Invitrogen Corporation (Carlsbad, CA). Coenzyme A trilithium salt was purchased from EMD biochemicals (San Diego, CA). 3'-phosphoadenosine-5'-phosphate disodium salt (PAP), 4-(2-hydroxyethyl)-1-piperazine ethanesulfonic acid (HEPES), dimethylsulfoxide (DMSO, Hybri-Max grade), and fluorescein-isothiocyanate isomer I (FITC) was purchased from Sigma (Saint Louis, MO). Concentrations of all fluorescently labeled reagents were quantified by UV-VIS spectroscopy with an Agilent 8354 diode array spectrophotometer (Agilent Technologies, Santa Clara, CA)

using the following extinction coefficients: DACM: 23,000 $\text{cm}^{-1}\text{M}^{-1}$, FITC: 77,000 $\text{cm}^{-1}\text{M}^{-1}$, TAMRA: 95,000 $\text{cm}^{-1}\text{M}^{-1}$.

Enzyme expression & Purification

Sfp was expressed and purified as described previously (Quadri et al., 1998a). The enzyme was concentrated to 40 mg/mL, diluted with an equal volume of 75 % glycerol, and stored in 100 μL aliquots at -80°C . For routine use, this stock (20 mg/mL, 765 μM) was diluted to 1 mg/mL in Sfp storage buffer (50 mM NaHEPES, 120 mM NaCl, 33 % v/v glycerol) supplemented with 0.1% w/v BSA and stored at -20°C . Under these conditions, there was no noticeable reduction in enzymatic activity with storage for periods longer than 6 months.

E. coli AcpS was expressed and purified as a native protein from pDPJ according to published procedures (Lambalot and Walsh, 1997). The protein concentration of the final preparation was adjusted to 10 mg/mL by addition of 2X storage buffer, an equal volume of glycerol added in 3 portions, and aliquots stored at -80°C . For routine work, single tubes (200 μL portions) were stored at -20°C , with no degradation of enzymatic activity observed after 1 year of storage.

Synthesis of assay components

An exploratory quantity (ca. 8 mg) of fluorescein-5-isothiocyanate-modified YbbR peptide (FITC-YbbR) **8** (sequence: Fluorescein-Ahx-DSLEFIASKLA-OH) was initially purchased from GL Biochem (Shanghai, China). For the final screen evaluation, the peptide was prepared on the 0.2 mmol scale using an automated solid phase peptide synthesizer (Applied Biosystems Pioneer) using standard 9-fluorenylmethyloxycarbonyl (Fmoc) chemistry with 2-(1H-7-Azabenzotriazol-1-yl)-

1,1,3,3-tetramethyl uronium hexafluorophosphate (HATU) activation (Fig. 3A) (Glover et al., 1999b). The sequence was appended with an N-terminal *N*-FMOC- ϵ -aminocaproic acid spacer, deprotected, and coupled overnight with FITC. Following cleavage from the solid support, the product was HPLC purified to yield 84 mg of FITC-YbbR **8** and its identity verified by ESI-MS.

Fluorescent reporter CoA (mCoA) analogues **11** and **12** were prepared by reaction of reduced CoA trilithium salt **2** (1 mg/mL in 50 mM NaH₂PO₄, pH 7.4) with 1.1 equivalents of maleimide bearing probe **9** or **10**, respectively (both dissolved at 1 mg/mL in methanol) (Fig. 3B). The reaction was followed to completion by HPLC, determined by disappearance of the CoA peak. Excess **9** and **10** were removed by extraction three times with ethyl acetate or dichloromethane, respectively. The resultant aqueous phase was placed under vacuum (< 2 mm/Hg) for 2h to remove residual organic solvent. The purity of mCoA analogues **11** and **12** were verified to be >95% by HPLC.

Kinetic evaluation of fluorescent substrates

Kinetic parameters for FITC-YbbR **8** and TAMRA-mCoA **12** were determined by HPLC. Reactions were conducted in a final volume of 50 μ L in a buffer containing 10 mM MgCl₂, 50 mM Na-HEPES, pH 7.6, 0.1 mg/mL BSA. Reactions were initiated by the addition of 0.5 μ M enzyme, allowed to progress for 15 minutes, and quenched by addition of 50 μ L 50 mM sodium ethylenediaminetetraacetic acid, pH 8.0. The reaction mixtures were then separated by reversed phase chromatography with an Agilent 1100 instrument fitted with a diode array detector (Agilent Technologies, Santa Clara, CA) using an OD5 C₁₈ column (250 x 4.6 mm, product

number 9575, Burdick & Jackson, Morristown, NJ). The separation was performed under the following conditions: Buffer A: 10 mM ammonium acetate, Buffer B: Acetonitrile, flow rate: 1.5 mL/min. After injection, the run initiated with a 2 minute isocratic flow of 10% Buffer B, followed by sample elution with a 10 minute linear gradient from 10% to 60% Buffer B. The column was regenerated with a 2 minute isocratic flow of 100% Buffer B, and then the column equilibrated to 10% Buffer B.

Fluorescence spectroscopy

Steady state single sample fluorescence spectra were recorded on a QuantaMaster 2000 spectrofluorometer (Photon Technologies International, Princeton, NJ), using excitation and emission slit widths of 4 nm and integration times of 0.1 sec.

FRET screen conditions

PAP parent inhibitor plates were made by dissolving the compound in dry DMSO at a concentration of 10 mM and serial diluting this (2-fold) in DMSO. The final protocol (Table 1) is as follows: 2.5 μ L of the parent DMSO solutions (or DMSO as a negative control) were transferred to individual wells of a black polystyrene 96 well plate (Costar # 3694) followed by 37.5 μ L of a 1.33 X Enzyme solution [16.62 nM Sfp or 66.6 nM AcpS in 1.33 X PPTase assay buffer (66 mM Na-HEPES, 13.3 mM MgCl₂, 1.33 mg/mL BSA, pH 7.6). Reactions were initiated by the addition of 10 μ L 5X reagent solution (50 μ M TAMRA-mCoA **12**, 25 μ M FITC-YbbR **8**, 10 mM NaH₂PO₄, pH 7.0). The reaction was monitored continuously (cycle time 2 minutes) for 15 cycles in a Perkin Elmer HTS7000plus microtiter plate reader with excitation filter $\lambda = 485$ nm, emission filter $\lambda = 535$ nm.

Data analysis

Kinetic data was processed with Microsoft Excel. Assay statistics were evaluated according to standard equations (Inglese et al., 2007b). Plotting and nonlinear regression was performed with GraphPad Prism version 5.00 (GraphPad Inc, La Jolla, CA), and IC50 curves were fit with the four-parameter dose response equation using the ordinary (least squares) setting. In all cases, error bars and reported error values represent one standard deviation.

Molecular graphics images (Figs. 1 & 2) are renditions of the *apo*-actinorhodin acyl carrier protein (PDB identifier: 2K0Y) and were generated using the UCSF Chimera package (Pettersen et al., 2004).

RESULTS & DISCUSSION

Design of a high-throughput PPTase assay

Traditionally, PPTase bioassays have been conducted in a low throughput manner, either by monitoring radiolabel incorporation to precipitated protein mass from [³H]-CoA [4] or by HPLC separation of the *apo*- and *holo*- states of the carrier protein substrate [3]. These systems utilize centrifugation and chromatographic separations, respectively, and are not readily amenable to high throughput screening. In designing a high throughput screen for PPTase activity, we desired a system that would allow direct monitoring of reaction progress to eliminate the probability of false-positive hits that arrive from inhibition of coupled enzyme systems. To accomplish this, we chose to exploit the synthetic aspect of the PPTase reaction in conjunction with a fluorescent reporter-CoA (mCoA) technology developed

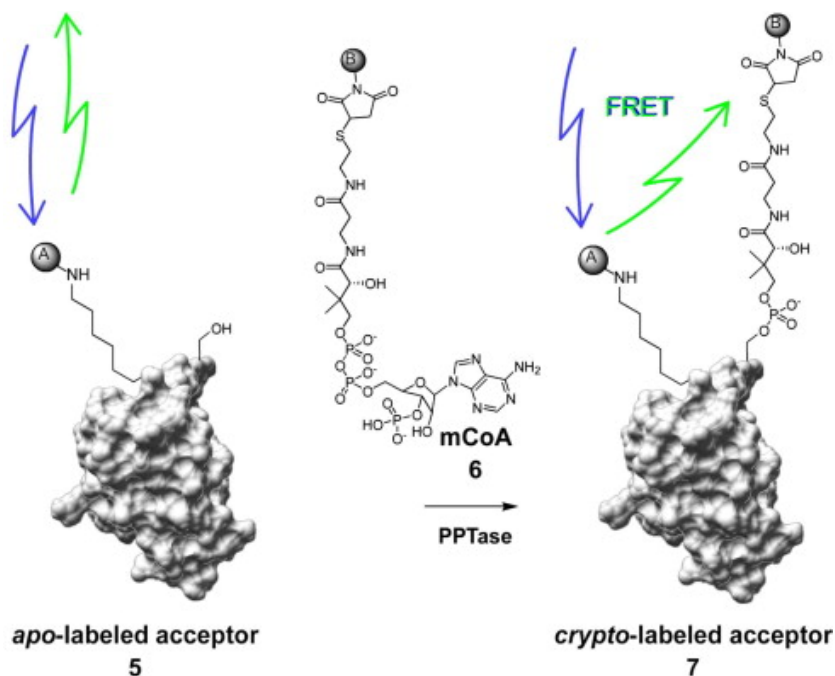


Figure 3.2 Fluorescence resonance energy transfer assay for phosphopantetheinyl transferase.

Action of PPTase on a fluorescently labeled acceptor substrate **5**, in conjunction with a fluorophore-modified coenzyme A analogue (mCoA) **6**, assembles a FRET pair upon conversion to the thiol-blocked *crypto*-acceptor substrate **7**. The assembly of this FRET pair can be detected with a fluorescence microplate reader.

previously in our laboratory (La Clair et al., 2004a). In this system, fluorophore-appended carrier protein domains/mimics **5** generate a FRET signal upon conversion to their thiol-blocked *crypto*- form **7** by modification with mCoA **6** analogs by PPTase (Fig. 2).

Fluorescent probe selection and substrate synthesis

We chose to make a fluorescein-5-isothiocyanate (FITC) modification to the protein-based substrate, as this fluorophore possesses absorption and emission centered about the visible light spectrum, allowing it to function as either FRET donor or acceptor, depending on the identity of compounds chosen for mCoA **6** preparation (Fig. 2). This would allow us to probe both modes of FRET from a singly prepared pool of reagent. In turning to select a carrier protein domain to function as the acceptor substrate, we initially considered the *E. coli* fatty acid synthase acyl carrier protein (ACP) as a candidate, as previous reports note that ACP contains a single tyrosine residue present at the C-terminus of α -helix 3 and modification of this residue with a dansyl-moiety does not hinder its function (Haas et al., 2000, Blommel and Fox, 2005). We found this protocol and other tyrosine-modifying techniques (Joshi et al., 2004, Schlick et al., 2005) to provide low yields of fluorescein-modified proteins due to the insolubility of FITC and its derivatives in low pH reaction conditions (data not shown), and the purification of this labeled material was insufficient for our needs.

Subsequently, we chose to investigate the use of the eleven residue YbbR peptide (sequence H-DSKLEFIASKLA-OH) identified by Yin *et al.* that undergoes modification by PPTases, thus serving as an ACP surrogate (Yin et al., 2005c). This choice was strengthened by the fact that solid phase peptide synthesis (SPPS) allows

access to large quantities of uniformly labeled material, a crucial requirement for FRET applications, and avoids the potential for batch-to-batch variability. In selecting the placement of the label, we noted that YbbR was isolated as a collection of N-terminal extensions to the consensus, suggesting a site for modification that would not abrogate activity. As such, we chose to attach FITC to the YbbR consensus via a 6-aminocaproic acid spacer unit to sufficiently distance the molecule from the central motif (Fig. 3A) and impart a number of freely rotatable bonds, thus ensuring a random spatial orientation upon FRET-pair assembly (*vide infra*).

In selecting complimentary probes containing modest spectral overlap with FITC for mCoA **6** production, we sought maleimide-bearing compounds that were amenable to organic extraction after reaction with CoA (Fig. 3B), as this would circumvent HPLC purification; a characteristic that would make the procedure easily scaleable for a high screening volume application. With this in mind, dimethylaminocoumarin (DACM) **9** and tetramethylrhodamine (TAMRA) **10** were chosen and used to prepare DACM-mCoA **11** and TAMRA-mCoA **12** (Fig. 3B) to be evaluated as a FRET donor (Fig. 4A) and FRET acceptor (Fig. 4E), respectively.

HPLC analysis of the labeled substrates

The labeled substrates were evaluated by HPLC to probe the effects that modification of the substrates would have upon the kinetic parameters displayed by the enzymes. Evaluation of FITC-YbbR **8** with AcpS and Sfp, with a saturating concentration of CoA **2** returned K_m values of 86 and 101 μM and K_{cat} values of 4.4 and 12.1 μM , respectively. These are in agreement with the values previously determined for the unmodified substrate (K_m values of 200 and 123 μM for AcpS and

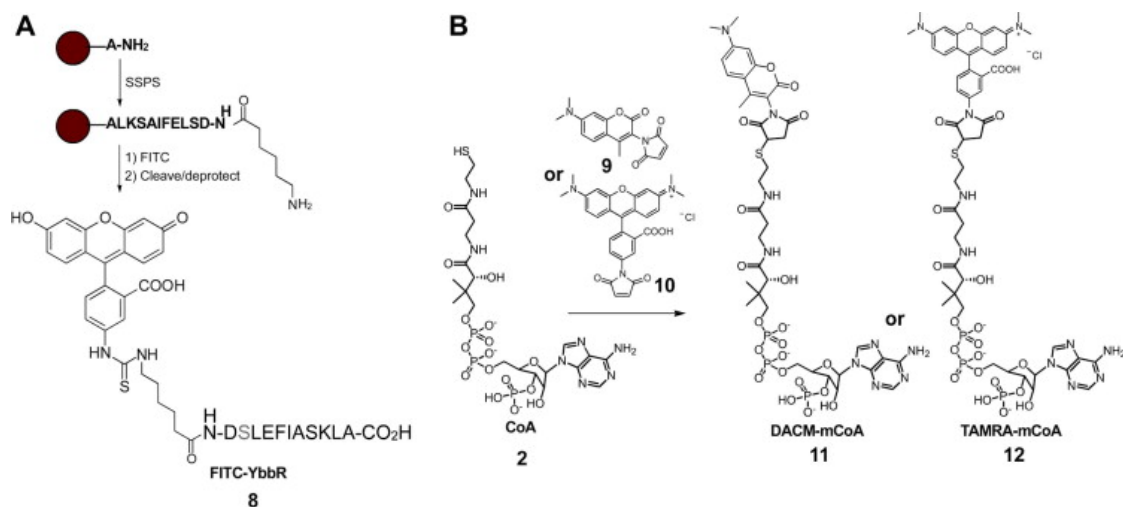


Figure 3.3 Synthesis of assay components.

(A) Beginning with L-alanine loaded polystyrene resin, standard SPPS procedures afford the YbbR sequence appended with an ϵ -aminocaproic acid residue. Reaction with FITC, followed by cleavage and HPLC purification gives the FITC-YbbR peptide substrate **8**. (B) CoA **2** is reacted with maleimide bearing probes **9** or **10** to produce their fluorescent mCoA derivatives **11** or **12**, respectively.

Sfp, respectively) (Yin et al., 2005c, Zhou et al., 2007). Additionally, the kinetic parameters for TAMRA-mCoA **12** were determined at a saturating concentration of FITC-YbbR **8** and gave K_m values of 22 and 6 μM for AcpS and Sfp, with K_{cat} values of 3.2 and 8.9, respectively. Again, these values were found to be in agreement with previously determined parameters (Yin et al., 2005c, Zhou et al., 2007) and demonstrate the modifications made to the substrates were well tolerated by the enzymes.

Determination of Förster Radius

In order to assess the viability of the donor and acceptor substrates chosen, we sought to determine the theoretical Förster's radius, R_0 , of these pairs. This value, the distance where transfer efficiency is 50%, is related to donor quantum yield Φ_D , the relative orientation of donor and acceptor transition dipoles κ , and $J(\lambda)$, the overlap integral of the donor emission F_D and the absorption of the acceptor ϵ_A (Lakowicz, 1999):

$$R_0^6 = \frac{\Phi_D \kappa^2 9000 (\ln 10)}{128 \pi^5 N_A \eta^4} J(\lambda) \quad (1)$$

For κ a value of $2/3$ is assumed and corresponds to a random orientation of the two fluorophores in space, given that they will be linked by numerous freely rotatable bonds. η , the index of refraction of the medium, is assumed to be 1.44 for biological samples (Lakowicz, 1999) and N_A , avagadro's number, is a constant, leaving R_0 to be determined by Φ_D , and $J(\lambda)$. Quantum yields for these fluorophores have been previously determined (Machida et al., 1975), $J(\lambda)$ is expressed as,

$$J(\lambda) = \int F_D(\lambda) \varepsilon_A(\lambda) \lambda^4 \delta\lambda \quad (2)$$

Simple equations cannot be written for $F_D(\lambda)$ and $\varepsilon_A(\lambda)$, and thus, $J(\lambda)$ is calculated as a summation (Campbell et al., 1984):

$$J(\lambda) \simeq \sum_{i=1}^{i=n} J_i = \sum_{i=1}^{i=n} F_D(\bar{\lambda}_i) \varepsilon_A(\bar{\lambda}_i) \bar{\lambda}_i^4 \Delta\lambda \quad (3)$$

Absorption and emission spectra were recorded for the three conjugated substrates **8**, **11** and **12** (Fig. 4B & F) and summation of the values at each wavelength according to Eq. (3) and use of these $J(\lambda)$ values in Eq. (1) gave Förster's radii of 38 Å and 56 Å for the DACM-FITC (Fig. 4A) and TAMRA-FITC pairs (Fig. 4E), respectively.

Photophysical evaluation of the phosphopantetheinylated peptide and efficiency of transfer determination

With the theoretical Förster's radii, we mathematically calculated the maximum distance that two fluorophores could achieve in the *crypto*-FITC-YbbR product (exemplified as **7**, Fig. 2) by summation of average bond lengths, and determined this to be 42 Å (radius, r , of 21 Å) if a rigid linear extension were to occur. This suggests a high theoretical FRET efficiency, E , which is strictly related to the radius separating the two fluorophores, r , by

$$E = \frac{R_0^6}{R_0^6 + r^6} \quad (4)$$

with a rapid decay in E when r exceeds R_0 . Using the R_0 values determined from Eq. (1) and our calculated r of 21Å; Eq. (4) gives theoretical E values of 97 %

and 99 % for the DACM-FITC and TAMRA-FITC pairs, respectively. However, r exists as a distribution due to the number of freely rotatable bonds, and thus transfer

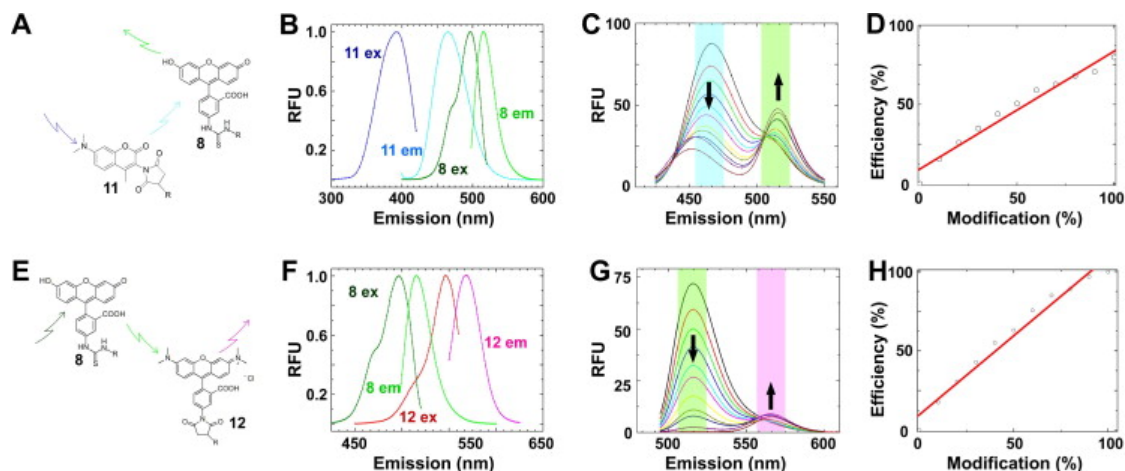


Figure 3.4 Probe selection and photophysical evaluation of the crypto-YbbR peptides.

DACM-mCoA **11** and TAMRA-mCoA **12** probes were evaluated for their FRET characteristics with FITC-YbbR **8**. (A) DACM-mCoA **11** acts as a FRET donor to FITC-YbbR **8**. (B) Excitation and emission spectra of probes **11** and **8** were recorded and normalized to determine the spectral overlap of **11** emission with **8** excitation to calculate an overlap integral $J(\lambda)$ [Eq. (3)] and theoretical Forster's radius R_0 [Eq. (2)] of this system. Summation of the normalized data gave a $J(\lambda)$ of $1.60 \times 10^{-13} \text{cm}^4$ and a $R_0 = 38 \text{\AA}$. (C) FRET characterization of the *crypto*-DACM-FITC-YbbR peptide. Equimolar solutions of **11** and **8** were prepared with varying degree of modification to the *crypto*-DACM-FITC-YbbR **7**, and their fluorescent spectra recorded with excitation at 403nm. The spectra are overlaid, and increase in 10% increments of modification from 0 to 100%; starting from the maximal emission observed at 462nm to minimum at this wavelength. (D) Eq. (5) was fitted to emission data from (C) and gave an efficiency of transfer value of 0.82. (E) FITC-YbbR **8** acts as a FRET donor to TAMRA-mCoA **12**. (F) Excitation and emission spectra of probes **11** and **12** were recorded and normalized to determine the spectral overlap of **11** emission with **12** excitation to calculate an overlap integral $J(\lambda)$ [Eq. (3)] and theoretical Forster's radius R_0 [Eq. (2)] of this system. Summation of the normalized data gave a $J(\lambda)$ of $3.01 \times 10^{-13} \text{cm}^4$ and a $R_0 = 56 \text{\AA}$. (G) FRET characterization of the *crypto*-TAMRA-YbbR peptide. Equimolar solutions of **11** and **12** were prepared with varying degree of modification to the *crypto*-TAMRA-YbbR **7**, and their fluorescent spectra recorded with excitation at 475nm. The spectra are overlaid, and increase in 10% increments of modification from 0 to 100%; starting from the maximal emission observed at 513nm to the spectrum with the minimum value at this wavelength. (H) Eq. (5) was fitted to emission data at 513nm from (G) and gave an efficiency of transfer value of 0.99.

efficiency must be experimentally determined by measurement of donor fluorescence in the absence (F_D) or presence (F_{DA}) of acceptor and fitting of Eq. (5) to the experimental data:

$$E = 1 - \frac{F_{DA}}{F_D} \quad (5)$$

Reactions were set up with mCoA analogues **11** and **12**, Sfp, and FITC-YbbR **8** and followed to completion by HPLC. The corresponding *crypto*-FITC-YbbR **7** peptides were then isolated by semi-preparative HPLC. These products were used to prepare equimolar mixtures of the probes with varying degrees of modification. Fluorescent emission spectra of these mixtures were recorded (Fig. 4C & G). Analysis of these data (Fig. 4D & H) by Eq. (5) yields efficiency of transfers of 0.82 and 0.99 for the DACM-FITC (Fig. 4A) and TAMRA-FITC (Fig. 4E) pairs, respectively.

Mode of observation

Data in Fig. 4 (C & G) was also informative with regard to the mode of monitoring for this biochemical system. FRET pairs offer flexibility in that their assembly can be detected by either the quench of the donor emission (down arrows) or by sensitization of acceptor fluorescence at shorter excitation wavelengths (up arrows). Evaluation of data for both systems shows a greater response for the quenching mode, with a 5-fold and 10-fold reduction in donor fluorescence upon conversion to *crypto*-FITC-YbbR **7** for the DACM-FITC and TAMRA-FITC pairs, respectively. Evaluation of acceptor sensitized emission at shorter excitation wavelengths showed an increase of 2-fold for complete conversion, indicating that the system would give a greater signal to background ratio by monitoring the quench of

donor fluorescence. This screen would therefore function optimally as a substrate-consumption assay.

Of these two FRET systems, TAMRA-mCoA probe **12** possessed better FRET characteristics (i.e. full attenuation of donor fluorescence upon complete conversion) and was chosen to be carried forward for screen implementation.

Determination of screen conditions

We arrived at initial assay conditions based on the requirement that the end point would need complete attenuation of donor fluorescence; requiring TAMRA-mCoA **12** to be present in excess of FITC-YbbR **8**. With this in mind, we probed the linearity of detector response with respect to FITC-YbbR **8** concentration. This was done to identify the maximal concentration that could be obtained before direct correlations between relative fluorescence units and substrate concentration became obscured by an inner filter effect, a phenomenon where all incident light irradiated upon the sample is absorbed and does not sufficiently transition all target molecules to the excited state. With our plate reader (Perkin Elmer HTS7000) we found delineation to occur at concentrations exceeding 10 μM , and thus chose to hold FITC-YbbR **8** at a concentration of 5 μM .

We then sought to determine the effects of increasing the concentration of TAMRA-mCoA **12** on FITC-YbbR **8** signal. The purpose of this analysis was to find an acceptably high concentration of TAMRA-mCoA **12** that did not impart an effect on FITC-YbbR **8** emission, as it displays some absorption at the FITC-YbbR **8** excitation wavelengths. We found the signal to be maintained at concentrations up to

12.5 μM and arrived at the final concentration in the screen for TAMRA-mCoA **12** to be 10 μM .

Assay optimization: Requirement of BSA for enzyme stability

The screen was first developed by initiating reactions in 96 well plates with varied enzyme concentration. These experiments were monitored continuously using standard fluorescein optics, and analysis of the progress curves revealed that reaction rate did not follow linearly with respect to enzyme concentration. This was identified to be a complication with time-dependent inactivation of the enzyme using Selwyn's method (Selwyn, 1965) (data not shown). A number of reaction additives, including buffer and salt composition, ionic strength, and detergents were screened in an attempt to stabilize the enzyme, and we found that inclusion of bovine serum albumin (BSA) at a concentration of 1 mg/mL (15 μM) stabilized the enzyme and eliminated this complication.

With this modification, stable reaction progress plots were observed (Fig. 5A & C) that displayed a linear relationship between rate and enzyme concentration (Fig. 5B & D). From this data, we determined optimal enzyme concentrations to be 50 and 12.5 nM for AcpS and Sfp, respectively, based on obtaining a complete progress curve terminating in approximately 30% substrate consumption over a 30 minute time interval (*vide infra*). It is noteworthy that while inclusion of BSA may be traditionally considered unattractive in a screening campaign, this carrier provides an excellent source of amine and thiol moieties and may serve to repress inhibition of the enzyme by nonspecific electrophilic species present in diverse compound libraries.

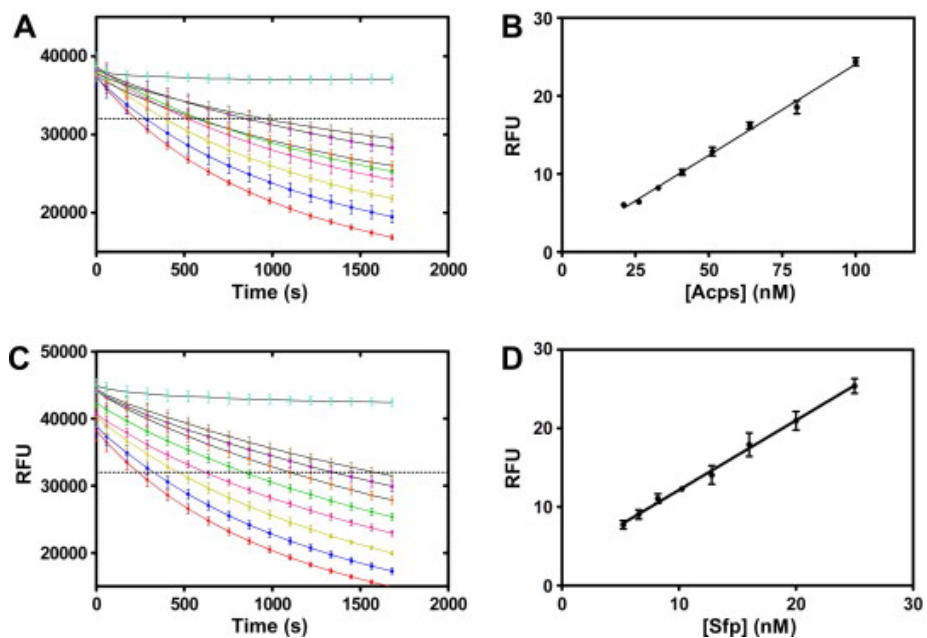


Figure 3.5 Reaction progress and enzyme titration.

(A) Reaction progress plots for eight concentrations of AcpS. Rates were determined for the experiments when they intersect the dashed threshold at 32,000 RFU. (B) Reaction rates for the progress curves in A are plotted against AcpS concentration and demonstrate a linear response. (C) Reaction progress curves for eight concentrations of Sfp. Rates were determined for the experiments when they intersect the dashed threshold at 32,000 RFU. (D) Reaction rates for the progress curves in C are plotted against Sfp concentration and demonstrate a linear response.

DMSO tolerance

Since most compound libraries are stocked as solutions in DMSO, we sought to evaluate the tolerance of the screen to this organic solvent. Inclusion of any organic solvent in the reaction caused an immediate 10% increase in RFU signal from the substrate mixture but did not deteriorate the observed rate until reaching a concentration greater than 10% total volume (data not shown). For our routine screening conditions, we maintained a final DMSO concentration of 5% v/v.

Progress curve analysis and signal statistics

With final assay conditions in hand, a screening protocol was developed and is presented in Table 1. Following this protocol, we recorded progress curves and analysed this data statistically to determine the appropriate time for analysis. Since known inhibitors of PPTases are not commercially available, an enzyme-free reaction was used as the fully inhibited (negative) control. Analysis of these data (presented in Fig. 6A & B) demonstrated the assay performance relied heavily on the amount of substrate consumption that was allowed to occur, with the parameter values becoming better with further consumption (Table 2). However, excessive substrate consumption can lead to erroneous determination of inhibition characteristics (Wu et al., 2003), and a progression of ~20% (Table 2, boxed values) was chosen as a balance of conditions where a minimum of substrate was consumed and assay statistics reached acceptable values, including Z' values of 0.7, and signal to noise of 20 (Table 2).

Table 3.1 Summaried homogenous protocol for PPTase assay

Table 1

Summarized assay protocol

step	parameter	value	description
1	compound library	2.5 μ L	transfer to COSTAR 3694 black 96 well plate; Row G & H = DMSO for control
2	Enzyme solution	37.5 μ L	1.33X solution: 1.33mg/mL BSA, 66.6mM NaHEPES, pH 7.6, 13.3mM MgCl ₂ ,
3	time	15 min	Room tempertature incubation
4	substrate reagent	10 μ L	5X solution: 25 μ M FITC-YbbR 8 , 50 μ M TAMRA-mCoA 12 in 10mM sodium phosphate
5	detection	Ex 485, Em 535 nm	Perkin-Elmer HTS7000 plus, kinetic read, once evey 2 min for 15 cycles

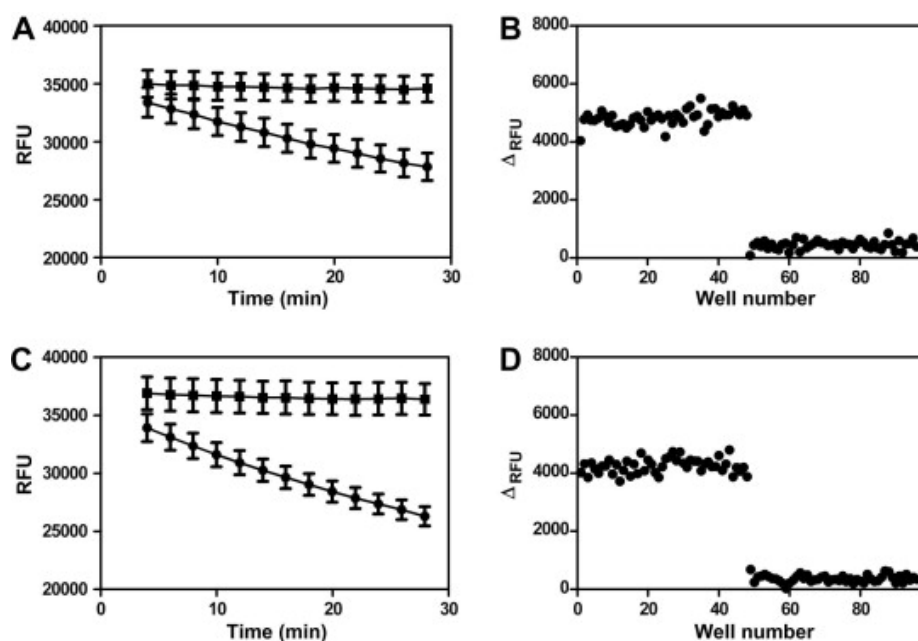


Figure 3.6 Determination of analysis timepoint and Z' .

(A) Progress curve for a 96 well plate containing 48 reactions in the presence (●) or absence (■) of 50 nM AcpS. The data for each timepoint were analysed statistically and presented in Table 2. The 24 minute time point was selected for routine analysis, as it gave acceptable assay statistics during the linear range of the screen. (B) Change in relative fluorescence units for the 24 minute time point (Table 2, boxed data) is plotted against well number. The Z' value for this data is 0.72. (C) Progress curve for a 96 well plate containing 48 reactions in the presence (●) or absence (■) of 12.5 nM Sfp. The data for each timepoint were analysed statistically and presented in Table 2. The 16 minute time point was selected for routine analysis, as it gave acceptable assay statistics during the linear range of the screen. (B) Change in relative fluorescence units for the 16 minute time point (Table 2, boxed data) is plotted against well number. The Z' value for this data is 0.71.

Table 3.2 Statistical analysis of reaction progress curves.

Boxed values signify the time points for routine analysis, where assay statistics reached plateaus and satisfactory Z' values.

Table 2

Statistical analysis of 50nM AcpS and 12.5 nM Sfp progress curves

time	6	8	10	12	14	16	18	20	22	24	26	28
<i>AcpS</i>												
Z'	-0.92	0.02	0.35	0.47	0.59	0.59	0.68	0.68	0.72	0.71	0.74	0.74
signal:noise	3.1	6.1	9.2	11.2	14.6	14.6	18.3	18.5	20.5	20.2	21.8	21.9
signal:background	4.0	8.2	6.4	8.4	8.6	8.3	8.1	11.4	10.7	10.8	10.7	13.3
signal window	-2.9	0.1	3.2	5.2	8.7	8.7	12.5	12.6	14.9	14.4	16.0	16.2
<i>Sfp</i>												
Z'	-0.11	0.33	0.51	0.62	0.64	0.70	0.70	0.73	0.76	0.76	0.77	0.78
signal:noise	5.4	8.9	12.2	15.4	15.5	19.2	19.4	20.8	23.5	23.4	24.5	25.5
signal:background	7.0	8.8	9.3	10.1	10.0	11.6	10.8	11.4	11.9	14.0	15.9	14.6
signal window	-0.6	2.9	6.2	9.6	9.9	13.5	13.7	15.2	17.8	17.8	19.0	19.9

Subsequently, this experiment was repeated on three separate days to assess the robustness of the method, and the data are presented in Table 3. The Z' factor (Zhang et al., 1999) is often used to evaluate the suitability of a screening method for high throughput implementation, with values greater than 0.5 being considered satisfactory. The assay performed well, and gave Z' values of 0.72 ± 0.01 and 0.75 ± 0.02 for Sfp and AcpS, respectively.

Screen validation for inhibitor identification

To demonstrate the ability of this screen to identify inhibitors of PPTases, we evaluated the effects of product inhibition by 3'-phosphoadenosine-5'-phosphate (PAP) **3** (Fig. 1), the nucleotide product released by the enzyme, utilized by McAllister *et al.* in their studies of the reaction mechanism of AcpS (McAllister et al., 2000). PAP was serially diluted (2-fold) from a top concentration of 10 mM in DMSO and stocked in polypropylene plates, and evaluated in the assay with both enzymes on three separate days (Fig. 7), again to demonstrate reproducibility of the screen. The method proved to yield consistent inhibition curves, with IC_{50} values $12.3 \pm 1.1 \mu\text{M}$ and $92 \pm 6 \mu\text{M}$ for Sfp and AcpS, respectively; and Hill coefficients for these analyses of -1.06 ± 0.09 for Sfp and -0.98 ± 0.11 for AcpS. Taken together, these data support the suitability of this method to determine inhibitory characteristics of compounds for these PPTase enzymes.

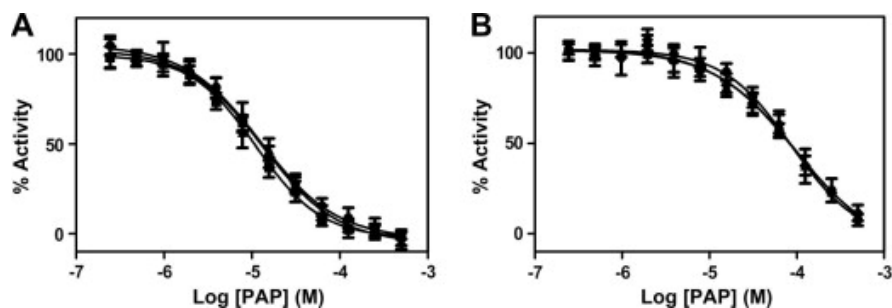


Figure 3.7 Reproducibility of IC₅₀ values for 3'-phosphoadenosine-5'-phosphate.

(A) Sfp was screened against 12 concentrations of PAP ranging from 244 nM to 500 μM on three separate days. The data were fit with the four-parameter dose response curve using GraphPad and returned IC₅₀ values of 13, 11, and 13 μM. (B) Replication of the same experiment as in A.) except using the AcpS enzyme. These curves returned IC₅₀ values of 86, 98 and 94 μM.

Table 3.3 Day-to-day variability of assay statistics for the FRET-based PPTase assay

Table 3

Day-to-day variability

statistical value	AcpS	Sfp
Z'	0.75 ± 0.02	0.72 ± 0.01
signal:noise	23.1 ± 2.1	19.9 ± 1.2
signal:background	10.8 ± 0.3	11.7 ± 1.5
signal window	17.3 ± 2.0	14.3 ± 1.1

CONCLUSIONS

In summary, we have developed a homogenous screen for PPTase that requires a minimum number of liquid handling steps, and meets the criteria set forth by the NIH Chemical Genomics Center as acceptable for automation (2009b). Importantly, this method utilizes simple reagents that can be prepared through traditional techniques (La Clair et al., 2004a, Wellings and Atherton, 1997b), and are pure chemical entities that do not require interbatch standardization, a luxury not afforded by complex biochemical reagents. It is anticipated that this method can be used to evaluate the crossreactivity of currently known AcpS inhibitors, and to identify new inhibitor architectures for Sfp and AcpS, and this work is currently in progress.

ACKNOWLEDGEMENTS

This work was funded by NIH R01GM075797 and 1R03MH083266. We thank Christopher T. Walsh (Harvard Medical School) for plasmids containing the Sfp and AcpS expression systems, Elizabeth A. Komives for guidance and assistance with peptide synthesis, and Adam Yasgar and Anton Simeonov (NIH Chemical Genomics Center) for helpful discussions.

Chapter 3, in whole, is a reprint of material as it appears in *Analytical Biochemistry* (2009) Vol. 394, pp. 39-47. I was the primary author of this work, and the research was performed under the guidance of Prof. Michael Burkart.

Chapter 4

PHOSPHOPANTETHEINYL TRANSFERASE INHIBITORS AND SECONDARY METABOLISM

ABSTRACT

Efforts to isolate carrier protein-mediated synthases from natural product producing organisms using reporter-linked post-translational modification have been complicated by the efficiency of the endogenous process. To address this issue, we have chosen to target endogenous phosphopantetheinyl transferases for inhibitor design to facilitate natural product synthase isolation through a chemical genetics approach. Herein we validate secondary metabolism-associated PPTase for chemical probe development. We synthesize and evaluate a panel of compounds based on the anthranilate 4*H*-oxazol-5-one pharmacophore previously described to attenuate phosphopantetheinyl transferase activity within bacterial cultures. Through the use of a new high-throughput FRET assay, we demonstrate that these compounds exclusively inhibit fatty acid synthase-specific PPTases. *In vivo*, a lead compound within this panel demonstrated selective antibiotic activity in a *Bacillus subtilis* model. Further evaluation demonstrated that the compound enhances actinorhodin production in *Streptomyces coelicolor*, revealing the ability of this class of molecules to stimulate precocious secondary metabolite production.

INTRODUCTION

Fatty acids, nonribosomal peptides, and polyketides represent three classes of metabolites that play important roles in human health, disease, and therapy (Paduch et al., 2007, Cimolai and Cimolai, 2007, Newman and Cragg, 2007, Cragg and Newman, 2005). Current studies of the modular synthases that produce these molecules aim to

both understand and engineer their multidomain biosynthesis (Hutchinson et al., 1989, Walsh, 2002, Kirschning et al., 2007). A limiting factor in these studies is the identification and elucidation of the gene clusters encoding the enzymatic machinery responsible for natural product biosynthesis (Van Lanen and Shen, 2006, Zazopoulos et al., 2003). This problem is particularly acute in the case of organisms possessing large or complex genomes in which genetics-based approaches have had limited success (Kubota et al., 2006).

All three classes of natural products are assembled by the polymerization small of amino and carboxylic acid precursors by large multienzyme complexes (i.e. synthases), and may contain as few as one, or as many as 47 enzymatic domains housed on a single polypeptide. A central theme in these biochemical pathways is tethering of the nascent polymer to small carrier protein domains of the synthases through thioester linkage. This thioester bond is not appending the β -sulphydryl group of a cysteine residue, but a 4'-phosphopantetheinyl (4'-PP) arm that is installed at a conserved serine residue as a post-translational modification from coenzyme A (CoA)

1. Phosphopantetheinyl transferase enzymes (PPTase, E.C. 2.7.8.7) catalyse this transfer, converting the translated proteins from their *apo*- to *holo*- forms, and is an obligatory requirement for processivity in the biochemical pathway (Fig. 1A).

These PPTase enzymes belong to a distinct structural superfamily organized into three classes based upon primary structure (Lambalot et al., 1996a). Two of these classes, the AcpS-type and Sfp-type PPTases, are responsible for modifying carrier protein domains in all secondary metabolic pathways. Typically, the former class is restrictive with regard to the identity of carrier protein substrates it will modify, acting

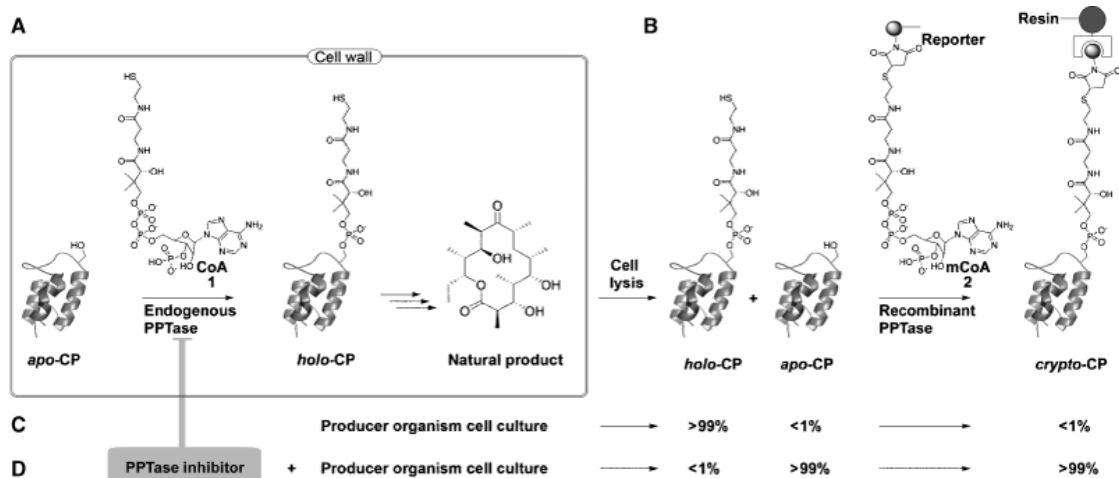


Figure 4.1 Isolation of carrier protein-dependent biosynthetic machinery.

(A) natural product synthases are converted from their *apo*- to *holo*- forms by action of phosphopantetheinyl transferase (PPTase) with coenzyme A (CoA) **1**, installing 4'-phosphopantetheinyl functionality on a conserved serine residue on carrier protein domains. (B) Cell lysis releases synthases for derivitization by treatment with modified CoA (mCoA) **2** and exogenously added PPTase. (C) Following this procedure with producer organisms generates cell lysates containing predominantly *holo*-carrier proteins and poor yield of *crypto*-synthases. (D) Culturing producer organisms with a phosphopantetheinyl transferase inhibitor may allow access to increased concentrations of *apo*-carrier proteins in cell extracts and improve *crypto*-synthase isolation.

only on dissociated fatty acid synthase-acyl carrier protein (FAS-ACP) and analogous type-II polyketide synthases. Similarly, the Sfp-type PPTases may exhibit a stringent specificity for carrier proteins domains of their associated pathway (e.g. EntD). However, a number of congeners of this latter division have been identified that possess a broad selectivity, and display cross-reactivity with FAS-ACP (Lambalot et al., 1996a).

In 2004, we reported the use of PPTases to selectively label carrier protein domains within modular biosynthetic machinery for the detection, isolation and identification of engineered systems (La Clair et al., 2004a). This method utilizes *apo*-carrier proteins, and converts them to their thiol-blocked or *crypto*- form with reporter labels originating from modified CoA (mCoA) analogues **2** (Fig. 1B). In applying this approach to natural product-producing organisms, we have found the technique complicated by the efficiency of endogenous protein modification (Fig. 1C). This method could be used to visualise natural product synthases via western blot, but it was insufficient as a means to isolate them from lysates of producer microbes due to the abundance of *holo*-synthases relative to their *apo*- form (Fig. 1C). We are currently investigating methods to either exploit (Clarke et al., 2005a, Meier et al., 2006b) or circumvent this issue. Toward this end, we envisioned a chemical genetics approach involving the culture of producer organisms in the presence of PPTase inhibitors as a means to increase the *apo*- vs. *holo*-carrier protein domain ratio from cellular extracts (Fig. 1D).

PPTase inhibitors have been of interest recently as possible antibiotics, with a focus on the modification of bacterial FAS-ACP. A number of groups have begun

focused programs to develop AcpS inhibitors as possible solutions to multi-drug resistance (Chu et al., 2003c, Gilbert et al., 2004, Joseph-McCarthy et al., 2005b, McAllister et al., 2000, Payne et al., 2007), and several scaffolds have recently been disclosed (Chu et al., 2003c, Gilbert et al., 2004, Joseph-McCarthy et al., 2005b). However, the lead compounds from these campaigns have not been evaluated for cross-reactivity against Sfp-type PPTases; and their characterization in this manner makes a logical starting point for our studies.

To this end, we recently reported the development of a high-throughput FRET-based assay for PPTase enzymes that was validated to characterize inhibitors against both PPTase classes (Foley and Burkart, 2009). In this report, we focus this assay to target secondary metabolism-associated PPTases for chemical probe development. We detail the preparation of a 25-compound panel based on the anthranilate 4*H*-oxazol-5-one pharmacophore, a scaffold of known activity with AcpS-PPTase. Using the FRET-based assay, we uncover the null-activity of this class of compounds with Sfp-PPTase. After identification and characterization of a lead compound, we reveal intriguing effects of this inhibitor to trigger precocious secondary metabolite production in *Streptomyces coelicolor*.

RESULTS & DISCUSSION

Chemical probe target validation: natural product synthase labeling in *Bacillus subtilis* deficient in secondary metabolism-associated PPTase

Because the overall goal of these studies is to achieve increased *apo-* vs. *holo-* synthase ratios by treating cell cultures with PPTase inhibitors, our first study was to determine whether inhibitors against Sfp-type PPTase would provide the desired phenotypic outcome. It is possible that an Sfp-targeting inhibitor merely downregulates modular synthase expression. Therefore, positive synthase detection in a PPTase deficient strain would confirm that our intent to block *in vivo* PPTase activity through use of inhibitors could be a viable chemical knock-out methodology (Hung et al., 1996). To this end, we chose to work in the Gram positive *Bacillus subtilis*, whose machinery responsible for the production of surfactin has served as a model to investigate the mechanism and regulation of nonribosomal peptide biosynthesis in prokaryotes (Steller et al., 2004, Tsuge et al., 1996, Ullrich et al., 1991, Kluge et al., 1988, Marahiel et al., 1993, Nakano and Zuber, 1990, Nakano and Zuber, 1989, Nakano et al., 1988). Within the genome of this organism are contained some 43-identified carrier protein-domains involved in secondary metabolism, with only a single PPTase responsible for their posttranslational modification (Mootz et al., 2001).

It was recognized that manipulation of this organism to render it competent resulted in the loss of capacity to produce surfactin by laboratory strains (PY79 and 168), while genetic experiments demonstrated that the genes necessary to produce these compounds had been retained within the genome (Nakano and Zuber, 1990, Nakano and Zuber, 1989, Nakano et al., 1988). Nakano *et al.* identified the *sfp* locus as a lesion point that disrupts the biosynthetic capacity of *B. subtilis* 168 by demonstrating that transfer of the wildtype locus to the laboratory strain (generating

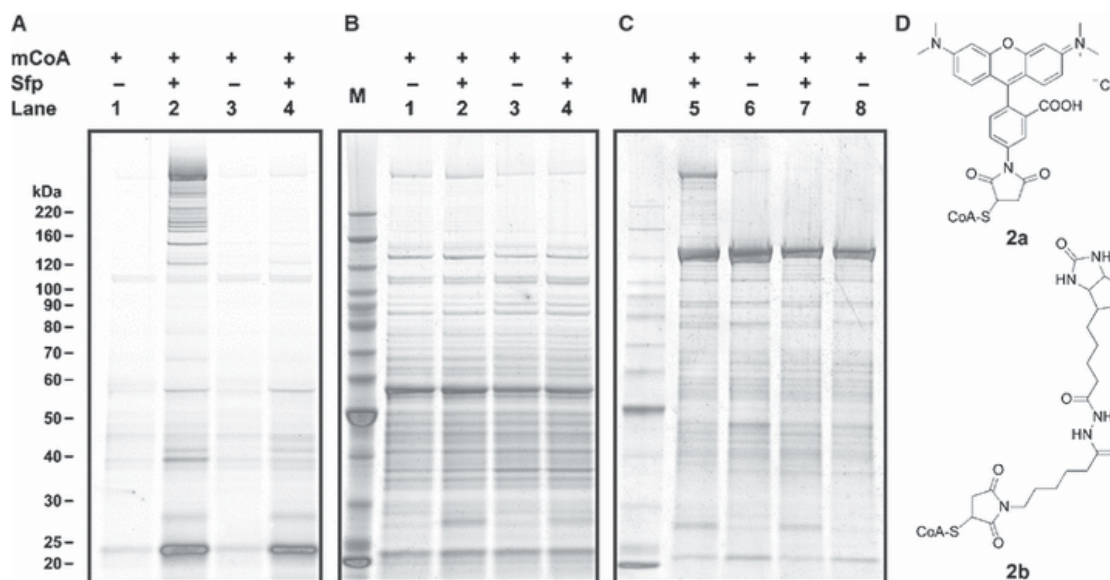


Figure 4.2 Target validation in *Bacillus subtilis* Sfp^{+/-}

B. subtilis 168 contains a lesion in the *sfp* gene and does not produce a viable gene product, and strain OKB105 is a gain of function mutant possessing the wild type allele. Extracts of early stationary phase *B. subtilis* were reacted with CoA analogues and recombinant Sfp PPTase, separated via SDS-PAGE and visualised by fluorescence scanning. (A) *B. subtilis* lysates were treated with 25 μ M rhodamine-mCoA **2a** (D) in the presence or absence of exogenously added Sfp. A number of high molecular weight proteins were labeled in an Sfp dependent manner in the 168 strain (Sfp⁻ genotype, lane 2 v. lane 1) that were undetectable in strain OKB105 (Sfp⁺ genotype, lane 4 v. lane 3). (B) Total protein stain of the gel in (A) demonstrating equal protein loading and the low relative abundance of fluorescently visualised proteins. (C) Reaction of cell lysates in (A) with biotin-mCoA **2b** (D) varying by treatment with or without exogenous Sfp. After removal of excess **2b**, biotinylated proteins were isolated with streptavidin-agarose, washed, and separated by SDS-PAGE. Sfp-dependent isolation is determined by comparing proteins observed in Sfp(+) lanes (5 and 7) vs. Sfp(-) controls (lanes 6 and 8). (D) structures of mCoA analogues used in these experiments.

OKB105) restores metabolite production (Nakano et al., 1988, Nakano et al., 1992). Thus, the common laboratory strain 168, and this gain-of-function mutant, OKB105, serve as pair of isogenic strains in which to assess the biochemical effects that inactivation of a PPTase locus may have on the stability of *apo*-synthases expressed at endogenous levels.

We evaluated our labeling technique with stationary phase cultures of *B. subtilis* 168 and OKB105, and data are presented in Fig. 2. Initially we verified synthase expression by probing the detection of Sfp-dependent modification with a fluorescent mCoA **2a**. Cellular extracts were reacted with rhodamine mCoA **2a** in the presence or absence of exogenously added Sfp, and separated on a gradient polyacrylamide gel. Fortuitously, fluorescence gel imaging showed that strain 168 produced a number of high molecular weight proteins labeled in an Sfp-dependent manner (Fig. 2A, lanes 1 and 2). However, these proteins were undetectable in OKB105 when the labeling reaction is compared to the control (Fig. 2A, lanes 3 and 4). The high molecular weight, and relative low abundance of the observed proteins suggests that they are polyketide and nonribosomal peptide synthases, and their detection with fluorescent probe **2b** may be enhanced by the multiplicity with which the carrier protein target of modification occurs in these modular enzymes. Total protein stain of the gel, presented in Fig. 2B, demonstrates that these observations were not a result of biased protein loading. The absence of detection in lane 4 relative to lane 2 (Fig. 2A) confirms the high efficiency of endogenous PPTase activity, and that successful detection with our method may be achieved in organisms possessing an appropriate genotype.

Building upon this, we sought to verify our enrichment procedure by demonstrating the selective isolation of these proteins with a biotin mCoA **2b** and immobilized streptavidin. Derivatization of the same protein samples as Fig. 2A & B with a biotin reporter **2b** and subsequent immobilization on streptavidin-agarose allows for the Sfp-dependent isolation of these proteins (Fig. 2C). Comparatively, there is correlation between fluorescently labeled and isolated proteins. With the latter technique, we have confirmed sequence from these proteins to be of polyketide and nonribosomal peptide synthase origins (Meier, J.L., Niessen, S., Hoover, H.S., Foley, T.L., Cravatt, B.J., Burkart, M.D., unpublished work). This method also isolated a number of lower molecular weight proteins in a nonspecific manner, and these presumably contain or bind to biotin carrier protein domains; with a significant enrichment of a 130 kD protein. This protein was identified as pyruvyl carboxylase by genomic and mass spectral analysis (data not shown). Furthermore, we found that the results observed above could be enhanced by increasing the quantity of input sample, and this gave a robust signal over background (fig. S1). It is noteworthy that while it is anticipated that the contaminants present in both samples may be achieved through background preclearing by treatment with streptavidin-agarose (Araga et al., 2000, Grosset et al., 2000, Schonhoff et al., 2006) before phosphopantetheinylation, their presence serves as a control for sufficient protein loading and successful protein isolation, as well as a standard for the correlation of relative protein abundance in the cellular extract.

Taken together, these experiments demonstrate that in the absence of phosphopantetheinylation, the expression and stability of polyketide and nonribosomal

peptide synthases is sufficient for their detection and isolation with our current strategy.

Anthranilate-4*H*-oxazol-5-ones are specific inhibitors of AcpS-Type PPTase

With a genetic rationale for a chemical genetic solution, we turned toward identifying a class of known PPTase inhibitor for our studies. When we began, two groups had published chemical structures with antagonistic activity with AcpS (Gilbert et al., 2004, Chu et al., 2003b). The first involved an anthranilic acid-based structure that had been identified by chemical library screening; the second had been isolated from the extract of an uncharacterized bacterial culture (Chu et al., 2003b). Of these, we chose anthranilate 4*H*-oxazol-5-ones described by Gilbert *et al.* (Gilbert et al., 2004) to be synthetically tractable as a starting point for our own studies.

The preparation of these compounds was accomplished by reported procedures, as outlined in Figure 3, and described in detail in the Supplementary Materials (documents S2 and S3). A parallel synthetic approach produced a 25 compound panel of anthranilate oxazolones (Fig. 3A). In designing the library we selected commercially available benzoyl chlorides **3a-e** (Fig. 3B) varying at the *o*-, *m*- and *p*- positions to obtain diverse functionality to allow for differences between the AcpS and Sfp enzymes, and chose to combine the 5-(ethoxymethylene)-oxazolone products **5a** with five anthranilic acids **6a-e** (Fig. 3C) that repeatedly gave the highest potency.

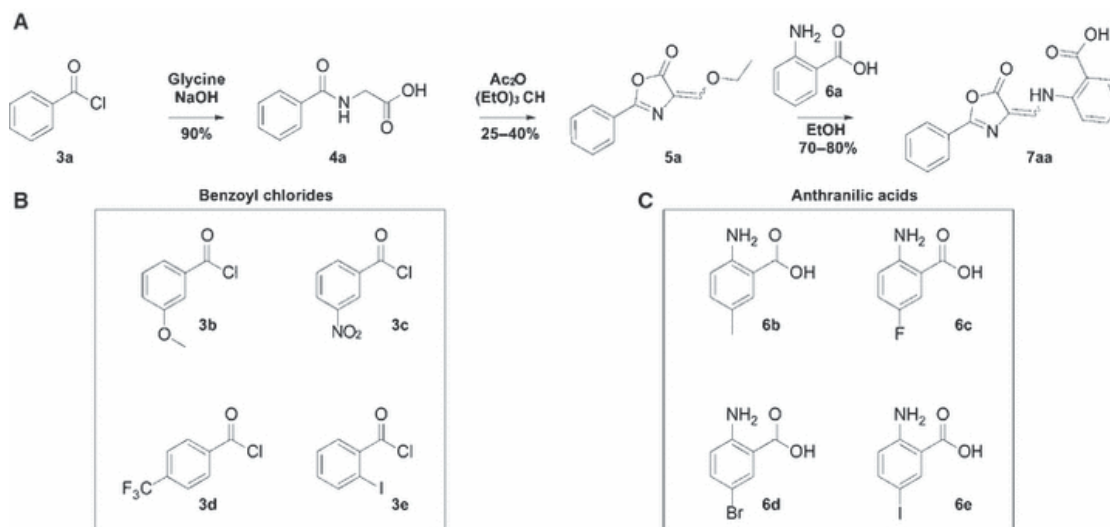


Figure 4.3 Synthesis of anthranilate 4*H*-oxazol-5-ones.

4*H*-anthranilate oxazol-5-one **7aa** and its derivatives are prepared following a 3 step reaction sequence. First, the benzoyl chloride **3a** is coupled to glycine to give hippuric acid **4a** as a filterable white solid. **4a** is then cyclized with acetic anhydride and condensed *in situ* with triethyl orthoformate to give the ethoxy (4*H*)-oxazol-5-one **5a**. Displacement of the ethyl enol ether with anthranilic acid **6a** in refluxing ethanol gives the desired product **7aa** as a precipitate. Systematic preparation of these compounds beginning with acyl halides **3a-e** and combination of their ethoxy (4*H*)-oxazol-5-ones **5a-e** with anthranilic acids **6a-e** yielded a 25 compound panel **7aa-ee** to be evaluated.

We screened this panel against *E. coli* AcpS and Sfp, the canonical models of both enzyme classes, using a high-throughput FRET assay format. This method utilizes a fluorescein-modified acceptor peptide (FITC-YbbR **8**) that generates a FRET pair upon conversion to the *crypto*- product **9** by action of PPTase in conjunction with rhodamine-mCoA **2a** as a cosubstrate (Fig. 4). This evaluation was performed at eight concentrations ranging from 0.4 - 50 μ M, and the data with Sfp revealed that none of the compounds inhibited the enzyme with IC₅₀ values below 50 μ M. IC₅₀ data for AcpS are presented in Fig. 5 and demonstrate that we had prepared only modest inhibitors of this enzyme. Analysis of this data identified compound **7ae** possessed the greatest inhibitory activity and was advanced as the lead for biological evaluation. This compound was prepared on a gram scale, and the integrity of the new material assessed spectroscopically and biochemically.

Antibiotic evaluation of 7ae in *B. subtilis*

Since we had an AcpS selective inhibitor in hand, biological studies of **7ae** began with antibiotic susceptibility assays in *B. subtilis* strains 168 and OKB105 (*vide supra*). In these studies, **7ae** exhibited minimum inhibitory concentration values of 62.5 and 200 μ M against *B. subtilis* 168 and the Sfp-containing mutant OKB105, respectively. These differential values suggest that the compound crosses the cell membrane and inhibits AcpS, and that the *sfp*⁺ genotype enhances tolerance to **7ae**. While the MIC value observed in strain 168 was not impressive in terms of an antibiotic development campaign, these concentrations are acceptable, for our

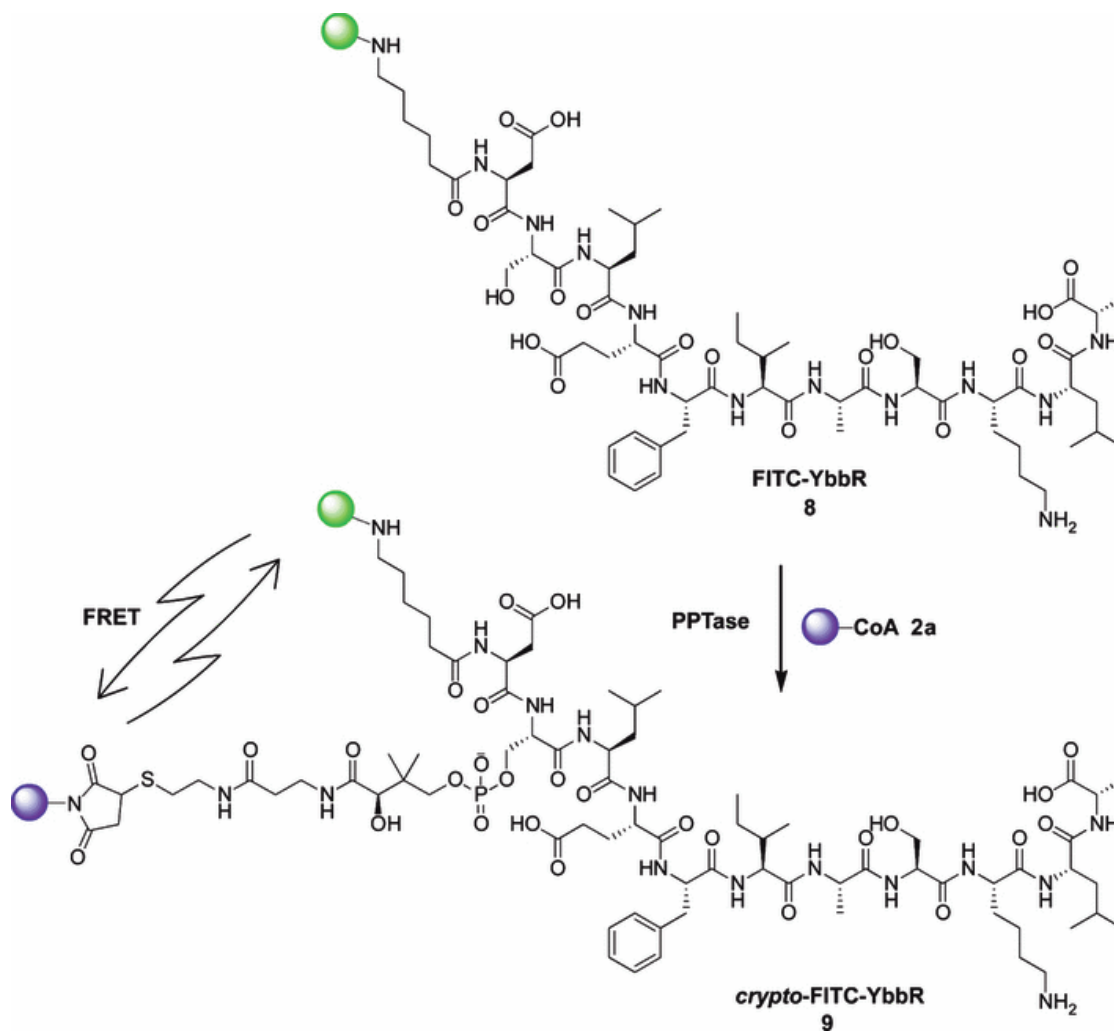
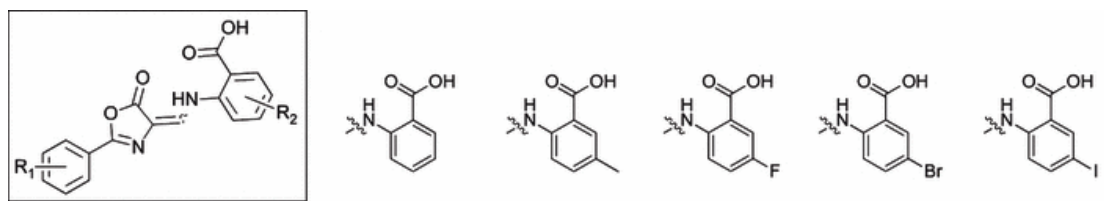


Figure 4.4 Design of a Förster resonance energy transfer assay for phosphopantetheinyl transferase.

The YbbR undecapeptide was recently described by Yin *et al.* to serve as a minimalized substrate for phosphopantetheinyl transferase. Fluorescein isothiocyanate modified YbbR **8** creates a FRET-paired *crypto*-YbbR upon reaction with a fluorescent mCoA and PPTase.



The figure shows the general structure of a 4H-oxazol-5-one library with substituents R₁ and R₂. Below it are five specific substituted benzamide derivatives used in the study, each with a different R₂ group: unsubstituted, methyl, fluorine, bromine, and iodine.

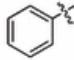
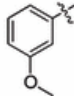
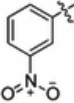
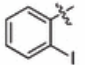
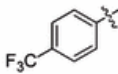
	>50	>50	>50	13.3	5.0
	24.3	34.4	>50	11.1	10.4
	>50	30.1	12.7	12.7	25.2
	>50	9.9	>50	8.4	8.2
	>50	40	>50	10.6	>50

Figure 4.5 Inhibition of PPTases from small 4*H*-oxazol-5-one library.

The library was screened against *E. coli* FAS PPTase (AcpS) and *B. subtilis* Sfp PPTase at 8 concentrations ranging from 0.4-50 μ M. K_i data for AcpS. Screening of Sfp revealed that none of the compounds inhibited the enzyme with IC₅₀ values less than 50 μ M. Compound **7ae**, bearing no functionalized R₁ and 5-iodo- substitution for R₂, was chosen as a lead for biological evaluation.

purposes, with regard to compound solubility and supply, and warranted further investigation.

An AcpS inhibitor precociously activates actinorhodin production in *S. coelicolor*

We next sought to evaluate the effects of **7ae** on fermentation yield of a natural product, with the tentative hypothesis that inactivation of a pathway's PPTase should preclude production. With this in mind, we chose to evaluate the effects of the lead on the yield of actinorhodin **10**, a type-II polyketide produced by the filamentous soil bacterium *Streptomyces coelicolor* A(3)2 (Fig. 6A) (Bystrykh et al., 1996) that can be rapidly observed and quantified by its blue color. Of the three PPTases identified within the genome, it has been suggested that posttranslational modification of actinorhodin acyl carrier protein (Act-ACP) is performed by AcpS itself (Cox et al., 2002, Stanley et al., 2006, Cerdano et al., 2001).

The investigation began by examining antimicrobial activity of **7ae** with zone of inhibition (ZOI) experiments. After 2 days at 25°C, no measurable ZOI was observed. However, at 4 days, a pronounced dark circle of actinorhodin **10** developed around the discs containing greater than 50 µg of **7ae**, indicating that production had been enhanced (Fig. 6B). These results were intriguing, as we had anticipated attenuation of fermentative yield upon treatment with **7ae**.

To further investigate this activity, we cultured *S. coelicolor* in defined liquid medium to control the growth conditions, in particular pH, which has been demonstrated to drastically affect fermentative yield (Wright and Hopwood, 1976, Elibol, 2002). Given this, we chose the iron deficient medium of Coisne

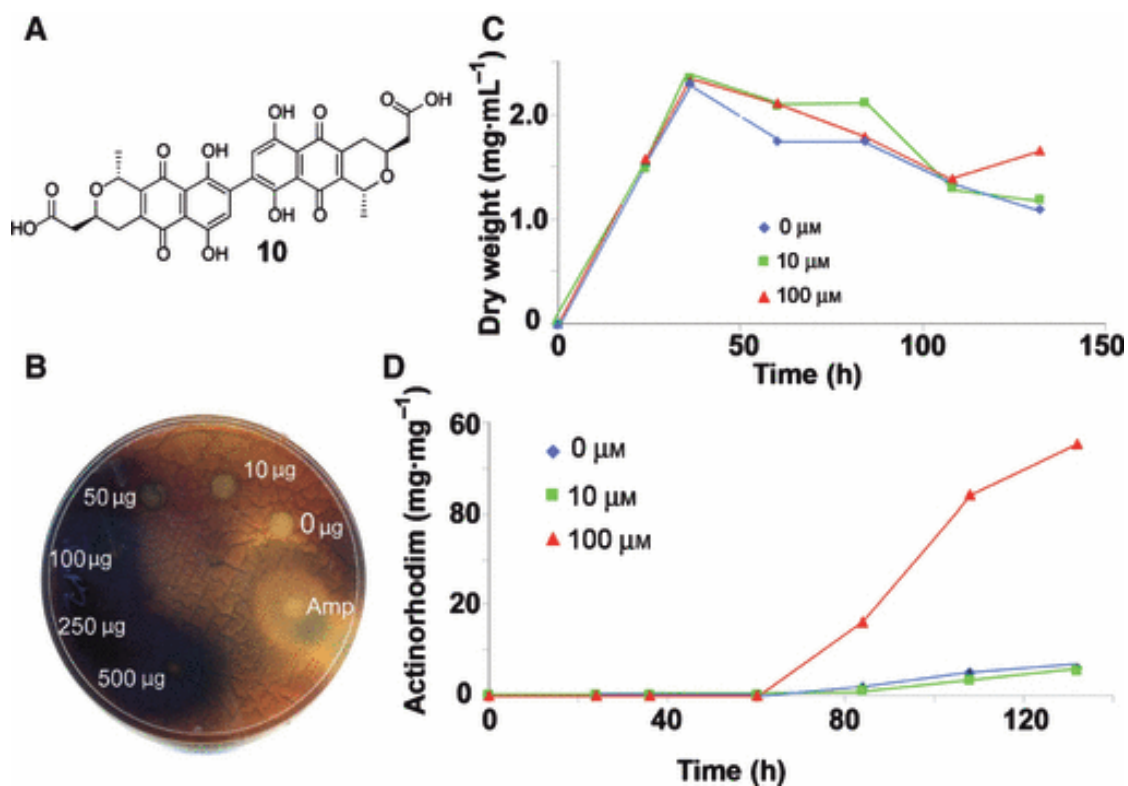


Figure 4.6 Biological evaluation of **7ae** in *Streptomyces coelicolor*.

Compound **7ae** was evaluated to determine effects on bacterial growth and natural product production in *Streptomyces coelicolor* A(3)2. (A) Upon entry into stationary phase, *S. coelicolor* produces the blue-pigment actinorhodin **10**. (B) Filter discs containing **7ae** were placed on lawns of *S. coelicolor* to assess antimicrobial activity of the compound. No zones of inhibition were observed and after 4 days incubation, increased production of **10** was triggered by discs containing higher amounts of **7ae**. (C) Dry mycelial weight curve for liquid culture evaluation of **7ae** showed no effects of the compound on growth. (D) Actinorhodin production as a function of time from the same cultures as (C). Culturing of the organism with 100 µM **7ae** increased actinorhodin titer 800 %.

(Coisne et al., 1999) that was shown to provide the most enhanced production of excreted pigments. Culturing of the organism over the course of seven days according to this protocol in the presence of 0, 10 or 100 μM **7ae**, confirmed our results observed on solid media and demonstrated that the compound has no effect on dry mycelial mass of the culture (Fig. 6C). In evaluating actinorhodin production, cultures containing 100 μM **7ae** showed an 800 % increase in actinorhodin production compared to DMSO controls (Fig. 6D).

The complex regulation of the actinorhodin biosynthetic pathway has been substantially investigated, and a number of metabolic stress sensing networks are capable of effecting fermentative yield (Coisne et al., 1999). These, coupled to our current understanding of cross-pathway phosphopantetheinyl transfer events, have led to our current hypothesis describing the effects of **7ae** on actinorhodin titer (Fig. 7). In this model, chemical inactivation of AcpS transduces a nutrient-deficiency signal, triggering up-regulation of secondary metabolic pathways and concomitant metabolite production. Included within the regulon of these pathways are Sfp-type PPTases that are immune to inhibitory effect of the compound. Crossover of one or more of these enzymes into primary metabolism rescues the organism from the growth inhibitory effects of **7ae**, consistent with null effects of the inhibitor on growth (Fig. 6C). While it cannot be overlooked that inhibition of FAS by this compound may increase the flux of acetate units through the actinorhodin biosynthetic pathway by decreasing the demand on a shared substrate pool, this is not supported by growth curve data or the current suggestions that AcpS modifies Act-ACP, as inhibition of this enzyme would simultaneously have deleterious effects on both pathways.

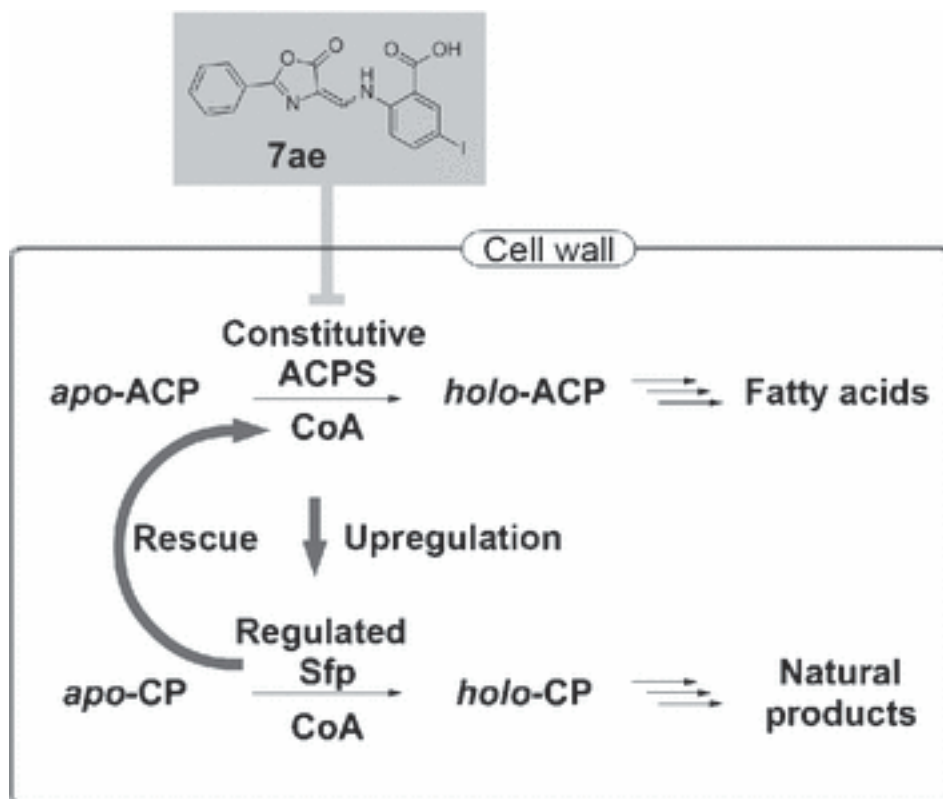


Figure 4.7 Working hypothesis of how PPTase inhibition increases natural product yield.

Culturing of an organism with **7ae** chemically inactivates constitutive AcpS, leaving fatty acid synthase acyl carrier protein (ACP) in the *apo*- form. A signal from this inactivation triggers the upregulation of natural product gene clusters that contain a Sfp-type PPTase. This Sfp-type PPTase is immune to the inhibitory effects of **7ae**. Sfp-PPTase can accept the fatty acid synthase ACP as a substrate, reactivating FAS and permitting continued growth. Concomitantly, global translation of the natural product operons and phosphopantetheinylation of PKS and NRPS enzymes initiates secondary metabolite production.

The inability of anthranilate oxazolones to act against Sfp-type PPTases offers caution to programs developing inhibitors targeting AcpS for clinical application (Gilbert et al., 2004, Joseph-McCarthy et al., 2005b, McAllister et al., 2000, Payne et al., 2007). In the classical model of phosphopantetheinyl transfer from *E. coli*, each carrier protein-dependent primary and secondary metabolic pathway contains a dedicated PPTase, and cross-pathway phosphopantetheinyl transfer does not occur (Lambalot et al., 1996a, Flugel et al., 2000). Hence, disruption of a pathway's cognate PPTase locus precludes metabolite production. While this model appears to hold in *E. coli*, it does not accurately describe the essentiality of PPTase loci when a Sfp-PPTase with broad substrate specificity is contained within the genome. Overlap of phosphopantetheinyl transfer from a secondary metabolic pathway into primary metabolism may rescue the chemical inactivation of the primary metabolism-associated gene product. This concept has been demonstrated genetically in wild type *B. subtilis*, where Sfp can rescue viability when lesions are introduced into *acpS* (Mootz et al., 2001); and organisms (i.e. *Pseudomonas*) have been identified where possession of a broad-specificity Sfp-PPTase has viably compensated for complete loss of the *acpS* locus (Barekzi et al., 2004, Mootz et al., 2001).

CONCLUSIONS

In conclusion, secondary metabolism-associated PPTase has been validated as a target for the development of chemical knockout probes to increase the *apo:holo*-carrier protein ratios in crude cellular extracts. We have used a new assay format to demonstrate the selectivity of anthranilate-4*H*-oxazol-5-one compounds for the AcpS-

type enzyme. These findings suggest that furthering of this chemical genetics approach to natural product synthase isolation will require a discovery campaign to identify inhibitory architectures of Sfp. Finally, evaluation of a lead selected from our panel has revealed a new route to elicit precocious effects on secondary metabolism in *Streptomyces coelicolor*. These results offer the tantalizing prospect of a general mode of induction for secondary metabolites, and further investigation into a metabolic rationale is ongoing.

MATERIALS AND METHODS

General

Unless otherwise stated, all chemicals were purchased from Sigma-Aldrich (St. Louis, MO). N,N,N',N'-tetramethylrhodamine-5-maleimide (TAMRA), Sypro Ruby, and Novex electrophoresis materials were purchased from Invitrogen Corporation (Carlsbad, CA). Biotin maleimide was purchased from Sigma (St. Louis, MO). Coenzyme A trilithium salt was purchased from EMD biochemicals (San Diego, CA).

***Bacillus subtilis* culturing and cellular extract preparation.** *Bacillus subtilis* 168 and OKB105 cultures were maintained on solid LB medium containing 1.5 % agar. 2 mL liquid cultures in LB medium were inoculated from a single colony and incubated overnight at 37 °C with shaking. The following morning, 0.1mL of overnight culture was used to seed 50 mL of LB medium in 250 mL furnbach flasks.

Cultures were grown at 37 °C in an Innova 4330 incubator (New Brunswick Scientific) with orbital shaking at 250 RPM. After 12 h, cells were harvested by centrifugation for 30 minutes at 4000 x g in a Beckman Coulter Avanti J-20 XP instrument fitted with a JLA 8.1000 rotor. The culture supernatant was decanted, and the cell pellets frozen at -80°C.

For analysis, the cell pellet was resuspended in 3 mL Lysis Buffer (50 mM Tris Cl pH 8.0, 250 mM NaCl, 1 mM phenylmethane sulfonyl fluoride, 10 µM leupeptin, 10 µM pepstatin), lysozyme (Worthington Biochemicals, Lakewood, NJ) added to a final concentration of 0.1 mg/mL and incubated 30 min at room temperature. Cells were then lysed by sonication and the cell debris cleared by centrifugation at 25,000 x g for 30'. The cellular extract was decanted, and quantified using the method of Bradford (Bradford, 1976).

Fluorescent *In vitro* phosphopantetheinylation of carrier protein domains in *B. subtilis*. To 400 µL of cellular extract (diluted to contain 1.0 mg protein, 2.5 mg/mL) was added 50 µL 10X PPTase reaction buffer (500 mM Na HEPES, 100 mM MgCl₂, pH 7.6), 25 µM 1 M MgSO₄, 25 µL 500 µM mCoA probe **2a**, and 1 µL Sfp (765 µM stock) or ddH₂O. Reactions were incubated 30 min at 37 °C and then quenched by the addition of 500 µL 0.5 M EDTA, pH 6.8. Unreacted probe was removed by passage over a PD-10 desalting column (Bio-Rad) equilibrated in Lysis Buffer while collecting 0.5 mL fractions. Those containing protein were pooled and protein concentrations determined. Samples were prepared for SDS-PAGE by dilution to 200 µg/mL, followed by addition of 1/3 volume 4 X LDS sample buffer (Invitrogen

Corporation) containing 50 mM DTT (final concentration). Samples were held at 70 °C for 20 min, cooled, and then separated on a Novex 4-12 % Bis-Tris gel using MOPS running buffer (Invitrogen Corporation) at a constant potential of 150 volts. The gels were imaged with a Typhoon Trio flatbed laser scanner (GE Healthcare) using the TAMRA settings. Total protein staining of the gel was routinely performed with Blue Silver colloidal Coomassie (Candiano et al., 2004) or Sypro Ruby (Invitrogen Corporation) and imaged with either a Perfection 3490 Photo scanner (Seiko Epson America, Long Beach, CA) or the Typhoon imager, respectively.

***In vitro* biotinylation and affinity purification on streptavidin agarose.** To 400 μ L of extract (1.0 mg protein) was added 50 μ L 10 X PPTase reaction buffer (*vide supra*) and 25 μ M mCoA **2b**, 1 μ M Sfp, and water to 0.5 mL total volume. The reaction was incubated at 37 °C for 30 minutes, quenched by addition of 500 μ L 0.5 M EDTA (pH 6.8), and desalted over a PD-10 column equilibrated in Lysis Buffer; to remove excess **2b** and endogenous biotin. The protein containing fraction was brought to 3 mL volume with column buffer in a 15 mL falcon tube, and 100 μ L of a 50 % slurry of Streptavidin-Agarose (Pierce Biochemicals) equilibrated in column buffer added. Tubes were shaken at room temperature for 1 h. The resin was collected by centrifugation at 300 x g for 30 s. The resin was washed 5 x 500 μ L of wash buffer (50 mM TrisCl, 1 M NaCl). After the final wash was decanted, 100 μ L of 1 X SDS-PAGE sample buffer was added and the samples boiled for 5 minutes. After cooling, the resin was pelleted by centrifugation for 30s at 100 x g and the 25 μ L of the supernatant

separated on a Novex 4-12 % Bis-Tris gradient gel as above. After completion, the gel was fixed and stained for total protein as above.

Synthesis of assay components. CoA analogues were prepared by reaction of reduced CoA trilithium salt (5 mg/mL in 50 mM $\text{NH}_4\text{CO}_2\text{H}$ in 50 % MeOH) with 1.1 equivalents of either maleimide bearing probe **11** or **12** (Fig. S1, both dissolved at 1 mg/mL in 100 % MeOH). Excess **11** was removed by extraction three times using dichloromethane (**11**), and **12** was removed by semipreparative HPLC. The purity of both substrates was confirmed to greater than 95 % by HPLC.

FITC-YbbR peptide **8** was synthesized using an automated SPPS synthesizer (Applied Biosystems Pioneer). The sequence was appended with an N-terminal N-FMOC- ϵ -aminocaproic acid spacer, deprotected, and coupled overnight with FITC. Following cleavage from the solid support, the product FITC-YbbR **8** was HPLC purified and its identity verified by ESI-MS.

FRET screen conditions. Compound screening was performed essentially as previously described (Foley and Burkart, 2009). Briefly, Parent compound plates were made by dissolving **7aa-7ee** in dry DMSO at a concentration of 1 mM and serial diluting this 2-fold in DMSO. Compound solution from the parent plate (2.5 μL) were transferred to individual wells of a black polystyrene 96 well plate (Costar # 3694). To this, a 1.33 X enzyme solution was then added (37.5 μL , 16.6 nM Sfp, 66.6 mM HEPES-Na, 13.3 nM MgCl_2). Reactions were initiated by the addition of a 5 X substrate solution [7.5 μL , 25 μM FITC-YbbR, 50 μM Rhodamine-mCoA **2a**, 1 mM

NaH₂PO₄]. The reaction was monitored continuously (cycle time 2 minutes) for 1h in a Perkin Elmer HTS7000 microtiter plate reader with excitation filter = 485 nm, emission filter = 535 nm.

***Streptomyces coelicolor* A(3)2 zone of inhibition experiments.** *Streptomyces coelicolor* A(3)2 was grown on ISP2 media containing 2.0 % w/v agar to obtain spore stocks prepared according to a general procedure (Kieser, 2000). Spore stocks were diluted to a standard inoculum concentration of 1×10^7 CFU/mL.

The lead compound was dissolved in methanol at a concentration of 10 mg/mL. The appropriate quantity of the lead was applied to sterile filter paper discs in a laminar flow hood and allowed to dry for 4 h. Filter discs were then stored in 15mL disposable corning tubes with dessication at -20°C until use.

In a sterile laminar flow hood, Petri dishes (100 mm x 15 mm) containing ~15 mL of solid media were inoculated with 1×10^5 spores in 250 μ L H₂O to give a lawn of mycelium. After allowing the inoculum to soak in for 1 h, filter discs containing various amounts of **7ae** (10 – 500 μ g) , ampicillin (50 μ g), or vehicle (0 μ g) were placed on the plates and incubated at 25 °C. Growth was checked at 18, 24, 48, and 72 h, and at no time was a zone of inhibition observable. The plates were checked again at 96 h and actinorhodin production had begun surrounding the discs containing 250 and 500 μ g of compound. On day 4 of the experiment, the plates were imaged by placing them directly on a flatbed Perfection 3490 Photo scanner (Seiko Epson America, Long Beach, CA).

Liquid culturing of *S. coelicolor*. Liquid medium was prepared according to Coisne (Coisne et al., 1999). Basal media is prepared as by adding the following to 500 mL dH₂O: 2 g K₂SO₄, 1 g NaCl, 15 mmol K₂HPO₄, 40 mmol KNO₃, 80 mg Mg₂SO₄·7H₂O, 2 mg ZnSO₄·7H₂O, and 100 µL of Streptomyces trace element solution. This trace element solution contained per Liter: 500 mg CuSO₄·5H₂O, 5.0 g MnSO₄·H₂O, 4.0 g H₃BO₃, 500 mg CoCl₂·6H₂O, 2.0 g NiCl₂·6H₂O, and 3.0 g Na₂MoO₄·2H₂O. 100 mL of 0.5 M K·TES [potassium N-tris(hydroxymethyl)methyl-2-aminoethanesulfonate] buffer pH 7.0 was added and the pH adjusted to 7.0 by the addition of KOH and the final volume brought to 900 mL. The following solutions are also prepared and autoclaved: 1M glucose in ddH₂O and 2 % w/v CaCl₂·2H₂O. These three solutions are autoclaved separately for 45 min at 121°C. After cooling, 50 mL 1M glucose was added to the base media. 5 mL of 2 % w/v CaCl₂·2H₂O is then added slowly to the media with gentle agitation to minimize precipitation. The medium is completed by the addition of 50 mL 1 mg/mL defferated yeast extract (prepared by passing a 1 mg/mL solution of yeast extract (250 mL total) over 25 mL of Chelex 100 (Bio-rad) preequilibrated in 50 mM K·TES pH 7.0).

Culturing was performed at each concentration of **7ae** in triplicate as follows: 100 mL the above medium in 500 mL fernbach flasks was inoculated with 1×10^7 CFU in a laminar flow hood, and the spores allowed to germinate 12 h at room temperature overnight without agitation. The cultures were then transferred to an incubator and incubated at 30 °C with shaking at 250 RPM. At 36 h after inoculation, 100 µL of the triethylammonium salt of **7ae** in DMSO was added [at stock concentrations of 100 mM, 10 mM or 0 mM (vehicle control)] and the culturing

continued at 30 °C with shaking at 250 RPM. At the given timepoints, 5 mL of each culture was withdrawn from the culture and the mycelial mass collected by centrifugation. The supernatant was decanted and processed under “Quantitation of actinorhodin”. The mycelial pellet was resuspended in 1mL sterile water, transferred to tared scintillation vials, and dried by incubation overnight in an 80 °C oven. The scintillation vials were removed from the oven, cooled to room temperature, and their mass recorded. This value was divided by 5 (corresponding to the milliliters removed from the culture) and plotted against a time coordinate in hours and is presented in Fig. 6C.

Quantitation of actinorhodin. The culture supernatant yielded after centrifugation was diluted with 1M KOH in a microtiter plate and the absorbance at 635 nm recorded with a Perkins-Elmer HTS7000 microtiter plate reader. Absorbance values ranging from 0.2-0.5 AU were corrected for the dilution factor and quantified using an extinction coefficient of $25,320 \text{ cm}^{-1}\text{M}^{-1}$ (Bystrykh et al., 1996).

Synthetic Procedures

General

All reagents and chemical compounds were purchased from commercial sources and used without further purification unless otherwise noted. Triethylamine (Et_3N) was distilled from sodium. Reactions were stirred magnetically with a Teflon-coated stir bar, and all non-aqueous reactions were performed under a balloon of dry argon in septum-sealed, oven-dried glassware. When required, compounds were

purified via flash chromatography on 230-400 mesh Silica Gel 60 (Merck). Analytical TLC was performed on 250 μm silica layers on glass plates (Silica Gel 60 F254, Merck) and separated compounds visualized by illumination with UV light or an appropriate stain (bromocresol green or I_2 on SiO_2). Characterization data and yields correspond to homogeneous materials. NMR data were collected on a 400 MHz Varian Mercury Plus spectrometer operating at 399.913 MHz for ^1H -NMR and 100.567 MHz for ^{13}C -NMR at the UCSD Department of Chemistry and Biochemistry NMR facility. FID files were processed using MestReNova software version 5.0.1. Chemical shifts were calibrated using the signal from residual D_6 -DMSO (δ 2.50, pentet, ^1H -NMR) and (δ 39.52, heptet, ^{13}C -NMR), D_1 -chloroform (δ 7.26, singlet, ^1H -NMR) and (δ 77.16, triplet, ^{13}C -NMR), or D_4 -methanol (δ 3.31, pentet, ^1H -NMR) or (δ 49.00, heptet, ^{13}C -NMR). Mass spectrometric data was collected by the UCSD Department of Chemistry and Biochemistry Small Molecule Mass Spectrometry facility on Finnigan LCQDECA and ThermoFinnigan MAT900XL spectrometers.

Hippuric acid general procedure. 1.877 g glycine (25mmol) is added to a 100 mL three-neck round bottom flask with a magnetic stirbar and dissolved with 12.5 mL H_2O , cooled to 0°C and three necks are closed with septa. Benzoyl chloride **1** is added dropwise, and complete dissolution maintained by the simultaneous addition of 5 mL 10 M NaOH. After addition is complete, the reaction is stirred for an additional 2 h. Any additional solids that formed were dissolved by addition a sufficient amount 10 M NaOH, and the reaction transferred to a 100 mL beaker, cooled on ice and 5 mL 6 M HCl added, and held on ice 10' to form a volumous white precipitate that is

collected via filtration. Collected solid was then boiled in 10 mL CHCl₃ for 10 min, and persisting solids recovered by filtration to give the title compound.

4a hippuric acid. 5.8 mL Benzoyl chloride **3a** (7.03 g, 50mmol) was added to 3.754 g glycine in 25 mL H₂O to give **4a** as a white solid (6.200 g, 69%). ¹H NMR (400 MHz, DMSO) δ 8.81 (t, 1H, J = 5.9 Hz), 7.39 (m, 3H), 7.09 (ddd, 1H, J = 0.8, 2.5, 8.0 Hz), 3.88 (d, 2H, J = 5.9 Hz), 3.78 (s, 3H). ¹³C NMR (100MHz, DMSO) δ 41.907, 127.904, 129.043, 132.128, 134.459, 167.233, 172.053. ESI-MS (M+H,100%) 180.02.

4b m-methoxy-hippuric acid. 3.0 mL **3b** (4.265 g, 25 mmol) was used following the general procedure to give **4b** as a white solid (1.255 g, 22%). ¹H NMR (400 MHz, DMSO) δ 8.81 (t, 1H, J = 5.9 Hz), 7.39 (m, 3H), 7.09 (ddd, 1H, J = 0.8, 2.5, 8.0 Hz), 3.88 (d, 2H, J = 5.9 Hz), 3.78 (s, 3H). ¹³C NMR (100MHz, DMSO) δ 41.897, 55.924, 113.009, 117.997, 120.132, 130.196, 135.892, 159.855, 166.909, 172.003. ESI-MS (M+H, 100%) 210.02.

4c m-nitro-hippuric acid. 4.639 g **3c** (25 mmol) dissolved in 2 mL isopropanol was used following the general procedure to give **4c** as a white solid (2.188 g, 42%). ¹H NMR (400 MHz, DMSO) δ 9.26 (t, 1H, J = 5.8 Hz), 8.68 (s, 1H), 8.39 (dd, 1H, J = 2.2, 8.1 Hz), 8.29 (d, 1H, J = 7.8 Hz), 7.79 (t, 1H, J = 9.0 Hz), 3.95 (d, 2H, J = 5.8 Hz). ¹³C NMR (100MHz, DMSO) δ 171.703, 165.141, 148.460,

140.079, 135.812, 134.333, 130.933, 126.784, 122.651, 41.999 . ESI-MS (M+NH₄,100%) 242.05.

4d *p*-(trifluoromethyl)-hippuric acid. 3.159 g **1d** (15.1 mmol) was added to 1.114 g glycine dissolved in 8 mL water to give **4d** as a white solid (2.530 g, 68%). ¹H NMR (400 MHz, DMSO) δ 9.09 (t, 1H, J = 5.8 Hz), 8.05 (d, 2H, J = 8.1 Hz), 7.86 (d, 2H, J = 8.3 Hz), 3.94 (d, 2H, J = 5.9 Hz). ¹³C NMR (100MHz, DMSO) δ 171.703, 165.141, 148.460, 140.079, 135.812, 134.333, 130.933, 126.784, 122.651, 41.999. ESI-MS (M+H, 100%) 248.05

4e *o*-iodo-hippuric acid. 3.97 g **3e** (14.9 mmol) dissolved in 2 mL isopropanol was added to 1.118 g glycine (14.9 mmol) dissolved in 7.5 mL H₂O and the general procedure followed to give **4e** as a white solid (2.618 g, 57%). ¹H NMR (400 MHz, DMSO) δ 8.70 (t, 1H, J = 5.9 Hz), 7.87 (d, 1H, J = 7.9 Hz), 7.44 (t, 1H, J = 7.5 Hz), 7.34 (dd, 1H, J = 1.5, 7.6 Hz), 7.16 (m, 1H), 3.87 (d, 2H, J = 6.0 Hz). ¹³C NMR (100MHz, DMSO) δ 171.6, 169.7, 142.8, 140.0, 131.7, 129.0, 128.7, 94.1, 41.6. ESI-MS (M+H, 100%) 305.94.

General procedure for 5-(ethoxymethylene)-2-phenyl-4H-oxazol-5-one. 1 g Hippuric acid **2** (4.6 mmol) is dissolved in 0.9 mL triethylorthoformate (683 mg, 4.6mmol) and 0.87 mL acetic anhydride (938 mg, 9 mmol) in a roundbottom flask, fitted with a watercooled condenser and heated to reflux 30 minutes. After heat was removed and the reaction allowed to cool to room temperature, solvent was removed

via vacuum to give a red syrup. Compounds were purified via flash chromatography on silica-gel columns (mobile phase 6:1 → 1:4 Hexanes:Ethyl acetate), and fractions containing the title compounds were pooled and evaporated to give the 5-(ethoxymethylene)-2-phenyl-4*H*-oxazol-5-one as a yellow solid.

5a 5-(ethoxymethylene)-2-phenyl-4*H*-oxazol-5-one. 2.0 g **4a** (11.17 mmol) was dissolved in 1.86 mL (EtO)₃CH (11.17 mmol) and 2.1 mL Ac₂O (22.34 mmol) and refluxed 30'. Purification via flash chromatography gave **5a** as a yellow solid (0.5727 g, 23.6%) ¹H NMR (400 MHz, DMSO) δ 7.92 (dd, 2H, J = 1.2, 8.3 Hz), 7.75 (s, 1H), 7.60 (m, 1H), 7.53 (t, 2H, J = 7.4 Hz), 4.43 (q, 2H, J = 7.1 Hz), 1.33 (t, 3H, J = 7.1 Hz) ¹³C NMR (100MHz, DMSO) δ 168.3, 158.2, 156.1, 133.1, 129.8, 127.7, 126.4, 117.0, 73.3, 15.9.

5b 5-(ethoxymethylene)-2-(3-methoxyphenyl)-4*H*-oxazol-5-one. 1.0 g **4b** (4.784 mmol) was dissolved in 0.795 mL (EtO)₃CH (4.784 mmol) and 0.90 mL Ac₂O (9.569 mmol) and refluxed 30'. Purification via flash chromatography gave **5b** as a yellow solid (0.681 g, 57%) ¹H NMR (400 MHz, DMSO) δ 7.75 (s, 1H), 7.48 (ddd, 2H, J = 4.6, 11.2, 25.2 Hz), 7.39 (m, 1H), 7.16 (ddd, 1H, J = 1.1, 2.7, 3.7 Hz), 4.44 (q, 2H, J = 7.1 Hz), 3.81 (s, 3H), 1.34 (t, 3H, J = 7.1 Hz) ¹³C NMR (100MHz, DMSO) δ 168.3, 160.2, 158.1, 156.2, 131.1, 127.7, 120.1, 119.4, 117.0, 111.8, 73.3, 56.0, 15.9

5c 5-(ethoxymethylene)-2-(3-nitrophenyl)-4*H*-oxazol-5-one. 1.0 g **4c** (4.46 mmol) was dissolved in 0.74 mL (EtO)₃CH (4.46 mmol) and 0.84 mL Ac₂O (8.92

mmol) and refluxed 30 minutes. Purification by flash chromatography gave **3c** as a yellow solid (0.430 g, 37%) ^1H NMR (400 MHz, DMSO) δ 8.55 (s, 1H), 8.41 (m, 1H), 8.31 (dd, 1H, $J = 0.7, 7.8$ Hz), 7.84 (m, 2H), 4.47 (m, 2H), 1.35 (t, 3H, $J = 7.1$ Hz) ^{13}C NMR (100MHz, DMSO) δ 167.8, 157.6, 156.4, 148.8, 133.5, 131.8, 128.0, 127.2, 121.9, 116.7, 73.7, 15.9.

5d 5-(ethoxymethylene)-2-(4-(trifluoromethyl)phenyl)-4H-oxazol-5-one.

1.0 g **4d** (4.05mmol) was dissolved in 0.67mL $(\text{EtO})_3\text{CH}$ (4.05mmol) and 0.76mL Ac_2O (8.09mmol) 90' Purification by flash chromatography gave **5d** as a yellow solid (0.270g, 23%). ^1H NMR (400 MHz, DMSO) δ 8.55 (s, 1H), 8.41 (m, 1H), 8.31 (dd, 1H, $J = 0.7, 7.8$ Hz), 7.84 (m, 2H), 4.47 (m, 2H), 1.35 (t, 3H, $J = 7.1$ Hz) ^{13}C NMR (100MHz, DMSO) δ 168.0, 157.4, 157.0, 132.4 (q, $J = 32.1$ Hz), 130.2, 128.4, 126.7 (q, $J = 3.8$ Hz), 125.8, 123.1, 116.9, 73.6, 15.9

5e 5-(ethoxymethylene)-2-(2-iodophenyl)-4H-oxazol-5-one. 1.500g **4e**

(5.15mmol) was dissolved in 0.86mL $(\text{EtO})_3\text{CH}$ (5.15mmol) and 0.97mL Ac_2O (10.3mmol) and refluxed 90'. Purification by flash chromatography gave **5e** as a yellow solid (0.910g, 51%). ^1H NMR (400 MHz, DMSO) δ 8.06 (d, 1H, $J = 8.7$ Hz), 7.80 (s, 1H), 7.77 (dd, 1H, $J = 1.5, 7.8$ Hz), 7.53 (t, 1H, $J = 7.8$ Hz), 7.27 (dd, 1H, $J = 8.7, 1.5$ Hz), 4.48 (q, 2H, $J = 7.1$ Hz), 1.33 (t, 3H, $J = 7.1$ Hz). ^{13}C NMR (100MHz, DMSO) δ 168.3, 158.1, 157.0, 141.9, 133.5, 131.8, 131.1, 129.1, 116.4, 95.5, 73.4, 15.9.

anthranilate-(2-phenyl)-4H-oxazol-5-one general procedure. 1.5mL each of 125mM ethanolic solutions of 5-ethoxymethylene-2-phenyl-4H-oxazol-5-one **5a-e** and anthranillic acid **6a-e** were combined and refluxed 3h to give a yellow precipitate. Heating was ceased and reactions allowed to cool to room temperature and solvent removed by evaporation. The resulting solids were titrated in methanol to give the title compounds as a fine yellow powder.

7aa ^1H NMR (400 MHz, DMSO) δ 8.36 (d, 1H, $J = 13.3$ Hz), 8.00 (td, 1H, $J = 2.3, 4.6$ Hz), 7.91 (m, 3H), 7.58 (m, 4H), 7.16 (dd, 1H, $J = 8.5, 16.0$ Hz). ESI-MS ($[\text{M}-\text{H}]^-$, 100%) 307.07

7ab ^1H NMR (400 MHz, DMSO) δ 8.66 (d, 0H, $J = 13.6$ Hz), 8.31 (d, 1H, $J = 13.4$ Hz), 7.90 (m, 2H), 7.78 (m, 2H), 7.56 (dd, 3H, $J = 5.9, 12.8$ Hz), 7.44 (t, 1H, $J = 6.9$ Hz), 2.29 (s, 3H) . ESI-MS ($[\text{M}-\text{H}]^-$, 100%) 321.06

7ac ^1H NMR (400 MHz, DMSO) δ 8.67 (d, 0H, $J = 13.5$ Hz), 8.33 (d, 1H, $J = 13.3$ Hz), 7.93 (m, 3H), 7.71 (dd, 1H, $J = 2.6, 8.9$ Hz), 7.54 (m, 4H) . ESI-MS ($[\text{M}-\text{H}]^-$, 100%) 325.04

7ad ^1H NMR (400 MHz, DMSO) δ 8.66 (d, 0H, $J = 13.3$ Hz), 8.32 (d, 1H, $J = 13.2$ Hz), 8.05 (t, 1H, $J = 2.3$ Hz), 7.93 (dd, 2H, $J = 1.7, 7.9$ Hz), 7.87 (m, 2H), 7.76

(ddd, 1H, J = 2.3, 9.0, 11.2 Hz), 7.56 (m, 3H) . ESI-MS ($[M-H]^-$, 100%) 384.94, 386.90

7ae . 1H NMR (400 MHz, DMSO) δ 8.66 (d, 1H, J = 13.3 Hz), 8.22 (m, 1H), 7.91 (m, 3H), 7.71 (dd, 1H, J = 9.0, 13.7 Hz), 7.55 (dd, 3H, J = 8.4, 12.4 Hz) ESI-MS ($[M-H]^-$, 100%) 342.89

7ba 1H NMR (400 MHz, DMSO) δ 8.71 (d, 0H, J = 13.4 Hz), 8.35 (d, 1H, J = 13.3 Hz), 8.00 (d, 1H, J = 7.9 Hz), 7.88 (t, 1H, J = 7.5 Hz), 7.61 (dd, 1H, J = 9.2, 17.0 Hz), 7.46 (m, 3H), 7.15 (m, 2H), 3.83 (s, 3H). ESI-MS ($[M-H]^-$, 100%) 337.08

7bb 1H NMR (400 MHz, DMSO) δ 8.31 (d, 1H, J = 13.4 Hz), 7.78 (dd, 2H, J = 6.0, 16.3 Hz), 7.45 (m, 4H), 7.13 (m, 1H), 3.82 (s, 3H), 2.30 (s, 3H). ESI-MS ($[M-H]^-$, 100%) 351.08.

7bc 1H NMR (400 MHz, DMSO) δ 8.33 (d, 1H, J = 13.3 Hz), 7.92 (m, 1H), 7.71 (dd, 1H, J = 2.6, 9.7 Hz), 7.49 (m, 4H), 7.14 (m, 1H), 3.82 (s, 3H). ESI-MS ($[M-H]^-$, 100%) 355.05

7bd 1H NMR (400 MHz, DMSO) δ 8.33 (d, 1H, J = 13.3 Hz), 7.92 (m, 1H), 7.71 (dd, 1H, J = 2.6, 9.7 Hz), 7.49 (m, 4H), 7.14 (m, 1H), 3.82 (s, 3H). ESI-MS ($[M-H]^-$, 100%) 414.91, 416.94.

7be $^1\text{H-NMR}$ (400MHz, DMSO) δ 8.33 (d, 1H, $J = 13.2$ Hz), 8.22 (t, 1H, $J = 2.0$ Hz), 7.87 (m, 1H), 7.71 (m, 1H), 7.47 (m, 3H), 7.15 (m, 1H), 3.83 (s, 3H) ($[\text{M-H}]^-$, 100%) 307.07

7ca. $^1\text{H NMR}$ (400 MHz, DMSO) δ 8.64 (s, 1H), 8.47 (d, 1H, $J = 13.4$ Hz), 8.33 (m, 2H), 7.92 (m, 3H), 7.62 (s, 1H), 7.17 (t, 1H, $J = 7.5$ Hz) ESI-MS ($[\text{M-H}]^-$, 100%) 352.05.

7cb $^1\text{H NMR}$ (400 MHz, DMSO) δ 8.64 (s, 1H), 8.47 (d, 1H, $J = 13.4$ Hz), 8.33 (m, 2H), 7.92 (m, 3H), 7.62 (s, 1H), 7.17 (t, 1H, $J = 7.5$ Hz), 2.30 (s, 3H). ESI-MS ($[\text{M-H}]^-$, 100%) 366.06.

7cd $^1\text{H NMR}$ (400 MHz, DMSO) δ 8.64 (m, 1H), 8.47 (d, 1H, $J = 13.3$ Hz), 8.41 (m, 1H), 8.28 (ddd, 1H, $J = 2.0, 3.1, 8.3$ Hz), 8.07 (t, 1H, $J = 2.1$ Hz), 7.84 (m, 4H). ESI-MS ($[\text{M-H}]^-$, 100%) 429.98, 431.94.

7ce $^1\text{H NMR}$ (400 MHz, DMSO) δ 8.79 (m, 1H), 8.63 (d, 1H, $J = 1.9$ Hz), 8.42 (dd, 4H, $J = 11.5, 15.0$ Hz), 8.17 (m, 4H), 7.84 (m, 5H), 7.46 (d, 1H, $J = 9.1$ Hz). ESI-MS ($[\text{M-H}]^-$, 100%) 477.96.

7da. $^1\text{H-NMR}$ (400MHz, DMSO) δ 8.43 (d, 1H, $J = 13.6$), 7.99 (m, 4H), 7.62 (m, 1H), 7.18 (m, 1H). ESI-MS ($[\text{M-H}]^-$, 100%) 375.07

7db ^1H NMR (400 MHz, DMSO) δ 8.79 (m, 1H), 8.63 (d, 1H, $J = 1.9$ Hz), 8.42 (dd, 4H, $J = 11.5, 15.0$ Hz), 8.17 (m, 4H), 7.84 (m, 5H), 7.46 (d, 1H, $J = 9.1$ Hz), 2.41 (s, 3H). ESI-MS ($[\text{M-H}]^-$, 100%) 389.07

7dc ^1H NMR (400 MHz, DMSO) δ 8.43 (d, 1H, $J = 13.4$ Hz), 8.09 (dd, 2H, $J = 8.2, 13.6$ Hz), 7.95 (m, 3H), 7.73 (dd, 1H, $J = 3.1, 9.2$ Hz), 7.56 (m, 1H). ESI-MS ($[\text{M-H}]^-$, 100%) 393.01

7dd ^1H NMR (400 MHz, DMSO) δ 8.43 (d, 1H, $J = 13.4$ Hz), 8.09 (dd, 2H, $J = 8.2, 13.6$ Hz), 7.95 (m, 3H), 7.73 (dd, 1H, $J = 3.1, 9.2$ Hz), 7.56 (m, 1H). ESI-MS ($[\text{M-H}]^-$, 100%) 452.92, 454.90

7de ^1H NMR (400 MHz, DMSO) δ 8.42 (d, 1H, $J = 13.3$ Hz), 8.24 (t, 1H, $J = 2.1$ Hz), 8.09 (dd, 2H, $J = 8.3, 12.8$ Hz), 7.91 (m, 3H), 7.75 (dd, 1H, $J = 9.0, 15.0$ Hz). ESI-MS ($[\text{M-H}]^-$, 100%) 500.90

7ea ^1H NMR (400 MHz, DMSO) δ 8.42 (d, 1H, $J = 13.3$ Hz), 8.24 (t, 1H, $J = 2.1$ Hz), 8.09 (dd, 2H, $J = 8.3, 12.8$ Hz), 7.91 (m, 3H), 7.75 (dd, 1H, $J = 9.0, 15.0$ Hz). ESI-MS ($[\text{M-H}]^-$, 100%) 432.96

7eb ^1H NMR (400 MHz, DMSO) δ 8.37 (d, 2H, $J = 13.5$ Hz), 8.09 (d, 2H, $J = 6.9$ Hz), 7.81 (d, 4H, $J = 7.9$ Hz), 7.55 (t, 2H, $J = 7.7$ Hz), 7.45 (dd, 2H, $J = 2.1, 8.5$ Hz), 7.26 (m, 2H), 2.30 (s, 3H). ESI-MS ($[\text{M-H}]^-$, 100%) 446.94

7ec ^1H NMR (400 MHz, DMSO) δ 8.72 (d, 1H, $J = 13.5$ Hz), 8.41 (d, 1H, $J = 13.4$ Hz), 8.01 (m, 2H), 7.82 (dd, 1H, $J = 2.4, 7.0$ Hz), 7.73 (m, 1H), 7.55 (dd, 2H, $J = 8.2, 16.0$ Hz), 7.26 (m, 1H) ESI-MS ($[\text{M-H}]^-$, 100%) 450.91

7ed ^1H NMR (400 MHz, DMSO) δ 8.36 (d, 1H, $J = 13.3$ Hz), 8.07 (dd, 2H, $J = 4.9, 13.0$ Hz), 7.80 (m, 3H), 7.56 (t, 1H, $J = 7.6$ Hz), 7.27 (t, 1H, $J = 7.7$ Hz) ESI-MS ($[\text{M-H}]^-$, 100%) 510.86, 512.81

7ee ^1H NMR (400 MHz, DMSO) δ 8.38 (d, 1H, $J = 13.3$ Hz), 8.23 (d, 1H, $J = 2.1$ Hz), 8.09 (d, 1H, $J = 7.9$ Hz), 7.90 (dd, 1H, $J = 2.2, 8.7$ Hz), 7.82 (dd, 1H, $J = 1.6, 7.8$ Hz), 7.75 (d, 1H, $J = 8.9$ Hz), 7.56 (t, 1H, $J = 8.1$ Hz), 7.28 (dt, 1H, $J = 1.6, 7.7$ Hz) ESI-MS ($[\text{M-H}]^-$, 100%) 558.80

ACKNOWLEDGEMENTS

This work was supported by the United States National Institutes of Health (NIH) awards R01GM075797 and 1R03MH083266. Mass spectral characterization was performed by Dr. Yongxuan Su at the Small Molecule Mass Spectrometry

Facility, Department of Chemistry and Biochemistry, University of California, San Diego.

Chapter 4, in whole, is a reprint of material as it appears in *FEBS Journal* (2009) Vol. 276, pp. 7134-7145. I was the primary author of this publication. Brian S. Young assisted in preparing the inhibitor panel. I prepared the lead compound, and performed all *in vitro* and *in vivo* experiments. This research was performed under the guidance of Prof. Michael Burkart.

Chapter 5

A STRATEGY TO DISCOVER INHIBITORS OF BACILLUS SUBTILIS SURFACTIN-TYPE PHOSPHOPANTETHEINYL TRANSFERASE

ABSTRACT

Surfactin-type phosphopantetheinyl transferases (Sfp-PPTases) are responsible for modifying type I polyketide and nonribosomal peptide synthases of prokaryotes and have been implicated in the activation of a variety of pathogen-associated virulence factors. As such, inhibitors of this enzyme class represent enticing leads for antibiotic development and can serve as tools in studies of bacterial metabolism. Currently, no small molecule inhibitors of Sfp-PPTase are known, highlighting the need for efficient methods for PPTase inhibitor identification and development. Herein, we present the design and implementation of a robust and miniaturized high-throughput kinetic assay for inhibitors of Sfp-PPTase using the substrate combination of rhodamine-labeled coenzyme A and Black Hole Quencher-2 labeled consensus acceptor peptide YbbR. Upon PPTase-catalyzed transfer of the rhodamine-labeled phosphopantetheinyl arm onto the acceptor peptide, the fluorescent donor and quencher are covalently joined and the fluorescence signal is reduced. This assay was miniaturized to a low 4 μ L volume in 1,536-well format and was used to screen the Library of Pharmacologically Active Compounds (LOPAC¹²⁸⁰). Top inhibitors identified by the screen were further characterized in secondary assays, including protein phosphopantetheinylation detected by gel electrophoresis. The present assay enables the screening of large compound libraries against Sfp-PPTase in a robust and automated fashion and is applicable to designing assays for related transferase enzymes.

INTRODUCTION

A key biosynthetic step in the formation of fatty acids, non-ribosomal peptides, and polyketides is the coupling of the respective monomeric precursor units to the carrier domains of synthases. The linker between a conserved serine residue of the carrier protein and the nascent polymer is a phosphopantetheinyl group, derived from coenzyme A (CoA). Phosphopantetheinyl moieties are attached as post-translational modifications via the catalytic action of phosphopantetheinyl transferases (PPTases). Within bacteria, PPTases are grouped into two classes, the AcpS-type and Sfp-type PPTases (AcpS-PPTase and Sfp-PPTase, respectively), based upon primary structure,(Lambalot et al., 1996a) and are responsible for modifying carrier protein domains in all primary and secondary metabolic pathways. The AcpS-type is named for *holo*-acyl carrier protein synthase and is typically associated with fatty acid biosynthesis,(Lambalot and Walsh, 1995) Sfp-type PPTases, corresponding to the activator of surfactin production in *Bacillus subtilis*, are generally responsible for modifying type I polyketide and nonribosomal peptide synthases of prokaryotes.(Quadri et al., 1998a)

The essential nature of PPTases to primary metabolism (i.e. fatty acid, teichoic acid, and lipid A biosynthesis) makes them enticing targets for antibiotic development.(Chu et al., 2003b, Gilbert et al., 2004, Joseph-McCarthy et al., 2005a, McAllister et al., 2000, Payne et al., 2007) Additionally, Sfp-type PPTases are responsible for activating biosynthetic pathways that manufacture a variety of pathogen-associated virulence factors. Among these compounds are toxins such as

mycolactone from *Mycobacterium ulcerans*, siderophores such as vibriobactin from *Vibrio cholerae* or mycobactin from *Mycobacterium tuberculosis*, as well as the mycolic acids that form the waxy cell wall of *Mycobacteria*; indeed, the biosyntheses of these compounds are now considered attractive targets for drug design.(Onwueme et al., 2005, Barry et al., 1998, Chalut et al., 2006a) Given the obligatory nature of this modification to these pathways, we have been interested in studying the effects that chemical modulation of this target will have on the virulence and viability of these pathogens.

While it has been suggested that the druggability of PPTases has been investigated,(Chu et al., 2003b, Gilbert et al., 2004, Joseph-McCarthy et al., 2005a, McAllister et al., 2000, Payne et al., 2007) there are only limited reports of inhibitor development against AcpS PPTase.(Chu et al., 2003b, Gilbert et al., 2004, Joseph-McCarthy et al., 2005a) Furthermore, there is a lack of a simple, robust assay for PPTase that could be applied in an automated manner to the screening of large compound libraries.(Michael et al., 2008) Existing assays have largely utilized radiolabeled substrates and involve cumbersome treatments and separation steps. A pair of reports on inhibitor development for AcpS-PPTase(Gilbert et al., 2004, Joseph-McCarthy et al., 2005a) presented a time-resolved fluorescence resonance energy-transfer (TR-FRET) based assay for the enzyme; however, no follow-up studies have since been disclosed. The TR-FRET method involved the use of expensive reagents and required multiple liquid handling and incubation steps, making it difficult to automate and scale up. Further, that format only generated end-point data, making it vulnerable to noise and false positives.(Inglese et al., 2007a)

To this end, we have recently described work to develop a FRET-based homogenous screen for PPTase activity that drew upon two recent developments in the field.(Foley and Burkart, 2009) Our prior work(La Clair et al., 2004a) has established that fluorescently modified-CoA (mCoA) is readily utilized as a substrate by Sfp-PPTase, converting the *apo*-acceptor substrate to the thiol blocked or *crypto*-product . Separately, Yin *et al*(Yin et al., 2005a) reported the identification of a consensus peptide motif (YbbR, sequence DSLEFIASKLA) which was shown to serve as a carrier protein surrogate for Sfp, accepting the phosphopantetheinyl arm transfer upon its second-position serine residue (Fig. 1A). Further, because YbbR was isolated as a collection of N-terminal extensions to the serine-containing motif, it was expected that attachment of detection labels to that end would be tolerated by the PPTase. Thus, we developed a first-generation assay using fluorescein-5-isothiocyanate modified-YbbR (FITC-YbbR) **1a** and rhodamine-mCoA **2b** substrates and observed a decrease in fluorescence intensity of the fluorescein donor emission when **1a** and **2b** are conjoined into the product **4ab**.(Foley and Burkart) These initial studies demonstrated that this fluorescein/rhodamine assay performed satisfactorily in 96-well format, and possessed the capacity to characterize an enzyme inhibitor.

With this method, we have determined that none of the currently disclosed chemical matter is active against Sfp,(Foley et al., 2007) thus necessitating a large-scale inhibitor screening campaign. To this end, we undertook a high throughput screening feasibility study, taking advantage of our access to HTS and chemical probe development technology being made available to the public by the Molecular Libraries and Initiative of the NIH Roadmap(Austin et al., 2004). We detail the evaluation of

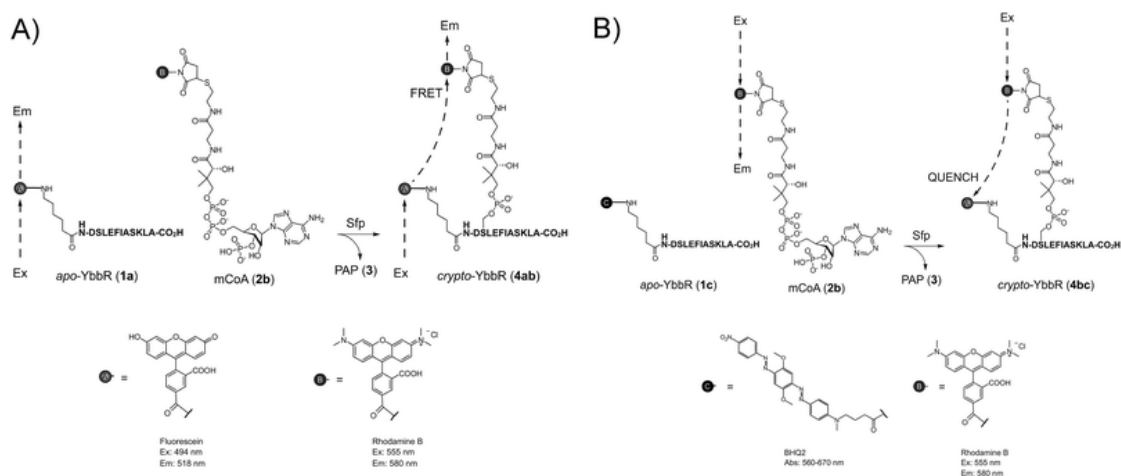


Figure 5.1 Assay Principle.

Panel A is the Fluorescein-rhodamine assay scheme. *Apo*-fluorescein-YbbR peptide **1a** is a fluorescently labeled acceptor peptide for Sfp phosphopantetheinyl transferase. Enzymatic modification of **1a** with the 4'-phosphopantetheinyl arm from rhodamine-mCoA **2b** generates the *crypto*-YbbR **4ab** FRET peptide and 3'-phosphoadenosine-5'-phosphate (PAP) **3** as products. Enzymatic activity is detected by observing the decrease of fluorescent emission from **1a** that is quenched in the FRET peptide **4ab**. Panel B is the Dark quench assay scheme. Rhodamine-mCoA **2b** and Black Hole Quencher-2 labeled acceptor peptide YbbR **1c** are used as substrates. Upon PPTase-catalyzed transfer of the rhodamine-labeled phosphopantetheinyl arm onto the acceptor peptide, the fluorescent donor and quencher are covalently joined in the reaction product and the fluorescence signal is reduced.

this fluorescein/rhodamine assay in highly miniaturized settings, where it functioned with significantly reduced performance in the 1,536-well format tested. To overcome this, we redesigned the assay to incorporate a non-emitting dark quencher to the peptide substrate. This modified assay was miniaturized to a low 4 μ L volume and was used to identify and characterize Sfp-PPTase inhibitors from the LOPAC¹²⁸⁰ collection of known bioactives.

MATERIALS AND METHODS

Chemicals and consumables. 4-(2-hydroxyethyl)-1-piperazine ethanesulfonic acid sodium salt (HEPES-Na) and $MgCl_2$ were purchased from GIBCO (Carlsbad, CA) and Quality Biological Inc. (Gaithersburg, MD), respectively. 7.5% bovine serum albumin (BSA) solution, Nonidet P-40 (NP-40), Tween-20, glycerol, coenzyme A (CoA), adenosine 3', 5'-diphosphate sodium salt (PAP), and 2'-Deoxy-N6-methyladenosine 3', 5'-bisphosphate (MRS 2179) were purchased from Sigma-Aldrich. Dimethyl sulfoxide (DMSO, certified ACS grade) was obtained from Thermo-Fisher Scientific (Pittsburg, PA). Medium binding black solid-bottom 384- and 1,536-well plates (assay plates), and 1,536-well polypropylene plates (compound plates) were purchased from Greiner Bio One (Monroe, NC), 384-well polypropylene V-bottom plates (compound storage) were from Matrix/Thermo Scientific (Hudson, NH), black flat-bottom Costar 96-well plates (assay plates) were from Thermo-Fisher Scientific, and skirted V-bottom 96-well polypropylene plates (compound storage) were from Genesee Scientific (San Diego, CA). An analog of the YbbR peptide [H-DALEFIASKLA-OH] containing an S2A point mutation to make it a non-processable

version of the original sequence was synthesized and HPLC purified by the Tufts University Core Facility (Medford, MA).

Instrumentation and equipment. Compound management and library plate compression to 1,536-well format was performed with a Cybi-well fixed tip automated pipettor (CyBio, Jena, Germany). Compound transfers for screening used a Kalypsys Workstation equipped with a 1,536 pin tool (Kalypsys Systems, San Diego, CA) and reagent dispenses were performed with a Flying Reagent Dispenser (FRD, Beckman Coulter, Fullerton, CA). Detection was accomplished with a ViewLux high-throughput CCD imager (Perkin Elmer, Waltham, MA).

Liquid handling for the FRET-quench and protein phosphopantetheinylation assays was performed with manual multichannel pipettors, and microplate detection accomplished with an HTS-7000 plus plate reader (Perkin Elmer). Gel electrophoresis was performed on a Multiphor-II horizontal electrophoresis unit (GE Healthcare, Piscataway, NJ) powered by a Fisher brand FB-600 power supply (Thermo-Fisher Scientific). Fluorescence gels were imaged with a Typhoon Trio laser-based scanner (GE Healthcare).

Enzymes and Fluorogenic Substrates. Sfp-PPTase was produced and purified as previously described.(Quadri et al., 1998a) Stock solutions of the enzyme (20 mg/mL, 765 μ M) were stored at -80°C in 50 mM HEPES-Na, 300 mM NaCl, pH 8.0, and 30% glycerol. Fluorescein-5-isothiocyanate (FITC) coupled to the 11 residue consensus peptide motif (FITC-YbBR) **1a** was purchased from GL Biochem (Shanghai, China) and supplied as a yellow powder of >95% purity.

Figure 1B depicts BHQ-2-YbbR **1c**, which was prepared from 6-aminocaproate-terminated YbbR that was assembled by standard Fmoc-based solid phase peptide synthesis methods using an automated synthesizer (Applied Biosystems Pioneers, Foster City, CA) with 2-(1H-7-Azabenzotriazol-1-yl)-1,1,3,3-tetramethyl uronium hexafluorophosphate (HATU) activation.(Wellings and Atherton, 1997a, Glover et al., 1999a) After removal of the resin from the synthesizer, BHQ-2-carboxylic acid (BHQ-2000, Biosearch Technologies Inc, Navato, CA) was activated with 2-(1H-benzotriazol-1-yl)-1,1,3,3-tetramethyl uronium hexafluorophosphate (HBTU) and allowed to couple to the peptide overnight at room temperature. In the morning the peptide was cleaved from the solid support in a cocktail containing 4% H₂O, 2% Triisopropylsilane in trifluoroacetic acid, and purified by HPLC.

Rhodamine-mCoA **2b** was prepared as previously described.(Foley and Burkart) Briefly, 1.1 equivalents of rhodamine maleimide (Invitrogen Corporation, Carlsbad, CA) was reacted with 1 equivalent of CoA in 10 mM NaH₂PO₄, pH 7.4 and followed to completion by HPLC. After completion, the reaction mixture was extracted 3 times with an equal volume of dichloromethane. The aqueous phase was placed under vacuum for two hours, and then stored in ~1 mM solutions in 10 mM NaH₂PO₄, at -20°C.

Miniaturized Fluorescein/rhodamine FRET-Quench Assay. The buffer consisted of 50 mM HEPES-Na, 10 mM MgCl₂, 0.1% BSA and 0.01% Tween-20. The substrate was a mixture of 5 μM FITC-YbbR **1a** and 10 μM rhodamine-mCoA **2b**. The assay was initiated by dispensing 3 μL of enzyme in buffer into a 1,536-well assay plates. The assay plate was then covered and incubated at room temperature for

10 minutes, followed by a 1 μL addition of substrate mixture in buffer to start the reaction, for a final assay volume of 4 μL . The plate was then centrifuged at 1,000 rpm for 15 seconds and kinetic fluorescence data were collected every minute for 30 minutes on a ViewLux high-throughput CCD imager with FITC [$E_x/E_m = 480(20)/530(20)$ nm] optics.

Rhodamine/BHQ-2 Dark Quench Assay. The buffer consisted of 50 mM HEPES-Na, 10 mM MgCl_2 , 0.1% BSA and 0.01% NP-40. The substrate was a mixture of 5 μM rhodamine-mCoA **2b** and 12.5 μM Black Hole Quencher-2 YbbR (BHQ-2-YbbR) **1c**. The assay was conducted as described above with the fluorescence signal collected using standard BODIPY [$E_x/E_m = 525(25)/598(25)$ nm] optics.

Model Inhibitor Studies: Substrate and Product Mimetics. A 50 mM initial stock solution of the YbbR peptide analog [H-DALEFIASKLA-OH] in DMSO was prepared and diluted (1:2.5, 8-points) down to 81.9 μM in a 384-well polypropylene V-bottom plate. The assay was performed in a 384-well plate by pipetting 27 μL of enzyme solution into a 384-well assay plate, followed by 4 μL of each dilution ($n = 3$). The plate was covered and incubated at room temperature for 10 min, followed by a 9 μL addition of substrate mixture (5 μM rhodamine-mCoA **2b** and 12.5 μM BHQ-2-YbbR **1c**) to start the reaction. The plate was then centrifuged at 1,000 rpm for 15 seconds, and an initial fluorescence read was collected on a ViewLux reader. The assay plate was removed from the reader, covered, incubated for 30 minutes at room temperature, and a second fluorescence read was performed.

50 mM stock solutions of CoA and PAP **3** in DMSO were prepared and diluted (1:3, 8-points) down to 68.6 μM in a 384-well polypropylene V-bottom plate.

Similarly, a 10 mM stock solution of MRS 2179 in DMSO was prepared and diluted (1:2, 16-points) down to 305 nM. Using a CyBi-well, the compound dilution series were transferred in duplicates to a 1,536-well compound plate. CoA, PAP, and MRS 2179 were assayed in 1,536-well format as described in the qHTS protocol section.

Compound Library. The Library of Pharmacologically Active Compounds (LOPAC¹²⁸⁰, Sigma-Aldrich) of 1,280 known bioactives were received as 10 mM DMSO solutions and formatted as 1,536-well compound plates of 6 concentrations (1:5 dilution) at 5 μ L per well. Additional details on the preparation of the compound library for quantitative high-throughput screening (qHTS) have been previously described.(Yasgar et al., 2008)

qHTS Protocol and Data Analysis. An FRD was used to dispense reagents into the assay plates. 3 μ L of reagents, consisting of enzyme (in columns 1 and 2 as the catalyzed control, 5 to 48 for compounds) and enzyme buffer (in columns 3 and 4 as the uncatalyzed control) were dispensed into 1,536-well assay plates. Compounds (23 nL) were transferred via Kalypsys pintoolequipped with 1,536-pin array.(Michael et al., 2008) The plate was incubated for 10 min at room temperature, followed by a 1 μ L addition of substrate to start the reaction, for a final assay volume of 4 μ L. The plate was then centrifuged at 1,000 rpm for 15 seconds, and kinetic fluorescence data were collected on a ViewLux reader. The plate was then covered, incubated for 30 minutes, and a second fluorescence read was performed. Library plates were screened starting from the lowest and proceeding to the highest concentration with pin-tool wash steps interleaved. The data were then analyzed as previously described.(Inglese et al., 2006, Michael et al., 2008, Yasgar et al., 2008) For activity calculations, delta

values were computed as the difference in fluorescence intensity between last and first time points. Percent activity was derived from the catalyzed, or neutral control, and the uncatalyzed, or 100% inhibited, control values, respectively, using in-house software (<http://ncgc.nih.gov/pub/openhts/>).

Re-test of Screening Actives. Candidate inhibitors selected for confirmatory testing were re-sourced as 10 mM initial stock solutions in DMSO or as powder from Sigma-Aldrich. The samples were then serially diluted (1:2, 22-points) row-wise down to 4.77 nM in a 384-well polypropylene V-bottom plate (leaving columns 1 and 2 empty for controls). Using a CyBi-well, the solutions were then transferred to columns 5 to 48 (n = 2 per dilution point) of a 1,536-well compound plate. The assay protocol for confirmation was identical to that described in the qHTS protocol section, with the first four columns of the 1,536-well compound plate being reserved for placement of controls. Pin-transfer of 23 nL of compound solution into 4 μ L of assay mixture resulted in final compound concentrations between 57.2 μ M and 27.3 pM.

FITC-Rhodamine and Gel Assays. These experiments were performed in the San Diego laboratory with inhibitor compounds that were resourced as solids from Sigma-Aldrich, dissolved as 10 mM stock solutions in DMSO, and further formulated as 1:3 dilution series over 12 points in full skirted 96-well polypropylene PCR plates, with top and bottom concentrations of 10 mM and 56.4 nM, respectively. These stocks were sealed with adhesive foil and stored at room temperature over CaCO₃ dessicant until use.

Compound activities were evaluated with the FITC-Quench assay as follows: 2.5 μ L of compound solution or DMSO were transferred to black half-well

polystyrene plates (Costar), followed by 37.5 μ L of a 1.33X enzyme solution (16.62 nM Sfp-PPTase in a buffer containing 13.3 mM MgCl₂, 66.6 mM HEPES-Na, 1.33 mg/mL BSA), and the plates incubated at room temperature for 15 minutes. Reactions were initiated by the addition of 10 μ L of 5X substrate solution (50 μ M Rhodamine-mCoA **2b** and 25 μ M FITC-YbbR **1a** in 10 mM Tris-HCl pH 7.4); the plate was centrifuged for 1 minute at 3,500 RPM in a Marathon 8K microplate centrifuge (Thermo-Fisher Scientific), and the reactions continuously monitored (15 reads, 2 minute cycle time) in a HTS7000 plus microplate reader with standard fluorescein filters [$E_x/E_m = 485(20)/535(30)$]. Data were analyzed by subtracting the RFU value at read 10 from the value at read 1, and converted to % activity using a slope generated from the inhibited and uninhibited controls present each plate. These data were plotted and fit with GraphPad Prism version 5.00 (Graphpad, Inc, La Jolla, CA) using the four-parameter dose response equation with the ordinary (least squares) setting, with error bars and error values representing one standard deviation.

Gel-based assay. Compounds were evaluated by monitoring of fluorescence transfer to whole carrier protein substrates via polyacrylamide gel electrophoresis. (La Clair et al., 2004a) Actinorhodin ACP was cloned from genomic DNA of *Streptomyces coelicolor* A(3)2 by initial amplification using Pfu DNA polymerase with primers 5'AATGGCAACCCTGCTGACCACCGACGATCTG (ActACP_F) and 5'TCATGCCGCCTCGGCAGTGCGCCGTTGATC (ActACP_R) into pET28b and expressed as a hexahistidine-tagged product using standard protocols. We elected to use the acyl carrier protein of the actinorhodin biosynthetic pathway (ActACP) as a protein substrate given its small size, high recombinant yield when expressed in *E.*

coli, and facile applicability to native polyacrylamide gel electrophoretic techniques. The final protein preparation was concentrated to 10 mg/mL, as determined using the Bradford assay with a BSA/lysozyme mixture as a standard, diluted with an equal volume of 50% glycerol, and stored in 1 mL aliquots at -80°C. The top 8 compound concentrations from the stock plates generated during evaluation with the FITC-Rhodamine assay were used in the present protein phosphopantetheinylation experiment. 1 μ L of compounds or DMSO were transferred to unskirted polypropylene 96 well PCR plates, followed by the addition of a 2X enzyme solution (30 nM Sfp-PPTase in a buffer containing 50mM HEPES-Na, 10 mM MgCl₂, 2 mg/mL BSA, pH 7.6); the plates were then incubated at room temperature for 15 minutes. Reactions were initiated by addition of 9 μ L of a 2.1X reagent solution (20 μ M Act-ACP, 20 μ M Rhodamine-mCoA **2b**, 50 mM KOAc, pH 8.0) After 30 minutes incubation, the reaction was terminated by the addition of a 2X quench/load solution containing 20 mM EDTA, 20 mM Tris, 192 mM glycine, 4 M Urea, pH 8.6 (pH unadjusted).

The samples were resolved on a non-denaturing 20% polyacrylamide gel containing 20 mM Tris and 192 mM glycine using the Multiphor-II horizontal electrophoresis unit. The gels were imaged with a Typhoon Trio laser scanner with standard tetramethylrhodamine (TAMRA) settings using the 532 nm green laser for excitation and 580(30) emission filter with a 50 μ m pixel size. The inhibition effect was scored visually, in a manner similar to that used by Dexheimer et al.(Dexheimer and Pommier, 2008), by comparing band intensities with control reactions that

contained 20, 15, 10, 5 and 0 nM Sfp-PPTase (100, 75, 50, 25 and 0% activity, respectively) as a reference.

RESULTS

Fluorescein/Rhodamine FRET-Quench Assay. Initially, we evaluated the existing FRET-quench system(Foley and Burkart) (Fig. 1A) for signal strength and viability in a miniaturized setting. The assay was miniaturized from 96- to 1,536-well format and tested according to the protocol described above utilizing FITC optics for fluorescence detection. 3 μ L of enzyme solution, or buffer serving as a no-enzyme control, were dispensed. The reaction was initiated by the addition of 1 μ L substrate. The time-course data revealed a significant baseline drift of the uncatalyzed control samples (substrate and buffer only, open circles Figure 2A). The signal from the catalyzed reaction decreased ~51% during the 30 minute reaction monitoring. However, the signal from the uncatalyzed control wells decreased also by a significant value of ~24%, ultimately resulting in a low signal-to-background ratio and a poor Z' factor(Zhang et al., 1999) of 0.27 (Fig. 2A). Attempts to stabilize this drift with increased concentrations of substrate or by dispensing the two substrates separately were unsuccessful (data not shown). This effect was also observed in 384-well format but was less dramatic and could be partially mitigated by running the reaction in low-binding plates (such an option was not available for the system-specific 1,536-well

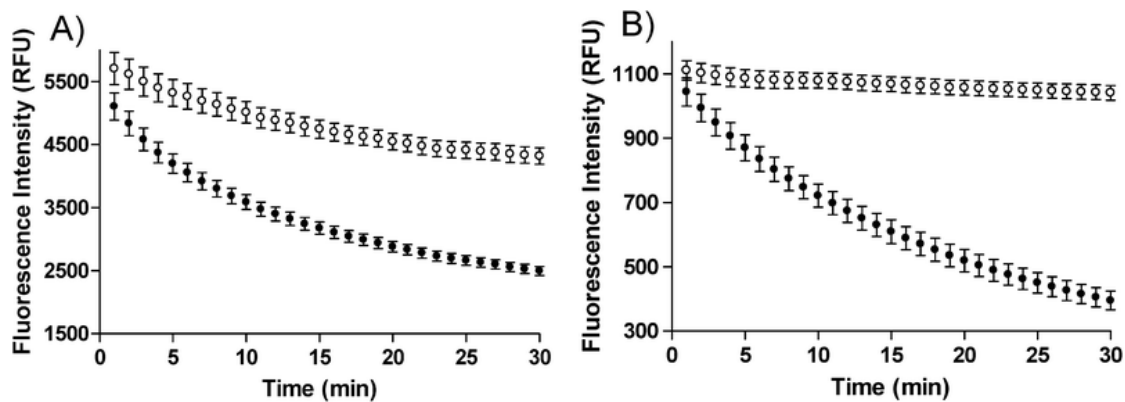


Figure 5.2 Assay Optimization

Panel A is the reaction progress of the uncatalyzed enzyme (\circ , $n = 64$) and catalyzed enzyme (\bullet , $n = 64$) at 100 nM using the FITC FRET Quench protocol in 1,536-well format (delta values were computed using the 30 minute and 1 minute time-point RFU). Panel B is the reaction progress of the uncatalyzed enzyme (\circ , $n = 64$) and catalyzed enzyme (\bullet , $n = 48$) at 50 nM using the Dark Quench protocol in 1,536-well format (delta values were computed using the 30 minute and 1 minute time-point RFU).

plates). Therefore we concluded that one or both substrates undergo irreversible binding and aggregation to the plate walls, an effect exacerbated by the high surface-to-volume ratio of 1,536-well plates.

Rhodamine/BHQ-2 Dark Quench Assay Design. To address the baseline drift and to increase the available signal window, we converted the initial donor-acceptor system to a pure fluorescence-quenching format by replacing the former fluorescein donor label with a dark, non-emitting quencher molecule, BHQ-2 (Simeonov et al., 2009, Cook et al., 2006) (Fig. 1B). This configuration was designed to spectrally match the emission of rhodamine, which in the new format serves as a fluorescence emission donor. Linking BHQ-2 to the YbbR peptide allowed us to maintain the rhodamine-mCoA 2b component of the reagent set and continue to report enzyme activity as a decrease in signal (hereinafter referred to as Δ RFU) relative to rhodamine quenching upon product formation. Further, we anticipated that by shifting detection to a longer wavelength, the assay would be less sensitive to autofluorescence from compound library members, a prevalent occurrence in the blue region of the light spectrum. (Simeonov et al., 2008)

Assay implementation. The new reagent, BHQ-2-YbbR 1c was assembled by conventional solid phase peptide synthesis and its identity confirmed by mass spectral analysis. With the new reagent in hand, the uncatalyzed reaction was screened for baseline drift in the presence of different detergents before assembling the complete dark quench assay. Substrate concentrations of 5 μ M rhodamine-mCoA 2b and 12.5 μ M BHQ-2-YbbR 1c were chosen based on previously estimated limits of inner filter effect, solubility of BHQ-2, and the K_m ratio of the two substrates. (Foley and Burkart,

2009) The substrate mixture, prepared as a 4X stock, was dispensed (1 μ L) into plates containing 3 μ L buffer. The baseline drift, expressed as the difference in fluorescence signal between reaction initiation and 30 minutes later, was monitored in the presence of 0.01% NP40, 0.01% Tween-20, and 0.01% Brij-35, respectively (Fig. 3). Tween-20 (Δ RFU = 263 ± 30) and Brij-35 (Δ RFU = 239 ± 19) conditions both exhibited a twofold larger drift as compared to NP40 (Δ RFU = 100 ± 14). Thus, the signal was best stabilized by the addition of 0.01% NP40 to the buffer. The use of detergent in the assay buffer carried an additional benefit in suppressing the interference from promiscuous inhibitors acting by colloidal aggregation.(Feng et al., 2007)

The above conditions were evaluated in a direct comparison run versus the fluorescein-rhodamine pair in 1,536-well format, with an Sfp-PPTase concentration of 50 nM. Only a minimal baseline drift of the uncatalyzed reaction control was observed with the new reagent set (Fig. 2B). The catalyzed reaction signal (black circles) decreased $\sim 62\%$ during the 30 minute reaction monitoring, versus only $\sim 6\%$ observed for the uncatalyzed (open circles) control, leading to a robust Z' factor of 0.76. This represented a dramatic improvement in assay performance when compared with the fluorescein-rhodamine system in 1,536-well format (Fig. 2A). Additionally, we note that only 50 nM enzyme was required to achieve $\sim 62\%$ signal change in the catalyzed reaction when using the Dark Quench reagent set, while double that concentration of PPTase was needed in the fluorescein-rhodamine assay to observe a smaller $\sim 51\%$ change. Utilization of NP40 instead of the originally used Tween-20 in the fluorescein-rhodamine FRET-quench assay did relieve some of the uncatalyzed reaction drift (similar to the trend observed with the rhodamine-BHQ2 Dark Quench

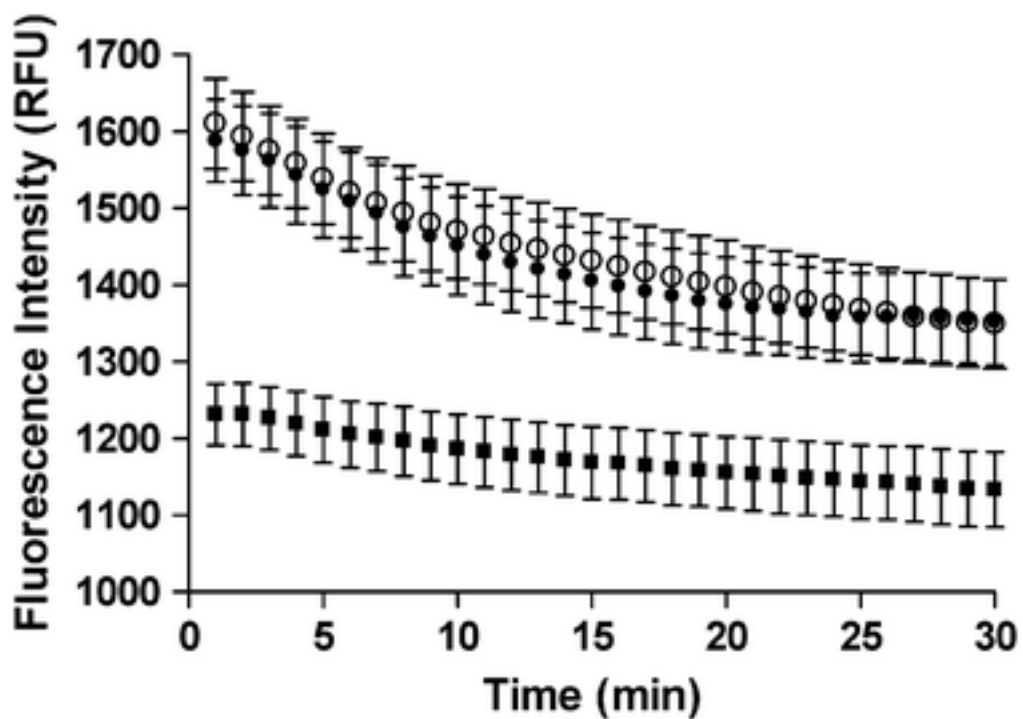


Figure 5.3 Effect of different detergents on the reaction progress of the uncatalyzed enzyme in the Dark Quench system.

Fluorescent intensity signal trend of substrate mixture (5 μM rhodamine-CoA **2b** and 12.5 μM BHQ-2-YbbR **1c**) in the presence of 0.01% NP40 (\blacksquare), Tween20 (\circ), or Brij35 (\bullet) freshly dispensed in 1,536-well plates ($n = 64/\text{condition}$).

pair in Fig. 3, data not shown) but the use of this detergent did not lead to a significant improvement in the signal increase (catalyzed rate) or signal-to-background ratio of that original reaction. Thus, aside from the issue of baseline stability, the improved donor-quencher format still yielded a superior signal-to-background.

These improvements in assay performance allowed us to optimize the dark quench system further in an effort to decrease enzyme concentration. We tested the reaction rate as a function of Sfp-PPTase concentration. Enzyme concentrations of 15, 50, and 100 nM were examined, with fluorescence data collection every 5 minutes over a 30 minute interval. Figure 4 shows the reaction progress of each enzyme concentration and the Z' factor calculated at each time-point. All enzyme concentrations tested exhibited robust assay performance, with Z' factor values at 30-minute reaction of 0.72, 0.84, and 0.74, respectively. Based on these results, an enzyme concentration of 15 nM was chosen for the 1,536-well screen. At this concentration, the 30 minute kinetic window was chosen to balance the need to run the reaction under initial-rates regime, at the lowest enzyme concentration possible and at minimal substrate conversion, and the desire for robust fluorescence intensity change of the catalyzed vs. uncatalyzed reactions, giving an acceptable Z' score. In the final screening mode, the 30-minute kinetic data were collected in a discontinuous manner (Michael et al., 2008) where, rather than measure fluorescence continuously for 30 minutes, we collected only two data points per well: the first read performed immediately after addition of the substrate reagent, and the second after 30 minutes of reaction. The net result from such implementation is that each plate spends a minimal amount of time inside the detector, thereby allowing a maximal screening throughput.

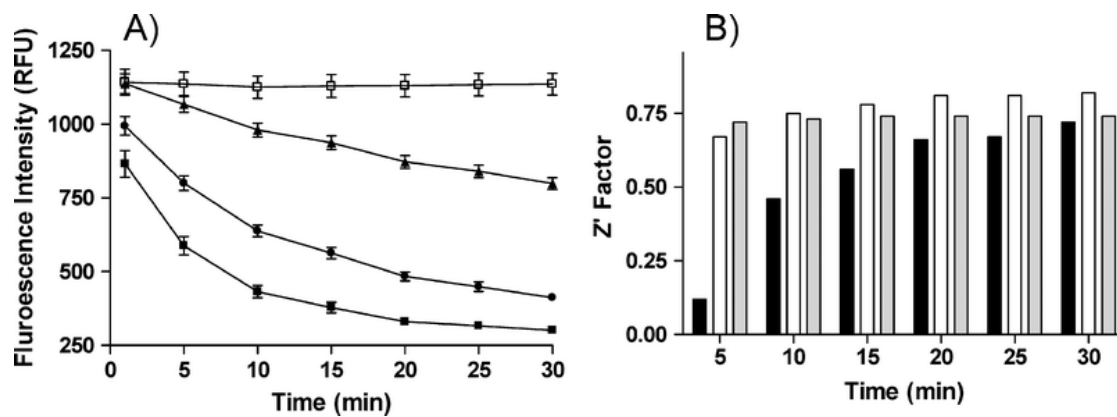


Figure 5.4 Sfp-PPTase Titration.

Panel A is the reaction progress at 0 (□), 15 (▲), 50 (●), and 100 nM (■) of Sfp-PPTase (n = 64 wells concentration/time-point). Panel B is the Z'-factor 15 (■), 50 (□), and 100 nM (■) after the plate has been incubated for 5, 10, 15, 20, 25, and 30 minutes.

With the basic assay parameters established, enzyme and substrate reagent components were tested for stability. Fresh enzyme and substrate solutions were prepared at time zero and stored at 4°C. At selected time points (0, 0.5, 1, 2, 4, and 21 hours), the reagents were tested by running the enzymatic assay in 1,536-well plates (*vide supra*). Excellent reagent integrity was noted for at least 21 hours of storage (Fig. 5), indicating that an unattended overnight screening using the present combination of enzyme and substrate was feasible.

Model Inhibitors: Substrate and Product Mimetics. In the absence of known inhibitors of Sfp-PPTase, we validated the assay by using several molecules which represented either components of the native reaction or were analogues thereof. This collection included CoA itself, representing a competitive substrate versus rhodamine-mCoA; MRS 2179, a competitive inhibitor versus CoA; a YbbR analogue peptide [sequence H-DALEFIASKLA-OH], unprocessable due to mutation of the acceptor serine residue; and PAP 3, one of the reaction products. Evaluation of these compounds with the developed conditions is presented in Figure 6. The CoA substrate and its analogue MRS 2179 yielded the strongest inhibition (IC_{50} values of 4.2 μ M for CoA and 7.7 μ M for MRS 2179, respectively), while the effect of the PAP 3 product was weaker (IC_{50} value of 14.6 μ M). Unsurprisingly, the point-mutant version of YbbR was weakly recognized by the enzyme, yielding an IC_{50} value of 616 μ M. We note the IC_{50} value obtained for PAP 3 in the present assay is within the error of measurement to that observed in the fluorescein-rhodamine assay investigated earlier.(Foley and Burkart)

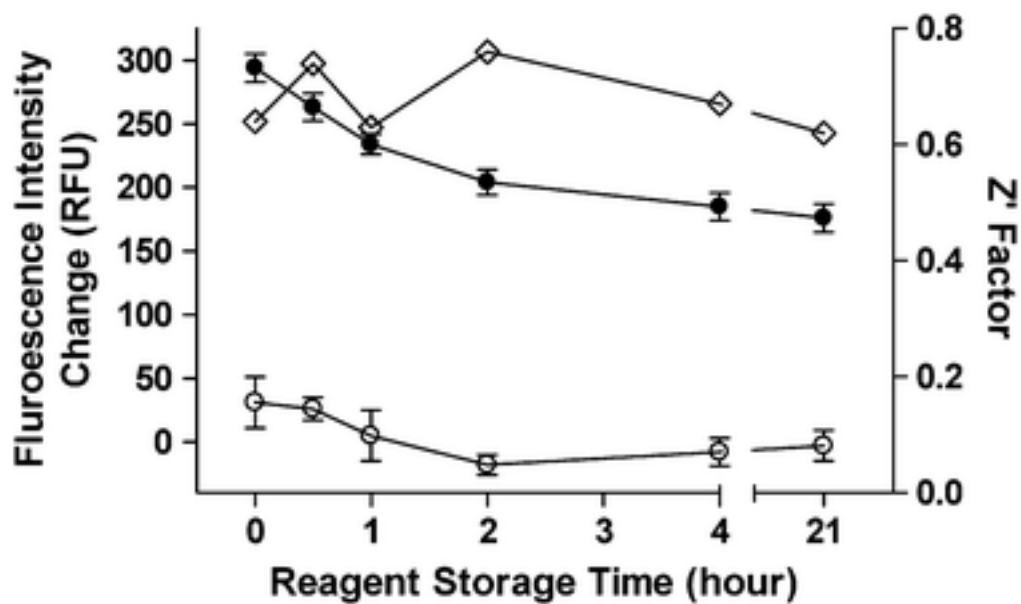


Figure 5.5 Reagent Stability.

The left axis is the signal change of the of the uncatalyzed enzyme (\circ , $n = 64$) and catalyzed enzyme (\bullet , $n = 64$) at 50 nM using the Dark Quench protocol in 1,536-well format at 0, 0.5, 1, 2, 4, and 21 hours of reagent storage. The right axis shows the corresponding Z'-factor (\diamond).

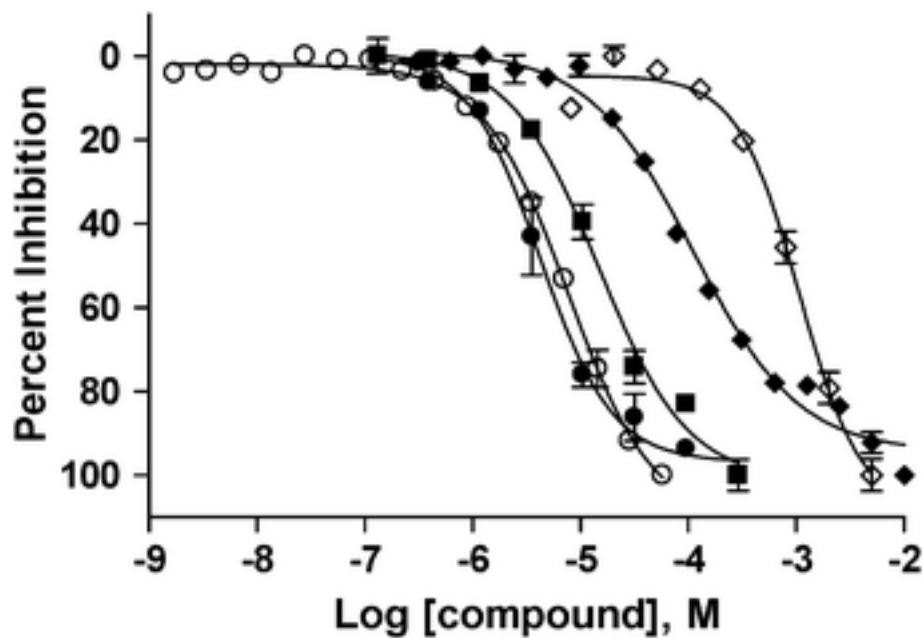


Figure 5.6 Substrate and Product Mimetics.

The percent inhibition activity of Coenzyme-A (unlabeled substrate, ●), MRS 2179 (substrate mimetic, ○), PAP (reaction product, ■), the unlabeled YbbR peptide (substrate mimic, ◆), and the YbbR analog peptide (substrate mimetic, ◇) containing a point mutation to make it a non-processable version of the original sequence.

qHTS of LOPAC¹²⁸⁰ Collection. Following this validation, the dark quench system was screened against a 6-point dilution series of the LOPAC¹²⁸⁰ compound library with final compound concentrations ranging from 18.3 nM to 57.2 μ M. At the end of the screen, data were analyzed, with top hits presented in Table 1. Importantly, the Z' factor remained nearly constant throughout the experiment, with an average value of 0.73, indicating a stable assay (Fig. 7A). In total, 163 samples exhibited inhibitory activity which tracked with sample concentration (Fig. 7B), with a small fraction, totaling 24 compounds, exhibiting complete concentration-response curves and 139 samples displaying incomplete responses (either partial curve without an upper asymptote or a single top-concentration activity point). The complete screening results are available in PubChem (bioassay identifier 1490).

Follow up screening and secondary assays. From these hits, nine compounds possessing complete concentration responses and lacking obvious highly reactive functionalities, and one partial-response compound (mitoxantrone **5**), were selected for follow-up testing in a set of secondary assays to validate the biochemical activity with Sfp-PPTase observed in the screen. This collection of experiments included a retest of the material in the donor-quencher screening assay on site at the screening center, followed by resourcing of the substances and evaluation in the FRET-quench screen at the San Diego laboratory. Afterward, an orthogonal enzymatic assay utilizing whole acyl carrier protein as a substrate and following the product formation by polyacrylamide gel electrophoretic separation was used as a secondary screen. (La Clair et al., 2004a) As seen in Table 1, 6 out of the 9 full-response inhibitors maintained remarkably similar IC₅₀ values when tested across the different assay

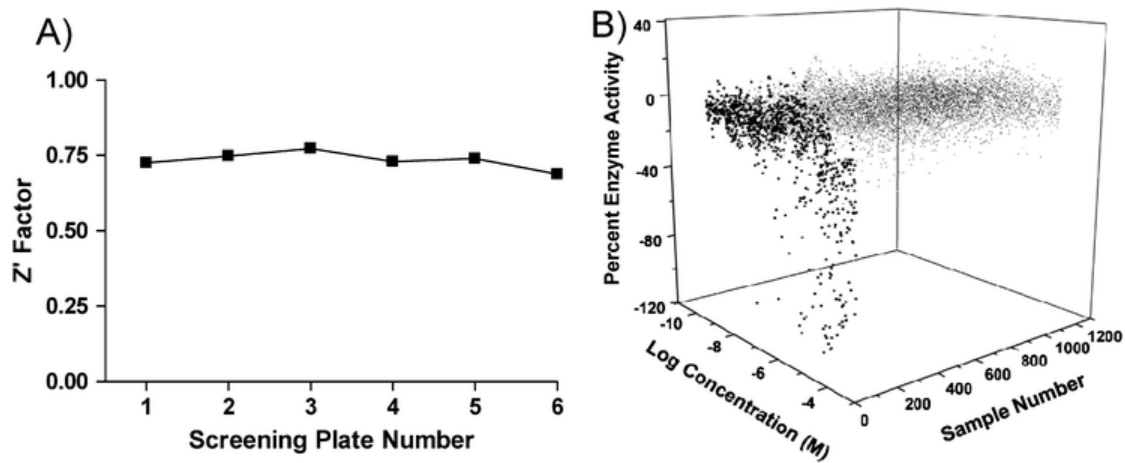
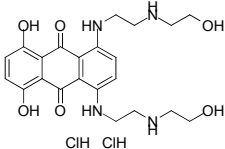
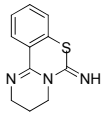
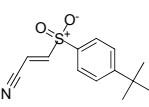
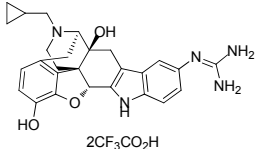
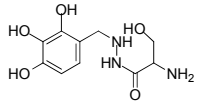
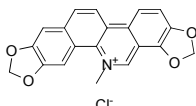
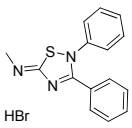
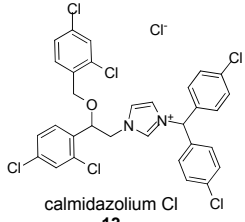
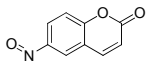
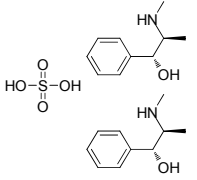


Figure 5.7 LOPAC¹²⁸⁰ qHTS.

Panel A is the screen performance represented by the reproducible high Z' factor as a function of screening plate number. Panel B is a compound activity plot of each LOPAC compound, with potential inhibitors positioned in the front (black solid dots ●), while the inactive samples are represented by open circles (○).

Table 5.1 Table 1. HTS Actives.

Values shown are IC_{50} 's in μM for Screen (six-point LOPAC HTS utilizing the rhodamine-BHQ-2 dark quench system), Retest (22-point concentration response using the HTS assay), FITC (12-point concentration response using the fluorescein-rhodamine FRET quench assay), and Gel (eight-point concentration response using whole protein assay with SDS PAGE separation). NC = not calculated. ND = no data available.

HTS Active	Screen	Retest	FITC	Gel	HTS Active	Screen	Retest	FITC	Gel
 Mitoxantrone 2HCl 5	35	Inactive	38	Inactive	 PD 404,182 10	3.5	10	1.7	1.0
 Bay 11-7085 6	2.2	9.8	19	Inactive	 2CF ₃ CO ₂ H guanidynil-naltrindole ditrifluoroacetate 11	1.3	3.4	4.9	3.1
 HCl benserazide HCl 7	22	Inactive	NC	9.3	 Cl ⁻ sanguinarine Cl 12	2.8	4.3	4.8	3.1
 HBr SCH-202676 HBr 8	0.20	0.37	0.19	0.38	 Cl ⁻ calmidazolium Cl 13	20	23	44	9.3
 6-nitroso-1,2-benzopyrone 9	2.2	6.0	2.8	3.1	 HO-SO ₃ -OH (-)-ephedrine hemisulfate 14	4.0	6.6	ND	ND

platforms and at different sites. From the three compounds which failed to confirm, mitoxantrone **5** was identified in the primary screen as being a partial-response weak active, and as such its failure to reproduce was not surprising. The variable assay results observed with BAY 11-7085 **6** and benserazide **7**, combined with the structural features of these molecules (vinyl nitrile and polyphenol, respectively), indicate that these hits may be unstable under the assay conditions and can thus be considered likely false positives or too reactive for further development.

DISCUSSION

As a first step toward identifying new inhibitor scaffolds of Sfp-PPTase, we attempted to miniaturize our recently described FRET-Quench assay using the FITC-YbbR **1a** and rhodamine mCoA **2b** acceptor (Fig. 1A).(Foley and Burkart) However, this method did not perform satisfactorily in 1,536-well format due to the overall weak signal difference and drift in the uncatalyzed control (Fig. 2A), the latter being attributed to the strong binding and aggregation of the FITC-YbbR **1a** reagent to the microtiter plates.

To circumvent this shortcoming, we embarked to overhaul the assay and address the following aspects. First, we wished to convert the assay from a FRET-quench format to a simple donor-quencher output. Doing so would eliminate the optical crosstalk effect where the fluorescence acceptor is partially excited at the wavelength used to excite the donor and produces a small amount of tail-band

emission, interfering with the donor signal being monitored. By implementing the simple donor-quencher format, the crosstalk effect is eliminated, as there is only one emitting species present in the assay. Second, we considered it advantageous to red-shift the reporter signal by utilizing a rhodamine fluorophore that excites/emits at longer wavelengths in order to avoid the fluorescein spectral region, where approximately 0.2% of a diverse compound collection has been shown to absorb or emit light.(Simeonov et al., 2008) Third, in realizing these reagent modifications, we aimed at placing the quencher onto the YbbR peptide to allow the use of the new substrates at concentrations which better reflect the K_m ratio of the native CoA and YbbR substrates. By keeping rhodamine attached to CoA and labeling the YbbR peptide with a non-emitting BHQ-2 (Fig. 1B), we were able to re-design the assay to meet all three criteria set above with only a single reagent modification.

In practice, this new assay system was greatly improved, with a stronger signal due to the more complete fluorescence quenching within the rhodamine-BHQ-2 product (Fig. 2B). This, in combination with the stability of the no-enzyme control, allowed a reduction of Sfp-PPTase level to a nanomolar concentration (Fig. 4), sensitizing the assay to inhibition and leading to significant savings of enzyme. The combination of having a low enzyme concentration and substrates used at concentrations close to their K_m ratio resulted in a more sensitive screening assay. The red-shifted nature of the assay detection combined with the micromolar concentration of rhodamine fluorophore was expected to reduce the number of fluorescent compounds capable of interfering with the signal, thereby effectively lowering the false-positive burden on the screen. Furthermore, any compounds interfering in this

manner can be easily identified because we perform the screen by monitoring reaction progress in kinetic mode. Given the limited number of sample handling steps, this is easily accomplished without limiting the throughput of the screen after complete robotic automation.

Before testing the present assay against a compound library, we assessed its ability to report on model inhibitors. The profiles observed for molecules native to the Sfp-PPTase system, such as unlabeled CoA (acting as a substrate competing with its labeled counterpart) and the reaction product PAP **3**, served as an initial proof of principle (Fig. 6). Further, we demonstrated that the enzyme is inhibited by a CoA-like molecule, MRS 2179. Lastly, as expected from changing the key serine residue to an alanine, the mutated YbbR peptide, exhibited only a minimal effect on the reaction. While we had anticipated that this peptide might serve as a representative inhibitor competitive with respect to YbbR, it should not be overlooked that deletion of a hydrogen bond donor/acceptor pair from such a minimalized motif may cause structural perturbations that significantly disrupt the peptide's binding capacity for Sfp-PPTase.

With the assay in hand, we proceeded to screen the LOPAC¹²⁸⁰ collection. The LOPAC¹²⁸⁰ represents a diverse makeup of bioactive compounds and approved drugs and is an excellent starting point to assess an assay's viability, identify preliminary inhibitor structures, and gauge the hit rate. To ensure a high quality screen, we performed the assay in concentration-response mode. In this format, the screen performed outstandingly with a stable signal window, and a high and consistent Z' factor. As anticipated from red-shifting the reporting fluorophore, and with its

micromolar concentration, there was practically no fluorescent interference affecting the data analysis. The only library compounds which affected the initial fluorescence read by values greater than three standard deviations from the median were the known fluorescent drug idamycin(Perez-Ruiz et al., 2001, Simeonov et al., 2008) and the intensely blue-colored Reactive Blue 2.(Marks et al., 2005) The identification of strong inhibitors possessing complete concentration-response curves, as well as a number of partial-response weak inhibitors demonstrated the ability of the present assay to respond to inhibitors of varying potencies expected to be found in diverse compound collections.

It is not unusual for a primary screening assay to be sensitive to both genuine enzyme inhibitors and to effectors acting by format- or assay technology-dependent mechanisms irrelevant to the enzymology at hand. To further prioritize the screening hits detected herein, we subjected the top actives to two additional comparative tests. First, the re-sourced compounds were assayed in the initial fluorescein-rhodamine reagent format in 96-well plates, an example of an orthogonal confirmation assay.(Inglese et al., 2007a) By maintaining the basic substrate composition but changing the reporter system, we wished to identify possible compounds which acted by nonspecifically disrupting the HTS reporters and confirm the activity of the newly resourced matter with a medium throughput technique. Further, we subjected the panel to analysis in an Sfp-PPTase enzymatic assay utilizing whole protein instead of the surrogate YbbR peptide. The excellent inter-assay concordance observed for the top inhibitors is indicative of the robustness of these different assay platforms and the similarity in their sensitivity, making them valuable as a panel to validate HTS actives.

The concordance also reaffirms the general reliability of the new donor-quencher assay as a tool for early discovery of PPTase inhibitors.

The top active compounds found in the screen represented a diverse set. The most potent trial HTS active, the thiadiazole SCH-202676 **8** has been reported as a reversible allosteric agonist and antagonist of G-protein coupled receptors (GPCR).(Fawzi et al., 2001) A recent mechanistic study of this compound by Lewandowicz *et al.* highlighted the possibility that it may act on GPCRs via a thiol-modification pathway dependent on the presence of dithiothreitol in the test medium.(Lewandowicz et al., 2006) Although additional studies into the mechanism of Sfp-PPTase inhibition by SCH-202676 **8** will be required, we note that our assay conditions do not contain reducing agents in any of the reagent formulations, and thereby would not be conducive to the mechanism advanced by Lewandowicz *et al.* This raises the possibility the SCH-202676 **8** may be the first true submicromolar inhibitor of Sfp-PPTase.

In addition to this compound, several low-micromolar hits deserve mention. 6-nitroso-1,2-benzopyrone (NOBP) **9** is a type of aromatic C-nitroso ligand capable of extracting zinc out of zinc-finger proteins such as HIV-1 nucleocapsid protein and poly(ADP-ribose) polymerase.(Rice et al., 1993) While it may be possible that in the present reaction NOBP **9** acts by binding the catalytic magnesium, this mechanism of action appears unlikely due to the thousand-fold excess of Mg^{2+} relative to the NOBP **9** concentration. Another hit, PD 404,182 **10**, was discovered as a phosphoenolpyruvate-competitive inhibitor of 3-deoxy-D-manno-octulosonic acid 8-phosphate (KDO) synthase and has been studied as a potential antibiotic against gram

negative bacteria.(Birck et al., 2000) Its further development was hampered by its hydrophobic nature, the absence of crystal structure, and lack of *in vivo* activity.(Sansom, 2001) Lastly, among the top actives were two molecules with extended ring systems: guanidinylnaltrindole di-trifluoroacetate (GNTI) **11** is a selective κ opioid receptor antagonist,(Stevens et al., 2000) while sanguinarine **12** is a natural product with noted anti-proliferative and pro-apoptotic effects in some cancer cell lines.(Ahmad et al., 2000) Further characterization of the top hit compounds for *in vivo* activity is currently underway.

In conclusion, we have designed and implemented an improved homogeneous assay for monitoring the Sfp-PPTase activity in real time. The mix-and-read scheme yielded a robust performance in miniaturized 1,536-well format and was used in an HTS setting to discover what we believe are the first low- and sub-micromolar small molecule inhibitors of this enzyme. The simplicity and universality of principle should make this format applicable to designing screening assays for other PPTases and transferase enzymes that have been shown to accept fluorescent substrate analogues.

ACKNOWLEDGEMENTS

This research was supported in part by the Molecular Libraries Initiative of the NIH Roadmap for Medical Research, the Intramural Research Program of the NHGRI, NIH, and grant 1R03MH083266 (M.D.B.).

Chapter 5, in whole, is a reprint of material as published in *Molecular Biosystems* (2010) Vol. 6, pp. 365-751 of which I am a primary author. Adam Yasgar performed all screening procedures at the NIH Chemical Genomics Center and Ajit Jadhav analysed the data. I prepared the assay reagents and performed all *in vitro* experiments at UCSD. This work was performed under the guidance of James Inglese, Anton Simeonov, and Michael Burkart.

Chapter 6

PREPARATION OF FRET REPORTERS TO SUPPORT CHEMICAL PROBE DEVELOPMENT

ABSTRACT

We describe an economical route to the preparation of rhodamine maleimides and non-emitting quencher probes to support a high throughput screening campaign

INTRODUCTION

Phosphopantetheinylation is an important and essential posttranslational modification representing an obligatory step during the biosynthesis of fatty acid, polyketide and nonribosomal peptide compounds. The phosphopantetheine functionality is installed on carrier domains of synthase enzymes by action of phosphopantetheinyl transferase using coenzyme A (CoA) as a donor.(Lambalot et al., 1996a) A number of synthases that undergo this modification are involved in membrane component biogenesis (fatty acids) and cell wall assembly in gram positive and gram negative organisms (teichoic acid and Lipid A, respectively), as well as the production of siderophores and small molecule virulence factors. The central role of this activation to bacterial primary metabolism and cellular maintenance has been demonstrated by genetic knockout, and chemical actuation of this process has potential to produce antimicrobial therapeutics with a novel mode of action.

In order to identify inhibitors of Sfp, a canonical representative of this enzyme class, we initially developed a fluorescent assay that utilized rhodamine-labeled CoA **1** and a fluorescein-containing acceptor peptide **2**. These are assembled into a FRET pair **3** upon action of the enzyme, thus allowing direct and continuous monitoring of the reaction (Fig. 1).(Foley and Burkart, 2009) We encountered complications during

miniaturization of this assay for a high-throughput screen (HTS) protocol; chief among them was spectral overlap of the dyes with library members. We therefore analyzed the use of tetramethylrhodamine (TAMRA) paired with a quencher such as Black Hole Quencher-2 (BHQ2) (Hamill et al., 2006, Polster et al., 2007) to overcome these obstacles and improve our method by red-shifting the signal.(Yasgar et al., 2010) We prepared pilot quantities of these reagents from commercially available TAMRA maleimide **4** and BHQ2 carboxylic acid **5** (Fig. 1). Evaluation of these initial reagents demonstrated satisfactory performance and stability, and we confirmed their viability in a miniaturized setting.(Yasgar et al., 2010) However, the high cost of reagents **4** and **5** to supply a large HTS campaign would prohibit their use.

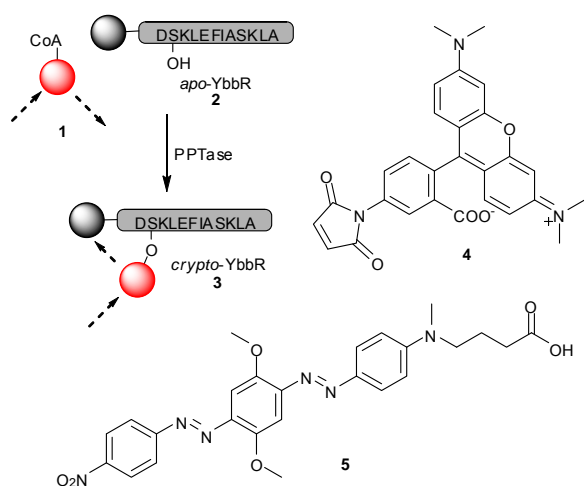


Figure 6.1 Phosphopantetheinyl transferase assay format and commercially available chemical probes.

Action of PPTase with rhodamine-CoA **1** on dark quencher –modified YbbR acceptor peptide **2**, assembles a FRET pair **3** and decreases the rhodamine-CoA fluorescence signal. These reagents were prepared from commercially available Tetramethylrhodamine maleimide **4** and Black Hole Quencher 2[®] carboxylic acid **5**.

RESULTS AND DISCUSSION

We estimated the minimum reagent need for completion of the quantitative HTS of the NIH Molecular Libraries Small Molecule Repository (311,260 compounds)(2009a) to be 120 mg of rhodamine CoA and 400 mg of quencher-peptide. The former was prepared from **4**, for which no inexpensive precursors could be identified. As such, we chose to evaluate Rhodamine WT **6**, a closely related carboxyrhodamine that is marketed for water-tracing applications as a mixture of isomers, that was recently adapted for use by McCafferty & coworkers.(Kruger et al., 2002) We acquired a sample of this material (60 g), provided as a powder and available for ~\$170/lb (Pylam Dyes, Tempe, AZ).

This mixture of isomers could be resolved by flash reversed-phase chromatography (Pedersen and Rosenbohm, 2001) using methanol : 0.003% phosphoric acid as a mobile phase (Vasudevan et al., 2001) to yield the pure isomers (Figure 2). We chose to carry forward isomer-II **7**, as it more closely resembles TAMRA maleimide **4** with respect to substitution about the benzoyl ring, given that FRET characteristics depend heavily on alignment of molecular dipoles.

The maleimide linker was assembled by mono-Boc protection of ethylene diamine **8**,(Dardonville et al., 2006) followed by conversion to maleimide **10** with *N*-(methoxycarbonyl)-maleimide **9** (Figure 2).(Huber et al., 1997) After purification, the BOC-group was removed with TFA/CH₂Cl₂ to afford TFA ammonium salt **11**.

We found that carboxylic acid **7** could be cleanly converted to the NHS-ester by treatment with *N,N'*-disuccinimidyl carbonate and a stoichiometric amount of *N,N'*-

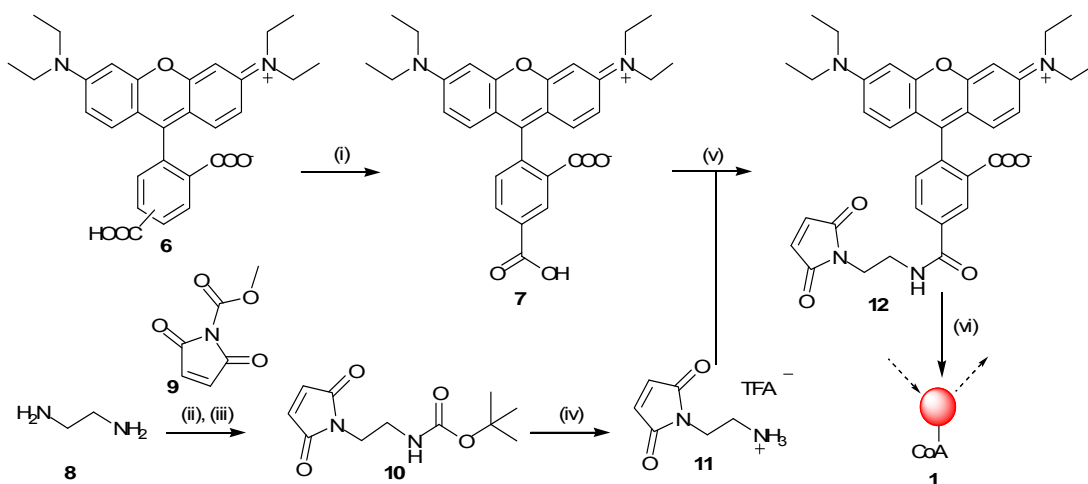


Figure 6.2 Synthetic route to Rhodamine WT-functionalized CoA

Rhodamine WT (i) C_{18} -silica, MeOH/ 0.003% H_3PO_4 , 20% (ii) $(BOC)_2O$, DCM, 87%. (iii) **9**, HCO_3^- , THF, 58%. (iv) TFA, DCM quant. (v) Et_3N , HBTU, DMF. 76% (vi) Coenzyme A, NaH_2PO_4 , quant.

dimethylaminopyridine.(Menchen and Fung, 1988, Bergot et al., 1995) Unfortunately, this compound was unreactive toward amine **11** in DMF and persisted after prolonged exposure to the reaction conditions. We achieved modest conversion to the product **12** using sodium phosphate buffer as a reaction medium. Subsequent evaluation of several activation schemes identified the HOBt ester of **7** to react readily with amine **11** in anhydrous DMF, which afforded **12** in very good yield (Figure 2). Conversion of maleimide **12** to the coenzyme A analogue **1** proceeded quantitatively in phosphate buffer and was biochemically indistinguishable from the analogue prepared using **4** as a reactive dye source.

Finding no preparative literature concerning BHQ2 carboxylic acid **5**, we developed a facile route based on published patents(Figure 3). (Cook et al., 2005, Gharavi and Saadeh, 2007) This sequence began with diazotization of aniline **13** in 3M HCl. Dilution with hydrofluoroboric acid gave the expected diazonium tetrafluoroborate salt as a precipitate. Conversion to diazoaniline **15** was accomplished by slow addition to **14** in DMF. Aqueous insolubility of **15** required conversion to the diazonium salt in concentrated sulfuric acid with nitrosylsulfuric acid as the oxidant. Subsequent reaction of the tetrafluoroborate salt with aniline **16** cleanly afforded alcohol **17**.

To activate alcohol **17** for peptide coupling, we had initially planned for oxidation to the corresponding carboxylic acid. However, the compound proved unreactive or prone to decomposition with common oxidants. As such, we investigated the use of activated carbonates or carbamates to install the alcohol onto

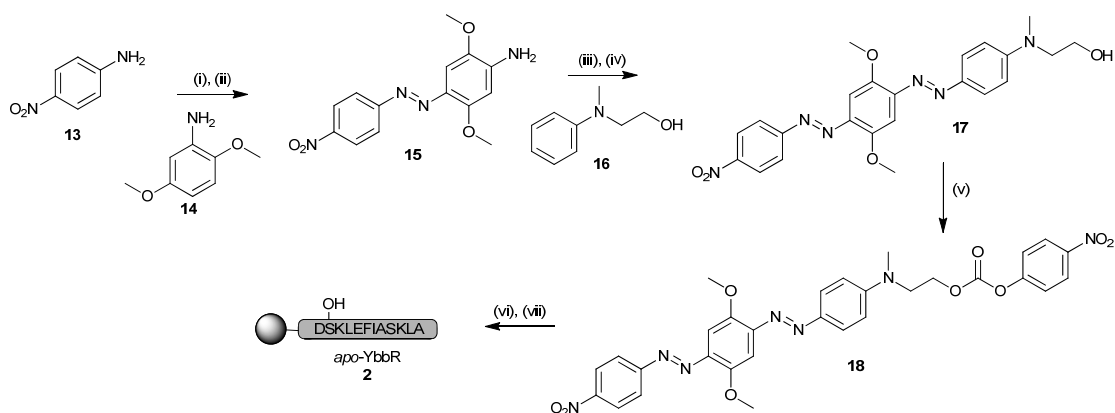


Figure 6.3 Synthetic route to dark quencher p-nitrophenyl carbonate

(i) 3M HCl, NaNO₂; HBF₄. (ii) 2,5-dimethoxyaniline, DMF, 69%. (iii) HSO₃NO, H₂SO₄; HBF₄. (iv) *N*-methyl-*N*-(2-hydroxyethyl)-aniline, DMF, 47% (2 steps). (v) *p*-NO₂PhCOCl, DIPEA, quant. (vi) H₂N-Ahx-DSKLEFIASKLA-O-[PEG]-PS resin, DIPEA. (vii) 96:2:2 TFA:TIPS:H₂O the peptide. We found that **17** could be readily converted to an imidazole carbamate or *p*-nitrophenyl carbonate **18** (Scheme 2). (Vatele, 2004)

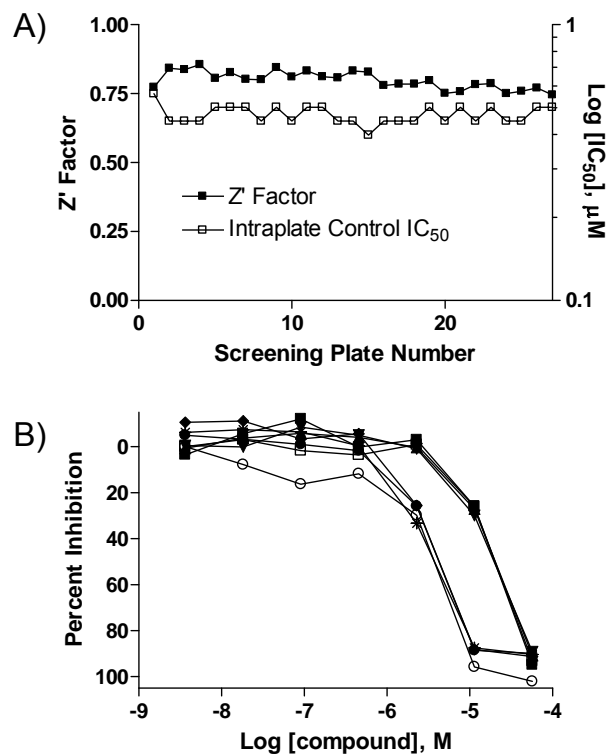


Figure 6.4 Utilization of the new reagents in a triplicate robotic screen of the LOPAC1280 library.

(A) Excellent screening assay performance as evidenced by the consistently high Z' factor and the unchanging IC_{50} for a control inhibitor SCH-202676. (B) Switching to the new reagents did not change the assay's sensitivity to inhibitors as evidenced by the nearly identical dose responses obtained for two inhibitors of different potency, PD 404,182 (average IC_{50} 3.2 μ M) and calmidazolium chloride (average IC_{50} 20 μ M) when old (PD 404,182, \circ ; calmidazolium chloride, \square) and new (PD 404,12: \blacklozenge , \bullet , and \ast ; calidazolium chloride: \blacksquare , \blacktriangle , and \blacktriangledown) reagents were used.

We prepared the final product by assembling the aminocaproate-terminated YbbR peptide (sequence: NH₂- DSKLEFIASKLA-CO₂H)(Yin et al., 2005b) using Fmoc-based solid phase peptide synthesis protocols on a 0.2 mmol scale.(Glover et al., 1999a) Treatment of the resin overnight with 4 molar equivalents (500 mg) of **18** gave clean conversion to peptide **2** that was HPLC purified to afford 228 mg of product at > 98% purity (Scheme 2). The process was iterated three times to afford sufficient material for HTS (> 500 mg).

The above-prepared reagents provided a stable and highly reproducible dose-response screen of the LOPAC¹²⁸⁰ (library of pharmacologically active compounds, Sigma-Aldrich) performed in triplicate using a fully-automated robotic screening system(Fig. 2).(Michael et al., 2008) As seen in Figure 6.4A, the robotic screen was associated with consistently high Z' screening factor (Zhang et al., 1999) and near-constant IC₅₀ for an inhibitor dose-response series included on every screening plate. Furthermore, two previously noted screening hits,(Yasgar et al., 2010) PD 404,182 and calmidazolium chloride, displayed uniform concentration-response triplicate curves which overlapped those obtained in an earlier screen performed with the initial reagent set (Figure 6.4B). These results confirmed that the assay retained its sensitivity to inhibitors with the new reagents.

The methods presented here for the general preparation of tetraethylrhodamine probes and quencher-modified peptides is economical and executable at a preparative scale. These procedures should be found applicable not only for the preparation of labeled peptides as above, but also as simple and direct source to quenchers for other FRET-based assay platforms (i.e. nucleic acids).

Notes and references

^a University of California, San Diego, 9500 Gilman Drive, San Diego, CA. USA. Tel: 001-858-534-5673 E-mail: mburkart@ucsd.edu

^b NIH Chemical Genomics Center, 9800 Medical Center Drive, Bethesda, MD 200892-3370, USA.

MATERIALS AND METHODS

All reagents and chemical compounds were purchased from commercial sources and used without further purification unless otherwise noted. Triethylamine (Et₃N) was distilled from sodium. Pyridine was distilled from KOH. Reactions were stirred magnetically with a teflon-coated stir bar, and all non-aqueous reactions were performed under a balloon of dry argon in septum-sealed, oven-dried glassware. When required, compounds were purified via flash chromatography [ref still] on 230-400 mesh Silica Gel 60 (Merck). Analytical TLC was performed on 250 μm silica layers on glass plates (Silica Gel 60 F254, Merck) and separated compounds visualized by illumination with UV light or an appropriate stain (bromocresol green or I₂ on SiO₂). Analytical reverse phase TLC was performed on 200 μm layers of Partisil[®] KC₁₈ layers on glass plates (Cat. No. 4801-425, Whatman). HPLC was performed on an Agilent 1100 series instrument equipped with a preparative scale autosampler (fitted with a 900 μL injection loop) and a diode array detector. Analytical separations were performed on a 4.6 x 150 mm Beckman Ultrasphere ODS column (Cat. No. 235330) with injection volumes ranging from 50 – 100 μL. Semipreparative separations were

performed on a 10 x 250 mm Biotage KP-C18-HS 35/70 μ column (Cat. No. S1L0-1119-95050) using an injection volume of 500 – 900 μ L.

Preparative separations were performed on a Waters instrument comprised of a model 680 gradient controller, model 510 pumps fitted with high flow volume 225 μ L heads, model 2487 dual wavelength detector, Hewlett Packard 3396-series II integrator and a Pharmacia Frac-100 fraction collector and a 22 x 250 mm Econosphere C18 (10 μ m) column (Cat. No. 50195422, Grace Davison). Prior to separation, samples were prepared using Waters SepPak C₁₈ solid phase extraction columns to remove salts and nonpolar contaminants that irreversibly adsorb to reverse phase media.

Characterization data and yields correspond to homogeneous materials. NMR data were collected on a 300 MHz Varian Mercury or 400 MHz Varian Mercury Plus spectrometers operating at 300.077 MHz or 399.913 MHz for ¹H-NMR and 75.462 MHz or 100.567 MHz for ¹³C-NMR, respectively, at the UCSD Department of Chemistry and Biochemistry NMR facility. FID files were processed using MestReNova software version 5.3.2. Chemical shifts were calibrated using the signal from residual D₆-DMSO (δ 2.50, pentet, ¹H-NMR) and (δ 39.52, heptet, ¹³C-NMR), D₁-chloroform (δ 7.26, singlet, ¹H-NMR) and (δ 77.16, triplet, ¹³C-NMR), or D₄-methanol (δ 3.31, pentet, ¹H-NMR) and (δ 49.00, heptet, ¹³C-NMR). Mass spectrometric data was collected by the UCSD Department of Chemistry and Biochemistry Small Molecule Mass Spectrometry facility on Finnigan LCQDECA and ThermoFinnigan MAT900XL spectrometers.

Rhodamine Coenzyme A 2

Coenzyme A (76 mg, 0.1 mmol) was dissolved in 20 mM NaH₂PO₄ pH 7.4 (100 mL) and cooled on ice. Rhodamine maleimide **12** (76 mg, 0.13 mmol) was dissolved in methanol (20 mL) and added in 1 mL portions. The reaction was wrapped in foil and stirred for 3 h at which point no detectable Coenzyme A was present (determined by HPLC). The reaction was transferred to a separatory funnel and washed with dichloromethane (5 x 100 mL). The resulting aqueous phase was passed over a Waters SepPak solid phase extraction column equilibrated in 0.05% TFA, washed with 5 column volumes 20% acetonitrile/0.05% TFA and rhodamine CoA **1** eluted with 80% acetonitrile/0.05% TFA. Acetonitrile was removed by rotary evaporation and provided **12** as a fine purple precipitate.

Separation of Rhodamine WT isomers

Rhodamine WT **3** (1 g) was dissolved in methanol (200 mL). Dichloromethane was added (400 mL) and the solution extracted with 1M HCl (400 mL). The organic phase was concentrated *in vacuo* to give a burgundy solid. The solid was dissolved in methanol (50 mL) and diluted with 0.003% phosphoric acid (70 mL). This solution was loaded on a preparative C₁₈-silica column (7 cm x 20 cm bed dimensions) equilibrated in 35:65 methanol: 0.003% phosphoric acid. The isomers were resolved by a step gradient from 35 to 60% methanol that increased in increments of 5% methanol. Fractions containing the separated isomers were pooled, diluted with an equal volume 1M HCl and extracted with dichloromethane (3 x total volume). The pooled organic phase was dried over Na₂SO₄ and evaporated to give the Rhodamine

WT isomer I and rhodamine WT isomer II **7** in a ratio of approximately 2:1 (isomer I : isomer II).

isomer I. δ H (400 MHz, CD₃OD) 8.90 (17 H, d, *J* 1.4), 8.41 (4 H, dd, *J* 7.9, 1.5), 7.53 (4 H, d, *J* 7.9), 7.10 (10 H, d, *J* 9.5), 7.03 (10 H, dd, *J* 9.5, 2.2), 6.97 (36 H, d, *J* 2.2), 3.67 (40 H, q, *J* 7.0), 1.30 (264 H, t, *J* 7.0). δ C (101 MHz, DMSO) 166.59, 166.53, 157.53, 155.37, 135.11, 131.56, 131.49, 131.06, 114.82, 113.10, 96.62, 45.91, 13.12. MS (ESI) *m/z* 487.40 ([M⁺]⁺, 100%); HRMS (ESI-FT) *m/z* calcd for C₂₉H₃₁N₂O₅ 487.2227, found 487.2229.

isomer II **7**. δ H (400 MHz, CD₃OD) 8.90 (17 H, d, *J* 1.4), 8.41 (4 H, dd, *J* 7.9, 1.5), 7.53 (4 H, d, *J* 7.9), 7.10 (10 H, d, *J* 9.5), 7.03 (10 H, dd, *J* 9.5, 2.2), 6.97 (36 H, d, *J* 2.2), 3.67 (40 H, q, *J* 7.0), 1.30 (264 H, t, *J* 7.0). δ C (75 MHz, CDCl₃) 170.72, 170.24, 162.60, 161.96, 159.85, 142.10, 137.20, 137.06, 136.98, 136.28, 136.11, 135.98, 135.04, 134.90, 118.31, 117.26, 100.13, 100.02, 49.65, 15.75, 15.60. MS (ESI) *m/z* 487.42 ([M⁺]⁺, 100%); HRMS (ESI-FT) *m/z* calcd for C₂₉H₃₁N₂O₅ 487.2227, found 487.2233.

tert-butyl 2-aminoethylcarbamate

1,2-diaminoethane **8** (7.7 mL, 114 mmol) was dissolved in chloroform (450 mL) and cooled to 0°C in an ice bath with stirring. A solution of t-butyl dicarbonate (5.26mL, 22.9 mmol) dissolved in chloroform (46mL) was cooled to 0°C and added dropwise to the ethylene diamine solution via pressure equalizing addition funnel over 2h. After addition was complete, the ice bath was removed and the reaction stirred overnight at room temperature to give a heterogenous solution. Solids were filtered off

and the filtrate evaporated to give a oil. The oil was dissolved in EtOAc (100 mL), washed with half-saturated brine (3 x 50 mL), dried over Na₂SO₄, and concentrated *in vacuo* to give monoamine (3.220 g, 20.1 mmol, 87 %). δ H (400 MHz, CDCl₃) 3.15 (1 H, dd, *J* 11.5, 5.7), 2.77 (1 H, t, *J* 5.9), 1.42 (5 H, s, *J* 9.4). δ C (101 MHz, CDCl₃) 177.14, 156.47, 79.28, 43.30, 41.63, 28.44. MS (ESI) *m/z* 160.95 ([M+H]⁺, 100%); HRMS (ESI-FT) *m/z* calcd for C₇H₁₇N₂O₂ 161.1285, found 161.1286.

N-(methoxycarbonyl)-maleimide 9

Maleimide (5 g, 51.5 mmol) was dissolved in ethyl acetate (250 mL). N-methyl morpholine (5.6 mL, 51.5 mmol) was added via syringe and the solution cooled on ice for 20 minutes. Methyl chloroformate (4.8 mL, 61.8 mmol) was added dropwise and the reaction stirred 30 min. Over this time, solids evolved and were collected on a büchner funnel, and washed with ethyl acetate (100 mL). The Filtrate and washes were combined, washed successively with water (1 x 100 mL) and brine (1 x 100 mL), dried of Na₂SO₄ and evaporated to dryness. The resulting solid was recrystallized from EtOAc/iPr₂O to give methyl carbamate **9** (6.211 g, 40 mmol, 78 %). NB: DIPEA is not an acceptable substitute for NMM. δ H (400 MHz, CDCl₃) 6.84 (1 H, s, *J* 4.6), 3.94 (1 H, s, *J* 0.4). δ C (101 MHz, CDCl₃) 165.89, 148.32, 135.53, 54.52. MS (ESI) *m/z* 156.04 ([M+H]⁺, 100%); HRMS (ESI-FT) *m/z* calcd for C₆H₆NO₄ 156.0291, found 156.0293.

tert-butyl 2-(2,5-dioxo-2,5-dihydro-1H-pyrrol-1-yl)ethylcarbamate 10

Tert-butyl 2-aminoethylcarbamate (1.13 g, 7.1 mmol) was dissolved in saturated sodium bicarbonate (35 mL), filtered, and cooled to 0°C. Finely ground N-methoxycarbonyl maleimide **9** (1.1 g, 7.09 mmol) was added and the reaction stirred for 15 minutes at room temperature. THF (55 mL) was added and the reaction stirred 45 min. Water (50 mL) was added and the solution washed with ethyl acetate (3 x 75 mL). The organic washes were pooled, dried over Na₂SO₄, and concentrated to give a oil that solidified upon standing. The residue was purified by chromatography on SiO₂ with a step gradient of hexane:ethyl acetate to give title compound **10** as a white solid (1.0922 g, 4.55 mmol, 58 %). δ H (400 MHz, CDCl₃) 6.68 (2 H, s), 3.67 – 3.55 (2 H, m), 3.29 (2 H, dd, *J* 11.1, 5.8), 1.36 (9 H, s). δ C (101 MHz, CDCl₃) 171.04, 134.37, 79.67, 39.53, 38.19, 28.51. MS (ESI) *m/z* 263.04 ([M+Na]⁺, 100%) ; HRMS (ESI-FT) *m/z* calcd for C₁₁H₁₆N₂O₄Na 263.1002, found 263.1008.

**2-(2,5-dioxo-2,5-dihydro-1H-pyrrol-1-yl)ethanammonium
trifluoroacetate **11****

tert-butyl 2-(2,5-dioxo-2,5-dihydro-1H-pyrrol-1-yl)ethylcarbamate **10** (1.000 g, 4.15 mmol) is dissolved in dichloromethane (10 mL) and cooled on ice. Trifluoroacetic acid (2 mL) is added and the solution stirred overnight. The reaction is diluted into diethylether (38 mL), cooled on ice 1 h, and filtered to provide the title compound **11** (1.051 g, 4.14 mmol) as a crystalline white solid. δ H (300 MHz, CD₃OD) 6.89 (1 H, s), 3.90 – 3.73 (1 H, t, *J* 5.6), 3.24 – 3.09 (1 H, t, *J* 5.6). δ C (75 MHz, cd3od) 171.19, 162.47, 162.01, 161.55, 161.09, 134.56, 38.65, 35.05. MS (ESI)

m/z 141.09 ($[M+H]^+$, 100%) ; HRMS (ESI-FT) m/z calcd for $C_6H_9N_2O_2$ 141.0658, found 141.0659.

Rhodamine-WT maleimide 12

Rhodamine WT isomer II **4** (10mg, 0.02 mmol) was dissolved in DMF (2 mL). HBTU (8.56mg, 0.02 mmol) and DIPEA (5.31 mg, 7.15 μ L, 0.04) are added successively with stirring. After 30 minutes, the reaction was checked by rp-TLC (MeOH/H₂O; 80/20) to ensure the formation of the HOBt ester (R_f = 0; deep purple) . N-(2-aminoethyl) maleimide TFA salt (10.43mg, 0.04 mmol) was added and the reaction followed to completion by rpTLC (product R_f = 0.5 in MeOH / 0.003% H₃PO₄; 80/20.) The reaction is diluted with dichloromethane (50 mL) and washed with NaH₂PO₄ buffer (50 mM, pH 7.4, 1 x 50 mL), brine (1 x 50 mL), dried over Na₂SO₄, and evaporated. The resulting purple solid was further purified by reverse phase HPLC to yield rhodamine WT isomer II- maleimide **12** (9.5 mg, 76 %). δ H (400 MHz, cd₃od) 8.69 (1 H, d, J 1.6), 8.16 (1 H, dd, J 7.9, 1.7), 7.51 (1 H, d, J 7.9), 7.12 (3 H, d, J 9.5), 7.03 (3 H, dd, J 9.5, 2.3), 6.98 (3 H, d, J 2.3), 6.84 (2 H, s), 3.87 – 3.76 (2 H, m), 3.75 – 3.60 (15 H, m), 1.30 (27 H, t, J 7.2). δ C (101 MHz, CDCl₃) 171.37, 159.61, 157.95, 155.64, 136.66, 135.98, 134.40, 131.80, 131.65, 130.27, 130.20, 114.16, 113.69, 96.21, 46.11, 39.02, 37.69, 12.67. MS (ESI) m/z 609.47 ($[M]^+$, 100%) ; HRMS (ESI-FT) m/z calcd for $C_{35}H_{37}N_4O_6$ 609.2708, found 609.2720.

(E)-2,5-dimethoxy-4-((4-nitrophenyl)diazenyl)aniline 15

2,5-dimethoxyaniline **14** was supplied by Sigma-Aldrich as pellets of a black solid, and required purification before proceeding. **14** (10 g) was dissolved in ethyl acetate (200 mL) and the persisting solids filtered to give a black solution. Activated carbon (2 g) is added and the solution stirred 20 minutes. Celite is added and the solution is filtered to give a faintly yellow solution which could not be further decolorized by reiteration of the above treatment. The solution is concentrated *in vacuo* and the crude material recrystallized from boiling EtOH or hexanes to give 2,5-dimethoxyaniline **14** as a white crystalline solid.

2,5-dimethoxyaniline **14** (0.9506 g, 6.21 mmol) is dissolved in DMF (10 mL). A solution of p-diazoniumnitrobenzene tetrafluoroborate (prepared from **13**) in DMF (10mL) is added slowly, and evolves a deep red color. Saturated sodium bicarbonate is added every 5' (6 x 1 mL additions). After 1h, the reaction is diluted with 200mL H₂O and placed on ice. A dark volumous precipitate forms and is collected by filtration, washed with water, dried over Ca₂CO₃ dessicant. The resulting solid is recrystallized from hexanes:EtOAc (3:1) to yield the title compound **15** (1.24 g, 4.1 mmol, 69%). δ H (400 MHz, CDCl₃) 8.30 (1 H, d, *J* 9.1), 7.90 (1 H, d, *J* 9.0), 7.40 (1 H, s), 6.35 (1 H, s), 4.61 (1 H, s), 3.98 (2 H, s), 3.90 (2 H, s). δ C (101 MHz, CDCl₃) 157.56, 156.74, 146.87, 145.79, 142.18, 133.64, 124.79, 122.59, 97.69, 97.00, 56.62, 55.86, 50.08. MS (ESI) *m/z* 303.06 ([M+H]⁺, 100%) ; HRMS (ESI-FT) *m/z* calcd for C₁₄H₁₅N₄O₄ 303.1088, found 303.1090.

2-((4-((E)-(2,5-dimethoxy-4-((E)-(4-nitrophenyl)diazenyl)phenyl)diazenyl)phenyl)(methylamino)ethanol 17

Diazoaniline **15** is dissolved in sulfuric acid (concentrated, 100 mL) at room temperature to give a thick, deep purple solution. The reaction is cooled on ice (20 minutes). Nitrososulfate is prepared separately by dissolving NaNO₂ in sulfuric acid and warming to 50°C in a water bath. After complete dissolution, the solution is cooled in an ice bath and added dropwise to diazoaniline **15**. After 1 hour of stirring, ice cold 1M hydrogen tetrafluoroborate (300 mL) is slowly added and the solution extracted with dichloromethane (5 x 100 mL). The organic extract is pooled, dried over Na₂SO₄ and evaporated to yield 0.661 g of the diazonium tetrafluoroborate salt that was dissolved in THF (200 mL) and to which a solution of N-methyl-N-(2-hydroxyethyl)-aniline **16** (0.286 g, 1.73 mmol) in THF (20 mL) was added dropwise. The reaction was stirred for 1 h and stripped of solvent. The residue was dissolved in dichloromethane (300 ml) and washed with 1M HCl (1 x 150 mL) and brine (1 x 150 mL) and dried over Na₂SO₄ to give **17** as a green-purple crystalline solid (0.748 g, 1.56 mmol, 47 %). δ H (400 MHz, CDCl₃) 8.38 (1 H, dd, *J* 9.3, 2.3), 8.05 (1 H, dd, *J* 9.3, 2.3), 7.95 (1 H, d, *J* 9.1), 7.49 (1 H, d, *J* 13.3), 6.85 (1 H, d, *J* 9.1), 4.10 (2 H, s), 4.05 (1 H, s), 3.91 (1 H, t, *J* 5.6), 3.66 (1 H, t, *J* 5.7), 3.17 (2 H, s). δ C (101 MHz, CDCl₃) 156.57, 153.71, 152.67, 150.98, 148.50, 146.82, 144.61, 142.19, 126.34, 124.90, 123.70, 111.74, 101.19, 100.18, 59.81, 56.87, 54.70, 50.40, 39.44. MS (ESI) *m/z* 465.10 ([M+H]⁺, 100%) ; HRMS (ESI-FT) *m/z* calcd for C₂₃H₂₄N₆O₅Na 487.1700, found 487.1702.

2-((4-((E)-(2,5-dimethoxy-4-((E)-(4-nitrophenyl)diazenyl)phenyl)diazenyl)phenyl)(methylamino)ethyl 4-nitrophenyl carbonate **18**

diazo-hydroxyethylaniline **17** (0.800 g, 1.72 mmol) was dissolved in 200 mL dry dichloromethane. p-nitrophenylchloroformate (0.382 g, 1.89 mmol) was added, followed by pyridine (0.416 mL, 0.408 g, 5.17 mmol), and stirred for 2h. The reaction was washed (1 x 200 mL each) with 1M HCl, 50% saturated sodium carbonate, brine, and dried over Na₂SO₄. Silica gel (5 g) was added and the mixture stripped of solvent. The silica was dried under vacuum (<10 mmHg), and used to dry load a silica gel column (60 g) and eluted with hexanes/ethylacetate (1:1) to give the p-nitrophenyl carbonate **18** (1.0551 g, 1.70 mmol, 97 %). δ H (400 MHz, CDCl₃) 8.38 (1 H, d, *J* 9.0), 8.25 (1 H, d, *J* 9.2), 8.05 (1 H, d, *J* 9.1), 7.96 (1 H, d, *J* 9.2), 7.49 (1 H, d, *J* 16.5), 7.24 (1 H, s, *J* 3.2), 6.85 (1 H, d, *J* 9.3), 4.53 (1 H, t, *J* 5.7), 4.10 (2 H, s, *J* 6.6), 4.06 (2 H, s), 3.87 (1 H, t, *J* 5.7), 3.18 (2 H, s, *J* 10.8). δ C (101 MHz, CDCl₃) 177.25, 156.56, 155.47, 153.65, 152.70, 151.96, 151.17, 148.60, 146.61, 145.10, 142.47, 126.26, 125.50, 124.93, 123.75, 122.01, 111.90, 101.25, 100.29, 66.29, 56.94, 50.86, 50.65, 39.10, 29.87. MS (ESI) *m/z* 630.15 ([M+H]⁺, 100%) ; HRMS (ESI-FT) *m/z* calcd for C₃₀H₂₈N₇O₉ 630.1943, found 630.1941.

ACKNOWLEDGEMENTS

Chapter 6, in whole, is material being prepared for publication. I am the primary author of this work. I performed all synthetic work and spectroscopic

characterization. Adam Yasgar evaluated the reagents, and Ajit Jadhav analysed the data. This research was performed under the guidance of Michael Burkart.

Chapter 7

INHIBITORS OF SURFACTIN-TYPE PHOSPHOPANTETHEINYL TRANSFERASE IDENTIFIED BY QUANTITATIVE HIGH THROUGHPUT SCREENING

ABSTRACT

A myriad of virulence factors of human pathogens are produced by fatty acid, polyketide and nonribosomal peptide biosynthetic pathways. These systems require covalent posttranslational modification with a 4'-phosphopantetheinyl group to their carrier protein domains, a process that is performed by phosphopantetheinyl transferase. Surfactin-Type PPTases, a subdivision of this enzyme family, are responsible for modifying most secondary metabolic pathways, and inhibitors of this enzyme would be useful to further current approaches looking to blockade these anabolic pathways to treat human disease. Herein we detail efforts to identify inhibitors of Sfp-Type phosphopantetheinyl transferase by automated quantitative high throughput screening of large chemical libraries, and efforts toward the nomination of a chemical probe that may serve to validate Sfp-PPTase for further therapeutic development.

INTRODUCTION

Fatty acids, non-ribosomal peptides, and polyketides are three classes of polymeric metabolites with key roles in human health and disease, both as therapeutic treatments and as virulence factors manufactured by pathogens. Unifying to biosynthesis of these compounds is the covalent tethering of intermediates to small carrier protein domains of the multienzyme complexes (i.e. synthases). A thioester bond holds the nascent polymer to these synthases, and is not of a proteogenic source. The corresponding thiol accomplishing this job is the functional terminus of a 4'-

phosphopantethiene group that is covalently installed as a posttranslational modification from coenzyme A (CoA) donor. This moiety is attached by the catalytic action of phosphopantetheinyl transferase enzymes (PPTases).

PPTase enzymes are structurally distinct, and constitute a novel enzyme superfamily. These are typically soluble proteins, the superfamily can be grouped into two denominations, the AcpS-type and Sfp-type classes (AcpS-PPTase and Sfp-PPTase, respectively), based upon primary structure (Lambalot et al., 1996a). Congeners of these classes are responsible for modifying carrier protein domains in all primary and secondary metabolic pathways found in prokaryotic life.

The pivotal role that PPTases play in activating cardinal processes of primary metabolism in bacteria (i.e. fatty acid, teichoic acid, lipid A and siderophore biosynthesis) has made them attractive targets for the development of therapeutics to combat multidrug resistance, and numerous reports have detailed efforts that pursued inhibitor development (Chu et al., 2003b, Gilbert et al., 2004, Joseph-McCarthy et al., 2005a, McAllister et al., 2000, Payne et al., 2007) However, we have found that at least one of class of these compounds possesses a narrow spectrum of activity, and may not provide adequate antagonism against all PPTase loci that bacteria may possess.

Furthermore, in pathogenic organisms, PPTases activate numerous biosynthetic pathways that produce a variety of virulence factors, including small molecule toxins such as mycolactone from *Mycobacterium ulcerans*, siderophores required for iron acquisition during infectivity, as well as cell wall components that may impart hypervirulency; and blockade of routes leading to the production of these molecules has received much attention as a new route for therapeutic

development.(Onwueme et al., 2005, Barry et al., 1998, Chalut et al., 2006a) Given the amplification that these pathways receive from PPTase enzymes (that is, many molecules are made for every 4'-PP arm that is installed), we are interested in evaluating the effects that inhibitors against this enzyme would have to dampen virulence factor production and thus pathogenicity.

As mentioned above, we have evaluated the currently known chemical matter that has been previously reported to act against AcpS-PPTase. In these experiments, we found that these compounds (the anthranilate 4H-oxazol-5-ones) were inactive against Sfp-PPTase. It has been shown that possession of a capable enzyme from the latter class can viably complement organisms when lesions are introduced in to the *acpS* locus, and this suggests that the effective targeting of PPTase must be accomplished with a compound of broader specificity to cover both enzyme classes, or be the combination of two or more narrow spectrum inhibitors. However, no disclosures describing Sfp-PPTase antagonist chemical entities have been made.

To fill this gap, we recently developed a miniaturized FRET-based homogenous screen for PPTase activity capable of robotic automation; and served to identify the first known small molecule inhibitors of Sfp-PPTase. The compounds that arose from this feasibility study were unlikely to provide PPTase specific antagonistic activity, and further evaluation demonstrated that we had not found a new PPTase-targeting antibiotic. Herein we detail the high throughput screening of large chemical libraries with this assay to identify new inhibitor architectures of Sfp-PPTase, and the evaluation of primary actives from this campaign in effort to nominate a PPTase chemical probe.

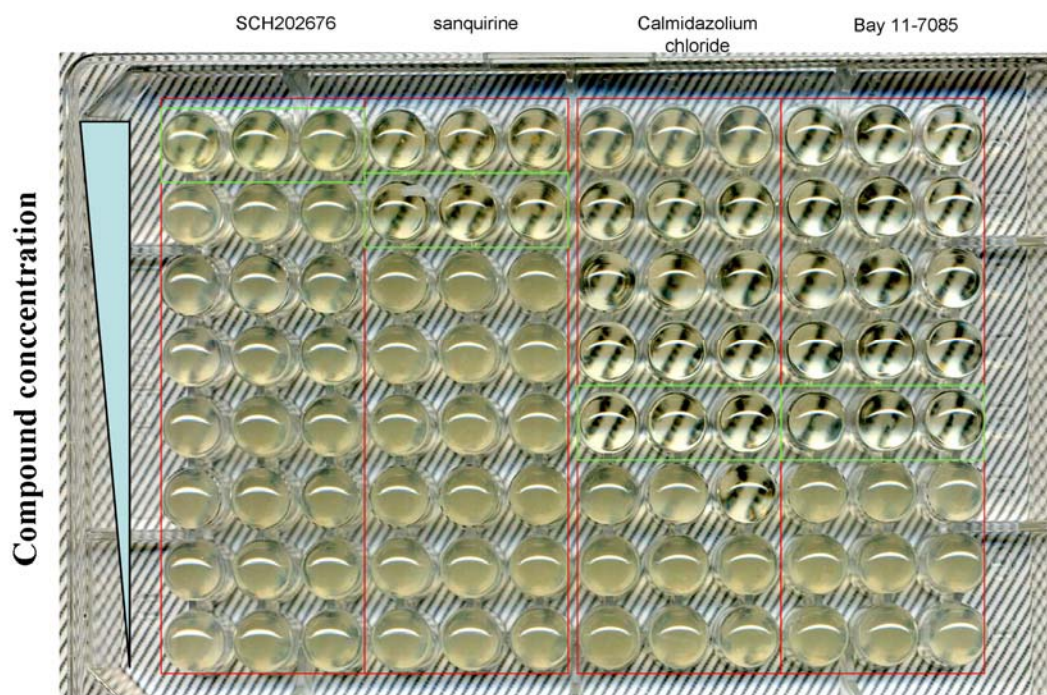
RESULTS

Assay Principle and known inhibitor evaluation.

We have previously reported the development of a FRET-Quench based assay for Sfp Phosphopantetheinyl transferase (Foley et al., 2009), and its optimization in a miniaturized high sample density format (Yasgar et al., 2010). This optimized assay functions in principle by observing the quench of fluorescence from a rhodamine CoA precursor upon attachment of the modified 4'-PP arm to a quencher-containing acceptor peptide (Figure 5.1). During these initial studies, we profiled the 1280 member Library Of Pharmacologically Active Compounds (LOPAC¹²⁸⁰) at 8 concentrations according to the qHTS paradigm, and identified the first known small molecule inhibitors of Sfp-PPTase. We further characterized these compounds in an antibiotic assay against *B. subtilis* strains and found that the top actives were either inactive or prone to metabolism in this biological context, and would serve insufficiently as base architectures for further optimization. As such, this warranted a large-scale inhibitor identification campaign.

Table 7.1 Antibiotic activity of LOPAC¹²⁸⁰ actives against *B. subtilis* M489

Table 7.1		
compound	MIC	
PD-404,18	>100	μM
6-NOBP	1.23	μM
GNTI	100	μM
mitoxanthrone x 2HCl	33	μM
BAY 11-7085	1.23	μM
calmidazolium chloride	1.23	μM
sanquinine HCl	33	μM
SCH202676	100	μM
Benzseridine	>100	μM

Figure 7.1 Data cataloging for antibiotic analysis of LOPAC¹²⁸⁰ hits.

Active compounds identified in Chapter 5 were evaluated against *B. subtilis* strains OKB105 and HM489 to assess their antibiotic properties against Sfp⁺ and Sfp⁻ genotypes. No compound showed a differential MIC, and data are presented in Table 7.1. Red boxes denote evaluation of each compound in replicate, and green boxes represent the dilution corresponding to the minimum inhibitory concentration.

Library composition

The qHTS of Sfp-PPTase was run against a library of 311,260 compounds. The collection spanned large diverse chemical sub-libraries including the NIH Molecular Libraries Small Molecule Repository (MLSMR) and the NCGC Exploratory Collection, the latter of which consisted of compounds with known pharmacological activity (e.g., LOPAC¹²⁸⁰, Prestwick, Microsource, Tocris, Biomol); a set of approved drugs; collections from the Centers for Chemical Methodology and Library Development (CMLD); and inhouse synthesized compounds. The total screened collection contained a few thousand duplicates overlapping the various sub-libraries.

qHTS Performance

The screening campaign consumed 2387 assay plates in three robotic runs over 162 hours on the Kalypys robotic system (Michael et al., 2008) to achieve 100% coverage of the entire library at 7 concentration points. A total of 1685 plates passed quality control analysis (Table 7.2). The bulk of the failed plates occurred during the first robotic run, and arose from an unforeseen instability of the reagent mixture to storing in large volumes, and resulted in diminished assay performance and Z' values for the intraplate controls that became evident 8 hours after preparation. As a result, the screen was implemented with routine replenishment of fresh reagent thrice per day. Such implementation provided satisfactory assay performance across the screen, as evidenced by a stable Z' value of 0.78. (Table 7.2) Overall, the Z'

Table 7.2 Summary of qHTS data collection and performance.

This table summarizes the data files collected and assay performance across three sets of experiments: the off-line (i.e. manual) validation performed in Chapter 5 (Assay Optimization), the triplicate run of LOPAC using the homemade probes performed with the Kalypsys robot and detailed in Chapter 6 (Validation), and the large scale qHTS of the MLSMR and NCGC collections (qHTS).

Sfp-PPTase Project	qHTS data summary		PubChem AID:1490 (validation only)
Parameter	Assay optimization	Validation	qHTS
system	off-line	Kalypsys robot	Kalypsys robot
plates screened	7	26	2387 (1685 passed)
plates failed QC	0	0	702
Total qHTS wells	8,960	26,880	2,588,160
Data points	17,920	53,760	5,176,320
% 7 pt titrations	100%	100%	100%
data layers	read 1 (bkg fluorescence) read 2 delta (calculated)	read 1 (bkg fluorescence) read 2 delta (calculated)	read 1 (bkg fluorescence) read 2 delta (calculated)
average Z'	0.73	0.90	0.78
Compounds tested	1,280	1,280	311,260
inactives	1197	1197	286,907
inconclusives	43	43	6911
weak actives	26	26	11,086
actives	13	13	10,959

factor remained flat over the screen, with minor valleys tracking with the maturation of the reagent mixture, and peaks indicating the replenishment of the solution (Figure 7.2A). As an interpolate control, we utilized a 2-fold dilution series of SCH-202676, the submicromolar inhibitor we identified previously. Remarkably, the control titration was stable throughout the screen, displaying an average IC₅₀ of 500 nM (Figure 7.2B) and a minimum significance ratio of 2.6. Each library compound was tested at seven concentrations, ranging from 114 μ M to 2.9 nM, totaling 2,588,160 wells with two time points collected for each, providing a dataset of 5,176,320 points.

Analysis of qHTS Screening Data

Given the small volume of the reaction assay, we performed the screen according to the qHTS paradigm. This method involves the acquisition of full concentration responses traces for all library members and allows for the extraction of an AC₅₀ value, defined as the half-maximal activity concentration, for each compound that elicits a change in response over control. This protocol provides the opportunity to triage false positives and negatives that may arise from errors in liquid handling; bestowing added confidence to the activity of primary hits. Additionally, the method lends itself to the formulation of structure-activity relationships directly from the primary dataset, and can allow for the identification and flagging of sparsely related core architectures to provide insight during the step of selecting compounds for follow up analysis.

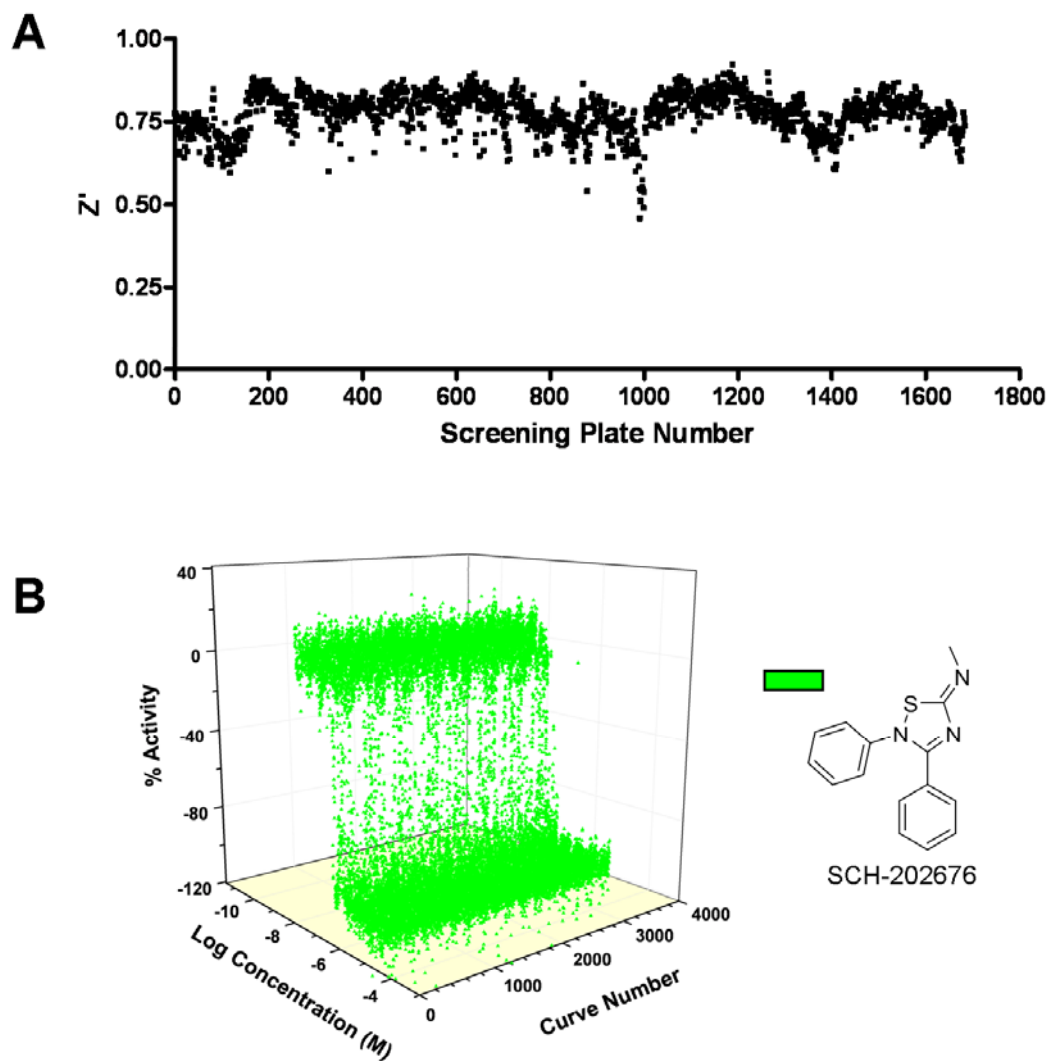


Figure 7.2 qHTS Z' and control titration performance

(A) The Z' value hovered around a value of 0.78 for the 1685 plates that passed quality control. (B) Titration plots of the interpolate IC50 control, SCH-202676 and show the consistent activity observed over the screen. The titration was included in duplicate on each assay plate (3,370 curves total).

For data handling, the activity associated with each well was calculated as a change of the secondary signal (read 2, collected after 30 minutes of progression) vs. the primary signal (read 1, read immediately after initiation); computed as [Read2-Read1] to give a decrease in signal corresponding inhibition, and normalized to the intraplate controls. In addition, values of the first reads were stored and used to scrutinize purported actives, with severe deviation of these data from the control serving to flag such compounds as artifacts arising from autofluorescence and signal quenching. This evaluation flagged 88 compounds as potentially interfering with the assay signal, and 44 of these were binned as actives or inclusives (*vide infra*).

These calculated values were used to construct dose-response curves for each compound, and were fit with a 4-parameter dose response equation using a proprietary qHTS software suite developed inhouse at NCGC. The generated curves were evaluated and distributed to four classes based on response magnitude (efficacy), presence of asymptotes across the top concentration points, and quality of curve fitting (r^2). An explanation of these classifications is given in Table 7.3, and analysis of the screening data according to these curve classifications is given in Table 7.4.

A plot of the screening data, presented as a plot of response vs. Log_{10} compound concentration vs. compound number, is provided in Figure 3. Evaluation of the data for inhibition provided the top actives (curve class 1.1 and 1.2, navy blue points) totaled and weak actives/inactives bins (curve class 2.1 and 2.2, true blue points) containing 10,959 and 11,962 compounds, respectively. With regard to

Table 7.3 Curve class description for qHTS data analysis.

* In addition Class 1 can have noisy curves (Class 1.3 = >80% efficacy and $r^2 > 0.9$; and Class 1.4 = min** – 80% efficacy and $r^2 > 0.9$).

** for these analyses, the minimum efficacy threshold was placed at 40%.

† Analogously there can be Classes 2.3 and 2.4; Class 5 curves did not receive an assignment

Curve Class	Description	Efficacy	r^2	Asymptotes	Inflection
1*	Complete response (a) Partial response (b)	> 80% (1.1) Min** - 80% (1.2)	= 0.9	2	yes
2†	Incomplete curve	> 80% (2.1) < 80% (2.2)	> 0.9 (2.1) < 0.9 (2.2)	1	yes
3	Single pt activity	> Min	NA	1	no
4	Inactive	NA	NA	0	no

Table 7.4 Curve class distribution of qHTS data.

Dose-response curves were fit to the qHTS data, and these were grouped according to the parameters in Table 7.3; and statistics regarding their distribution between these classes are presented.

Table 7.4 Curve class distribution of HTS data											
Activity	Distribution	Curve Classification									
		1.1	1.2	1.3	1.4	2.1	2.2	2.3	2.4	3	4
Inhibition	total compounds	2572	2288	8	976	2240	8846	56	1417	4518	286907
	% library	0.83	0.74	0.00	0.31	0.72	2.84	0.02	0.46	1.45	
	total compounds	0	30	0	106	0	197	0	175	924	
Activation	% library	0.00	0.01	0.00	0.03	0.00	0.06	0.00	0.06	0.30	

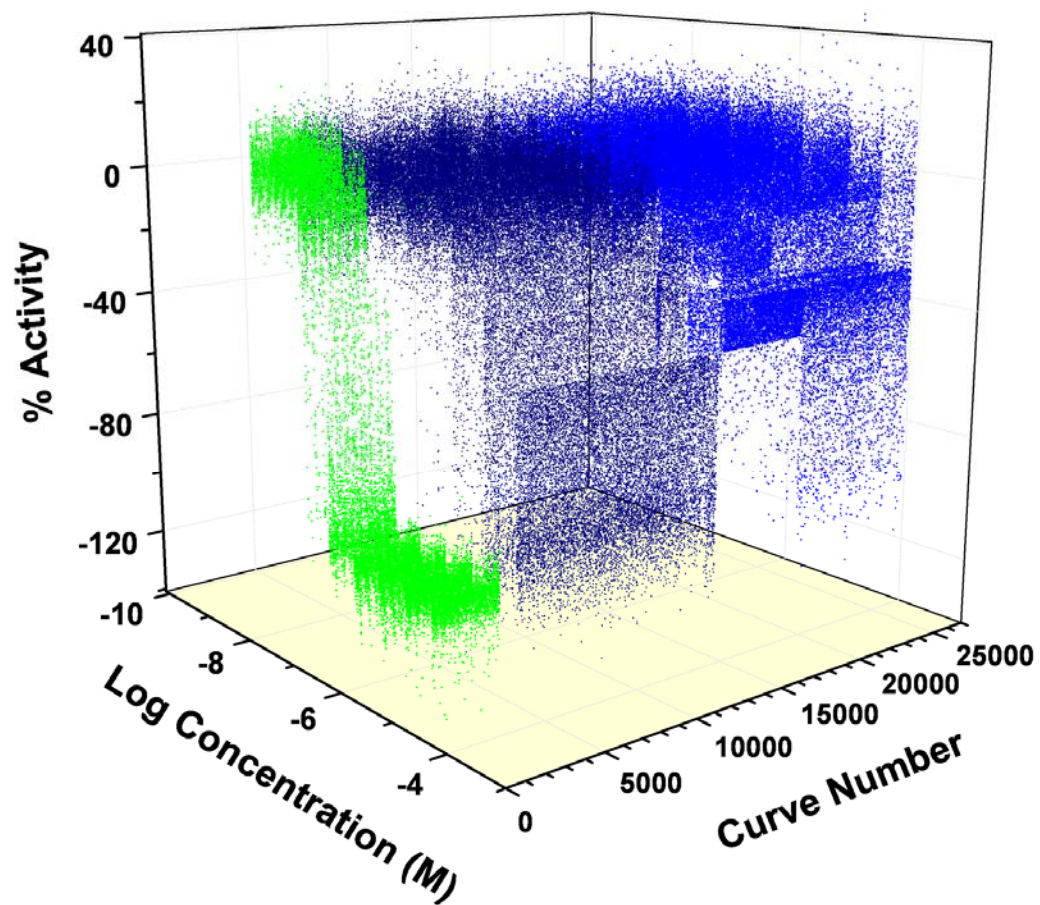


Figure 7.3 waterfall plot of qHTS actives and inconclusives

Plotted above are the signal vs. Log_{10} of inhibitor concentration plots for active compounds found in the qHTS. The SCH-202676 control traces are plotted alongside the ranked actives (navy blue) and weak actives and inconclusives (true blue) to give a gauge of potency.

activators, 1,447 compounds showed a signal enhancement of greater than six standard deviations above the control, and the rest were inactive. Representative chemical structures of the top actives are presented in Figure 7.4, and demonstrate the chemically diverse set of potential inhibitors of Sfp-PPTase. These examples include known actives containing reactive functionalities or problematic moieties, compounds approved for medical use, and small drug-like compounds. The high hit rate, 7.36% of the total library screened, was remarkable, and required further refinement before compounds for follow up could be selected.

Filtering of reactive functional groups: primary hit refinement

A list of 247 substructure filters were implemented using a combination of published and NCGC generated queries of reactive or undesirable functional groups and were used to reduce the population of the combined 'actives' bin. These filters were split into two categories: Level 1 were likely reactive or highly undesirable while Level 2 filters are less problematic and are provided as warning flags for activity analysis. Representative functionalities that were flagged by these filters include thiols, acyl halides, thioesters and malimides (Level 1) and hydrazines, acetals, and Michael acceptors (Level 2).

Triaging was performed in an automated fashion according to Filter 1, while Filter 2 was used to only to flag compounds, and their inclusion or exclusion from the final actives pool was accomplished manually. This evaluation resulted in the removal of 3,903 actives and 3,413 inconclusives from the hit pool. Representatives of triaged compounds are shown in Figure 7.5, and demonstrate some of the problematic

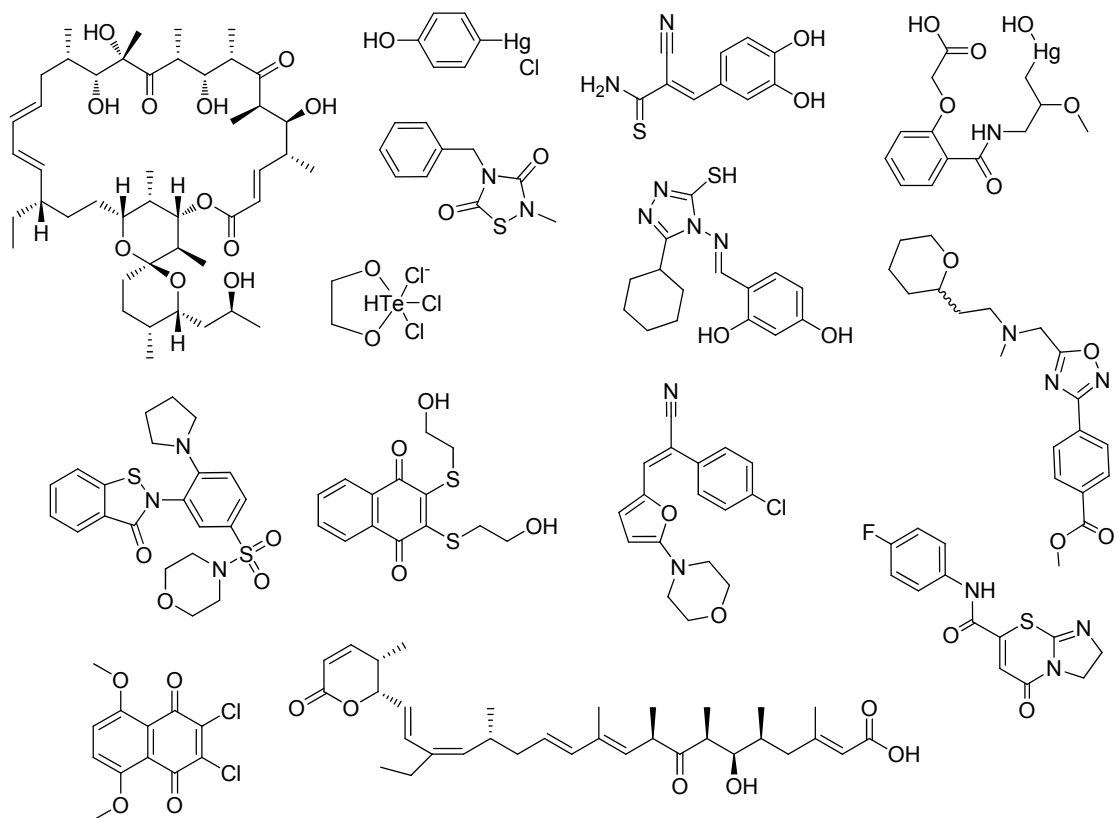


Figure 7.4 Representative top actives

Shown above are representative top actives identified by qHTS of the MLSMR and internal NCGC collections

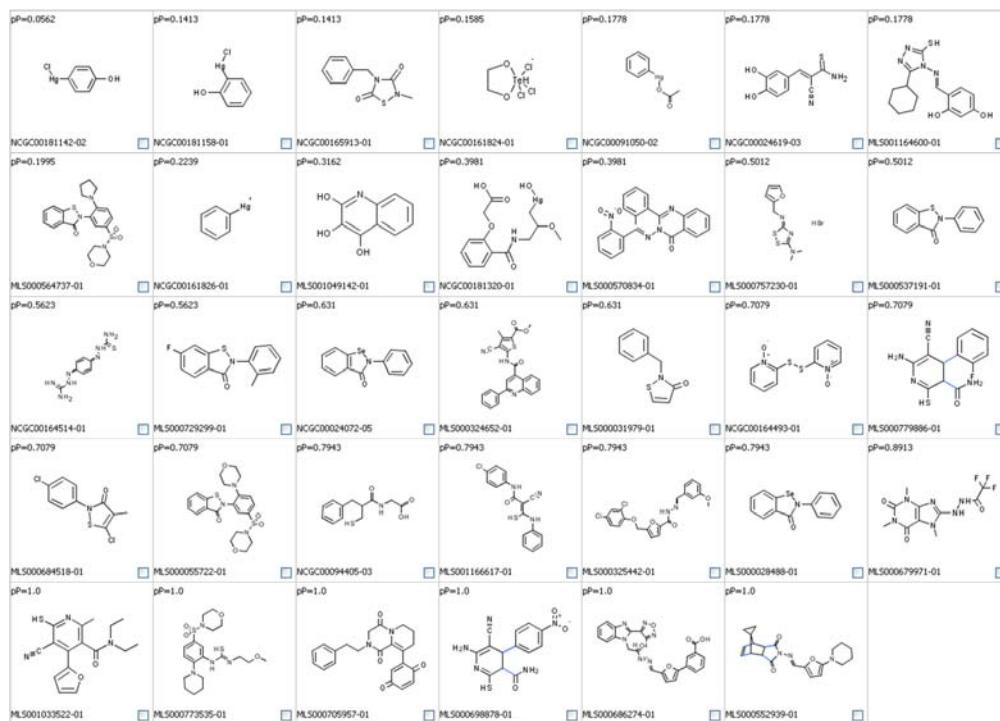


Figure 7.5 Compounds triaged for undesirable functionalities

Structures of the 70 compounds with IC₅₀ values less than 1 μ M 34 (49 %) that did not pass the 247 filters. Contained within these are numerous mercury and tellurium containing compounds, as well as free thiols, disulfides and hydrazide functionalities.

compounds within the libraries, including organo-mercury, disulfide, thiol and imine functionalities that were excluded. In summary, 64% of actives and 71% of inconclusives passed filters.

Compound Clustering

The resulting 7,038 compounds in the top actives pool that passed fluorescence and functionality filters were evaluated with Leadscape to group the compounds into clusters based on core molecular structures. In total, 488 clusters were identified that contained 4 or more active entities, with an additional 356 clusters containing 2 or 3 compounds. Finally, 247 compounds were identified as structurally unique from the other actives, and were binned as 'singletons'. Representative core structures (centroids) are shown in Figure 7.6 and display the number of actives with IC₅₀ values below 10 μ M, paired with the total cluster population.

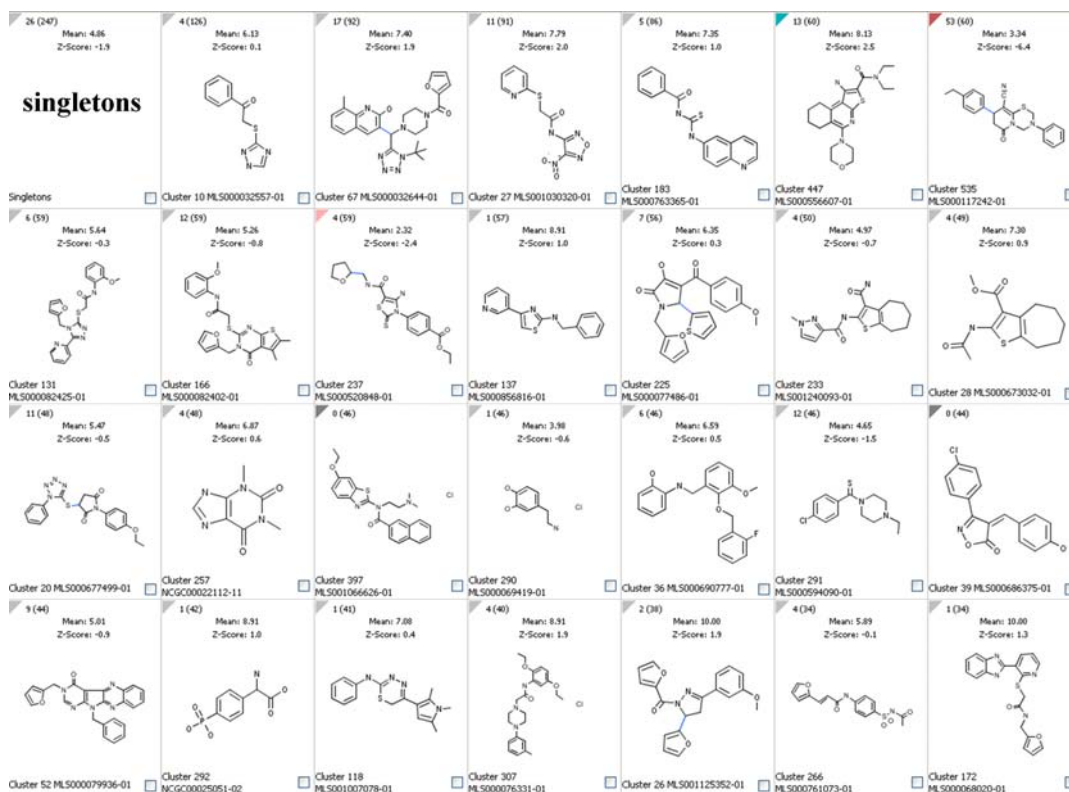


Figure 7.6 Clusters of disparate active structures.

A representative selection of compound substructures whose congeners showed activity in the qHTS screen of Sfp-PPTase. The numbers in the upper left of each cell represent compounds within the cluster that showed potency below 10 μ M, followed by the total cluster population in parentheses.

Further analysis of the actives to identify known PPTase architectures turned up the 4H-oxazol-5-one core, While this rediscovery was gratifying, the overall marginal activity and our prior experiments with this core structure (Chapter 4) excluded this cluster from further evaluation. Choice among these active series was the cyclohexa-/cyclohepta-/thiophene cluster (Figure 7.7), and contained a total of 13 compounds with high potency (IC₅₀ values less than 10 μ M) and 14 with values of modest potency (ranging between 10 and 30 μ M). Another top cluster identified was the thienopyrimidinones (Figure 7.8) and contained 9 considered highly active, and 10 more falling into the modest category. The third high priority ranking cluster was the 3-amino-N-phenylbenzene sulfonamide class (Figure 7.9), with 7 highly active structures, and another 15 displaying modest activity.

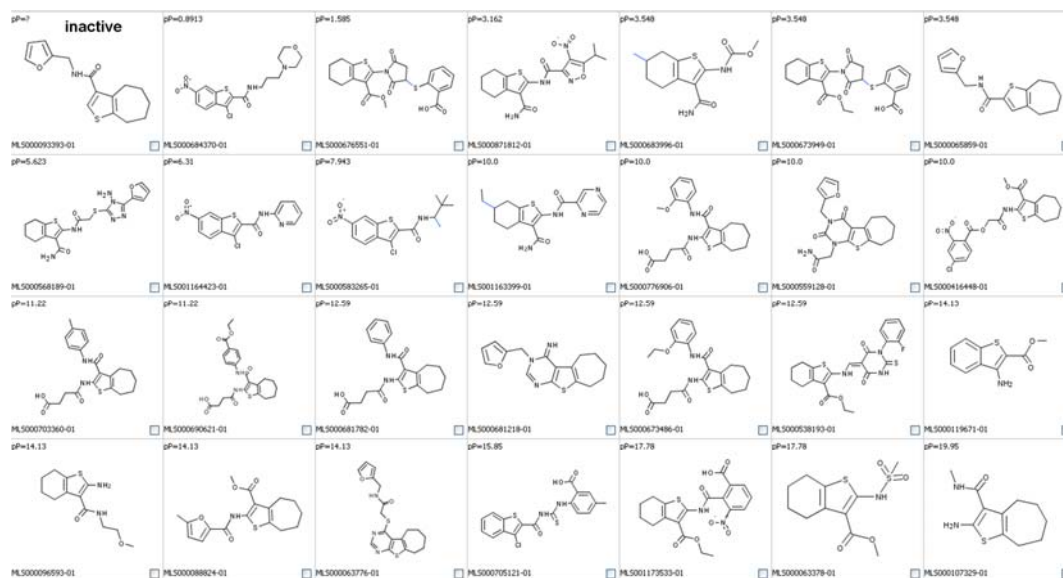


Figure 7.7 Cyclohexa-/cyclohepta-/thiophene cluster

Cyclohexa-/cyclohepta-/thiophene cluster contained 13 compounds with potency below 10 μM and 14 with potency ranging between 10 and 30 μM . Note: pP values are IC50 values.

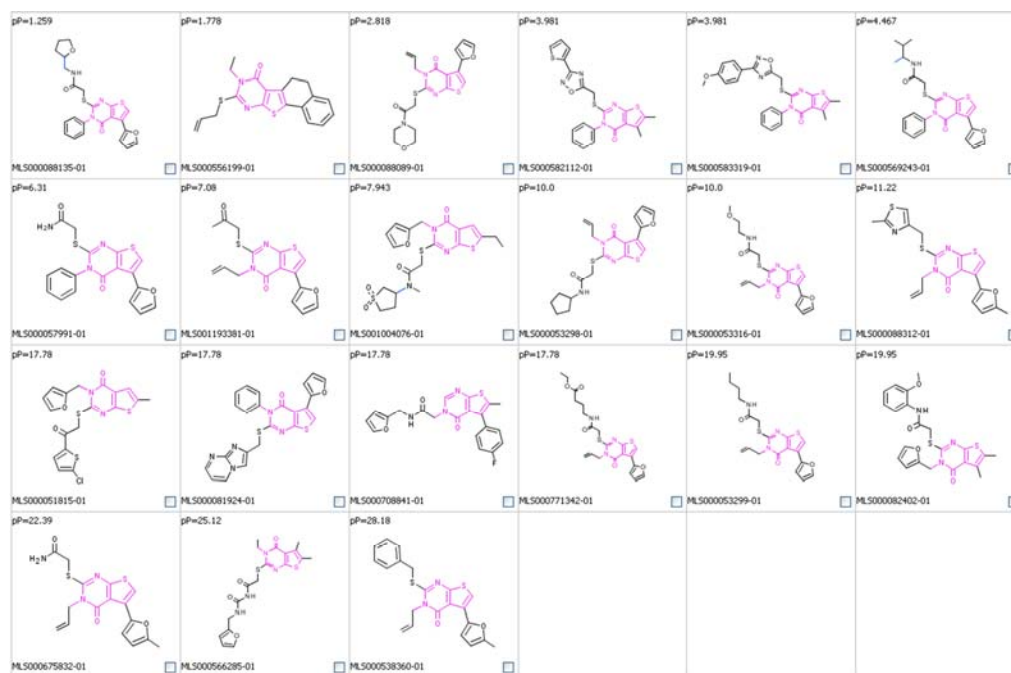


Figure 7.8 Thienopyrimidinone cluster.

The thienopyrimidinone cluster contained 9 compounds with potency below 10 μM and 10 with potency ranging between 10 and 30 μM . Note: pP values are IC_{50} values.

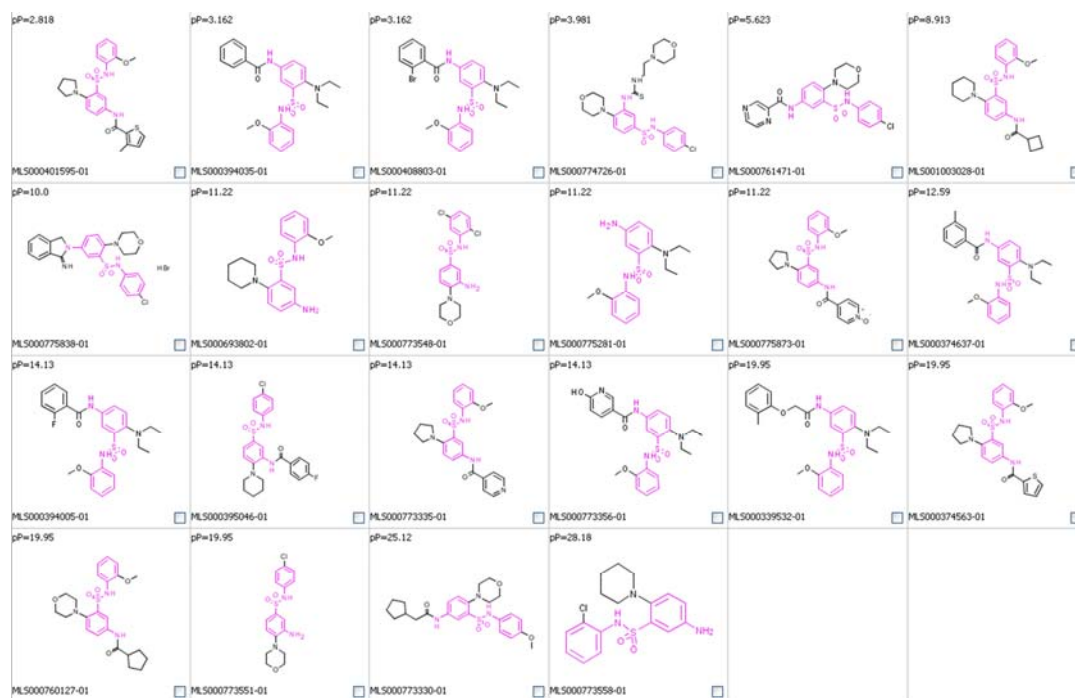


Figure 7.9 3-amino-N-phenylbenzene sulfonamide cluster

The 3-amino-N-phenylbenzene sulfonamide cluster contained 7 compounds with potency below 10 μM and 15 with potency ranging between 10 and 30 μM . Note: pP values are IC₅₀ values.

First pass hit selection and followup analysis

For follow-up evaluation, representative compounds were selected across top active clusters and singletons. The selected actives span MW, logP, polar surface area (PSA) property distributions. 388 compounds were selected for retesting and acquired from three sources: Biofocus DPI, curator of the MLSMR; inhouse cherry picks from NCGC collections including approved drugs; and dry powder orders that were unavailable from the former two sources.

This pool was retested in the qHTS protocol as described. Independent of this analysis, the compounds were also evaluated in the gel-based phosphopantetheinylation assay that provides an orthogonal method of detection to confirm the activity of the hits. Data for both of these analyses are compiled in Table 7.5. Additionally, the compounds were profiled against AcpS PPTase to evaluate them for crossreactivity with the primary metabolism associated PPTase. Interestingly, all of the compounds retested in the qHTS assay with IC₅₀ values similar to those found primary screen, but 120 (31%) showed no activity in the gel-based assay. The summation of these three datasets was used to assign a priority rank to the active compounds for further evaluation and resynthesis.

Table 7.5 Analysis of primary actives selected for follow up.

A collection of 387 compounds were selected from the clusters and singleton pools from the qHTS. Congeners that were inactive members of clusters were also included in the selection process to strengthen confidence in the structure activity relationships that could be deduced from the primary data.

Compounds are sorted by activity in the Gel-based phosphopantetheinylation assay, and include IC50 and curve classification data from the primary screen as well as a counterscreen against AcpS.

Table 7.5 Followup results from the first pool of primary actives

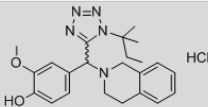
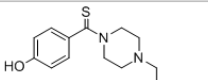
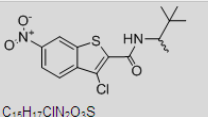
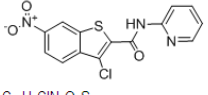
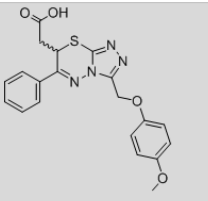
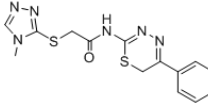
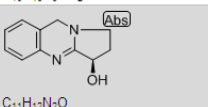
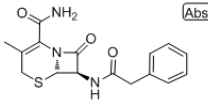
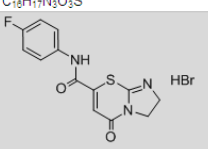
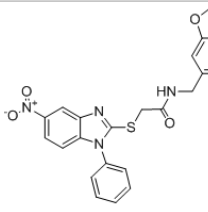
compound number	Structure	Substance ID	gel assay IC50 (µM)	sfp qHTS Potency (µM)	sfp qHTS CurveClass	AcpS qHTS Potency (µM)	AcpS qHTS CurveClass
1	 C ₂₃ H ₃₀ ClN ₆ O ₂	MLS000123156-01	0.69	3.55	-1.1	25.72	-2.2
2	 C ₁₃ H ₁₃ N ₂ OS	MLS000621546-01	0.69	2.82	-1.1	32.39	-3
3	 C ₁₂ H ₁₇ ClN ₂ O ₃ S	MLS000583265-01	0.69	7.94	-1.1	9.13	-2.2
4	 C ₁₄ H ₈ ClN ₃ O ₃ S	MLS001164423-01	0.69	6.31	-1.1	11.49	-2.2
5	 C ₂₀ H ₁₃ N ₄ O ₄ S	MLS001172074-01	0.69	4.47	-1.1	20.43	-2.2
6	 C ₂₁ H ₁₆ N ₆ OS ₂	MLS000683944-01	0.69	8.91	-1.1	32.39	-3
7	 C ₁₁ H ₁₂ N ₂ O	NCGC00163661-01	0.69	2.82	-2.1	18.21	-2.2
8	 C ₁₈ H ₁₇ N ₃ O ₃ S	NCGC00160285-01	0.92	25.12	-1.1		Inactive
9	 C ₁₃ H ₁₁ BrFN ₃ O ₂ S	MLS000681557-01	2.06	0.56	-1.1	45.75	-3
10	 C ₂₃ H ₁₃ N ₄ O ₅ S	MLS000417738-01	2.06	1.00	-1.1	28.86	-2.2

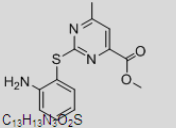
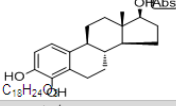
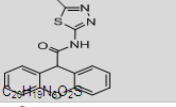
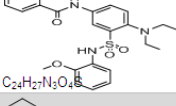
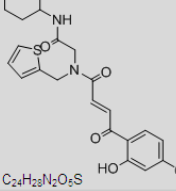
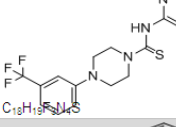
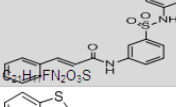
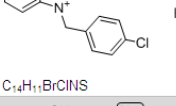
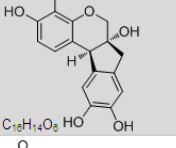
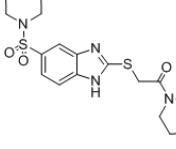
Table 7.5 continued							
compound number	Structure	Substance ID	gel assay IC50 (µl)	sfp qHTS Potency (µl)	sfp qHTS CurveClas	AcpS qHTS Potency (µl)	AcpS qHTS CurveClass
11	 C ₁₃ H ₁₃ N ₃ O ₂ S	MLS000835010-01	2.06	2.00	-1.1	18.21	-2.2
12	 C ₁₈ H ₂₄ O ₄	MLS000069567-01	2.06	3.16	-1.1	36.34	-2.2
13	 C ₂₂ H ₁₉ N ₃ O ₂ S	MLS000121444-01	2.06	2.82	-1.1	40.77	-3
14	 C ₂₄ H ₂₇ N ₃ O ₄ S	MLS000394035-01	2.06	3.16	-1.1		Inactive
15	 C ₂₄ H ₂₈ N ₂ O ₂ S	MLS000714573-01	2.06	3.16	-1.1	18.21	-2.2
16	 C ₁₈ H ₁₉ F ₃ N ₃ S	MLS001172437-01	2.06	2.51	-1.1	20.43	-2.2
17	 C ₂₂ H ₂₇ FN ₂ O ₃ S	MLS000339519-01	2.06	3.98	-1.1		Inactive
18	 C ₁₄ H ₁₁ BrClNS	MLS000699544-01	2.06	3.98	-1.1	18.21	-2.2
19	 C ₁₈ H ₁₄ O ₅	NCGC00142609-01	2.06	3.98	-1.1		Inactive
20	 C ₁₇ H ₂₂ N ₄ O ₂ S ₂	MLS000081697-01	2.06	6.31	-1.1		Inactive

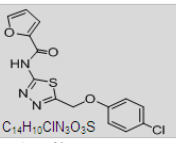
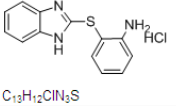
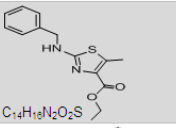
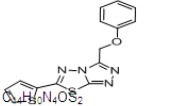
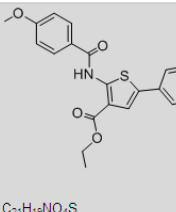
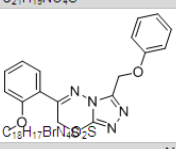
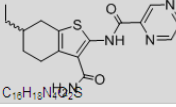
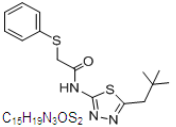
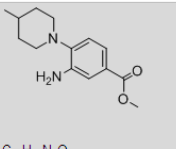
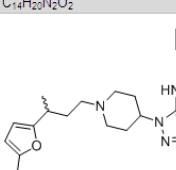
Table 7.5 continued							
compound number	Structure	Substance ID	gel assay IC50 (µl)	sfp qHTS Potency (µl)	sfp qHTS CurveClas	AcpS qHTS Potency (µl)	AcpS qHTS CurveClass
21	 <chem>C14H10ClN2O3S</chem>	MLS000708356-01	2.06	7.08	-1.1	28.86	-2.2
22	 <chem>C13H12ClN2S</chem>	MLS000770492-01	2.06	7.94	-1.1	32.39	-3
23	 <chem>C14H16N2O2S</chem>	MLS001172429-01	2.06	8.91	-1.1	20.43	-2.2
24	 <chem>C14H16N2O2S</chem>	MLS000035335-01	2.06	10.00	-1.1	25.72	-2.2
25	 <chem>C21H19NO4S</chem>	MLS000573010-01	2.06	14.13	-1.1		Inactive
26	 <chem>C19H17BrN2O2S</chem> HBr	MLS001006872-01	2.06	14.13	-1.1	18.21	-2.2
27	 <chem>C18H19N2O2S</chem>	MLS001163399-01	2.06	10.00	-1.1		Inactive
28	 <chem>C15H19N2OS2</chem>	MLS001211798-01	2.06	14.13	-1.1		Inactive
29	 <chem>C14H20N2O2</chem>	MLS000520963-01	2.06	31.62	-1.2	32.39	-3
30	 <chem>C22H32N4O3</chem>	MLS001105336-01	2.06	50.12	-2.2	32.39	-2.2

Table 7.5 continued

compound number	Structure	Substance ID	gel assay IC50 (µl)	sfp qHTS Potency (µl)	sfp qHTS CurveClass	AcpS qHTS Potency (µl)	AcpS qHTS CurveClass
31	 <chem>C22H17N3O3S</chem>	MLS000324652-01	6.17	0.63	-1.1	25.72	-2.4
32	 <chem>C23H21N3O4S2</chem>	MLS000088135-01	6.17	1.26	-1.1	28.86	-2.2
33	 <chem>C14H13BrN2O3</chem>	MLS000097046-01	6.17	1.59	-1.1	20.43	-2.2
34	 <chem>C12H12N4O</chem>	MLS000540817-01	6.17	1.26	-1.1	28.86	-2.2
35	 <chem>C12H12BrN2S</chem>	MLS000679518-01	6.17	1.26	-1.1	Inactive	
36	 <chem>C12H12ClN2O4S</chem>	MLS000684370-01	6.17	0.89	-1.1	20.43	-2.2
37	 <chem>C13H12BrN2OS</chem>	MLS000665240-01	6.17	1.26	-1.1	32.39	-2.2
38	 <chem>C22H22N2S</chem>	MLS000679877-01	6.17	2.24	-1.1	36.34	-3
39	 <chem>C14H13N2O3S</chem>	MLS000720425-01	6.17	1.26	-1.1	Inactive	
40	 <chem>C22H23N3O2S</chem>	MLS000032944-01	6.17	3.55	-1.1	18.21	-2.2

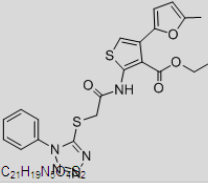
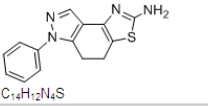
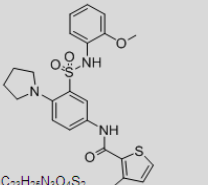
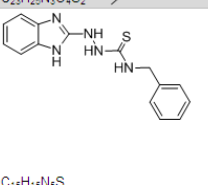
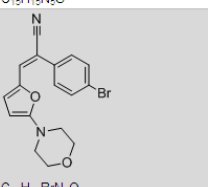
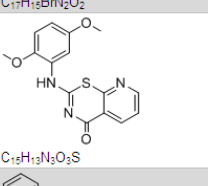
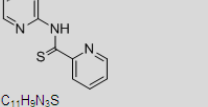
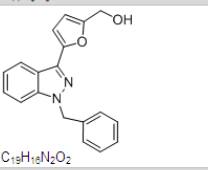
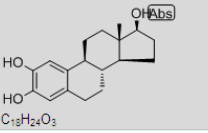
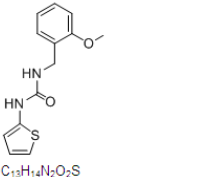
Table 7.5 continued								
compound number	Structure	Substance ID	gel assay IC50 (μM)	sfp qHTS Potency (μM)	sfp qHTS CurveClass	AcpS qHTS Potency (μM)	AcpS qHTS CurveClass	
41	 <chem>C21H19N3O2S2</chem>	MLS000057277-01	6.17	3.55	-1.1	10.24	-1.1	
42	 <chem>C14H12N4S</chem>	MLS000085948-01	6.17	2.51	-1.1	25.72	-2.2	
43	 <chem>C23H29N3O4S2</chem>	MLS000401595-01	6.17	2.82	-1.1	45.75	-2.4	
44	 <chem>C13H15N5S</chem>	MLS000516615-01	6.17	3.98	-1.1	32.39	-2.4	
45	 <chem>C17H15BrN2O2</chem>	MLS000572730-01	6.17	2.82	-1.1	10.24	-1.1	
46	 <chem>C18H13N3O3S</chem>	MLS000664030-01	6.17	2.82	-1.1	36.34	-3	
47	 <chem>C11H9N3S</chem>	MLS000756413-01	6.17	3.16	-1.1	Inactive	Inactive	
48	 <chem>C18H19N2O2</chem>	NCGC00094472-03	6.17	4.47	-1.1	5.76	-2.2	
49	 <chem>C18H24O3</chem>	MLS000069506-01	6.17	3.98	-1.1	36.34	-3	
50	 <chem>C13H14N2O2S</chem>	MLS000093633-01	6.17	3.98	-1.1	36.34	-3	

Table 7.5 continued

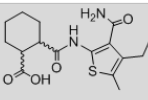
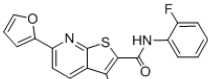
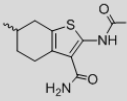
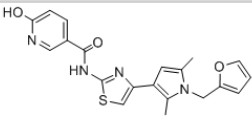
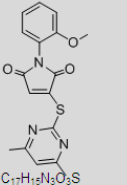
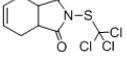
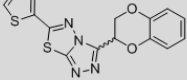
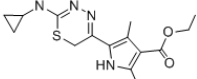
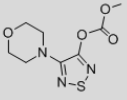
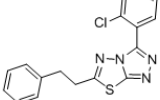
compound number	Structure	Substance ID	gel assay	sfp qHTS	sfp qHTS	AcpS qHTS	AcpS qHTS
			IC50 (µM)	Potency (µM)	CurveClass	Potency (µM)	CurveClass
51		MLS000109947-01	6.17	4.47	-1.1	45.75	-3
	<chem>C18H22N2O4S</chem>						
52		MLS000559030-01	6.17	3.98	-1.1	14.47	-2.2
	<chem>C18H12FN3O2S</chem>						
53		MLS000683996-01	6.17	3.55	-1.1		Inactive
	<chem>C12H18N2O3S</chem>						
54		MLS000760175-01	6.17	4.47	-1.1	12.89	-1.2
	<chem>C20H18N4O3S</chem>						
55		MLS000775985-01	6.17	3.16	-1.1	12.89	-1.1
	<chem>C17H12N3O3S</chem>						
56		NCGC00091034-02	6.17	6.31	-1.1	32.39	-3
	<chem>C8H8Cl2NO2S</chem>						
57		MLS000066380-01	6.17	7.94	-1.1		Inactive
	<chem>C18H10N4O2S2</chem>						
58		MLS001033010-01	6.17	7.08	-1.1	28.86	-2.2
	<chem>C19H20N4O2S</chem>						
59		MLS000029111-01	6.17	12.59	-1.1	25.72	-2.4
	<chem>C8H11N3O4S</chem>						
60		MLS000050191-01	6.17	12.59	-1.1	28.86	-2.2
	<chem>C17H13ClN4S</chem>						

Table 7.5 continued

compound number	Structure	Substance ID	gel assay	sfp qHTS	sfp qHTS	AcpS qHTS	AcpS qHTS
			IC50 (µl)	Potency (µl)	CurveClass	Potency (µl)	CurveClass
61	 <chem>C19H19N6S</chem>	MLS000052001-01	6.17	10.00	-1.1	25.72	-3
62	 <chem>C17H14N6OS</chem>	MLS000064648-01	6.17	14.13	-1.1	32.39	-2.2
63	 <chem>C19H17NO2S</chem>	MLS000521458-01	6.17	14.13	-1.1	32.39	-3
64	 <chem>C22H18ClNO3S</chem>	MLS000555674-01	6.17	11.22	-1.1	10.24	-1.2
65	 <chem>C17H14ClN3O2S2</chem>	MLS000579968-01	6.17	14.13	-1.1	20.43	-2.2
66	 <chem>C13H13F3N2S</chem>	MLS001173914-01	6.17	15.85	-1.1	16.23	-2.2
67	 <chem>C10H14N2O4</chem>	NCGC00024596-05	6.17	19.95	-1.1		Inactive
68	 <chem>C14H8ClN3S</chem>	MLS000099929-01	6.17	15.85	-1.2		Inactive
69	 <chem>C28H19ClN2O7S</chem>	MLS000416448-01	6.17	10.00	-1.2	20.43	-2.2
70	 <chem>C10H9NO2S</chem>	MLS000119671-01	6.17	14.13	-2.1	28.86	2.4

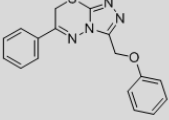
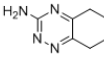
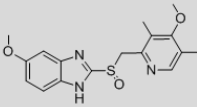
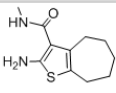
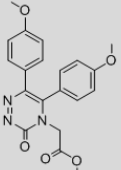
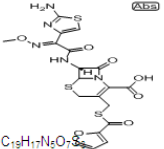
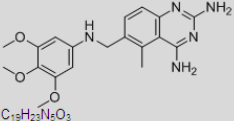
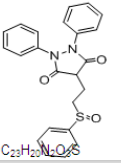
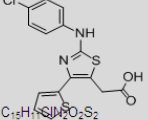
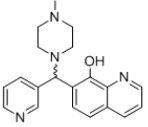
Table 7.5 continued								
compound number	Structure	Substance ID	gel assay IC50 (µl)	sfp qHTS Potency (µl)	sfp qHTS CurveClass	AcpS qHTS Potency (µl)	AcpS qHTS CurveClass	
71	 <chem>C17H14N4OS</chem>	MLS000685849-01	6.17	15.85	-2.1	45.75	-3	
72	 <chem>C7H10N4</chem>	MLS000040395-01	6.17	44.67	-2.1		Inactive	
73	 <chem>C17H19N3O3S</chem>	MLS000069373-01	6.17	19.95	-2.1	32.39	-2.2	
74	 <chem>C11H16N2OS</chem>	MLS000107329-01	6.17	19.95	-2.1	28.86	-3	
75	 <chem>C20H19N3O5</chem>	MLS001208868-01	6.17	50.12	-2.1	22.93	2.4	
76	 <chem>C19H17N5O7S</chem>	NCGC00167543-01	6.17	56.23	-2.2	45.75	-3	
77	 <chem>C19H23N5O3</chem>	NCGC00161419-02	6.17	31.62	-2.2	28.86	-2.2	
78	 <chem>C23H22N4O4S</chem>	NCGC00016255-01	8.28	35.48	-2.2		Inactive	
79	 <chem>C19H17ClN3O2S2</chem>	MLS000760703-01	18.52	1.26	-1.1	40.77	-3	
80	 <chem>C20H22N4O</chem>	MLS000081800-01	18.52	2.82	-1.1		Inactive	

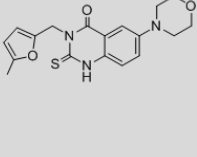
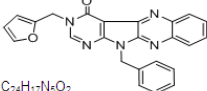
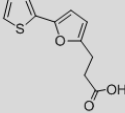
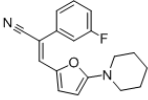
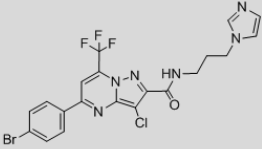
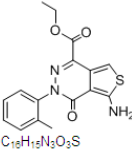
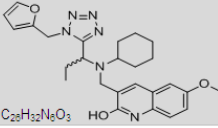
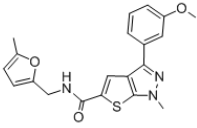
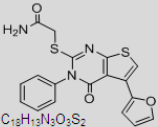
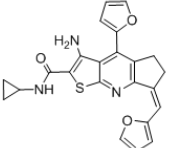
Table 7.5 continued							
compound number	Structure	Substance ID	gel assay	sfp qHTS	sfp qHTS	AcpS qHTS	AcpS qHTS
			IC50 (μM)	Potency (μM)	CurveClass	Potency (μM)	CurveClass
81	 C ₁₉ H ₁₉ N ₃ O ₃ S	MLS000095421-01	18.52	2.51	-1.1	7.25	-1.1
82	 C ₂₄ H ₁₇ N ₅ O ₂	MLS000079936-01	18.52	2.82	-1.1	20.43	-2.2
83	 C ₁₁ H ₁₀ O ₃ S	MLS000112485-01	18.52	2.82	-1.1	12.89	-2.2
84	 C ₁₈ H ₁₇ FN ₂ O	MLS000539295-01	18.52	2.82	-1.1	14.47	-2.2
85	 C ₂₃ H ₁₂ BrClF ₃ N ₄ O	MLS000702616-01	18.52	1.12	-1.1		Inactive
86	 C ₁₈ H ₁₅ N ₃ O ₃ S	MLS000707247-01	18.52	3.16	-1.1	32.39	-3
87	 C ₂₈ H ₃₂ N ₆ O ₃	MLS000032291-01	18.52	3.55	-1.1		-2.4
88	 C ₂₁ H ₁₉ N ₃ O ₃ S	MLS000045350-01	18.52	3.55	-1.1	28.86	-3
89	 C ₁₈ H ₁₇ N ₃ O ₃ S ₂	MLS000057991-01	18.52	6.31	-1.1	20.43	-2.2
90	 C ₂₃ H ₁₉ N ₃ O ₃ S	MLS000390291-01	18.52	5.01	-1.1	16.23	-2.1

Table 7.5 continued

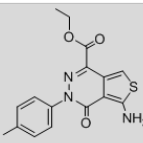
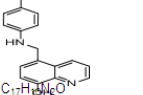
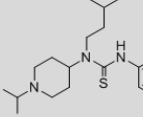
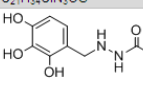
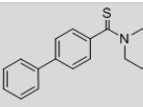
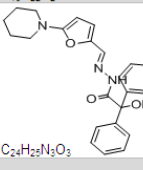
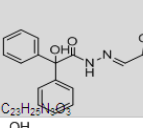
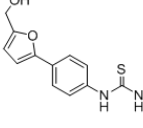
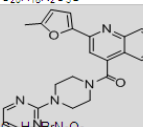
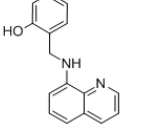
compound number	Structure	Substance ID	gel assay	sfp qHTS	sfp qHTS	AcpS qHTS	AcpS qHTS
			IC50 (μM)	Potency (μM)	CurveClass	Potency (μM)	CurveClass
91	 C ₁₉ H ₁₉ N ₃ O ₃ S	MLS000528230-01	18.52	3.55	-1.1	40.77	-2.4
92	 C ₁₇ H ₁₆ N ₂ O	MLS000715757-01	18.52	3.55	-1.1	45.75	-3
93	 C ₂₁ H ₃₄ ClN ₃ O ₂ S	MLS001200831-01	18.52	3.98	-1.1	32.39	-3
94	 C ₁₀ H ₁₀ ClN ₃ O ₅	MLS000028424-01	18.52	6.31	-1.1	22.93	-2.2
95	 C ₁₉ H ₂₂ N ₂ O ₂ S	MLS000559855-01	18.52	7.08	-1.1	40.77	-2.2
96	 C ₂₄ H ₂₆ N ₃ O ₃	MLS000587277-01	18.52	8.91	-1.1		Inactive
97	 C ₂₃ H ₂₅ N ₃ O ₂ S	MLS000587278-01	18.52	7.08	-1.1	25.72	-2.2
98	 C ₂₀ H ₁₉ N ₂ O ₃ S	MLS000625102-01	18.52	7.08	-1.1	11.49	-1.1
99	 C ₂₃ H ₂₂ BrN ₃ O ₂	MLS000672543-01	18.52	7.94	-1.1	5.76	-1.1
100	 C ₁₈ H ₁₄ N ₂ O	MLS000715552-01	18.52	7.94	-1.1		2.4

Table 7.5 continued

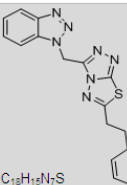
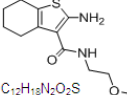
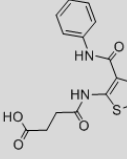
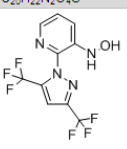
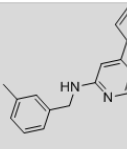
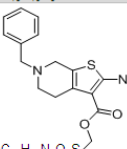
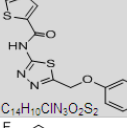
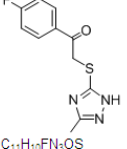
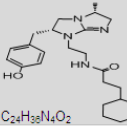
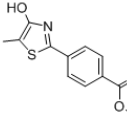
compound number	Structure	Substance ID	gel assay IC50 (μl)	sfp qHTS Potency (μl)	sfp qHTS CurveClass	AcpS qHTS Potency (μl)	AcpS qHTS CurveClass
101	 C ₁₉ H ₁₉ N ₇ S	MLS000042630-01	18.52	12.59	-1.1		Inactive
102	 C ₁₂ H ₁₈ N ₂ O ₂ S	MLS000096593-01	18.52	14.13	-1.1		Inactive
103	 C ₂₀ H ₂₂ N ₂ O ₄ S	MLS000681782-01	18.52	12.59	-1.1	32.39	-3
104	 C ₁₀ H ₈ F ₂ N ₄ O	MLS000763604-01	18.52	8.91	-1.1	28.86	-3
105	 C ₁₈ H ₁₅ N ₃ O	NCGC00011814-01	18.52	14.13	-1.1		Inactive
106	 C ₁₇ H ₂₀ N ₂ O ₂ S	NCGC00159451-02	18.52	10.00	-1.1		Inactive
107	 C ₁₄ H ₁₀ ClN ₃ O ₂ S ₂	MLS000049235-01	18.52	14.13	-1.1		Inactive
108	 C ₁₇ H ₁₀ FN ₂ OS	MLS000111303-01	18.52	19.95	-1.1		Inactive
109	 C ₂₄ H ₃₀ N ₄ O ₂	MLS000697947-01	18.52	15.85	-1.1		Inactive
110	 C ₁₂ H ₁₁ NO ₃ S	MLS000755422-01	18.52	14.13	-1.1		Inactive

Table 7.5 continued

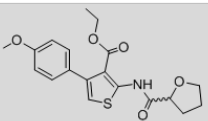
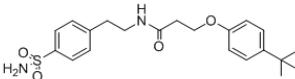
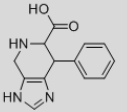
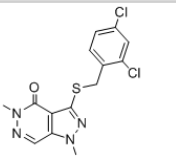
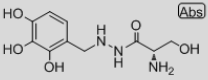
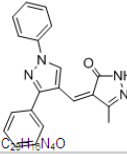
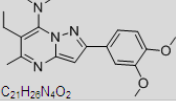
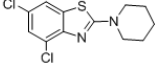
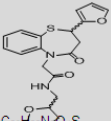
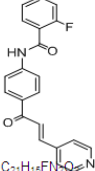
compound number	Structure	Substance ID	gel assay	sfp qHTS	sfp qHTS	AcpS qHTS	AcpS qHTS
			IC50 (µl)	Potency (µl)	CurveClass	Potency (µl)	CurveClass
111	 <chem>C19H21NO2S</chem>	MLS000765499-01	18.52	15.85	-1.1	28.86	-3
112	 <chem>C21H28N2O2S</chem>	MLS001151090-01	18.52	19.95	-1.1		Inactive
113	 <chem>C13H13N3O2</chem>	NCGC00167998-01	18.52	15.85	-1.1		-1.4
114	 <chem>C14H12Cl2N4OS</chem>	MLS000851063-01	18.52	25.12	-1.1		Inactive
115	 <chem>C10H15N3O5</chem>	NCGC00016709-01	18.52	28.18	-1.1		Inactive
116	 <chem>C20H16N4O</chem>	MLS000391932-01	18.52	3.55	-1.2	12.89	-2.2
117	 <chem>C21H28N4O2</chem>	MLS000035091-01	18.52	6.31	-1.2	40.77	-3
118	 <chem>C12H12Cl2N2S</chem>	MLS000045496-01	18.52	10.00	-1.2	32.39	-3
119	 <chem>C20H22N2O2S</chem>	MLS000093166-01	18.52	11.22	-1.2	18.21	-2.2
120	 <chem>C21H15FN2O2</chem>	MLS000699929-01	18.52	5.62	-1.2	28.86	2.4

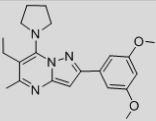
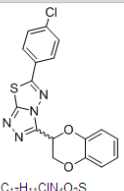
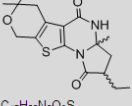
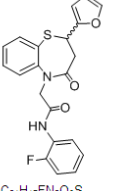
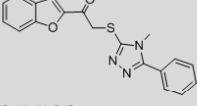
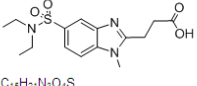
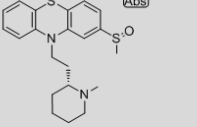
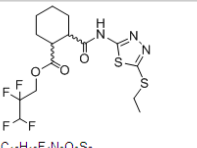
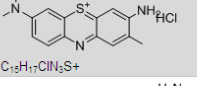
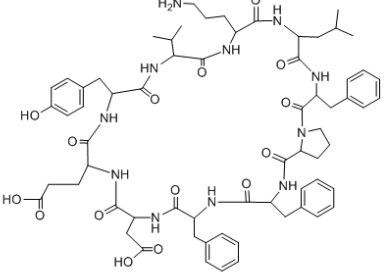
Table 7.5 continued								
compound number	Structure	Substance ID	gel assay IC50 (µM)	sfp qHTS Potency (µM)	sfp qHTS CurveClass	AcpS qHTS Potency (µM)	AcpS qHTS CurveClass	
121	 <chem>C21H29N4O2</chem>	MLS000035293-01	18.52	15.85	-1.2	18.21	-2.2	
122	 <chem>C17H17ClN4O2S</chem>	MLS000042624-01	18.52	14.13	-1.2	32.39	-2.2	
123	 <chem>C17H22N2O3S</chem>	MLS000077638-01	18.52	15.85	-1.2		Inactive	
124	 <chem>C21H17FN2O3S</chem>	MLS000102382-01	18.52	15.85	-1.2	32.39	-2.2	
125	 <chem>C19H19N3O2S</chem>	MLS000115919-01	18.52	12.59	-1.2		Inactive	
126	 <chem>C19H21N3O4S</chem>	MLS001002059-01	18.52	19.95	-1.2		Inactive	
127	 <chem>C21H29N2OS2</chem>	NCGC00014529-01	18.52	19.95	-1.2		Inactive	
128	 <chem>C19H19F4N3O3S2</chem>	MLS000085121-01	18.52	22.39	-1.2		Inactive	
129	 <chem>C19H17ClN3S+</chem>	MLS000738130-01	18.52	25.12	-1.2	16.23	-2.2	
130	 <chem>C69H89N11O19</chem>	NCGC00094807-01	18.52	25.12	-1.2		Inactive	

Table 7.5 continued

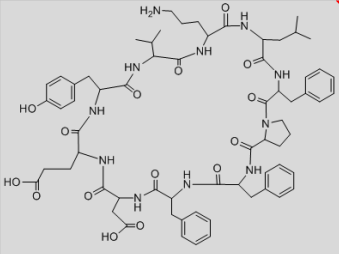
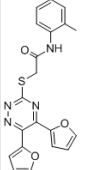
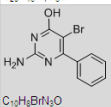
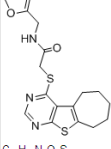
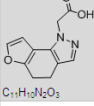
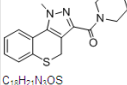
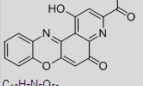
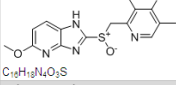
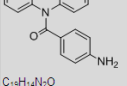
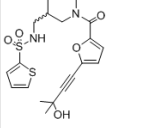
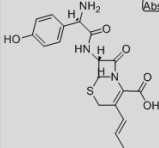
compound number	Structure	Substance ID	gel assay IC50 (μM)	sfp qHTS Potency (μM)	sfp qHTS CurveClass	AcpS qHTS Potency (μM)	AcpS qHTS CurveClass
130	 <chem>C26H32N4O12</chem>	NCGC00094807-01	18.52	25.12	-1.2		Inactive
131	 <chem>C22H18N4O3S</chem>	MLS000556526-01	18.52	10.00	-2.1	32.39	-2.2
132	 <chem>C17H14BrN2O</chem>	NCGC00181015-01	18.52	70.79	-2.1	5.13	-1.1
133	 <chem>C18H19N2O2S2</chem>	MLS000063776-01	18.52	14.13	-2.2		Inactive
134	 <chem>C17H12N2O3</chem>	MLS000120749-01	18.52	44.67	-2.1		Inactive
135	 <chem>C18H21N2OS</chem>	MLS001115532-01	18.52	44.67	-2.1	32.39	-2.2
136	 <chem>C18H12N2O2</chem>	NCGC00167452-01	18.52	44.67	-2.1	28.86	-2.2
137	 <chem>C18H13N4O3S</chem>	NCGC00167521-01	18.52	44.67	-2.1		Inactive
138	 <chem>C19H14N2O</chem>	MLS000527643-01	18.52	44.67	-2.2		Inactive
139	 <chem>C22H24N2O3S2</chem>	MLS001090546-01	18.52	39.81	-2.2	40.77	-3
140	 <chem>C18H19N3O2S</chem>	NCGC00159513-02	18.52	39.81	-2.2		Inactive

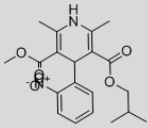
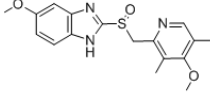
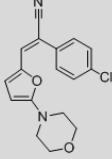
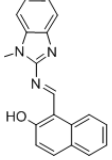
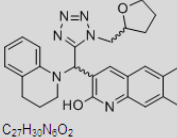
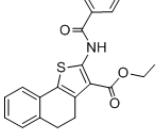
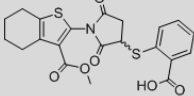
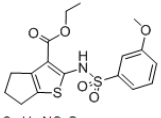
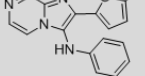
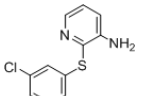
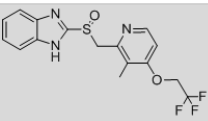
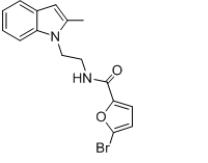
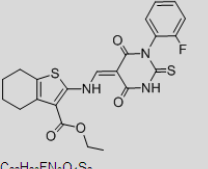
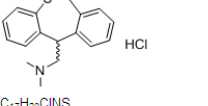
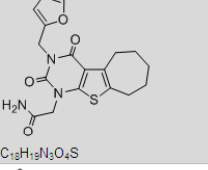
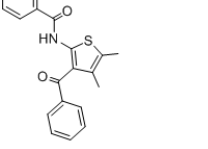
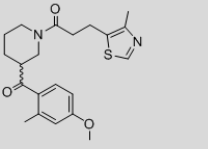
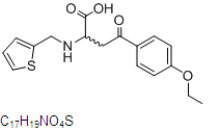
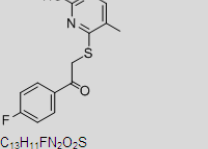
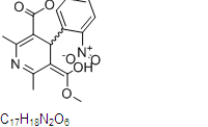
Table 7.5 continued							
compound number	Structure	Substance ID	gel assay IC50 (μl)	sfp qHTS Potency (μl)	sfp qHTS CurveClas	AcpS qHTS Potency (μl)	AcpS qHTS CurveClass
141	 C ₂₃ H ₂₄ N ₂ O ₃	NCGC00164633-01	18.52	39.81	-2.2		Inactive
142	 C ₁₇ H ₁₃ N ₃ O ₂ S	NCGC00016925-01	24.83	28.18	-2.1		Inactive
143	 C ₁₇ H ₁₅ ClN ₂ O ₂	MLS000560294-01	55.56	0.71	-1.1	9.13	-1.1
144	 C ₁₃ H ₁₂ N ₂ O	MLS000106285-01	55.56	0.89	-1.1		Inactive
145	 C ₂₇ H ₃₃ N ₅ O ₂	MLS000072735-01	55.56	1.41	-1.1		Inactive
146	 C ₂₂ H ₁₃ NO ₂ S	MLS000555575-01	55.56	1.26	-1.1	14.47	-2.2
147	 C ₂₁ H ₁₃ NO ₅ S ₂	MLS000676551-01	55.56	1.59	-1.1		Inactive
148	 C ₁₇ H ₁₃ NO ₂ S ₂	MLS000088664-01	55.56	2.82	-1.1	32.39	-3
149	 C ₁₇ H ₁₄ N ₄ O	MLS000116166-01	55.56	4.47	-1.1	3.24	-1.1
150	 C ₁₁ H ₉ ClN ₂ S	MLS000543573-01	55.56	3.16	-1.1	45.75	-3

Table 7.5 continued							
compound number	Structure	Substance ID	gel assay IC50 (μl)	sfp qHTS Potency (μl)	sfp qHTS CurveClass	AcpS qHTS Potency (μl)	AcpS qHTS CurveClass
161	 C ₁₈ H ₁₄ F ₃ N ₃ O ₂ S	MLS000069705-01	55.56	12.59	-1.1		Inactive
162	 C ₁₈ H ₁₂ BrN ₂ O ₂	MLS000419204-01	55.56	12.59	-1.1	40.77	-3
163	 C ₂₂ H ₂₀ FN ₃ O ₄ S ₂	MLS000538193-01	55.56	12.59	-1.1	36.34	-3
164	 C ₁₇ H ₂₀ ClNS	MLS000538220-01	55.56	14.13	-1.1	45.75	-3
165	 C ₁₈ H ₁₉ N ₃ O ₄ S	MLS000559128-01	55.56	10.00	-1.1	32.39	-2.2
166	 C ₂₃ H ₁₇ NO ₂ S	MLS000569098-01	55.56	12.59	-1.1	20.43	-2.2
167	 C ₂₁ H ₂₈ N ₂ O ₃ S	MLS000731852-01	55.56	12.59	-1.1	36.34	2.4
168	 C ₁₇ H ₁₉ NO ₄ S	MLS000736256-01	55.56	11.22	-1.1		Inactive
169	 C ₁₃ H ₁₁ FN ₂ O ₂ S	MLS001167450-01	55.56	14.13	-1.1		Inactive
170	 C ₁₇ H ₁₉ N ₂ O ₅	MLS000028521-01	55.56	17.78	-1.1	32.39	-2.4

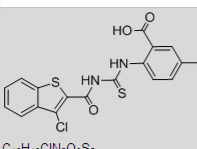
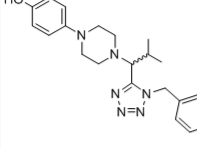
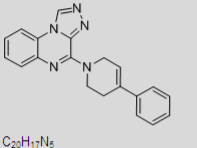
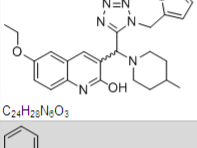
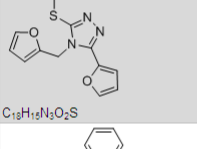
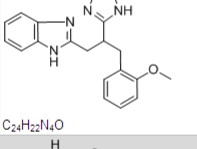
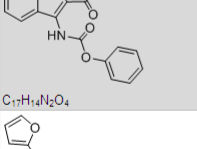
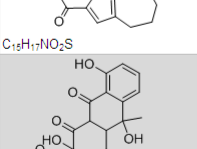
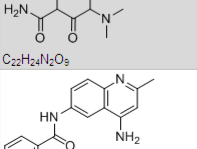
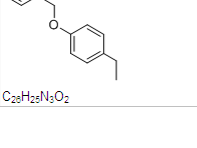
compound number	Structure	Substance ID	gel assay	sfp qHTS	sfp qHTS	AcpS qHTS	AcpS qHTS
			IC50 (μl)	Potency (μl)	CurveClass	Potency (μl)	CurveClass
171	 C ₁₈ H ₁₃ ClN ₂ O ₃ S ₂	MLS000705121-01	55.56	15.85	-1.1	25.72	-3
172	 C ₂₂ H ₂₇ FN ₃ O	MLS000716371-01	55.56	15.85	-1.1		Inactive
173	 C ₂₀ H ₁₇ N ₅	MLS000119007-01	55.56	28.18	-1.1		Inactive
174	 C ₂₄ H ₂₃ N ₃ O ₃	MLS000071870-01	55.56	3.55	-1.2	32.39	-3
175	 C ₁₈ H ₁₅ N ₃ O ₃ S	MLS000082409-01	55.56	3.98	-1.2	40.77	-3
176	 C ₂₄ H ₂₂ N ₄ O	NCGC00142347-01	55.56	5.01	-1.2	28.86	-2.2
177	 C ₁₇ H ₁₄ N ₂ O ₄	MLS000037451-01	55.56	11.22	-1.2		Inactive
178	 C ₁₅ H ₁₇ NO ₂ S	MLS000065859-01	55.56	3.55	-1.2		Inactive
179	 C ₂₂ H ₂₄ N ₂ O ₉	NCGC00159490-02	55.56	7.94	-1.2		Inactive
180	 C ₂₈ H ₂₅ N ₃ O ₂	NCGC00161418-01	55.56	12.59	-1.2	40.77	-3

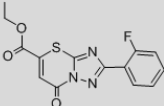
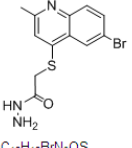
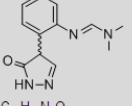
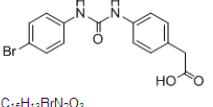
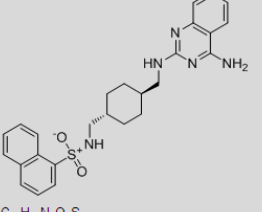
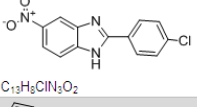
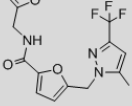
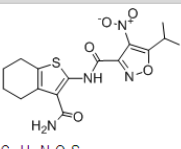
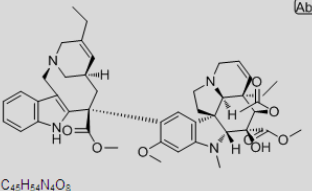
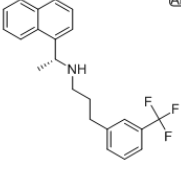
Table 7.5 continued							
compound number	Structure	Substance ID	gel assay IC50 (µM)	sfp qHTS Potency (µM)	sfp qHTS CurveClass	AcpS qHTS Potency (µM)	AcpS qHTS CurveClass
181	 C ₁₄ H ₁₀ FN ₃ O ₃ S	MLS000081797-01	55.56	14.13	-1.2		Inactive
182	 C ₁₂ H ₁₂ BrN ₃ OS	MLS000770041-01	55.56	22.39	-1.2		Inactive
183	 C ₁₂ H ₁₄ N ₄ O	MLS000830729-01	55.56	17.78	-1.2		Inactive
184	 C ₁₃ H ₁₃ BrN ₂ O ₃	MLS000661040-01	55.56	39.81	-1.2		Inactive
185	 C ₂₈ H ₂₉ N ₉ O ₂ S	NCGC00159542-01	55.56	28.18	-1.2		Inactive
186	 C ₁₃ H ₉ ClN ₃ O ₂	MLS000702274-01	55.56	0.35	-2.2		Inactive
187	 C ₁₈ H ₁₄ F ₃ N ₃ O ₃	MLS000088912-01	55.56	0.89	-2.2	40.77	-3
188	 C ₁₉ H ₁₉ N ₄ O ₅ S	MLS000871812-01	55.56	3.16	-2.1		Inactive
189	 C ₄₉ H ₅₄ N ₄ O ₉	NCGC00165966-01	55.56	14.13	-2.2	25.72	-3
190	 C ₂₂ H ₂₂ F ₃ N	NCGC00181002-01	55.56	79.43	-2.2		Inactive

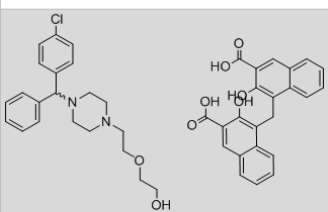
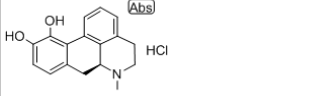
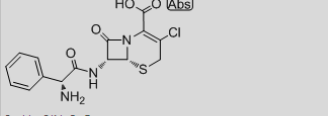
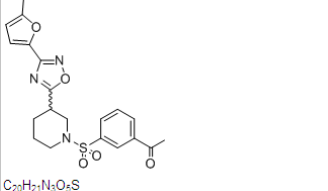
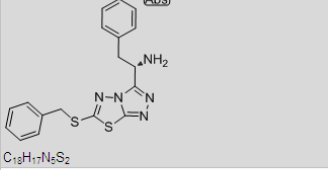
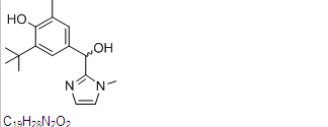
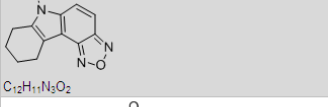
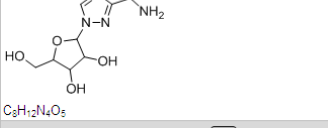
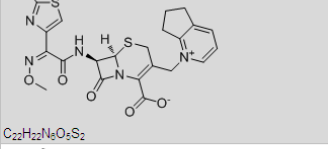
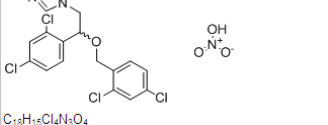
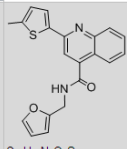
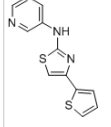
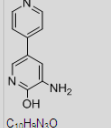
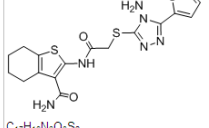
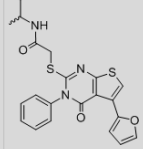
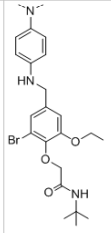
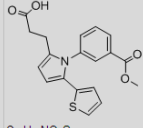
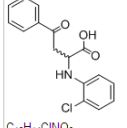
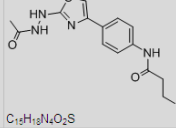
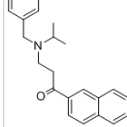
Table 7.5 continued								
compound number	Structure	Substance ID	gel assay IC50 (μl)	sfp qHTS Potency (μl)	sfp qHTS CurveClass	AcpS qHTS Potency (μl)	AcpS qHTS CurveClass	
191	 C ₄₄ H ₄₃ ClN ₂ O ₃	MLS000028605-01	55.56	50.12	-2.2	32.39	-3	
192	 C ₁₇ H ₁₃ ClNO ₂	MLS000028867-01	55.56	44.67	-2.1		Inactive	
193	 C ₁₅ H ₁₄ ClN ₃ O ₄ S	MLS000069617-01	55.56	50.12	-2.2		Inactive	
194	 C ₂₃ H ₂₁ N ₃ O ₃ S	MLS000075525-01	55.56	56.23	-2.2	28.86	-2.2	
195	 C ₁₃ H ₁₇ N ₅ S ₂	MLS000083775-01	55.56	44.67	-2.2		Inactive	
196	 C ₁₉ H ₂₃ N ₂ O ₂	MLS000107149-01	55.56	44.67	-2.2		Inactive	
197	 C ₁₂ H ₁₁ N ₃ O ₂	MLS000525866-01	55.56	44.67	-2.1		Inactive	
198	 C ₈ H ₁₂ N ₄ O ₂	NCGC00095898-01	55.56	56.23	-2.1		Inactive	
199	 C ₂₂ H ₂₂ N ₈ O ₅ S ₂	NCGC00181339-01	55.56	56.23	-2.1		Not tested	
200	 C ₁₈ H ₁₂ Cl ₄ N ₃ O ₄	MLS000028674-01	55.56	35.48	-2.1	28.86	-3	

Table 7.5 continued							
compound number	Structure	Substance ID	gel assay IC50 (µl)	sfp qHTS Potency (µl)	sfp qHTS CurveClass	AcpS qHTS Potency (µl)	AcpS qHTS CurveClass
201	 C ₁₂ H ₉ N ₅	MLS000075752-01	55.56	39.81	-2.1	36.34	Inactive
202	 C ₁₃ H ₇ NO ₂	MLS000104216-01	55.56	35.48	-2.1	40.77	-3
203	 C ₁₂ H ₁₇ ClN ₂ S ₂	MLS001002012-01	55.56	35.48	-2.2		Inactive
204	 C ₁₉ H ₂₁ FN ₄ O ₃	NCGC00093935-01	55.56	35.48	-2.1	32.39	-2.2
205	 C ₁₄ H ₁₃ N ₂ O ₂ S ₂	NCGC00159512-02	55.56	31.62	-2.2	0.00	Inactive
206	 C ₁₈ H ₁₇ N ₄ O ₂ S ₄	NCGC00181012-01	55.56	39.81	-2.2	8.13	2.4
207	 C ₈ H ₉ N ₄	NCGC00015501-02	74.50	5.01	-1.2	0.62	Inactive
208	 C ₈ H ₉ NO ₃	NCGC00016542-01	74.50	35.48	-2.2	17.41	-2.4
209	 C ₁₉ H ₁₉ FN ₂ O	MLS000539028-01	166.67	0.56	-1.1	20.43	-2.2
210	 C ₁₈ H ₁₂ ClN ₃ S	MLS000392755-01	166.67	1.41	-1.1		Inactive

Table 7.5 continued

compound number	Structure	Substance ID	gel assay IC50 (μl)	sfp qHTS Potency (μl)	sfp qHTS CurveClass	AcpS qHTS Potency (μl)	AcpS qHTS CurveClass
211	 C ₂₂ H ₁₉ N ₂ O ₂ S	MLS000325444-01	166.67	2.82	-1.1	40.77	-3
212	 C ₁₂ H ₉ N ₃ S ₂	MLS000064768-01	166.67	5.01	-1.1	45.75	Inactive
213	 C ₁₀ H ₉ N ₃ O	MLS000069829-01	166.67	6.31	-1.1	32.39	-2.2
214	 C ₁₇ H ₁₃ N ₆ O ₃ S ₂	MLS000568189-01	166.67	5.62	-1.1	32.39	-2.4
215	 C ₂₃ H ₂₃ N ₂ O ₃ S ₂	MLS000569243-01	166.67	4.47	-1.1	40.77	-3
216	 C ₂₃ H ₂₂ BrN ₃ O ₃	MLS000580588-01	166.67	3.55	-1.1	28.86	-3
217	 C ₁₉ H ₁₇ NO ₄ S	MLS000621481-01	166.67	3.98	-1.1	25.72	-2.2
218	 C ₁₈ H ₁₄ ClNO ₃	MLS000626824-01	166.67	3.98	-1.1	0.03	Inactive
219	 C ₁₉ H ₁₉ N ₄ O ₂ S	MLS000768916-01	166.67	5.01	-1.1		Inactive
220	 C ₂₃ H ₂₂ NO	NCGC00025126-01	166.67	3.98	-1.1	36.34	-2.2

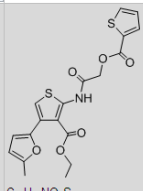
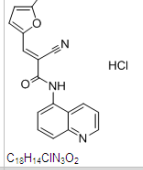
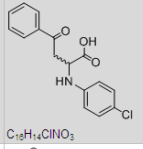
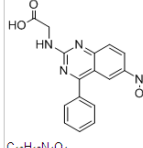
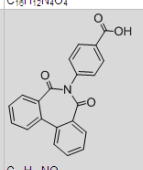
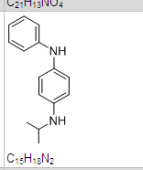
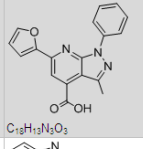
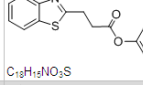
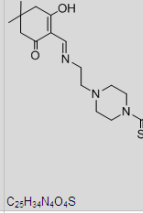
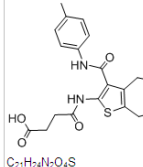
compound number	Structure	Substance ID	gel assay IC50 (μM)	slp qHTS Potency (μM)	slp qHTS CurveClass	AcpS qHTS Potency (μM)	AcpS qHTS CurveClass
221	 C ₁₈ H ₁₇ NO ₆ S ₂	MLS000053288-01	166.67	10.00	-1.1	20.43	-2.2
222	 C ₁₈ H ₁₄ ClN ₃ O ₂ HCl	MLS000402164-01	166.67	8.91	-1.1	20.43	-2.2
223	 C ₁₈ H ₁₄ ClNO ₃	MLS000549895-01	166.67	7.08	-1.1	0.00	Inactive
224	 C ₁₈ H ₁₂ N ₄ O ₄	MLS000594859-01	166.67	6.31	-1.1	45.75	-3
225	 C ₂₁ H ₁₃ NO ₄	MLS000713943-01	166.67	7.94	-1.1		Inactive
226	 C ₁₅ H ₁₃ N ₂	NCGC00091826-01	166.67	8.91	-1.1	12.89	-2.2
227	 C ₁₈ H ₁₃ N ₃ O ₃	MLS000060726-01	166.67	12.59	-1.1	51.33	-2.4
228	 C ₁₈ H ₁₂ NO ₃ S	MLS000516608-01	166.67	15.85	-1.1		Inactive
229	 C ₂₂ H ₂₄ N ₄ O ₄ S	MLS000687270-01	166.67	11.22	-1.1		Inactive
230	 C ₂₁ H ₂₄ N ₄ O ₄ S	MLS000703360-01	166.67	11.22	-1.1	25.72	-2.2

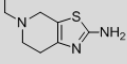
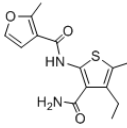
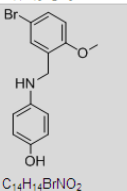
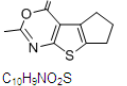
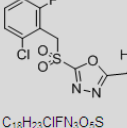
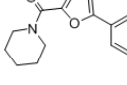
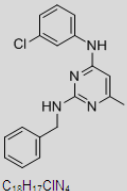
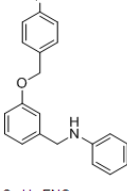
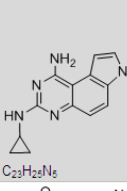
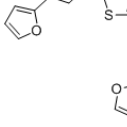
Table 7.5 continued							
compound number	Structure	Substance ID	gel assay IC50 (µl)	sfp qHTS Potency (µl)	sfp qHTS CurveClas	AcpS qHTS Potency (µl)	AcpS qHTS CurveClass
231	 C ₉ H ₁₃ N ₃ S	MLS001005691-01	166.67	11.22	-1.1		Inactive
232	 C ₁₄ H ₁₆ N ₂ O ₃ S	MLS001125689-01	166.67	11.22	-1.1	32.39	-3
233	 C ₁₄ H ₁₄ BrNO ₂	MLS000064028-01	166.67	19.95	-1.1		Inactive
234	 C ₁₀ H ₉ NO ₂ S	MLS000068653-01	166.67	15.85	-1.1	0.36	Inactive
235	 C ₁₈ H ₂₃ ClFNO ₃ S	MLS000084061-01	166.67	14.13	-1.1	25.72	Inactive
236	 C ₁₆ H ₁₆ N ₂ O ₄	MLS000552970-01	166.67	15.85	-1.1	32.39	-2.2
237	 C ₁₈ H ₁₇ ClN ₄	MLS000591844-01	166.67	15.85	-1.1	40.77	-3
238	 C ₂₀ H ₁₃ FNO ₂	MLS000693361-01	166.67	15.85	-1.1	12.89	Inactive
239	 C ₂₃ H ₂₅ N ₅	NCGC00025225-01	166.67	5.01	-1.2	32.39	-2.2
240	 C ₁₄ H ₁₀ N ₂ O ₄ S ₃	MLS000054210-01	166.67	14.13	-1.2	2.57	Inactive

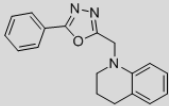
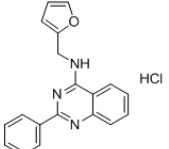
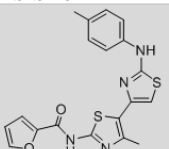
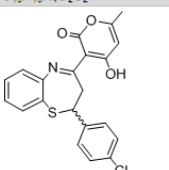
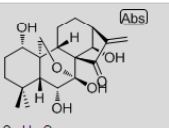
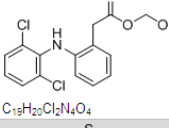
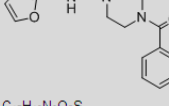
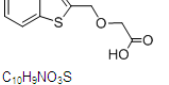
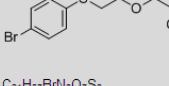
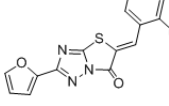
Table 7.5 continued							
compound number	Structure	Substance ID	gel assay IC50 (µl)	sfp qHTS Potency (µl)	sfp qHTS CurveClas	AcpS qHTS Potency (µl)	AcpS qHTS CurveClass
241	 C ₁₈ H ₁₇ N ₃ O	MLS000066744-01	166.67	14.13	-1.2		Inactive
242	 C ₁₉ H ₁₆ ClN ₃ O	MLS000121782-01	166.67	11.22	-1.2	20.43	Inactive
243	 C ₁₉ H ₁₆ N ₄ O ₂ S ₂	MLS000561530-01	166.67	15.85	-1.2		Inactive
244	 C ₂₁ H ₁₈ ClNO ₃ S	MLS000595006-01	166.67	14.13	-1.2	18.21	-2.2
245	 C ₂₀ H ₂₅ O ₅	NCGC00161610-01	166.67	12.59	-1.2	18.21	-2.2
246	 C ₁₉ H ₂₀ Cl ₂ N ₄ O ₄	NCGC00168162-01	166.67	22.39	-1.2	32.39	-2.2
247	 C ₁₇ H ₁₉ N ₃ O ₂ S	MLS000772404-01	166.67	35.48	-1.2		Inactive
248	 C ₁₉ H ₉ NO ₃ S	MLS000773812-01	166.67	25.12	-1.2	0.51	Inactive
249	 C ₂₁ H ₂₇ BrN ₂ O ₇ S ₂	MLS000402458-01	166.67	3.55	-2.1	0.00	Inactive
250	 C ₁₈ H ₁₁ N ₃ O ₃ S	MLS000085633-01	166.67	2.00	-2.2	18.21	-2.1

Table 7.5 continued

compound number	Structure	Substance ID	gel assay IC50 (μl)	sfp qHTS Potency (μl)	sfp qHTS CurveClas	AcpS qHTS Potency (μl)	AcpS qHTS CurveClass
251	 <chem>C19H14N4OS</chem>	MLS000589681-01	166.67	7.94	-2.1		Inactive
252	 <chem>C17H10ClN3</chem>	MLS000695034-01	166.67	15.85	-2.1	36.34	-3
253	 <chem>C19H19N3O4S</chem>	MLS000028120-01	166.67	39.81	-2.1	0.51	Inactive
254	 <chem>C14H13N3NaO4S3</chem>	MLS000028706-01	166.67	44.67	-2.2	2.89	Inactive
255	 <chem>C19H20ClN2O4</chem>	MLS000040261-01	166.67	56.23	-2.2	45.75	Inactive
256	 <chem>C17H10ClN3S</chem>	MLS000522808-01	166.67	56.23	-2.2	10.24	Inactive
257	 <chem>C17H15ClN3S</chem>	MLS000719838-01	166.67	17.78	-2.2	32.39	-2.2
258	 <chem>C18H20N2</chem>	NCGC00024926-04	166.67	44.67	-2.2	22.93	Inactive
259	 <chem>C19H14N4O5S2</chem>	NCGC00095137-01	166.67	56.23	-2.1	0.00	Inactive
260	 <chem>C17H15N3S</chem>	NCGC00163160-01	166.67	56.23	-2.1	5.13	Inactive

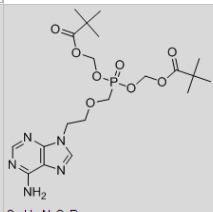
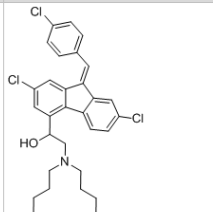
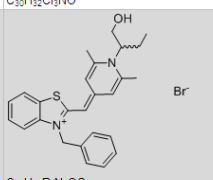
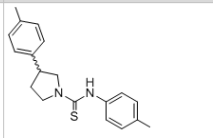
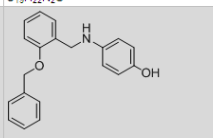
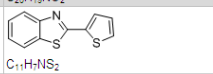
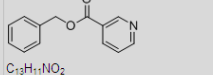
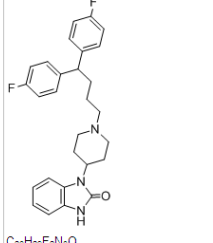
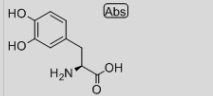
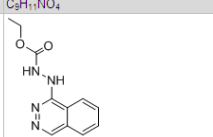
compound number	Structure	Substance ID	gel assay IC50 (μM)	sfp qHTS Potency (μM)	sfp qHTS CurveClass	AcpS qHTS Potency (μM)	AcpS qHTS CurveClass
261	 C ₂₂ H ₃₂ N ₄ O ₅ P	NCGC00164624-01	166.67	56.23	-2.2	28.86	-3
262	 C ₃₃ H ₃₂ Cl ₃ NO	NCGC00167490-01	166.67	44.67	-2.2	32.39	-3
263	 C ₂₅ H ₂₃ BrN ₂ OS	MLS000392277-01	166.67	35.48	-2.2	1.45	Inactive
264	 C ₁₉ H ₂₂ N ₂ S	MLS000683715-01	166.67	31.62	-2.1	45.75	Inactive
265	 C ₂₃ H ₁₉ NO ₂	MLS000704391-01	166.67	25.12	-2.2	45.75	Inactive
266	 C ₁₁ H ₇ NS ₂	MLS000851105-01	166.67	35.48	-2.2		Inactive
267	 C ₁₃ H ₁₁ NO ₂	NCGC00166105-01	166.67	31.62	-2.2	18.21	-2.2
268	 C ₂₈ H ₂₅ F ₂ N ₃ O	NCGC00016601-01	223.50	19.95	-1.2	17.41	-3
269	 C ₉ H ₁₁ NO ₄	NCGC00016270-01	223.50	39.81	-2.2	2.76	Inactive
270	 C ₁₁ H ₁₂ N ₄ O ₂	NCGC00016640-01	223.50	35.48	-2.2	2.46	Inactive

Table 7.5 continued

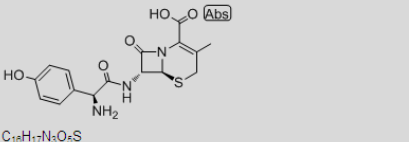
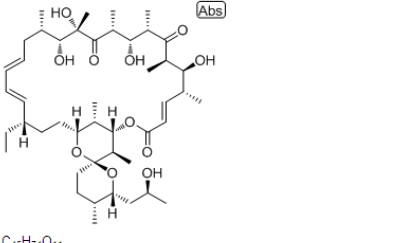
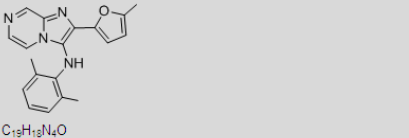

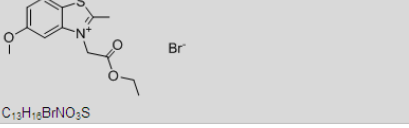
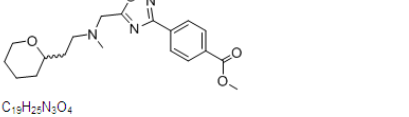


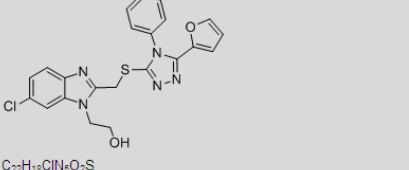
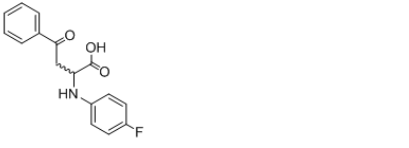
compound number	Structure	Substance ID	gel assay IC ₅₀ (µl)	slp qHTS Potency (µl)	slp qHTS CurveClass	AcpS qHTS Potency (µl)	AcpS qHTS CurveClass
271	 C ₁₂ H ₁₇ N ₃ O ₂ S	NCGC00016858-01	223.50	31.62	-2.2		Inactive
272	 C ₂₅ H ₄₂ O ₁₁	NCGC00163472-01	>114	0.00	-1.1	9.13	Inactive
273	 C ₁₃ H ₁₃ N ₄ O	MLS000522365-01	>114	0.50	-1.1	18.21	-2.1
274	 C ₁₃ H ₁₃ N ₂ O ₂	MLS000557738-01	>114	1.41	-1.1	10.24	-1.1
275	 C ₁₃ H ₁₆ BrNO ₂ S	MLS000568400-01	>114	1.00	-1.1	18.21	-2.1
276	 C ₁₅ H ₂₂ N ₂ O ₄	MLS000733657-01	>114	0.71	-1.1	6.46	Inactive
277	 C ₁₃ H ₁₇ ClN ₂ S	MLS000594090-01	>114	2.24	-1.1	25.72	-2.2
278	 C ₂₀ H ₂₈ O ₄	NCGC00161623-01	>114	1.41	-1.1		Inactive
279	 C ₂₂ H ₁₉ ClN ₂ O ₂ S	MLS000058557-01	>114	3.98	-1.1	28.86	-2.2
280	 C ₁₈ H ₁₄ FNO ₃	MLS000088817-01	>114	2.24	-1.1	22.93	Inactive

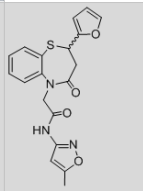
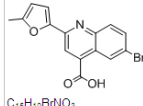
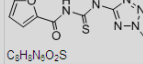
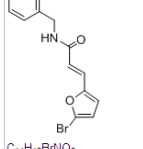
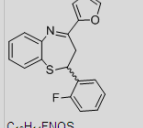
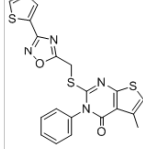
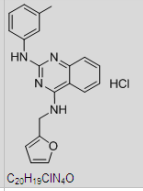
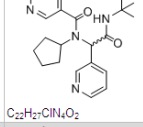
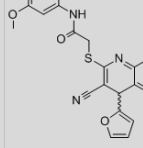
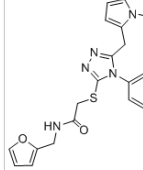
Table 7.5 continued							
compound number	Structure	Substance ID	gel assay IC50 (µM)	sfp qHTS Potency (µM)	sfp qHTS CurveClass	AcpS qHTS Potency (µM)	AcpS qHTS CurveClass
281	 C ₁₉ H ₁₇ N ₃ O ₄ S	MLS000102384-01	>114	2.51	-1.1	20.43	-2.2
282	 C ₁₉ H ₁₀ BrNO ₃	MLS000699043-01	>114	3.16	-1.1	9.13	-1.1
283	 C ₈ H ₉ N ₃ O ₂ S	MLS000331956-01	>114	6.31	-1.1	0.58	Inactive
284	 C ₁₄ H ₁₂ BrNO ₂	MLS000388925-01	>114	6.31	-1.1	25.72	-2.2
285	 C ₁₉ H ₁₄ FNO ₃ S	MLS000516585-01	>114	3.55	-1.1	36.34	-2.2
286	 C ₂₁ H ₁₉ N ₄ O ₂ S ₃	MLS000582112-01	>114	3.98	-1.1	1.82	-1.1
287	 C ₂₀ H ₁₉ ClN ₄ O	MLS000662793-01	>114	2.51	-1.1	40.77	-3
288	 C ₂₂ H ₂₇ ClN ₄ O ₂	MLS000706307-01	>114	3.55	-1.1	1.82	Inactive
289	 C ₂₃ H ₂₁ N ₄ O ₄ S	MLS000079525-01	>114	7.94	-1.1	20.43	Inactive
290	 C ₂₂ H ₂₃ N ₃ O ₂ S	MLS000092949-01	>114	6.31	-1.1		Inactive

Table 7.5 continued							
compound number	Structure	Substance ID	gel assay IC50 (µl)	sfp qHTS Potency (µl)	sfp qHTS CurveClass	AcpS qHTS Potency (µl)	AcpS qHTS CurveClass
291	 <chem>C12H9N3O2S</chem>	MLS000552509-01	>114	5.01	-1.1	28.86	-3
292	 <chem>C22H20N4OS</chem>	MLS000559383-01	>114	8.91	-1.1	11.49	-1.2
293	 <chem>C21H23N2O2</chem>	MLS000594533-01	>114	10.00	-1.1	20.43	Inactive
294	 <chem>C17H15ClNO3</chem>	MLS000704279-01	>114	7.94	-1.1	22.93	Inactive
295	 <chem>C18H15N3OS</chem>	MLS000706712-01	>114	6.31	-1.1	45.75	Inactive
296	 <chem>C13H13N4OS</chem>	MLS000764665-01	>114	4.47	-1.1	45.75	Inactive
297	 <chem>C12H10N2O3</chem>	MLS000766249-01	>114	6.31	-1.1	45.75	Inactive
298	 <chem>C14H13FN2OS</chem>	MLS000780456-01	>114	7.94	-1.1	22.93	-2.2
299	 <chem>C18H17NO2</chem>	MLS001001346-01	>114	7.94	-1.1	28.86	-2.1
300	 <chem>C18H14ClNO4</chem>	MLS001017925-01	>114	7.94	-1.1	0.02	Inactive

Table 7.5 continued

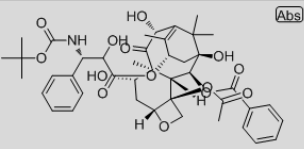
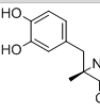
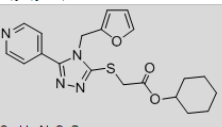
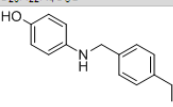
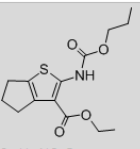
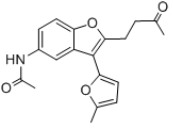
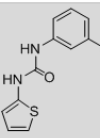
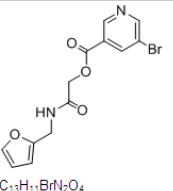
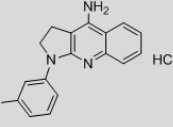
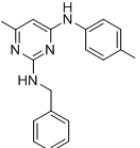
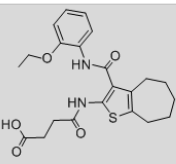
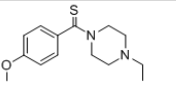
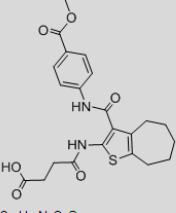
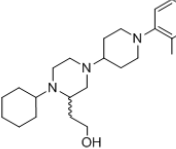
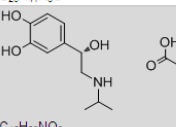
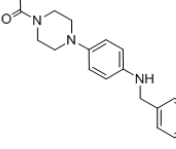
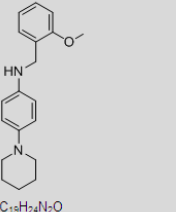
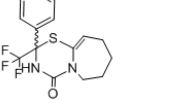
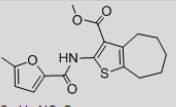
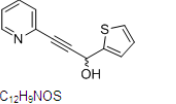
compound number	Structure	Substance ID	gel assay IC50 (µM)	sfp qHTS Potency (µM)	sfp qHTS CurveClas	AcpS qHTS Potency (µM)	AcpS qHTS CurveClass
301	 C ₄₃ H ₅₃ NO ₁₄	NCG00181306-01	>114	6.31	-1.1	45.75	Inactive
302	 C ₁₀ H ₁₃ NO ₄	MLS000028644-01	>114	12.59	-1.1	0.00	Inactive
303	 C ₂₀ H ₂₂ N ₄ O ₂ S	MLS000033403-01	>114	14.13	-1.1	28.86	-2.2
304	 C ₁₅ H ₁₇ NO	MLS000063679-01	>114	11.22	-1.1		Inactive
305	 C ₁₄ H ₁₉ NO ₄ S	MLS000088484-01	>114	14.13	-1.1	45.75	-3
306	 C ₁₉ H ₁₉ NO ₄	MLS000090236-01	>114	12.59	-1.1	28.86	-2.2
307	 C ₁₂ H ₁₂ N ₂ O ₂ S	MLS000093622-01	>114	11.22	-1.1		Inactive
308	 C ₁₃ H ₁₁ BrN ₂ O ₄	MLS000098199-01	>114	12.59	-1.1	22.93	-2.2
309	 C ₁₉ H ₁₉ ClN ₃	MLS000120350-01	>114	11.22	-1.1		Inactive
310	 C ₁₉ H ₂₀ N ₄	MLS000574704-01	>114	12.59	-1.1	28.86	-2.1

Table 7.5 continued							
compound number	Structure	Substance ID	gel assay IC50 (μl)	sfp qHTS Potency (μl)	sfp qHTS CurveClass	AcpS qHTS Potency (μl)	AcpS qHTS CurveClass
311	 <chem>C22H26N2O8S</chem>	MLS000673486-01	>114	12.59	-1.1	36.34	-2.2
312	 <chem>C14H20N2OS</chem>	MLS000674926-01	>114	11.22	-1.1	0.51	Inactive
313	 <chem>C23H26N2O8S</chem>	MLS000690621-01	>114	11.22	-1.1	20.43	-2.2
314	 <chem>C28H44N2O</chem>	MLS000732232-01	>114	10.00	-1.1	32.39	Inactive
315	 <chem>C19H23NO9</chem>	MLS000028736-01	>114	19.95	-1.1	45.75	Inactive
316	 <chem>C20H23N3O3</chem>	MLS000049429-01	>114	15.85	-1.1	28.86	3
317	 <chem>C18H24N2O</chem>	MLS000062416-01	>114	17.78	-1.1	32.39	-3
318	 <chem>C18H18F3N2OS</chem>	MLS000081947-01	>114	19.95	-1.1	0.14	Inactive
319	 <chem>C17H19NO4S</chem>	MLS000088824-01	>114	14.13	-1.1	22.93	-2.2
320	 <chem>C12H9NOS</chem>	MLS000090235-01	>114	17.78	-1.1	0.41	Inactive

compound number	Structure	Substance ID	gel assay IC50 (µM)	sfp qHTS Potency (µM)	sfp qHTS CurveClass	AcpS qHTS Potency (µM)	AcpS qHTS CurveClass
321	 <chem>CC(=O)N1C=NC(S1)S(=O)(=O)N</chem> C ₅ H ₅ N ₄ O ₃ S ₂	MLS000028532-01	>114	25.12	-1.1	16.23	Inactive
322	 <chem>O=[N+]([O-])c1ccc(cc1)C2=CC=CN2C3=CC=C(C=C3)C4=NC5=CC=NS5C4=O</chem> C ₁₃ H ₁₃ N ₅ O ₃ S	MLS0005683159-01	>114	1.00	-1.2	16.23	-2.2
323	 <chem>COc1ccc(cc1)C(=O)NCC2=NC3=CC=CC=C3N=C2C4=CC=CC=C4N</chem> C ₂₁ H ₁₉ N ₄ O ₃ S	MLS000082425-01	>114	4.47	-1.2	45.75	-3
324	 <chem>COc1ccc(cc1)N2CCN(C2)C(=O)C3=C4C=CC(=C34)N5C=NC=C5</chem> C ₂₃ H ₂₂ N ₂ O ₃	MLS000547118-01	>114	2.00	-1.2	32.39	-2.2
325	 <chem>C1=CC=C(C=C1)N2C=NC=C2C3=CC=CC=C3C4=CC=CC=C4C5=CC=CC=C5N</chem> C ₂₃ H ₁₉ N ₄ O ₂	MLS000560787-01	>114	2.82	-1.2	0.10	Inactive
326	 <chem>COc1ccc(cc1)N2=CN=C(S2)C3=CC=CC=C3C4=CC=CC=C4C5=CC=CC=C5N</chem> C ₂₄ H ₂₂ N ₄ O ₃ S ₂	MLS0005683319-01	>114	3.98	-1.2	1.62	-1.1
327	 <chem>Oc1ccc(cc1)N2=NC(=S2)C3=CC=CC=C3C4=CC=CC=C4C5=CC=CC=C5N</chem> C ₁₃ H ₁₁ N ₃ O ₃ S	MLS000689789-01	>114	3.98	-1.2	45.75	-3
328	 <chem>Oc1ccc(cc1)N2=NC(=S2)C3=CC=CC=C3C4=CC=CC=C4C5=CC=CC=C5N</chem> C ₁₄ H ₁₂ N ₃ O ₃ S	MLS000088166-01	>114	7.94	-1.2	1.02	Inactive
329	 <chem>Oc1ccc(cc1)N2=NC(=S2)C3=CC=CC=C3C4=CC=CC=C4C5=CC=CC=C5N</chem> C ₁₄ H ₁₂ N ₄ O ₃ S	MLS000716947-01	>114	3.55	-1.2	0.46	Inactive
330	 <chem>Oc1ccc(cc1)N2=NC(=S2)C3=CC=CC=C3C4=CC=CC=C4C5=CC=CC=C5N</chem> C ₄₇ H ₅₁ NO ₁₄	MLS000863266-01	>114	10.00	-1.2	10.24	-2.2

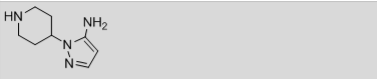
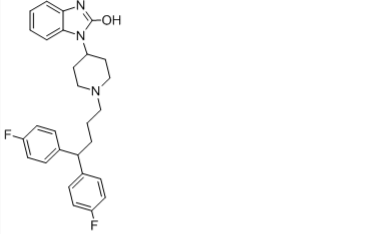
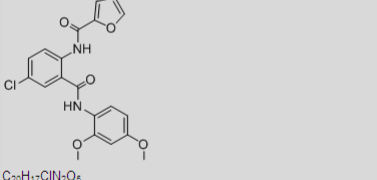
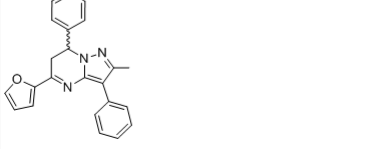
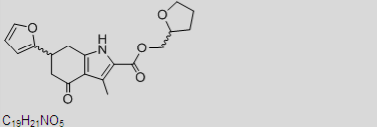

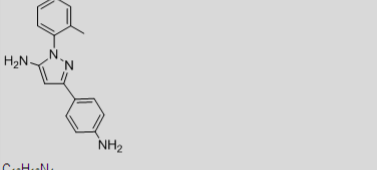
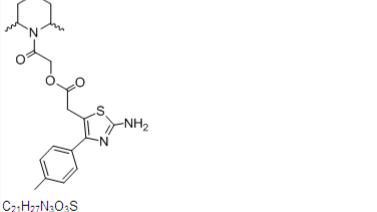
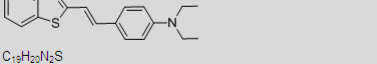

Table 7.5 continued							
compound number	Structure	Substance ID	gel assay IC50 (µl)	sfp qHTS Potency (µl)	sfp qHTS CurveClass	AcpS qHTS Potency (µl)	AcpS qHTS CurveClass
331	 C ₉ H ₁₄ N ₄	MLS000027810-01	>114	17.78	-1.2	36.34	Inactive
332	 C ₂₈ H ₂₉ F ₂ N ₃ O	MLS000028410-01	>114	22.39	-1.2	28.86	-2.2
333	 C ₂₀ H ₁₇ ClN ₂ O ₅	MLS000075270-01	>114	15.85	-1.2	20.43	-2.2
334	 C ₂₃ H ₁₉ N ₃ O	MLS000084315-01	>114	15.85	-1.2	36.34	-2.2
335	 C ₁₉ H ₂₁ NO ₅	MLS000090966-01	>114	15.85	-1.2	20.43	-2.2
336	 C ₁₈ H ₁₅ NO ₃	MLS000098379-01	>114	15.85	-1.2	20.43	-2.4
337	 C ₁₈ H ₁₆ N ₄	MLS000104399-01	>114	14.13	-1.2	8.13	2.4
338	 C ₂₁ H ₂₃ N ₃ O ₃ S	MLS000335438-01	>114	17.78	-1.2	1.15	Inactive
339	 C ₁₈ H ₂₀ N ₂ S	MLS000581120-01	>114	17.78	-1.2	11.49	-1.1
340	 C ₁₈ H ₁₇ N ₃ OS	MLS000681218-01	>114	12.59	-1.2		Inactive

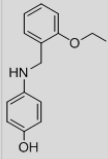
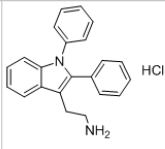
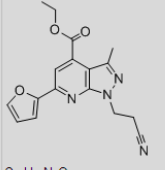
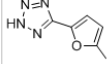
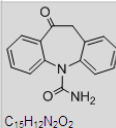
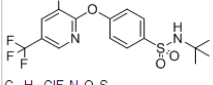
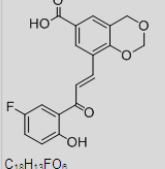
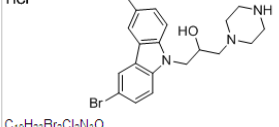
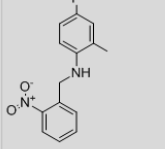
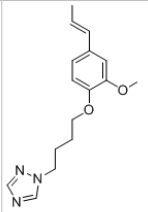
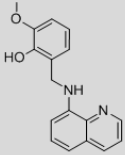
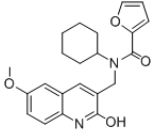
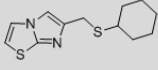
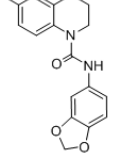
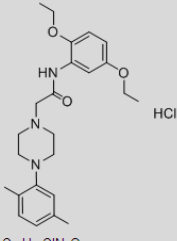
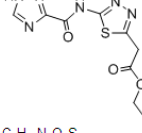
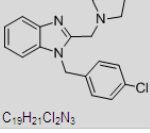
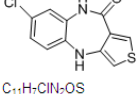
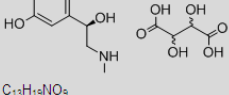
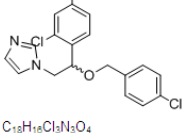
Table 7.5 continued							
compound number	Structure	Substance ID	gel assay IC50 (µM)	sfp qHTS Potency (µM)	sfp qHTS CurveClass	AcpS qHTS Potency (µM)	AcpS qHTS CurveClass
341	 C ₁₂ H ₁₇ NO ₂	MLS000693814-01	>114	10.00	-1.2	0.03	Inactive
342	 C ₂₂ H ₂₁ ClN ₂	MLS000723515-01	>114	15.85	-1.2	36.34	-2.1
343	 C ₁₇ H ₁₉ N ₄ O ₃	MLS000053974-01	>114	28.18	-1.2	0.10	Inactive
344	 C ₆ H ₆ N ₄ O	MLS000068683-01	>114	25.12	-1.2	32.39	-2.2
345	 C ₁₃ H ₁₂ N ₂ O ₂	MLS000084586-01	>114	35.48	-1.2	12.89	Inactive
346	 C ₁₈ H ₁₉ ClF ₃ N ₂ O ₂ S	MLS000328021-01	>114	25.12	-1.2	18.21	-2.2
347	 C ₁₉ H ₁₃ FO ₃	MLS000777851-01	>114	22.39	-1.2	0.00	Inactive
348	 C ₁₉ H ₂₃ Br ₂ Cl ₂ N ₃ O	NCGC00092317-01	>114	35.48	-1.2	0.00	Inactive
349	 C ₁₄ H ₁₃ FN ₂ O ₂	MLS000711244-01	>114	2.82	-2.1	36.34	Inactive
350	 C ₁₈ H ₂₁ N ₃ O ₂	MLS000063579-01	>114	1.12	-2.2		Inactive

Table 7.5 continued							
compound number	Structure	Substance ID	gel assay IC50 (μl)	sfp qHTS Potency (μl)	sfp qHTS CurveClas	AcpS qHTS Potency (μl)	AcpS qHTS CurveClass
351	 C ₁₇ H ₁₆ N ₂ O ₂	MLS000088258-01	>114	4.47	-2.1	0.00	Inactive
352	 C ₂₂ H ₂₄ N ₂ O ₄	MLS000041029-01	>114	7.94	-2.1	40.77	-2.4
353	 C ₁₂ H ₁₆ N ₂ S ₂	MLS000054248-01	>114	3.16	-2.2	1.62	Inactive
354	 C ₁₈ H ₁₉ N ₂ O ₃	MLS000064379-01	>114	3.16	-2.2	0.00	Inactive
355	 C ₂₄ H ₃₄ ClN ₃ O ₃	MLS000076291-01	>114	5.62	-2.2	10.24	-2.2
356	 C ₉ H ₁₂ N ₄ O ₂ S	MLS000087964-01	>114	14.13	-2.2	0.00	Inactive
357	 C ₁₉ H ₂₁ Cl ₂ N ₃	MLS000120342-01	>114	79.43	-2.1	36.34	Inactive
358	 C ₁₁ H ₇ ClN ₂ OS	NCGC00167991-01	>114	79.43	-2.1		Inactive
359	 C ₁₃ H ₁₉ NO ₃	MLS000028381-01	>114	56.23	-2.1	0.00	Inactive
360	 C ₁₈ H ₁₆ Cl ₃ N ₃ O ₄	MLS000028626-01	>114	56.23	-2.1	32.39	-3

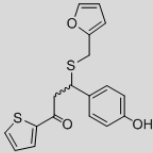
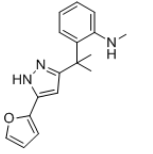
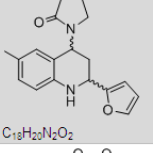
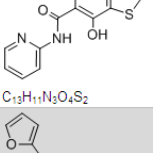
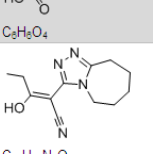
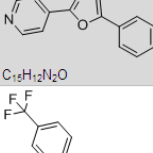
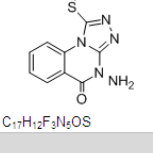
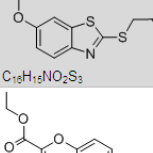
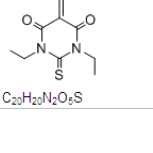

compound number	Structure	Substance ID	gel assay IC50 (µM)	sfp qHTS Potency (µM)	sfp qHTS CurveClas	AcpS qHTS Potency (µM)	AcpS qHTS CurveClass
361	 <chem>C18H16O3S2</chem>	MLS000054235-01	>114	56.23	-2.2		-1.4
362	 <chem>C17H19N3O</chem>	MLS000054520-01	>114	56.23	-2.2	28.86	-2.2
363	 <chem>C18H20N2O2</chem>	MLS000063165-01	>114	39.81	-2.1	32.39	-3
364	 <chem>C13H11N3O4S2</chem>	MLS000069830-01	>114	50.12	-2.2	0.41	Inactive
365	 <chem>C8H6O4</chem>	MLS000071185-01	>114	44.67	-2.1	25.72	-2.2
366	 <chem>C12H16N4O</chem>	MLS000087858-01	>114	14.13	-2.2	6.46	Inactive
367	 <chem>C13H12N2O</chem>	MLS000105516-01	>114	56.23	-2.2	3.63	Inactive
368	 <chem>C17H12F3N2OS</chem>	MLS000122581-01	>114	44.67	-2.2	0.00	Inactive
369	 <chem>C18H15NO2S3</chem>	MLS000535329-01	>114	17.78	-2.2	40.77	-3
370	 <chem>C20H20N2O5S</chem>	MLS001018332-01	>114	50.12	-2.1	0.10	Inactive

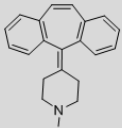
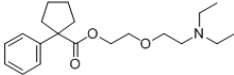
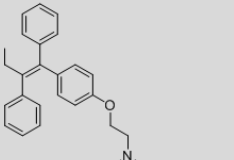
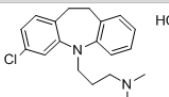
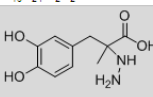
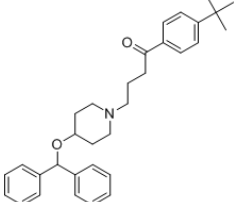
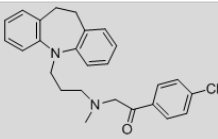
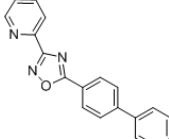
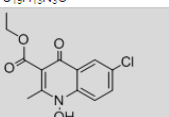
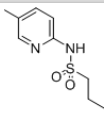
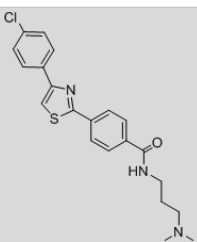
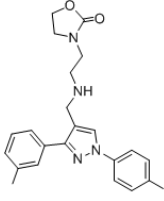
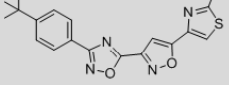
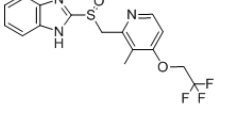
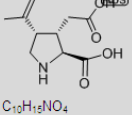
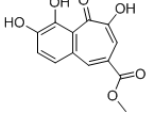
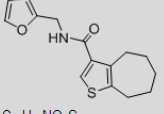
Table 7.5 continued							
compound number	Structure	Substance ID	gel assay IC50 (μ M)	sfp qHTS Potency (μ M)	sfp qHTS CurveClass	AcpS qHTS Potency (μ M)	AcpS qHTS CurveClass
371	 C ₂₁ H ₂₁ N	NCGC00024293-05	>114	44.67	-2.1	32.39	-3
372	 C ₂₀ H ₃₁ NO ₃	NCGC00024595-03	>114	50.12	-2.2		Inactive
373	 C ₂₈ H ₂₉ NO	NCGC00024928-01	>114	56.23	-2.2	20.43	-2.2
374	 C ₁₉ H ₂₄ Cl ₂ N ₂ HCl	NCGC00093756-02	>114	56.23	-2.1	0.00	Inactive
375	 C ₁₀ H ₁₄ N ₂ O ₄	NCGC00095918-01	>114	50.12	-2.1	32.39	-2.2
376	 C ₃₂ H ₃₉ NO ₂	NCGC00164603-01	>114	50.12	-2.2		Inactive
377	 C ₂₈ H ₂₇ ClN ₂ O	NCGC00166397-02	>114	50.12	-2.1	25.72	Inactive
378	 C ₁₉ H ₁₃ N ₃ O	MLS000107901-01	>114	39.81	-2.2	36.34	-3
379	 C ₁₃ H ₁₂ ClNO ₄	MLS000111501-01	>114	35.48	-2.1	22.93	Inactive
380	 C ₁₀ H ₁₆ N ₂ O ₂ S	MLS000394725-01	>114	39.81	-2.2		Inactive

Table 7.5 continued

compound number	Structure	Substance ID	gel assay IC50 (μl)	sfp qHTS Potency (μl)	sfp qHTS CurveClas	AcpS qHTS Potency (μl)	AcpS qHTS CurveClass
381	 <chem>C21H22ClN3OS</chem>	MLS000546266-01	>114	25.12	-2.2	16.23	-2.2
382	 <chem>C23H26N4O2</chem>	MLS000735811-01	>114	44.67	-2.2	18.21	2.4
383	 <chem>C19H18N4O2S</chem>	MLS000834019-01	>114	39.81	-2.2	20.43	-2.2
384	 <chem>C16H14F3N3O2S</chem>	NCGC00015615-02	>114	28.18	-2.2	6.46	Inactive
385	 <chem>C10H12NO4</chem>	NCGC00024504-05	>114	39.81	-2.2		Inactive
386	 <chem>C13H10O5</chem>	NCGC00095922-01	>114	31.62	-2.1	3.24	Inactive
387	 <chem>C16H17NO2S</chem>	MLS000093393-01	>114		Inactive	0.00	Inactive

Antibiotic activity of lead compounds

After evaluation of the data in Table 7.5, 36 top actives were chosen for further characterization. These compounds were resourced from BioFocus DPI as stock solutions in DMSO. These compounds were evaluated in a pair of antimicrobial susceptibility assays against *B. subtilis* strains OKB105 and HM489. The former strain is a mutant of the common laboratory strain 168 that has been complimented with a viable copy of the *sfp* locus, and contains the PPTase genotype $acpS^+/sfp^+$. The latter strain is a mutant of OKB105, and contains a lesion in the *acpS* locus, and thus the PPTase genotype $acpS^-/sfp^+$. In these experiments, we expected to see compounds that cross the cell membrane, are not metabolized, and are acting on target exhibit antibiotic activity since PPTase function is tied to cell viability. Given the differential in activity of most compounds between Sfp and AcpS, we anticipated a differential activity of compounds acting on target. This evaluation revealed that 7 compounds, MLS001173914-01, MLS001172437-01, MLS000394035-01, MLS000081697-01, MLS000685849-01, MLS001172074-01, and MLS000339519-01 possessed modest biochemical activity and were antibiotics at concentrations below 25 μ M, and revealed that the 3-amino-N-benzenesulfonamide series (representative MLS000339519-01) looked promising for further characterization.

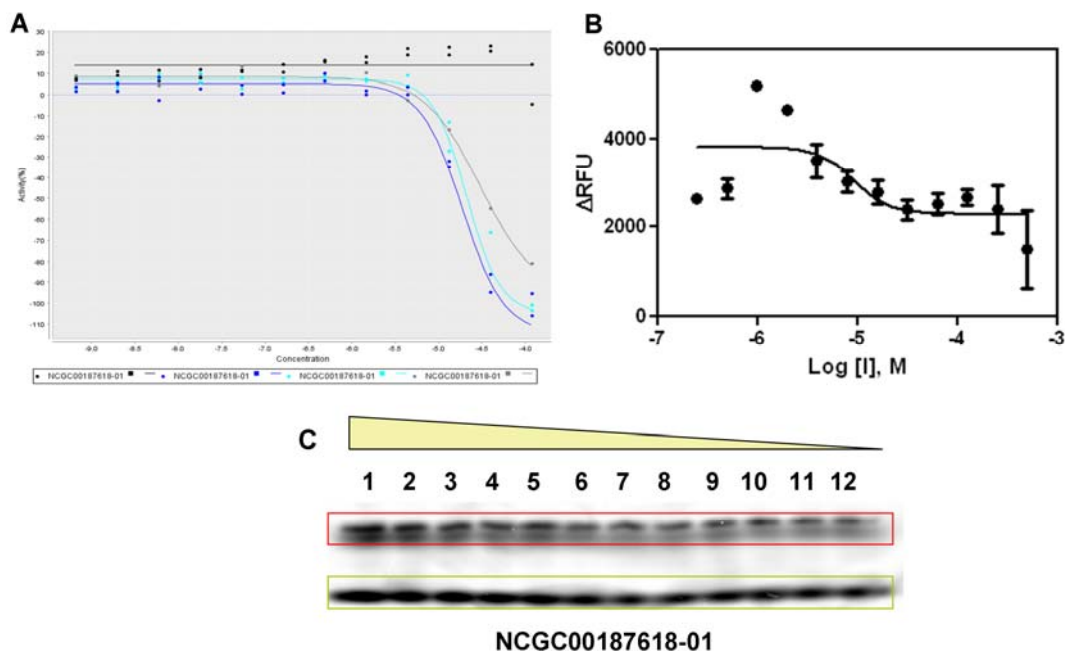


Figure 7.10 Evaluation of thiourea active after resynthesis

NCGC00187618-01 was evaluated in three biochemical assays after resynthesis to confirm its activity before nomination as a lead structure for optimization.

(A). dose response curves from titration of the compound in the qHTS assay. the compound exhibited appropriate behavior with an IC₅₀ value of $23 \pm 6 \mu\text{M}$, and a max response of 90 ± 10 percent inhibition.

(B). Dose response behavior of the compound in the FITC/Rhodamine screen. the compound exhibited moderate inhibition at the lowest concentrations that were alleviated and then enhanced upon higher dosing.

(C). Gel-based assay of NCGC00187618-01. Compound decreases in concentration two-fold every step from lanes 1 to 12, with a top concentration of $500 \mu\text{M}$. The green box contains bands of Rhodamine-CoA, and the red box bands of *crypto*-ActACP. The compound showed no attenuation of fluorescent label incorporation to the protein target.

Activity confirmation by resourcing and purification or resynthesis

With compounds displaying antibiotic activity, we proceeded to confirm the activity of leads by resourcing the compounds as solids from an independent supplier and purifying the provided material, or through resynthesis. In total, 40 compounds were pursued, and 27 were able to be acquired or prepared in a timely manner. The compounds were evaluated in the qHTS assay. Dishearteningly, only the thiourea compound, resynthesized ID NCGC00187618-01, was active after resynthesis. The concentration response curve for this lead evaluated in triplicate using the qHTS protocol is presented in Figure 7.10A.

This compound was further evaluated using the FiTC-Rhodamine quench and gel assays to validate the retention of activity before advancing it as our lead for series expansion and probe development. The data from these experiments are presented in Figure 7.10B and C, respectively. This analysis demonstrated a peculiar behavior of the compound, with perturbation of the assay signal at the lowest concentrations, and an atypical dose response curve that could not be fit by the Hill Equation with confidence. These observations may be due to nonspecific aggregation of the compound in the assay medium, although this could not be confirmed by simple solubility evaluation in a buffered solution. Taken together with the reduced activity in the qHTS protocol (23 μM IC₅₀ v. 2.5 μM from the library deposited sample), this eliminated the compound from the actives pool, and it will not be pursued as a lead for probe nomination.

CONCLUSIONS

We have screened large chemical libraries with the goal of identifying new scaffolds that possess inhibitory activity with Sfp PPTase. This screening was accomplished according to the qHTS paradigm, and has provided an extraordinary amount of information about the activity of the library components. This large dataset (5.2 million points) identified 10,959 compounds with inhibitory characteristics. We chose 387 representatives from this pool and evaluated them in three biochemical assays, and followed up the top 27 that remained active by resynthesis. These 27 compounds failed to retain potent antagonistic activity at this step, and we have not yet identified a scaffold to advance as a lead structure for optimization and nomination as a chemical probe. We are currently advancing this work through the evaluation of a second pool of actives, and the results of this are forthcoming.

ACKNOWLEDGEMENTS

Chapter 7 describes work that is an ongoing collaboration between the Laboratory of Michael D. Burkart and the NIH Chemical Genomics Center. I am a primary author of this work, and performed all *in vitro* and *in vivo* experiments at UCSD. Adam Yasgar and Anton Simeonov executed the robotic screen of the MLSMR. Ajit Jadhav analysed the data and performed compound clustering. David Maloney performed compound resynthesis and purification. This work was performed under the guidance of Christopher P. Austin, James Inglese and Michael D. Burkart.

REFERENCES

- 2009a. Molecular Libraries Small Molecule Repository.
http://mlsmr.glp.gov/MLSMR_HomePage/project.html.
- 2009b. NCGC Assay Guidance Criteria.
http://www.ncgc.nih.gov/guidance/HTS_Assay_Guidance_Criteria.html.
March 31, 2009
- AGARD, N. J., PRESCHER, J. A. & BERTOZZI, C. R. (2004) A strain-promoted [3+2] azide-alkyne cycloaddition for covalent modification of biomolecules in living systems. *Journal of the American Chemical Society*, 126, 15046-15047.
- AHMAD, N., GUPTA, S., HUSAIN, M. M., HEISKANEN, K. M. & MUKHTAR, H. (2000) Differential Antiproliferative and Apoptotic Response of Sanguinarine for Cancer Cells versus Normal Cells. *Clin Cancer Res*, 6, 1524-1528.
- ALLEN, J. J., LAZERWITH, S. E. & SHOKAT, K. M. (2005) Bio-orthogonal affinity purification of direct kinase substrates. *Journal of the American Chemical Society*, 127, 5288-5289.
- ANHAUSER, M. (2003) Pharmacists seek the solution of a shaman. *Drug Discov Today*, 8, 868-9.
- ANNE, J. & VAN MELLAERT, L. (1993) *Streptomyces lividans* as host for heterologous protein production. *FEMS Microbiol Lett*, 114, 121-8.
- ANTOS, J. M. & FRANCIS, M. B. (2006) Transition metal catalyzed methods for site-selective protein modification. *Current Opinion in Chemical Biology*, 10, 253-262.
- ARAGA, S., XU, L., NAKASHIMA, K., VILLAIN, M. & BLALOCK, J. E. (2000) A peptide vaccine that prevents experimental autoimmune myasthenia gravis by specifically blocking T cell help. *The FASEB Journal*, 14, 185-196.
- AUSTIN, C. P., BRADY, L. S., INSEL, T. R. & COLLINS, F. S. (2004) NIH Molecular Libraries Initiative. *Science*, 306, 1138-9.
- BAREKZI, N., JOSHI, S., IRWIN, S., ONTL, T. & SCHWEIZER, H. P. (2004) Genetic characterization of pcpS, encoding the multifunctional phosphopantetheinyl transferase of *Pseudomonas aeruginosa*. *Microbiology*, 150, 795-803.
- BARRY, C. E., 3RD, LEE, R. E., MDLULI, K., SAMPSON, A. E., SCHROEDER, B. G., SLAYDEN, R. A. & YUAN, Y. (1998) Mycolic acids: structure, biosynthesis and physiological functions. *Progress Lipid Res*, 37, 143-79.

- BEDFORD, D. J., SCHWEIZER, E., HOPWOOD, D. A. & KHOSLA, C. (1995) Expression of a Functional Fungal Polyketide Synthase in the Bacterium *Streptomyces-Coelicolor* A3(2). *Journal of Bacteriology*, 177, 4544-4548.
- BERGOT, J. B., CHAKERIAN, V., CONNELL, C. R., EADIE, S. J., FUNG, S., HERSHEY, D. N., LEE, L. G., MENCHEN, S. M. & WOO, S. L. (1995) SPECTRALLY RESOLVABLE RHODAMINE DYES FOR NUCLEIC ACID SEQUENCE DETERMINATION. IN PAT., E. (Ed.), Applied Biosystems.
- BHATT, A., MOLLE, V., BESRA, G. S., JACOBS, W. R. & KREMER, L. (2007) The Mycobacterium tuberculosis FAS-II condensing enzymes: their role in mycolic acid biosynthesis, acid-fastness, pathogenesis and in future drug development. *Molecular Microbiology*, 64, 1442-1454.
- BINNIE, C., WARREN, M. & BUTLER, M. J. (1989) Cloning and heterologous expression in *Streptomyces lividans* of *Streptomyces rimosus* genes involved in oxytetracycline biosynthesis. *J Bacteriol*, 171, 887-95.
- BIRCK, M. R., HOLLER, T. P. & WOODARD, R. W. (2000) Identification of a Slow Tight-Binding Inhibitor of 3-Deoxy-d-manno-octulosonic Acid 8-Phosphate Synthase. *J Am Chem Soc*, 122, 9334-9335.
- BLOMMEL, P. G. & FOX, B. G. (2005) Fluorescence anisotropy assay for proteolysis of specifically labeled fusion proteins. *Analytical Biochemistry*, 336, 75-86.
- BRADFORD, M. M. (1976) Rapid and Sensitive Method for Quantitation of Microgram Quantities of Protein Utilizing Principle of Protein-Dye Binding. *Analytical Biochemistry*, 72, 248-254.
- BUNKOCZI, G., PASTA, S., JOSHI, A., WU, X., KAVANAGH, K. L., SMITH, S. & OPPERMANN, U. (2007) Mechanism and substrate recognition of human holo ACP synthase. *Chem Biol*, 14, 1243-53.
- BYSTRYKH, L. V., FERNANDEZMORENO, M. A., HERREMA, J. K., MALPARTIDA, F., HOPWOOD, D. A. & DIJKHUIZEN, L. (1996) Production of actinorhodin-related "blue pigments" by *Streptomyces coelicolor* A3(2). *J Bacteriol*, 178, 2238-2244.
- CAMPBELL, I. D., DWEK, R. A. & DWEK, R. A. (1984) *Biological spectroscopy*, Menlo Park, Calif., Benjamin/Cummings Pub. Co.
- CANDIANO, G., BRUSCHI, M., MUSANTE, L., SANTUCCI, L., GHIGGERI, G. M., CARNEMOLLA, B., ORECCHIA, P., ZARDI, L. & RIGHETTI, P. G.

- (2004) Blue silver: A very sensitive colloidal Coomassie G-250 staining for proteome analysis. *Electrophoresis*, 25, 1327-1333.
- CANE, D. E., WALSH, C. T. & KHOSLA, C. (1998) Biochemistry - Harnessing the biosynthetic code: Combinations, permutations, and mutations. *Science*, 282, 63-68.
- CERDENO, A. M., BIBB, M. J. & CHALLIS, G. L. (2001) Analysis of the prodiginine biosynthesis gene cluster of *Streptomyces coelicolor* A3(2): new mechanisms for chain initiation and termination in modular multienzymes. *Chem Biol*, 8, 817-829.
- CHALUT, C., BOTELLA, L., DE SOUSA-D'AURIA, C., HOUSSIN, C. & GUILHOT, C. (2006a) The nonredundant roles of two 4'-phosphopantetheinyl transferases in vital processes of Mycobacteria. *Proc. Nat. Acad. Sci. USA*, 103, 8511-6.
- CHALUT, C., BOTELLA, L., DE SOUSA-D'AURIA, C., HOUSSIN, C. & GUILHOT, C. (2006b) The nonredundant roles of two 4'-phosphopantetheinyl transferases in vital processes of Mycobacteria. *Proceedings of the National Academy of Sciences of the United States of America*, 103, 8511-8516.
- CHEN, I., HOWARTH, M., LIN, W. Y. & TING, A. Y. (2005) Site-specific labeling of cell surface proteins with biophysical probes using biotin ligase. *Nature Methods*, 2, 99-104.
- CHEN, I. & TING, A. Y. (2005) Site-specific labeling of proteins with small molecules in live cells. *Current Opinion in Biotechnology*, 16, 35-40.
- CHIN, J. W., CROPP, T. A., ANDERSON, J. C., MUKHERJI, M., ZHANG, Z. W. & SCHULTZ, P. G. (2003) An expanded eukaryotic genetic code. *Science*, 301, 964-967.
- CHU, M., MIERZWA, R., XU, L., YANG, S. W., HE, L., PATEL, M., STAFFORD, J., MACINGA, D., BLACK, T., CHAN, T. M. & GULLO, V. (2003a) Structure elucidation of Sch 538415, a novel acyl carrier protein synthase inhibitor from a microorganism. *Bioorganic & Medicinal Chemistry Letters*, 13, 3827-3829.
- CHU, M., MIERZWA, R., XU, L., YANG, S. W., HE, L., PATEL, M., STAFFORD, J., MACINGA, D., BLACK, T., CHAN, T. M. & GULLO, V. (2003b) Structure elucidation of Sch 538415, a novel acyl carrier protein synthase inhibitor from a microorganism. *Bioorg Med Chem Lett*, 13, 3827-9.

- CHU, M., MIERZWA, R., XU, L., YANG, S. W., HE, L., PATEL, M., STAFFORD, J., MACINGA, D., BLACK, T., CHAN, T. M. & GULLO, V. (2003c) Structure elucidation of Sch 538415, a novel acyl carrier protein synthase inhibitor from a microorganism. *Bioorg Med Chem Lett*, 13, 3827-3829.
- CIMOLAI, N. & CIMOLAI, T. (2007) The cranberry and the urinary tract. *European Journal of Clinical Microbiology & Infectious Diseases*, 26, 767-776.
- CISAR, J. S., FERRERAS, J. A., SONI, R. K., QUADRI, L. E. N. & TAN, D. S. (2007) Exploiting ligand conformation in selective inhibition of non-ribosomal peptide synthetase amino acid adenylation with designed macrocyclic small molecules. *Journal of the American Chemical Society*, 129, 7752-+.
- CLARKE, K. M., MERCER, A. C., LA CLAIR, J. J. & BURKART, M. D. (2005a) In vivo reporter labeling of proteins via metabolic delivery of coenzyme A analogues. *J Am Chem Soc*, 127, 11234-5.
- CLARKE, K. M., MERCER, A. C., LA CLAIR, J. J. & BURKART, M. D. (2005b) In vivo reporter labeling of proteins via metabolic delivery of coenzyme A analogues. *Journal of the American Chemical Society*, 127, 11234-11235.
- COISNE, S., BECHET, M. & BLONDEAU, R. (1999) Actinorhodin production by *Streptomyces coelicolor* A3(2) in iron-restricted media. *Letters in Applied Microbiology*, 28, 199-202.
- COOK, R. M., LYTTLE, M. & DICK, D. (2005) Dark quenchers for donor-acceptor energy transfer IN PAT., U. S. (Ed.) U.S.A., Biosearch Technologies, Inc. .
- COOK, R. M., LYTTLE, M. & DICK, D. (2006) Dark quenchers for donor-acceptor energy transfer IN USPTO (Ed.) USA, Biosearch Technologies, Inc.
- COX, R. J., CROSBY, J., DALTROP, O., GLOD, F., JARZABEK, M. E., NICHOLSON, T. P., REED, M., SIMPSON, T. J., SMITH, L. H., SOULAS, F., SZAFRANSKA, A. E. & WESTCOTT, J. (2002) *Streptomyces coelicolor* phosphopantetheinyl transferase: a promiscuous activator of polyketide and fatty acid synthase acyl carrier proteins. *Journal of the Chemical Society-Perkin Transactions 1*, 1644-1649.
- CRAGG, G. M. & NEWMAN, D. J. (2001) Medicinals for the millennia: the historical record. *Ann N Y Acad Sci*, 953, 3-25.
- CRAGG, G. M. & NEWMAN, D. J. (2005) International collaboration in drug discovery and development from natural sources. *Pure and Applied Chemistry*, 77, 1923-1942.

- CRAGG, G. M., NEWMAN, D. J. & SNADER, K. M. (1997) Natural products in drug discovery and development. *J Nat Prod*, 60, 52-60.
- CRAWFORD, J. M., VAGSTAD, A. L., EHRLICH, K. C., UDWARY, D. W. & TOWNSEND, C. A. (2008) Acyl-carrier protein-phosphopantetheinyltransferase partnerships in fungal fatty acid synthases. *Chembiochem*, 9, 1559-63.
- DARDONVILLE, C., FERNANDEZ-FERNANDEZ, C., GIBBONS, S. L., RYAN, G. J., JAGEROVIC, N., GABILONDO, A. M., MEANA, J. J. & CALLADO, L. F. (2006) Synthesis and pharmacological studies of new hybrid derivatives of fentanyl active at the mu-opioid receptor and I-2-imidazoline binding sites. *Bioorganic & Medicinal Chemistry*, 14, 6570-6580.
- DEXHEIMER, T. S. & POMMIER, Y. (2008) DNA cleavage assay for the identification of topoisomerase I inhibitors. *Nat Prot*, 3, 1736-50.
- DU, L. H., SANCHEZ, C. & SHEN, B. (2001) Hybrid peptide-polyketide natural products: Biosynthesis and prospects toward engineering novel molecules. *Metabolic Engineering*, 3, 78-95.
- DUBE, D. H., PRESCHER, J. A., QUANG, C. N. & BERTOZZI, C. R. (2006) Probing mucin-type O-linked glycosylation in living animals. *Proceedings of the National Academy of Sciences of the United States of America*, 103, 4819-4824.
- ELIBOL, M. (2002) Product shifting by controlling medium pH in immobilised *Streptomyces coelicolor* A3(2) culture. *Process Biochemistry*, 37, 1381-1386.
- ELOVSON, J. & VAGELOS, P. R. (1968) Acyl carrier protein. X. Acyl carrier protein synthetase. *J Biol Chem*, 243, 3603-11.
- FAWZI, A. B., MACDONALD, D., BENBOW, L. L., SMITH-TORHAN, A., ZHANG, H., WEIG, B. C., HO, G., TULSHIAN, D., LINDER, M. E. & GRAZIANO, M. P. (2001) SCH-202676: An allosteric modulator of both agonist and antagonist binding to G protein-coupled receptors. *Mol Pharmacol*, 59, 30-7.
- FENG, B. Y., SIMEONOV, A., JADHAV, A., BABAOGLU, K., INGLESE, J., SHOICHET, B. K. & AUSTIN, C. P. (2007) A high-throughput screen for aggregation-based inhibition in a large compound library. *J. Med. Chem.*, 50, 2385-90.
- FERRERAS, J. A., STIRRETT, K. L., LU, X. Q., RYU, J. S., SOLL, C. E., TAN, D. S. & QUADRI, L. E. N. (2008) Mycobacterial phenolic glycolipid virulence

factor biosynthesis: Mechanism and small-molecule inhibition of polyketide chain initiation. *Chemistry & Biology*, 15, 51-61.

- FINKING, R., SOLSBACHER, J., KONZ, D., SCHOBERT, M., SCHAFER, A., JAHN, D. & MARAHIEL, M. A. (2002) Characterization of a new type of phosphopantetheinyl transferase for fatty acid and siderophore synthesis in *Pseudomonas aeruginosa*. *J Biol Chem*, 277, 50293-302.
- FLUGEL, R. S., HWANGBO, Y., LAMBALOT, R. H., CRONAN, J. E., JR. & WALSH, C. T. (2000) Holo-(acyl carrier protein) synthase and phosphopantetheinyl transfer in *Escherichia coli*. *Journal of Biological Chemistry*, 275, 959-68.
- FOLEY, T. L. & BURKART, M. D. (2009) A homogenous resonance energy transfer assay for phosphopantetheinyl transferase. *Anal Biochem*, 394, 39-47.
- FOLEY, T. L., YOUNG, B. S. & BURKART, M. D. (2007) Synthesis and evaluation anthranilate 4H-oxazol-5-one compounds to inhibit phosphopantetheinyl transferase involved in secondary metabolism. *The 233rd Natl Meeting of the Am Chem Soc*. Chicago, IL.
- FOLEY, T. L., YOUNG, B. S. & BURKART, M. D. (2009) Phosphopantetheinyl transferase inhibition and secondary metabolism. *Febs J*.
- GHARAVI, A. & SAADEH, H. (2007) Substituted-polyaryl chromophoric compounds IN PAT., U. S. (Ed.) U.S.A., Trans Photonics, LLC. .
- GIEPMANS, B. N. G., ADAMS, S. R., ELLISMAN, M. H. & TSIEN, R. Y. (2006) Review - The fluorescent toolbox for assessing protein location and function. *Science*, 312, 217-224.
- GILBERT, A. M., KIRISITS, M., TOY, P., NUNN, D. S., FAILLI, A., DUSHIN, E. G., NOVIKOVA, E., PETERSEN, P. J., JOSEPH-MCCARTHY, D., MCFADYEN, I. & FRITZ, C. C. (2004) Anthranilate 4H-oxazol-5-ones: novel small molecule antibacterial acyl carrier protein synthase (AcpS) inhibitors. *Bioorg Med Chem Lett*, 14, 37-41.
- GILMORE, J. M., SCHECK, R. A., ESSER-KAHN, A. P., JOSHI, N. S. & FRANCIS, M. B. (2006) N-terminal protein modification through a biomimetic transamination reaction. *Angewandte Chemie-International Edition*, 45, 5307-5311.
- GLOVER, K. J., MARTINI, P. M., VOLD, R. R. & KOMIVES, E. A. (1999a) Preparation of insoluble transmembrane peptides: Glycophorin-A, prion (110-137), and FGFR (368-397). *Anal Biochem*, 272, 270-274.

- GLOVER, K. J., MARTINI, P. M., VOLD, R. R. & KOMIVES, E. A. (1999b) Preparation of insoluble transmembrane peptides: Glycophorin-A, prion (110-137), and FGFR (368-397). *Analytical Biochemistry*, 272, 270-274.
- GROSSET, C., CHEN, C.-Y. A., XU, N., SONENBERG, N., JACQUEMIN-SABLON, H. & SHYU, A.-B. (2000) A Mechanism for Translationally Coupled mRNA Turnover: Interaction between the Poly(A) Tail and a c-fos RNA Coding Determinant via a Protein Complex. *Cell*, 103, 29-40.
- GUO, S. & BHATTACHARJEE, J. K. (2004) Posttranslational activation, site-directed mutation and phylogenetic analyses of the lysine biosynthesis enzymes alpha-aminoadipate reductase Lys1p (AAR) and the phosphopantetheinyl transferase Lys7p (PPTase) from *Schizosaccharomyces pombe*. *Yeast*, 21, 1279-88.
- HAAS, J. A., FREDERICK, M. A. & FOX, B. G. (2000) Chemical and posttranslational modification of *Escherichia coli* acyl carrier protein for preparation of dansyl-acyl carrier proteins'. *Protein Expr Purif*, 20, 274-284.
- HAMILL, P., HUDSON, D., KAO, R. Y., CHOW, P., RAJ, M., XU, H., RICHER, M. J. & JEAN, F. (2006) Development of a red-shifted fluorescence-based assay for SARS-coronavirus 3CL protease: identification of a novel class of anti-SARS agents from the tropical marine sponge *Axinella corrugata*. Walter De Gruyter & Co.
- HERMANSON, G. T. (1996) *Bioconjugate Techniques*, San Diego, Academic Press.
- HOFFMANN, R. W. (2000) Conformation Design of Open-Chain Compounds. *Angew Chem Int Ed Engl*, 39, 2054-2070.
- HORBACH, R., GRAF, A., WEIHMANN, F., ANTELO, L., MATHEA, S., LIERMANN, J. C., OPATZ, T., THINES, E., AGUIRRE, J. & DEISING, H. B. (2009) Sfp-type 4'-phosphopantetheinyl transferase is indispensable for fungal pathogenicity. *Plant Cell*, 21, 3379-96.
- HORSMAN, G. P., VAN LANEN, S. G. & SHEN, B. (2009) Iterative type I polyketide synthases for enediynes core biosynthesis. *Methods Enzymol*, 459, 97-112.
- HOWARTH, M., CHINNAPEN, D. J. F., GERROW, K., DORRESTEIN, P. C., GRANDY, M. R., KELLEHER, N. L., EL-HUSSEINI, A. & TING, A. Y. (2006) A monovalent streptavidin with a single femtomolar biotin binding site. *Nature Methods*, 3, 267-273.

- HOWARTH, M., TAKAO, K., HAYASHI, Y. & TING, A. Y. (2005) Targeting quantum dots to surface proteins in living cells with biotin ligase. *Proceedings of the National Academy of Sciences of the United States of America*, 102, 7583-7588.
- HUBER, E., KLEIN, C., BATZ, H. G. & ZINK, B. (1997) Aminoalkylmaleimides and Hapten and Antigen Derivatives derived therefrom as well as conjugates with peptides and proteins. IN PAT., U. S. (Ed.), Boehringer Mannheim GmbH.
- HUNG, D. T., JAMISON, T. F. & SCHREIBER, S. L. (1996) Understanding and controlling the cell cycle with natural products. *Chem Biol*, 3, 623-39.
- HUTCHINSON, C. R. (1994) Drug synthesis by genetically engineered microorganisms. *Biotechnology (NY)*, 12, 375-80.
- HUTCHINSON, C. R. (1998) Combinatorial biosynthesis for new drug discovery. *Current Opinion in Microbiology*, 1, 319-329.
- HUTCHINSON, C. R., BORELL, C. W., OTTEN, S. L., STUTZMANENGWALL, K. J. & WANG, Y. G. (1989) Drug Discovery and Development through the Genetic-Engineering of Antibiotic-Producing Microorganisms. *J Med Chem*, 32, 929-940.
- HUTCHINSON, C. R. & MCDANIEL, R. (2001) Combinatorial biosynthesis in microorganisms as a route to new antimicrobial, antitumor and neuroregenerative drugs. *Curr Opin Investig Drugs*, 2, 1681-90.
- INGLESE, J., AULD, D. S., JADHAV, A., JOHNSON, R. L., SIMEONOV, A., YASGAR, A., ZHENG, W. & AUSTIN, C. P. (2006) Quantitative high-throughput screening: a titration-based approach that efficiently identifies biological activities in large chemical libraries. *Proc. Nat. Acad. Sci. USA*, 103, 11473-8.
- INGLESE, J., JOHNSON, R. L., SIMEONOV, A., XIA, M., ZHENG, W., AUSTIN, C. P. & AULD, D. S. (2007a) High-throughput screening assays for the identification of chemical probes. *Nat Chem Biol*, 3, 466-79.
- INGLESE, J., JOHNSON, R. L., SIMEONOV, A., XIA, M. H., ZHENG, W., AUSTIN, C. P. & AULD, D. S. (2007b) High-throughput screening assays for the identification of chemical probes. *Nature Chemical Biology*, 3, 466-479.
- JAMES, J. S. (1999) Diarrhea: new treatment option from Shaman. *AIDS Treat News*, 1-2.

- JOSEPH-MCCARTHY, D., PARRIS, K., HUANG, A., FAILLI, A., QUAGLIATO, D., DUSHIN, E. G., NOVIKOVA, E., SEVERINA, E., TUCKMAN, M., PETERSEN, P. J., DEAN, C., FRITZ, C. C., MESHULAM, T., DECENZO, M., DICK, L., MCFADYEN, I. J., SOMERS, W. S., LOVERING, F. & GILBERT, A. M. (2005a) Use of structure-based drug design approaches to obtain novel anthranilic acid acyl carrier protein synthase inhibitors. *J MedChem*, 48, 7960-9.
- JOSEPH-MCCARTHY, D., PARRIS, K., HUANG, A., FAILLI, A., QUAGLIATO, D., DUSHIN, E. G., NOVIKOVA, E., SEVERINA, E., TUCKMAN, M., PETERSEN, P. J., DEAN, C., FRITZ, C. C., MESHULAM, T., DECENZO, M., DICK, L., MCFADYEN, I. J., SOMERS, W. S., LOVERING, F. & GILBERT, A. M. (2005b) Use of structure-based drug design approaches to obtain novel anthranilic acid acyl carrier protein synthase inhibitors. *J Med Chem*, 48, 7960-9.
- JOSHI, N. S., WHITAKER, L. R. & FRANCIS, M. B. (2004) A three-component Mannich-type reaction for selective tyrosine bioconjugation. *Journal of the American Chemical Society*, 126, 15942-15943.
- KAO, C. M., KATZ, L. & KHOSLA, C. (1994) Engineered Biosynthesis of a Complete Macrolactone in a Heterologous Host. *Science*, 265, 509-512.
- KEALEY, J. T., LIU, L., SANTI, D. V., BETLACH, M. C. & BARR, P. J. (1998) Production of a polyketide natural product in nonpolyketide-producing prokaryotic and eukaryotic hosts. *Proceedings of the National Academy of Sciences of the United States of America*, 95, 505-509.
- KIESER, T., BIBB, M.J., BUTTNER, M.J., CHATER, K.F., HOPWOOD, D.A. (2000) *Practical Streptomyces genetics*, John Innes Foundation.
- KIM, E. S., CRAMER, K. D., SHREVE, A. L. & SHERMAN, D. H. (1995) Heterologous Expression of an Engineered Biosynthetic-Pathway - Functional Dissection of Type-Ii Polyketide Synthase Components in Streptomyces Species. *Journal of Bacteriology*, 177, 1202-1207.
- KINGSTON, D. G. & NEWMAN, D. J. (2005) Natural products as drug leads: an old process or the new hope for drug discovery? *IDrugs*, 8, 990-2.
- KIRSCHNING, A., TAFT, F. & KNOBLOCH, T. (2007) Total synthesis approaches to natural product derivatives based on the combination of chemical synthesis and metabolic engineering. *Organic & Biomolecular Chemistry*, 5, 3245-3259.

- KLUGE, B., VATER, J., SALNIKOW, J. & ECKART, K. (1988) Studies on the biosynthesis of surfactin, a lipopeptide antibiotic from *Bacillus subtilis* ATCC 21332. *FEBS Lett*, 231, 107-10.
- KRUGER, R. G., DOSTAL, P. & MCCAFFERTY, D. G. (2002) An economical and preparative orthogonal solid phase synthesis of fluorescein and rhodamine derivatized peptides: FRET substrates for the *Staphylococcus aureus* sortase SrtA transpeptidase reaction. *Chemical Communications*, 2092-2093.
- KUBOTA, T., IINUMA, Y. & KOBAYASHI, J. (2006) Cloning of polyketide synthase genes from amphidinolide-producing, dinoflagellate *Amphidinium* sp. *Biological & Pharmaceutical Bulletin*, 29, 1314-1318.
- LA CLAIR, J. J., FOLEY, T. L., SCHEGG, T. R., REGAN, C. M. & BURKART, M. D. (2004a) Manipulation of carrier proteins in antibiotic biosynthesis. *Chem Biol*, 11, 195-201.
- LA CLAIR, J. J., FOLEY, T. L., SCHEGG, T. R., REGAN, C. M. & BURKART, M. D. (2004b) Manipulation of carrier proteins in antibiotic biosynthesis. *Chemistry & Biology*, 11, 195-201.
- LAKOWICZ, J. R. (1999) *Principles of fluorescence spectroscopy*, New York, Kluwer Academic/Plenum.
- LAM, H. M., TANCULA, E., DEMPSEY, W. B. & WINKLER, M. E. (1992a) Suppression of Insertions in the Complex Pdxj Operon of *Escherichia-Coli* K-12 by Ion and Other Mutations. *J Bacteriol*, 174, 1554-1567.
- LAM, H. M., TANCULA, E., DEMPSEY, W. B. & WINKLER, M. E. (1992b) Suppression of insertions in the complex pdxJ operon of *Escherichia coli* K-12 by Ion and other mutations. *J Bacteriol*, 174, 1554-67.
- LAMBALOT, R. H., GEHRING, A. M., FLUGEL, R. S., ZUBER, P., LACELLE, M., MARAHIEL, M. A., REID, R., KHOSLA, C. & WALSH, C. T. (1996a) A new enzyme superfamily - the phosphopantetheinyl transferases. *Chem Biol*, 3, 923-36.
- LAMBALOT, R. H., GEHRING, A. M., FLUGEL, R. S., ZUBER, P., LACELLE, M., MARAHIEL, M. A., REID, R., KHOSLA, C. & WALSH, C. T. (1996b) A new enzyme superfamily - The phosphopantetheinyl transferases. *Chemistry & Biology*, 3, 923-936.
- LAMBALOT, R. H. & WALSH, C. T. (1995) Cloning, overproduction, and characterization of the *Escherichia coli* holo-acyl carrier protein synthase. *J Biol Chem*, 270, 24658-61.

- LAMBALOT, R. H. & WALSH, C. T. (1997) Holo-[acyl-carrier-protein] synthase of *Escherichia coli*. *Methods in Enzymology*, 279, 254-62.
- LEWANDOWICZ, A. M., VEPSALAINEN, J. & LAITINEN, J. T. (2006) The 'allosteric modulator' SCH-202676 disrupts G protein-coupled receptor function via sulphhydryl-sensitive mechanisms. *British J Pharmacol*, 147, 422-9.
- LIN, C. W. & TING, A. Y. (2006) Transglutaminase-catalyzed site-specific conjugation of small-molecule probes to proteins in vitro and on the surface of living cells. *Journal of the American Chemical Society*, 128, 4542-4543.
- LINK, A. J., VINK, M. K. S., AGARD, N. J., PRESCHER, J. A., BERTOZZI, C. R. & TIRRELL, D. A. (2006) Discovery of aminoacyl-tRNA synthetase activity through cell-surface display of noncanonical amino acids. *Proceedings of the National Academy of Sciences of the United States of America*, 103, 10180-10185.
- MACHIDA, M., USHIJIMA, N., MACHIDA, M. I. & KANAOKA, Y. (1975) Fluorescent Thiol Reagents .9. N-(7-Dimethylamino-4-Methyl-Coumariny)Maleimides (Dacm) - Novel Fluorescent Thiol Reagents. *Chemical & Pharmaceutical Bulletin*, 23, 1385-1386.
- MANDEL, A. L., LA CLAIR, J. J. & BURKART, M. D. (2004) Modular synthesis of pantetheine and phosphopantetheine. *Organic Letters*, 6, 4801-4803.
- MARAHIEL, M. A., NAKANO, M. M. & ZUBER, P. (1993) Regulation of peptide antibiotic production in *Bacillus*. *Mol Microbiol*, 7, 631-6.
- MARKS, B. D., QADIR, N., ELIASON, H. C., SHEKHANI, M. S., DOERING, K. & VOGEL, K. W. (2005) Multiparameter Analysis of a Screen for Progesterone Receptor Ligands: Comparing Fluorescence Lifetime and Fluorescence Polarization Measurements. *Assay Drug Dev Technol*, 3, 613-622.
- MCALLISTER, K. A., PEERY, R. B., MEIER, T. I., FISCHL, A. S. & ZHAO, G. (2000) Biochemical and molecular analyses of the *Streptococcus pneumoniae* acyl carrier protein synthase, an enzyme essential for fatty acid biosynthesis. *J Biol Chem*, 275, 30864-72.
- MEIER, J. L., BARROWS-YANO, T., FOLEY, T. L., WIKE, C. L. & BURKART, M. D. (2008) The unusual macrocycle forming thioesterase of mycolactone. *Molecular Biosystems*, 4, 663-671.

- MEIER, J. L. & BURKART, M. D. (2009a) Chapter 9. Synthetic probes for polyketide and nonribosomal peptide biosynthetic enzymes. *Methods Enzymol*, 458, 219-54.
- MEIER, J. L. & BURKART, M. D. (2009b) The chemical biology of modular biosynthetic enzymes. *Chem Soc Rev*, 38, 2012-45.
- MEIER, J. L., MERCER, A. C., RIVERA, H. & BURKART, M. D. (2006a) Synthesis and evaluation of bioorthogonal pantetheine analogues for in vivo protein modification. *Journal of the American Chemical Society*, 128, 12174-12184.
- MEIER, J. L., MERCER, A. C., RIVERA, H., JR. & BURKART, M. D. (2006b) Synthesis and evaluation of bioorthogonal pantetheine analogues for in vivo protein modification. *J Am Chem Soc*, 128, 12174-84.
- MENCHEN, S. M. & FUNG, S. (1988) 5- and 6-succinimidyl-carboxylate isomers of rhodamine dyes. IN PAT., E. (Ed.), Applied Biosystems.
- MERCER, A. C. & BURKART, M. D. (2007) The ubiquitous carrier protein--a window to metabolite biosynthesis. *Nat Prod Rep*, 24, 750-73.
- MEYER, B. H., MARTINEZ, K. L., SEGURA, J. M., PASCOAL, P., HOVIUS, R., GEORGE, N., JOHNSON, K. & VOGEL, H. (2006a) Covalent labeling of cell-surface proteins for in-vivo FRET studies. *Febs Letters*, 580, 1654-1658.
- MEYER, B. H., SEGURA, J. M., MARTINEZ, K. L., HOVIUS, R., GEORGE, N., JOHNSON, K. & VOGEL, H. (2006b) FRET imaging reveals that functional neurokinin-1 receptors are monomeric and reside in membrane microdomains of live cells. *Proceedings of the National Academy of Sciences of the United States of America*, 103, 2138-2143.
- MICHAEL, S., AULD, D., KLUMPP, C., JADHAV, A., ZHENG, W., THORNE, N., AUSTIN, C., INGLESE, J. & SIMEONOV, A. (2008) A Robotic Platform for Quantitative High-Throughput Screening. *Assay Drug Dev Technol*, 6, 637-657.
- MILLER, L. W. & CORNISH, V. W. (2005) Selective chemical labeling of proteins in living cells. *Current Opinion in Chemical Biology*, 9, 56-61.
- MOOTZ, H. D., FINKING, R. & MARAHIEL, M. A. (2001) 4'-phosphopantetheine transfer in primary and secondary metabolism of *Bacillus subtilis*. *J Biol Chem*, 276, 37289-98.
- NAKANO, M. M., CORBELL, N., BESSON, J. & ZUBER, P. (1992) Isolation and characterization of *sfp*: a gene that functions in the production of the

- lipopeptide biosurfactant, surfactin, in *Bacillus subtilis*. *Mol Gen Genet*, 232, 313-21.
- NAKANO, M. M., MARAHIEL, M. A. & ZUBER, P. (1988) Identification of a genetic locus required for biosynthesis of the lipopeptide antibiotic surfactin in *Bacillus subtilis*. *J Bacteriol*, 170, 5662-8.
- NAKANO, M. M. & ZUBER, P. (1989) Cloning and characterization of *srfB*, a regulatory gene involved in surfactin production and competence in *Bacillus subtilis*. *J Bacteriol*, 171, 5347-53.
- NAKANO, M. M. & ZUBER, P. (1990) Molecular biology of antibiotic production in *Bacillus*. *Crit Rev Biotechnol*, 10, 223-40.
- NERES, J., LABELLO, N. P., SOMU, R. V., BOSHOFF, H. I., WILSON, D. J., VANNADA, J., CHEN, L., BARRY, C. E., BENNETT, E. M. & ALDRICH, C. C. (2008) Inhibition of siderophore biosynthesis in *Mycobacterium tuberculosis* with nucleoside bisubstrate analogues: Structure-activity relationships of the nucleobase domain of 5'-O-[N-(salicyl)sulfamoyl]adenosine. *Journal of Medicinal Chemistry*, 51, 5349-5370.
- NEWMAN, D. J. & CRAGG, G. M. (2004a) Advanced preclinical and clinical trials of natural products and related compounds from marine sources. *Curr Med Chem*, 11, 1693-713.
- NEWMAN, D. J. & CRAGG, G. M. (2004b) Marine natural products and related compounds in clinical and advanced preclinical trials. *J Nat Prod*, 67, 1216-38.
- NEWMAN, D. J. & CRAGG, G. M. (2007) Natural products as sources of new drugs over the last 25 years. *Journal of Natural Products*, 70, 461-477.
- NEWMAN, D. J., CRAGG, G. M., HOLBECK, S. & SAUSVILLE, E. A. (2002) Natural products and derivatives as leads to cell cycle pathway targets in cancer chemotherapy. *Curr Cancer Drug Targets*, 2, 279-308.
- NEWMAN, D. J., CRAGG, G. M. & SNADER, K. M. (2003) Natural products as sources of new drugs over the period 1981-2002. *J Nat Prod*, 66, 1022-37.
- NGUYEN, T., JOSHI, N. S. & FRANCIS, M. B. (2006) An affinity-based method for the purification of fluorescently-labeled biomolecules. *Bioconjugate Chemistry*, 17, 869-872.
- NIELSEN, J. (1998) The role of metabolic engineering in the production of secondary metabolites. *Current Opinion in Microbiology*, 1, 330-336.

- OBeregger, H., EISENDLE, M., SCHRETTL, M., GRAESSLE, S. & HAAS, H. (2003) 4'-phosphopantetheinyl transferase-encoding *npgA* is essential for siderophore biosynthesis in *Aspergillus nidulans*. *Curr Genet*, 44, 211-5.
- ONWUEME, K. C., VOS, C. J., ZURITA, J., FERRERAS, J. A. & QUADRI, L. E. (2005) The dimycocerosate ester polyketide virulence factors of mycobacteria. *Progress Lipid Res*, 44, 259-302.
- PADUCH, R., KANDEFER-SZERSZEN, M., TRYTEK, M. & FIEDUREK, J. (2007) Terpenes: substances useful in human healthcare. *Archivum Immunologiae Et Therapiae Experimentalis*, 55, 315-327.
- PARRIS, K. D., LIN, L., TAM, A., MATHEW, R., HIXON, J., STAHL, M., FRITZ, C. C., SEEHRA, J. & SOMERS, W. S. (2000) Crystal structures of substrate binding to *Bacillus subtilis* holo-(acyl carrier protein) synthase reveal a novel trimeric arrangement of molecules resulting in three active sites. *Structure with Folding & Design*, 8, 883-895.
- PAYNE, D. J., GWYNN, M. N., HOLMES, D. J. & POMPLIANO, D. L. (2007) Drugs for bad bugs: confronting the challenges of antibacterial discovery. *Nat Rev Drug Discov*, 6, 29-40.
- PAYNE, G. F., DELACRUZ, N. & COPPELLA, S. J. (1990) Improved production of heterologous protein from *Streptomyces lividans*. *Appl Microbiol Biotechnol*, 33, 395-400.
- PEDERSEN, D. S. & ROSENBOHM, C. (2001) Dry column vacuum chromatography. *Synthesis-Stuttgart*, 2431-2434.
- PEREZ-RUIZ, T., MARTINEZ-LOZANO, C., SANZ, A. & BRAVO, E. (2001) Simultaneous determination of doxorubicin, daunorubicin, and idarubicin by capillary electrophoresis with laser-induced fluorescence detection. *Electrophoresis*, 22, 134-8.
- PETTERSEN, E. F., GODDARD, T. D., HUANG, C. C., COUCH, G. S., GREENBLATT, D. M., MENG, E. C. & FERRIN, T. E. (2004) UCSF chimera - A visualization system for exploratory research and analysis. *Journal of Computational Chemistry*, 25, 1605-1612.
- PFEIFER, B. A. & KHOSLA, C. (2001) Biosynthesis of polyketides in heterologous hosts. *Microbiology and Molecular Biology Reviews*, 65, 106-+.
- POLSTER, B. M., ARZE, R., LYTTLE, M. H., NICHOLLS, D. G. & HUDSON, D. (2007) Solid phase synthesis of dual labeled peptides: Development of cell

permeable calpain specific substrates. *International Journal of Peptide Research and Therapeutics*, 13, 83-91.

- PORTEVIN, D., SOUSA-D'AURIA, C. C., HOUSSIN, C., GRIMALDI, C., CHAMI, M., DAFFE, M. & GUILHOT, C. (2004) A polyketide synthase catalyzes the last condensation step of mycolic acid biosynthesis in mycobacteria and related organisms. *Proceedings of the National Academy of Sciences of the United States of America*, 101, 314-319.
- POWELL, G. L., ELOVSON, J. & VAGELOS, P. R. (1969) Acyl carrier protein. XII. Synthesis and turnover of the prosthetic group of acyl carrier protein in vivo. *J Biol Chem*, 244, 5616-24.
- PRESCOTT, D. J., ELOVSON, J. & VAGELOS, P. R. (1969) Acyl carrier protein. XI. The specificity of acyl carrier protein synthetase. *J Biol Chem*, 244, 4517-21.
- QUADRI, L. E., WEINREB, P. H., LEI, M., NAKANO, M. M., ZUBER, P. & WALSH, C. T. (1998a) Characterization of Sfp, a *Bacillus subtilis* phosphopantetheinyl transferase for peptidyl carrier protein domains in peptide synthetases. *Biochemistry*, 37, 1585-95.
- QUADRI, L. E. N., SELLO, J., KEATING, T. A., WEINREB, P. H. & WALSH, C. T. (1998b) Identification of a *Mycobacterium tuberculosis* gene cluster encoding the biosynthetic enzymes for assembly of the virulence-conferring siderophore mycobactin. *Chemistry & Biology*, 5, 631-645.
- RABUKA, D., HUBBARD, S. C., LAUGHLIN, S. T., ARGADE, S. P. & BERTOZZI, C. R. (2006) A chemical reporter strategy to probe glycoprotein fucosylation. *Journal of the American Chemical Society*, 128, 12078-12079.
- REED, M. B., DOMENECH, P., MANCA, C., SU, H., BARCZAK, A. K., KREISWIRTH, B. N., KAPLAN, G. & BARRY, C. E. (2004) A glycolipid of hypervirulent tuberculosis strains that inhibits the innate immune response. *Nature*, 431, 84-87.
- REUTER, K., MOFID, M. R., MARAHIEL, M. A. & FICNER, R. (1999) Crystal structure of the surfactin synthetase-activating enzyme Sfp: a prototype of the 4'-phosphopantetheinyl transferase superfamily. *Embo Journal*, 18, 6823-6831.
- RICE, W. G., SCHAEFFER, C. A., HARTEN, B., VILLINGER, F., SOUTH, T. L., SUMMERS, M. F., HENDERSON, L. E., BESS, J. W., ARTHUR, L. O., MCDUGAL, J. S., ORLOFF, S. L., MENDELEYEV, J. & KUN, E. (1993)

- Inhibition of HIV-1 infectivity by zinc-ejecting aromatic C-nitroso compounds. *Nature*, 361, 473-475.
- SAGHATELIAN, A. & CRAVATT, B. F. (2005) Assignment of protein function in the postgenomic era. *Nature Chemical Biology*, 1, 130-142.
- SANSOM, C. (2001) LPS inhibitors: key to overcoming multidrug-resistant bacteria? *Drug Disc Today*, 6, 499-500.
- SATHYAMOORTHY, M., STEMKE, D. & SPEEDIE, M. K. (1996) Native and heterologous protein secretion by *Streptomyces lividans*. *Appl Microbiol Biotechnol*, 46, 347-52.
- SAWA, M., HSU, T. L., ITOH, T., SUGIYAMA, M., HANSON, S. R., VOGT, P. K. & WONG, C. H. (2006) Glycoproteomic probes for fluorescent imaging of fucosylated glycans in vivo. *Proceedings of the National Academy of Sciences of the United States of America*, 103, 12371-12376.
- SAXON, E. & BERTOZZI, C. R. (2000) Cell surface engineering by a modified Staudinger reaction. *Science*, 287, 2007-2010.
- SCHLICK, T. L., DING, Z. B., KOVACS, E. W. & FRANCIS, M. B. (2005) Dual-surface modification of the tobacco mosaic virus. *Journal of the American Chemical Society*, 127, 3718-3723.
- SCHONHOFF, C. M., MATSUOKA, M., TUMMALA, H., JOHNSON, M. A., ESTEVÃZ, A. G., WU, R., KAMAID, A. S., RICART, K. C., HASHIMOTO, Y., GASTON, B., MACDONALD, T. L., XU, Z. & MANNICK, J. B. (2006) S-nitrosothiol depletion in amyotrophic lateral sclerosis. *Proc. Nat. Acad. Sci. USA*, 103, 2404-2409.
- SELWYN, M. J. (1965) A Simple Test for Inactivation of an Enzyme During Assay. *Biochimica Et Biophysica Acta*, 105, 193-4.
- SIMEONOV, A., JADHAV, A., THOMAS, C. J., WANG, Y. H., HUANG, R. L., SOUTHALL, N. T., SHINN, P., SMITH, J., AUSTIN, C. P., AULD, D. S. & INGLESE, J. (2008) Fluorescence spectroscopic profiling of compound libraries. *J Med Chem*, 51, 2363-2371.
- SIMEONOV, A., KULKARNI, A., DORJSUREN, D., JADHAV, A., SHEN, M., MCNEILL, D. R., AUSTIN, C. P. & WILSON III, D. M. (2009) Identification and Characterization of Inhibitors of Human Apurinic/aprimidinic Endonuclease APE1. *PLoS ONE*, 4, e5740.

- SPRUNG, R., NANDI, A., CHEN, Y., KIM, S. C., BARMA, D., FALCK, J. R. & ZHAO, Y. M. (2005) Tagging-via-substrate strategy for probing O-GlcNAc modified proteins. *Journal of Proteome Research*, 4, 950-957.
- STANLEY, A. E., WALTON, L. J., ZERIKLY, M. K., CORRE, C. & CHALLIS, G. L. (2006) Elucidation of the *Streptomyces coelicolor* pathway to 4-methoxy-2,2'-bipyrrole-5-carboxaldehyde, an intermediate in prodiginine biosynthesis. *Chemical Communications*, 3981-3983.
- STELLER, S., SOKOLL, A., WILDE, C., BERNHARD, F., FRANKE, P. & VATER, J. (2004) Initiation of surfactin biosynthesis and the role of the SrfD-thioesterase protein. *Biochemistry*, 43, 11331-43.
- STEVENS, W. C., JONES, R. M., SUBRAMANIAN, G., METZGER, T. G., FERGUSON, D. M. & PORTOGHESE, P. S. (2000) Potent and Selective Indolomorphinan Antagonists of the Kappa-Opioid Receptor. *J Med Chem*, 43, 2759-2769.
- STIRRETT, K. L., FERRERAS, J. A., JAYAPRAKASH, V., SINHA, B. N., REN, T. & QUADRI, L. E. N. (2008) Small molecules with structural similarities to siderophores as novel antimicrobials against *Mycobacterium tuberculosis* and *Yersinia pestis*. *Bioorganic & Medicinal Chemistry Letters*, 18, 2662-2668.
- STRICKLAND, K. C., HOEFERLIN, L. A., OLEINIK, N. V., KRUPENKO, N. I. & KRUPENKO, S. A. (2009) Acyl carrier protein-specific 4'-phosphopantetheinyl transferase activates 10-formyltetrahydrofolate dehydrogenase. *J Biol Chem*.
- STROHL, W. R. (2001) Biochemical engineering of natural product biosynthesis pathways. *Metabolic Engineering*, 3, 4-14.
- TAKAOKA, Y., TSUTSUMI, H., KASAGI, N., NAKATA, E. & HAMACHI, I. (2006) One-pot and sequential organic chemistry on an enzyme surface to tether a fluorescent probe at the proximity of the active site with restoring enzyme activity. *Journal of the American Chemical Society*, 128, 3273-3280.
- TAKIFF, H. E., BAKER, T., COPELAND, T., CHEN, S. M. & COURT, D. L. (1992) Locating Essential *Escherichia-Coli* Genes by Using Mini-Tn10 Transposons - the Pdxj Operon. *J Bacteriol*, 174, 1544-1553.
- TSUGE, K., ANO, T. & SHODA, M. (1996) Isolation of a gene essential for biosynthesis of the lipopeptide antibiotics plipastatin B1 and surfactin in *Bacillus subtilis* YB8. *Arch Microbiol*, 165, 243-51.

- ULLRICH, C., KLUGE, B., PALACZ, Z. & VATER, J. (1991) Cell-free biosynthesis of surfactin, a cyclic lipopeptide produced by *Bacillus subtilis*. *Biochemistry*, 30, 6503-8.
- VAN LANEN, S. G. & SHEN, B. (2006) Microbial genomics for the improvement of natural product discovery. *Current Opinion in Microbiology*, 9, 252-260.
- VASUDEVAN, D., FIMMEN, R. L. & FRANCISCO, A. B. (2001) Tracer-grade rhodamine WT: Structure of constituent isomers and their sorption behavior. *Environmental Science & Technology*, 35, 4089-4096.
- VATELE, J. M. (2004) Prenyl carbamates: preparation and deprotection. *Tetrahedron*, 60, 4251-4260.
- VOCADLO, D. J., HANG, H. C., KIM, E. J., HANOVER, J. A. & BERTOZZI, C. R. (2003) A chemical approach for identifying O-GlcNAc-modified proteins in cells. *Proceedings of the National Academy of Sciences of the United States of America*, 100, 9116-9121.
- WALSH, C. (2003) *Antibiotics : actions, origins, resistance*, Washington, D.C., ASM Press.
- WALSH, C. T. (2002) Combinatorial biosynthesis of antibiotics: Challenges and opportunities. *Chembiochem*, 3, 125-134.
- WELLINGS, D. A. & ATHERTON, E. (1997a) Standard Fmoc protocols. *Meth Enzymol*, 289, 44-67.
- WELLINGS, D. A. & ATHERTON, E. (1997b) Standard Fmoc protocols. *Methods in Enzymology*, 289, 44-67.
- WORTHINGTON, A. S. & BURKART, M. D. (2006) One-pot chemo-enzymatic synthesis of reporter-modified proteins. *Organic & Biomolecular Chemistry*, 4, 44-46.
- WORTHINGTON, A. S., HUR, G. H., MEIER, J. L., CHENG, Q., MOORE, B. S. & BURKART, M. D. (2008) Probing the compatibility of type II ketosynthase-carrier protein partners. *Chembiochem*, 9, 2096-103.
- WORTHINGTON, A. S., RIVERA, H.R.JR., TOPEY, J.W., BURKART, M.D. (2006) Mechanism-based protein crosslinking probes to investigate carrier protein mediated synthesis. *American Chemical Society Chemical Biology*, in press.

- WRIGHT, L. F. & HOPWOOD, D. A. (1976) Actinorhodin Is a Chromosomally-Determined Antibiotic in *Streptomyces-Coelicolor* A3(2). *Journal of General Microbiology*, 96, 289-297.
- WU, G., YUAN, Y. & HODGE, C. N. (2003) Determining appropriate substrate conversion for enzymatic assays in high-throughput screening. *Journal of Biomolecular Screening*, 8, 694-700.
- XIE, J. & SCHULTZ, P. G. (2006) A chemical toolkit for proteins - an expanded genetic code. *Nature Reviews Molecular Cell Biology*, 7, 775-782.
- YAN, S. C. B., GRINNELL, B. W. & WOLD, F. (1989) Post-Translational Modifications of Proteins - Some Problems Left to Solve. *Trends in Biochemical Sciences*, 14, 264-268.
- YASGAR, A., FOLEY, T. L., JADHAV, A., INGLESE, J., BURKART, M. D. & SIMEONOV, A. (2010) A strategy to discover inhibitors of *Bacillus subtilis* surfactin-type phosphopantetheinyl transferase. *Mol. Biosyst.*, *in press*.
- YASGAR, A., SHINN, P., MICHAEL, S., ZHENG, W., JADHAV, A., AULD, D., AUSTIN, C., INGLESE, J. & SIMEONOV, A. (2008) Compound Management for Quantitative High-Throughput Screening. *J Assoc Lab Automat*, 13, 79-89.
- YIN, J., LIN, A. J., BUCKETT, P. D., WESSLING-RESNICK, M., GOLAN, D. E. & WALSH, C. T. (2005a) Single-cell FRET imaging of transferrin receptor trafficking dynamics by Sfp-catalyzed, site-specific protein labeling. *Chemistry & Biology*, 12, 999-1006.
- YIN, J., LIU, F., LI, X. H. & WALSH, C. T. (2004) Labeling proteins with small molecules by site-specific posttranslational modification. *Journal of the American Chemical Society*, 126, 7754-7755.
- YIN, J., STRAIGHT, P. D., MCLOUGHLIN, S. M., ZHOU, Z., LIN, A. J., GOLAN, D. E., KELLEHER, N. L., KOLTER, R. & WALSH, C. T. (2005b) Genetically encoded short peptide tag for versatile protein labeling by Sfp phosphopantetheinyl transferase. *Proceedings of the National Academy of Sciences of the United States of America*, 102, 15815-15820.
- YIN, J., STRAIGHT, P. D., MCLOUGHLIN, S. M., ZHOU, Z., LIN, A. J., GOLAN, D. E., KELLEHER, N. L., KOLTER, R. & WALSH, C. T. (2005c) Genetically encoded short peptide tag for versatile protein labeling by Sfp phosphopantetheinyl transferase. *Proc Natl Acad Sci U S A*, 102, 15815-20.

- ZAZOPOULOS, E., HUANG, K. X., STAFFA, A., LIU, W., BACHMANN, B. O., NONAKA, K., AHLERT, J., THORSON, J. S., SHEN, B. & FARNET, C. M. (2003) A genomics-guided approach for discovering and expressing cryptic metabolic pathways. *Nature Biotechnology*, 21, 187-190.
- ZHANG, J. H., CHUNG, T. D. Y. & OLDENBURG, K. R. (1999) A simple statistical parameter for use in evaluation and validation of high throughput screening assays. *Journal of Biomolecular Screening*, 4, 67-73.
- ZHANG, Z. W., ALFONTA, L., TIAN, F., BURSULAYA, B., URYU, S., KING, D. S. & SCHULTZ, P. G. (2004) Selective incorporation of 5-hydroxytryptophan into proteins in mammalian cells. *Proceedings of the National Academy of Sciences of the United States of America*, 101, 8882-8887.
- ZHOU, Z., CIRONI, P., LIN, A. J., XU, Y. Q., HRVATIN, S., GOLAN, D. E., SILVER, P. A., WALSH, C. T. & YIN, J. (2007) Genetically encoded short peptide tags for orthogonal protein labeling by sfp and AcpS phosphopantetheinyl transferases. *Acs Chemical Biology*, 2, 337-346.
- ZIRKLE, R., LIGON, J. M. & MOLNAR, I. (2004) Heterologous production of the antifungal polyketide antibiotic soraphen A of *Sorangium cellulosum* So ce26 in *Streptomyces lividans*. *Microbiology*, 150, 2761-74.